UNIVERSITÀ DI SIENA 1240

Dipartimento di Scienze Fisiche, della Terra e dell'Ambiente

Dottorato in Scienze e Tecnologie Ambientali, Geologiche e Polari

34°Ciclo

Coordinatore: Prof. Simone Bastianoni

"Micro and nanoplastic: a growing threat to marine organisms, the case of the sea urchin *Paracentrotus lividus* "

Settore scientifico disciplinare: BIO/07

Candidato

Carola Murano
Università di Siena
Stazione Zoologica Anton Dohrn

Firma del Candidato

Tutori

Prof.ssa Ilaria Corsi *(Università di Siena)*

Firma del Tutore

Dott.ssa Anna Palumbo (*Stazione Zoologica Anton Dohrn*)

Firma del Tutore

Anno accademico di conseguimento del titolo di Dottore di ricerca
2020/2021

Università degli Studi di Siena

Dottorato in Scienze e tecnologie ambientali, geologiche e polari

34° Ciclo

Data dell'esame finale

13/12/2021

Commissione giudicatrice

Prof. Giovanni Libralato- Università Federico II di Napoli, Napoli, Italy

Prof.ssa Elena Fabbri- Università degli Studi di Bologna, Bologna, Italy

Prof.ssa Maria Cristina Fossi- Università degli Studi di Siena, Siena, Italy

Supplenti

Prof.ssa Camilla Della Torre- Università degli Studi di Milano Statale, Milano, Italy

Table of contents

Abstract

It is common knowledge that the marine environment is facing a great challenge nowadays against the smallest fraction of marine litter known as microplastics (MP; < 5 mm) and nanoplastics (< 1μm). The Mediterranean Sea, due to its geographic conformation, is recognized as one of the main areas with a high accumulation of both MPs and nanoplastics. The most affected compartment seems to be the sediments, especially those bordering marine coastal areas, which act as a long-term sink of legacy and emerging contaminants of anthropogenic origin. How MPs and nanoplastics interact with marine species and in particular with benthic organisms is a research topic not yet completely understood. This knowledge-gap results in the absence of a fitting ecological risk assessment with consequent severe damages to the marine ecosystems. Among the benthic organisms of environmental concern, the sea urchin *Paracentrotus lividus* could be a target of MPs and nanoplastics with consequences on its ecological role and function in Mediterranean coastal areas. It is widely recognized as the key species of the Mediterranean benthic communities being grazer who defines structural complexity as well as the dynamic supply of energy, mass, and nutrients from detritus to higher trophic levels.

In order to fill current knowledge gaps on the impact and interaction of MPs and nanoplastics on benthic species populating Mediterranean coastal areas, the aim of the present study was to explore mechanisms of uptake, biodisposition and clearance, and toxicological responses of selected MPs and nanoplastics in different organs and cells of the sea urchin *P. lividus.* In addition, a special focus was reserved on the nanoscale dimension of plastics (<100 nm), by looking at the mechanisms of the bio-nano interactions between nanoplastics and the sea urchin immune cells. The research described here has been divided in 4 chapters in which findings on polystyrene (PS) MPs and nanoparticles (PS NPs) in *P. lividus* have been obtained by using 3 approaches: 1) an *in vivo* study has been designed in order to identify mechanisms of uptake, toxicity and immunological response of either virgin or colonized MPs of different sizes; 2) an *in vitro* study has been performed to examine the cellular trafficking of PS NPs having negative surface charges in immune cells coupled to the evaluation of immune function and ultrastructural properties; 3) a *field* study was performed to assess the occurrence of MPs in wild specimens collected from various locations in the Gulf of Naples (Italy). Concerning the *in vivo* study, adult specimen's sea urchins were exposed to two different sizes of PS MPs, 10 and 45 μm (10 MPs mL^{-1}), for 72h. A size-dependent MPs uptake in sea urchins was observed; while the smallest MPs resulted located in the aquifer system, the largest ones were mainly found in the digestive system. As far as the observed effects upon exposure, PS MPs regardless of their different size both affected the immune response in terms of quantity/quality of cells, antioxidant capacity, reactive oxygen and nitrogen species. Another important finding concerns the evidence that the

naturally occurring colonized MPs are higher internalized by sea urchins compared to virgin ones after 48h of exposure. Colonized microplastics were obtained by 1-week incubation in unfiltered natural sea water (NSW) collected from a coastal site in the Gulf of Naples. The biofilm formation on MPs surface targets immune cells in terms of counts and morphology as well as redox status. Therefore, it can be concluded that colonized PS MPs exhibit greater effects on sea urchin immune cells compared to virgin ones as those most commonly used in ecotoxicological studies. These results encourage the use of colonized rather than virgin MPs for a more environmentally relevant risk assessment, since once released in marine waters MPs are soon colonized both chemically and biologically.

Regarding the bio-nano interactions, our *in vitro* study with sea urchin's immune cells confirmed the role of surface charges (negative *vs* positive) as drivers of ecotoxicity. Precisely, immune cells were exposed to negatively charged PS NPs (PS-COOH; 50nm) (0, 5, 25 µg mL^{-1}) and to PS NPs (PS-NH$_2$; 50nm) (25 µg mL^{-1}) for 4h. In detail, our study showed a fast uptake by phagocytes of negatively charged PS NPs and sequestration into lysosomal compartments associated with low acute toxicity in comparison with their positively charged counterparts as amino-modified PS NPs (PS-NH$_2$).

In the *field* study, the occurrence of MPs, mostly microfibers (MFs), in adult sea urchin specimens sampled in four sites in the Gulf of Naples was demonstrated. MFs were found both in gonads, coelomic fluid and digestive system of wild sea urchins, although in the latter in higher amounts. Polyester-based fibers were the most abundant together with natural fibers such as cotton. Potential sources could be represented by fishing lines and textiles whole fibers could be released by the sewage treatment plants.

Overall these findings provided for the first time the evidence of the multisided interactions between MPs/nanoplastics and the sea urchin *P. lividus* with important ecological implications. This thesis provided key answers to the scientific existing gaps by establishing how MPs uptake and biodistribution occur and how these are transformed according to their surface biological characteristics. Furthermore, the key factors for estimating how the sea urchin immune response counteract exposure to MPs as well as toxicokinetic/toxicodynamic elements underlying the bio-nano-interaction have been revealed. The use of the adult sea urchin *P. lividus* as a suitable model has been proved to be instrumental in shedding light on the potential effects of MPs and nanoplastics on benthic marine grazer species thus stimulating future research in deepening the understanding of the potential impacts on marine communities and ecosystems.

List of Abbreviations

List of the abbreviations used, in alphabetical order:

ABTS: 2,2′-azinobis-3-ethylbenzothiazoline-6-sulfonic acid

ANOVA: Analysis of variance

CAT: catalase

CCM: cell culture medium

CDNB: 1-chloro- 2,4- dinitrobenzene

CF: coelomic fluid

DAF: 4-amino-5-methylamino-2',7'-difluororescein diacetate

DCF: 2',7'-dichlorohydro-fluoresceindiacetate

DMSO: dimethyl sulfoxide

DTT: threo-1,4-Dimercapto-2,3-butanediol

FAD: flavin adenine dinucleotide disodium salt hydrate

FTIR: fourier-transform infrared spectroscopy

GFP: green fluorescent protein

GPx: glutathione peroxidase

GSH: reduced glutathione

GST: glutathione-S-transferase

LDA: linear discriminant analysis

MFs: microfibers

MPs: microplastics

Micro-PS: polystyrene microparticles

NED: N-(1-naphthyl) ethylenediamine

NM: nanomaterial

NMDS: non metric multidimensional scaling

NO: nitric oxide

NOM: natural organic matter

NPs: nanoparticles

NSW: natural sea water

OTU: operational taxonomic unit

PBS: phosphate-Buffered Saline

PC: phagocytic capacity

PDI: polydispersion index

PI: phagocytic index

PMSF: phenylmethanesulfonyl fluoride

PS: polystyrene

PS-COOH: carboxyl-modified polystyrene nanoparticles

PS-NH$_2$: amino-modified polystyrene nanoparticles

PS NPs: polystyrene nanoparticles

ROS: reactive oxygen species

RNS: reactive nitrogen species

SD: standard deviation

SE: standard error

SEM: scanning electron microscopy

SOD: superoxide dismutase

TAC: total antioxidant capacity

TEM: transmission electron microscopy

Structure of the thesis

This thesis work begins with an introduction in which an overview of microplastic/nanoplastic pollution was provided with a particular focus on the current situation in the Mediterranean Sea. More deeply, a detailed description of the sea urchin *Paracentrotus lividus*, the model organism used in this study, was added. As a matter of fact, the sea urchin is a key species in benthic communities, important not only for its ecological function but also for the high commercial value. In spite of these premises, prior to this thesis no research had been performed on the effects of microplastics (MPs) and nanoplastics on the adult's sea urchin. After the introduction, the main objectives of this study and the description of the content of each chapter are presented. The entire work is divided into 4 chapters. In detail, each chapter is characterized by a general introduction in which the research context and research goals are described followed by materials and methods that consist of all the methodologies used to achieve the set objectives. The results obtained were presented and discussed either in separate sections or combined: results and discussions. Afterwards, a concluding remarks summarizing the results obtained by contextualizing them in future perspectives has been added at the end of each chapter. Furthermore, supplementary material and a bibliographic research list are provided. This thesis work ends with a general concluding paragraph of the work carried out during the 3 years, unravelling the objectives achieved and the future scientific challenges to be faced.

Part of the work presented in this PhD thesis has been published as manuscript, listed below:

- <u>Chapter 1</u>**: Murano C.,** Agnisola C., Castellano I., Casotti R., Corsi, I., Palumbo A. (2020). "How sea urchin face microplastics: Uptake, tissue distribution and immune system response". Environmental Pollution 264, 114685. https://doi.org/10.1016/j.envpol.2020.114685
- <u>Chapter 2</u>**: Murano C.,** Donnarumma V., Corsi I., Casotti R., Palumbo A. (2021). "Impact of Microbial Colonization of Polystyrene Microbeads on the Toxicological Responses in the Sea Urchin *Paracentrotus lividus*". Environmental Science & Technology 55 (12), 7990-8000. https://doi.org/10.1021/acs.est.1c00618
- <u>Chapter 4</u>: **Murano C.,** Bergami E., Liberatori G., Palumbo A., Corsi I. (2021). "Interplay Between Nanoplastics and the Immune System of the Mediterranean Sea Urchin *Paracentrotus lividus*". Frontiers in Marine Science 8, 234. https://doi.org/10.3389/fmars.2021.647394

Introduction

1.1 Plastic pollution at sea: sources, fate and impacts

Plastic pollution is not a recent issue. Indeed, the first research on plastic debris retrieved on the sea is back in 1972, when for the first time the presence of polystyrene (PS) spherules covered by bacteria and polychlorinated biphenyls was reported along the New England coasts (Carpenter et al., 1972). At the same time, the first gyre of marine plastic debris in the central North Pacific Ocean was documented (the Great Pacific Garbage Patch) (Wong et al., 1974). Currently, it is expected that 87k metric tons of plastic items are floating on it (Lebreton et al., 2018). Up to now, plastics have transformed our lives radically by changing our habits thanks to their low costs and versatility and huge introduction in consumer products (e.g. packaging, high-tech and clothes industries, building and medicine) (Andrady et al., 2009). Nowadays, the production of plastic is estimated to be around 368 million metric tons worldwide (2019) with a global plastic market size of USD 579.7 billion in 2020 (Plastic Europe, 2020). Unfortunately, as a result of the plastic short lifetime and waste mismanagement, the occurrence and accumulation of plastic debris in the natural environment is now widespread (Jambeck et al., 2015) including even the most remote regions of the Earth such as the Arctic and Antarctica (Peeken et al., 2018; Suaria et al., 2020). Known as the ultimate sink of man-made pollutants, the sea is the environmental compartment most affected by plastic pollution, in which end up about 60-80% of the total plastic litter (Barboza et al., 2019). Reliable quantitative estimations suggested that, every year, almost 8 million tonnes of plastics reach the ocean (Gallo et al., 2018). Nevertheless, the predominance of plastics in litter is not only due to their increasing use but also to their exceptional durability and persistence into the environment (Bessenling, 2018). Conventionally, plastic debris are classified according to dimensional criteria (Eriksen et al., 2014):

- Macroplastics as above 200 mm

- Mesoplastics between 5-200 mm

- Microplastics (MPs) < 5 mm

- Nanoplastics <1 µm

However, for the latter, a conventional definition is missing or is anyway under continuous debate (Koelmans, 2019). According to some authors, the nanoplastics definition should follow the common criteria used for engineered nanomaterials (ENMs) (<100 nm in at least one dimension) while others consider the metric system more suitable for nanoplastics definition (Koelmans et al., 2015; Gigault et al., 2018; Harmann et al., 2019). Moreover, in the case of MPs, there is a further subdivision by which they are classified in large-MPs (1-5 mm) and small-MPs or sub-micron MPs (0.1 nm-1mm)

(Hartmann et al., 2019). In order to be clear, in the following text, the following definitions are applied here: MPs (<5 mm) and nanoplastics (<1 μm).

In recent years, both MPs and nanoplastics have attracted particular attention in the scientific community for their physical-chemical properties and the effects that they may exert on the surrounding environment and associated wildlife. Depending on their origin, both MPs and nanoplastics are currently classified as primary or secondary. Primary MPs/nanoplastics are defined as plastics intentionally produced at micro/nano scale for different applications such as drug delivery, cosmetics and clothes (Al-Thawadi, 2020). Instead, secondary MPs/ nanoplastics are the results of the fragmentation and degradation of larger plastic debris by chemical, physical, and biological processes (Singh and Sharma, 2008; Gago et al., 2016; Andrady, 2017; Horton et al., 2018). Late evidence suggests that most of the plastics that are found in the environment are secondary and have a land-based rather than sea-based origin (Koutsodendris et al., 2008; Galgani, 2013; Pasquini et al., 2016). One of the most current challenges for the scientific and technological research of MPs/nanoplastics is the improvement in the detection technologies. Indeed, the current data relating to the amount of plastics in the seas and oceans includes only fragments with dimensions greater than 330 μm (manta mesh size) with the exclusion of smaller fragments and fibers below such size. Therefore, while there is a partial view of the global abundance of MPs, very little is known about nanoplastics (<1 μm) whose information can be only inferred from controlled laboratory conditions (Gigault et al., 2016; Lambert & Wagner, 2016). Only in 2018, the presence of nanoplastics in sea water from the North Atlantic Subtropical Gyre was reported for the first time (Ter Halle et al., 2018).

Environmental life-cycle of plastic

Over the lifecycle in the aquatic environment, MPs and nanoplastics undergo a series of transformations, which set their environmental fate, bioavailability as well as toxicity for marine organisms (Figure 1). In detail, these transformations involve their surface properties (shape, roughness, charge) that play an important role in determining their ecological impacts driving the rapid changes in seawater (Galloway et al., 2017). However, also the features of the surrounding environment (pH, temperature, ionic strength, natural organic matter concentration) affect the transformations of MPs/nanoplastics in water (Sharma et al., 2021). As far as for NM, the interactions occurring with natural biomolecules and chemical substances present in the natural aquatic media led to the formation of the so-called "eco-corona" (Canesi and Corsi, 2016). The key aspect of the eco-corona formation concerns the surface of MPs/nanoplastics that acts as a magnet towards substances from the surrounding environment including natural organic matter (NOM), nutrients and toxic chemicals (Galloway et al., 2017; Paul et al., 2020; Kihara et al., 2021). NOM, humic acids and

exopolymeric substances (EPS) produced by microalgae attached onto the surface of MPs/nanoplastics alter their density and aggregation as well as the surface charge that is expected to be negative in marine environment also for the weathering processes (Fotopoulou and Karapanagioti, 2012; Gigault et al., 2016; Andrady, 2017). Deeply inside in this concept of absorbed layers, MPs/nanoplastics provide a suitable substrate also for hydrophobic contaminants and heavy metals contributing to their release and transport in sea water and in biological systems (Koelmans et al., 2013; Lee et al., 2014; Wang et al., 2019; Yu et al., 2019). In the case of nanoplastics of lower dimension below 100 nm, another important aspect is the formation of the protein-corona. This is a kind of process at a finer level, which involves the interaction of nanoscale polymeric particles with proteins that characterize biological fluids (serum, haemolymph, coelomic fluid) whereby the surface of the nanoparticles (NPs) adsorbs the surrounding proteins on its surface creating the bridge at the bio-nano interface (Corsi et al., 2020). As fitting frame, MPs surface represents a new pelagic substrate rapidly colonized by different microorganisms such as bacteria, fungi, diatoms and algae including potential fish and human pathogens which together form the so-called "Plastisphere" (Zettler et al., 2013). The effect of biofouling/coverage surface together with the contribution of marine snow aggregates promote significant variations in density with consequent vertical transport of MPs/ nanoplastics towards the seafloor (Porter et al., 2018; Kvale et al., 2020). In fact, there is a conspicuous disparity between the quantities of plastic potentially introduced and that actually found on the surface, generally referred to as the "missing 99%" surface plastic (Còzar et al., 2015; Kooi et al., 2017; Choy et al., 2019). This suggests that all these transformations over the time, that allow the MPs/nanoplastics transfer up to the deep waters and sediments, play a fundamental role in their fate (Figure 1). Resuspension patterns from the seafloor due to natural processes or to the contribution of bioturbators cannot be excluded but are currently poorly understood (Bulleri et al., 2021).
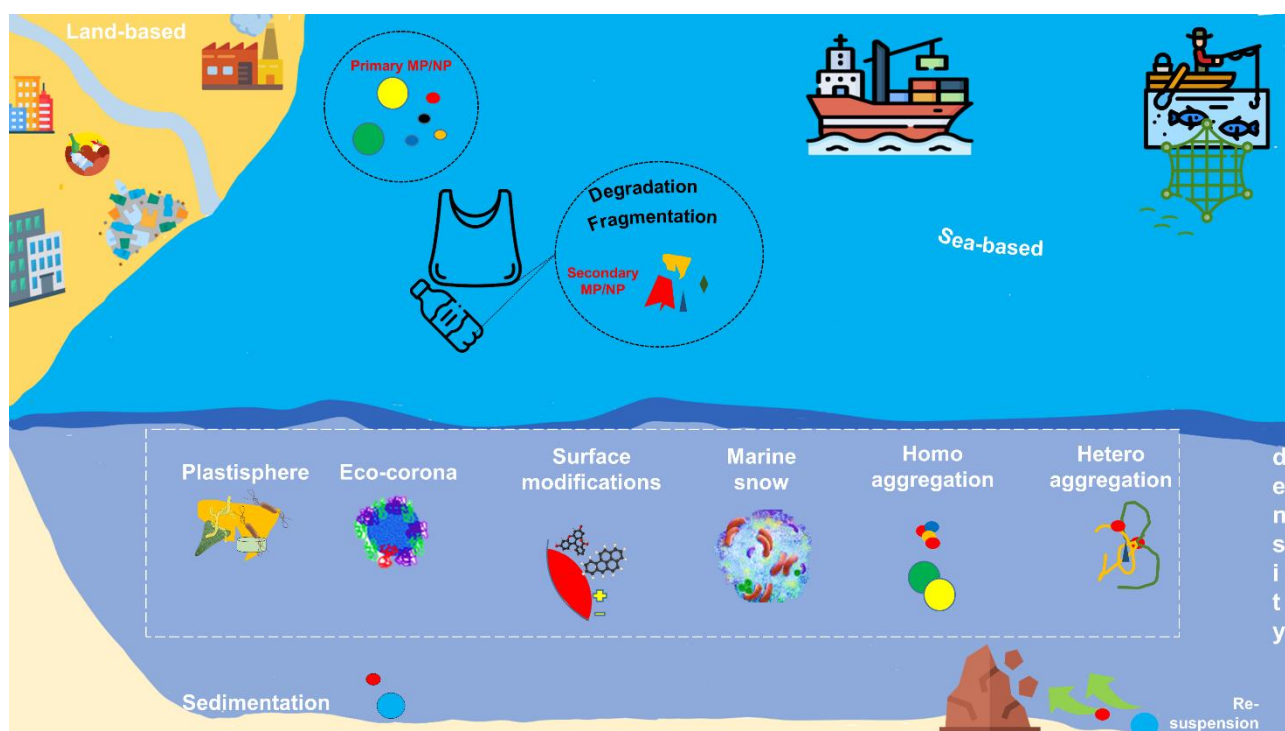
Figure 1. Conceptualization of the MPs/nanoplastics dynamic transformations in the marine environment.

How microplastics and nanoplastics affects marine biota

A growing concern worldwide is related to the MPs/nanoplastics interactions with marine organisms that can occur at the cellular/molecular level up to the community/ecosystem level. Generally, the downsizing of any type of particle involves an increase in the surface area with a consequent increase in chemical, physical and biological reactivity (da Costa et al., 2016). This concept supports the notion that at the nanoscale level the characteristics of particles will differ substantially from macro and micro-sized ones also in terms of the hazardous effects/biological interaction according to the NM paradigm (Klaine et al., 2012). The ingestion of MPs by biota and eventual accumulation in the food chain is well documented from zooplankton to fish and large mammals (Fossi et al., 2012; Romeo et al., 2015; Bellas et al., 2016; Güven et al., 2017; Compa et al., 2018; Digka et al., 2018; Duncan et al., 2018; Phuong et al., 2018; Giani et al., 2019; Lefebvre et al., 2019). Different physical effects are reported following the ingestion of varying size particles (20 nm to 1 mm) that affect feeding performance and food intake, tissue damage, mortality (Chen et al., 2011; Chua et al., 2014; Paul-Pont et al., 2016; Pedà et al., 2016; Sussarellu et al., 2016). Translocation events of MPs/nanoplastics across biological membranes were demonstrated in laboratory studies for particles less than 10 μm (Browne et al., 2008; Magni et al., 2018). However, the harmful effects not only depend on physical impairments but also on chemical aspects due to the polymeric nature and the leaching of plastic additives and adsorbed pollutants on their surfaces (Wang et al., 2019; Chen et al., 2021). Available literature underlines that both MP/nanoplastics can cause cytotoxicity (e.g. especially nanoplastics

9

<100 nm nominal size), developmental toxicity, neurotoxicity, and immunotoxicity as well as genotoxicity (Marques-Santos et al., 2018; Tallec et al., 2018; Begami et al., 2019; Cole et al., 2020; Eliso et al., 2020) (Figure 2). Beyond these aspects, the lethal and sub-lethal effects reported in various marine organisms, belonging to different trophic levels, seem to indicate that oxidative stress and the activated pathways, including inflammatory responses, could represent key events in MPs/nanoplastics toxicity (Hu & Palic, 2020).
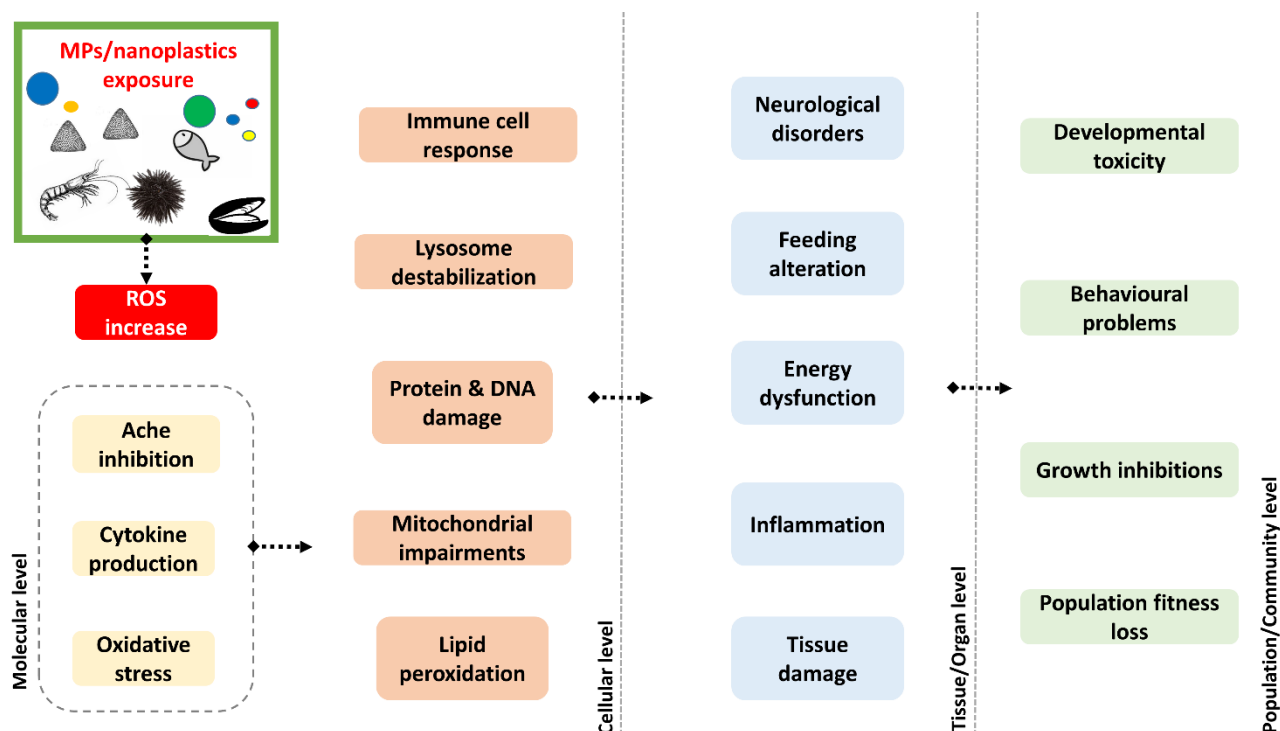
Figure 2. Summary of MPs/nanoplastics-induced effects in aquatic organisms at the cellular/molecular level up to the community/ecosystem level. The adverse effects are summarized with emphasis on the oxidative stress subsequent to the increase of reactive oxygen species, the key event in MPs / nanoplastics toxicity (modified from Hu & Pralic, 2020).

1.2. Mediterranean Sea: the case in point of plastic pollution

With its 46.000 km of densely populated and urbanized coastlines, the Mediterranean Sea has always been identified as one of the most polluted areas in the world (Danovaro, 2003; Deudero & Alomar, 2015). Showing a semi-enclosed geographical configuration with limited outlet flow in the Atlantic Ocean, it has become over the years the sixth gyre with accumulation of plastics comparable to that found in the inner Subtropical Gyres (Còzar et al., 2015; Suaria et al., 2016; Macias et al., 2019; Everaert et al., 2020) (Figure 3). The Mediterranean area hosts a large number of important freshwater rivers (such as Po, Nile, Ebro, Adige) that discharges into the sea contributing for almost half (40%) of the mean annual water discharge into the sea of plastic waste (Guerranti et al., 2020; Schmid et al., 2021). Precisely, recent estimates have identified the presence of approximately 3.2×10^{12}-28.2×10^{12} small plastic particles floating on the sea surface of the Mediterranean Sea (van

Sebille et al., 2015; Suaria et al., 2016). The existing data on MPs highlighted geographical differences between Mediterranean sub-basins (Cincinelli et al., 2019).
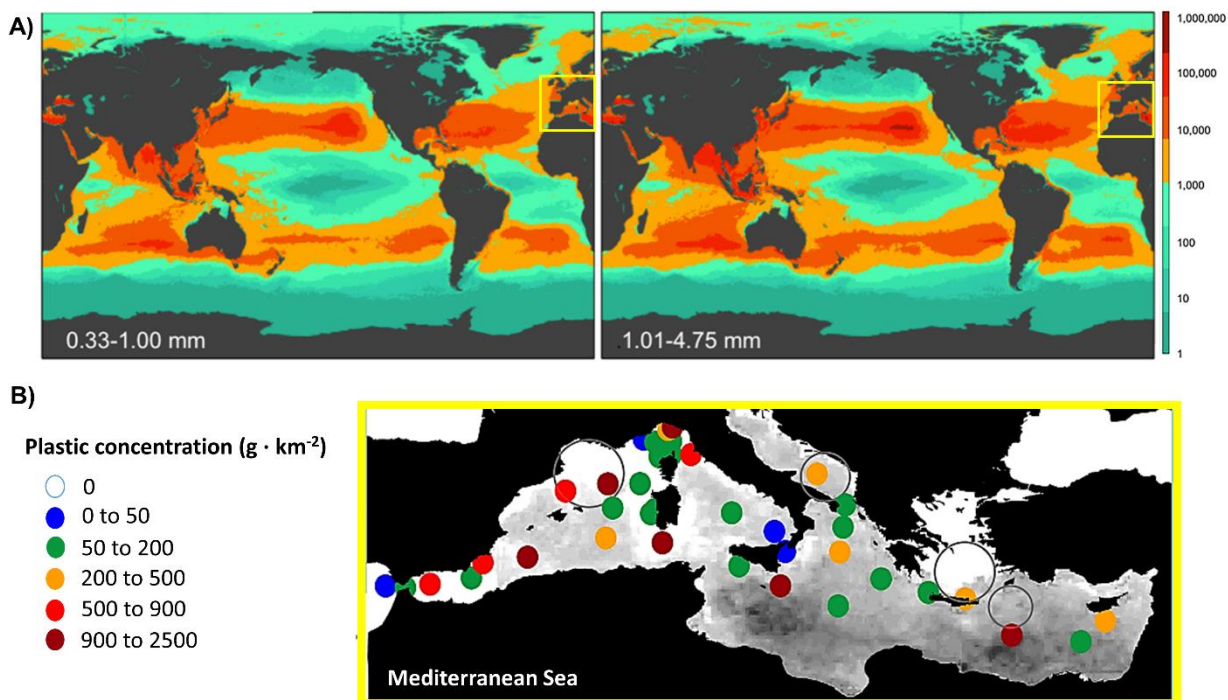
Figure 3. Plastic pollution in the Mediterranean Sea. (A) World map for global count density (MPs km^{-2}, legend on the right) from the model results in two size classes (0.33–1.00 mm, 1.01–4.75 mm). In the yellow box is highlighted the Mediterranean Sea. Image modified from Eriksen et al., 2015. (B) Concentrations of plastic debris in surface waters in Mediterranean Sea. Coloured circles indicate mass concentrations (legend on the left). Image modified from Còzar et al., 2015.

The presence of nanoplastics in Mediterranean Sea still remains unknown even if a first study from Schirinzi et al. (2019) reported for the first time the presence of nano-sized PS (1.08 -136.7 ng L^{-1}) in estuarine and surface waters of the West Mediterranean Sea. The predominant plastic type collected in surface waters includes fragments, films, beads, fishing thread and MFs, ubiquitous shape of emerging concern (Còzar et al., 2015; Suaria et al., 2020). Regarding polymer type, polyethylene (PE), (PS), polypropylene (PP), polyamides (PA) are the most abundant (Suaria et al., 2016; Baini et al., 2018). The management criticalities of plastic waste mainly reside for land-based sources. In fact, half of the annual plastic input originates from various sources (deriving from domestic, industrial, business, and touristic activities), while 30% comes from river channels and 20% is from the sea, mainly cruise liners and fishing activities (WWF 2018; Cincinelli et al., 2019). In turn, plastic loading from rivers depends on the massive production of plastic waste that is quickly dumped into landfills and across rivers, stormwater and runoffs ending then to the sea (Sharma et al., 2021). In populated coasts where the input of plastics can reach very high levels, model-based studies evidenced that species with smaller home ranges are more likely to be exposed to plastic compared

to species with larger home ranges. Moreover, concerning the habitat type, demersal species (benthic and benthopelagic) are at a higher risk of ingesting marine plastics than pelagic ones (Compa et al., 2019). Indeed, in the benthic environment of coastal areas, the concentrations of MPs are much higher than in the rest of the basin due to the close proximity to the potential sources (Navarro et al., 2021). As a matter of fact, sediments are suggested to be long term- sinks for MPs (Cózar et al., 2014, Fries et al., 2014; Nuelle et al., 2014; Courtene-Jones et al., 2017). In Mediterranean coastal sediments, MPs show a heterogeneous distribution, with abundances between 480 ± 9 and 2052 ± 746 MPs kg^{-1} of sediment (Alomar et al., 2016; Abidli et al., 2018; Simon-Sánchez et al., 2019) with the Eastern area more contaminated than the Western one (Lots et al., 2018) (Figure 4).
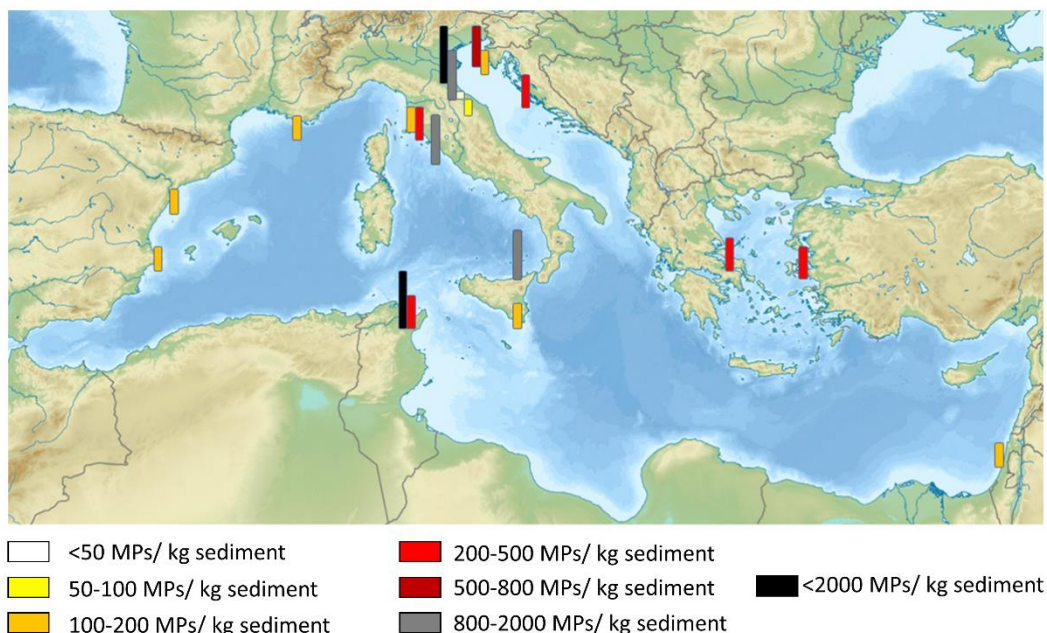
Figure 4. Mediterranean map summarizing the maximum concentrations (MPs/kg sediment) reported for marine sediments (lagoon and canal, beach, coastlines, shorelines) (modified from Martellini et al., 2018).

Given the extraordinary richness of the Mediterranean Sea as a biodiversity hotspot, such levels of plastic highlight the potential risk for marine species up to marine coastal areas and benthic environments. However, in spite of the growing concern about MPs/nanoplastics pollution, the interactions and the effects on the benthic organisms that populate the coasts of the Mediterranean Sea are overlooked. However, the most employed benthic organisms in laboratory studies of the last three years are mostly molluscs such as mussels and oysters (Brandts et al., 2018; Tallec et al., 2018; Rist et al., 2019; Sendra et al., 2020; Cole et al., 2020; Capolupo et al., 2021). Instead, field studies in the Mediterranean area mainly concern pelagic and demersal species such as fish and large mammals (reviewed by Fossi et al., 2018).

Benthic species play a fundamental role in sediment bioturbation and in the dynamic supply of energy, mass, and nutrient from detritus to higher trophic levels (Purcell, 2019). Climate change, overfishing and human activities have been shown to have severe consequences on benthic species and consequently on ecosystem health, especially in coastal zones (Griffiths et al., 2017). For these reasons, further knowledge of how MPs/ nanoplastics interact with these species is needed to shed light on ecological risks and to improve our actions to mitigate their effect preserving ecosystem functioning.

1.3 Sea urchin *Paracentrotus lividus*

The deuterostome invertebrate sea urchin *Paracentrotus lividus* (Lamark, 1816) is a shallow subtidal species belonging to Echinodermata phylum in the class of Echinoidea. Sea urchins are mainly distributed throughout the Mediterranean Sea and in the North-eastern Atlantic and in areas where water temperatures range in winter from 10°C to 15°C and in summer from 18°C to 25°C (Boudouresque & Verlaque, 2020). They are herbivorous inhabitants of seagrass meadows *Posidonia oceanica*, kelp beds and other assemblages of macroalgae and intertidal rock pools. Like other echinoderms, sea urchins are broadcast-spawners and development starts through a dispersal-stage planktonic larva (*pluteus*), which exhibits bilateral symmetry and swims and feeds through the activities of surface cilia and the ciliary band. Metamorphosis occurs when the larva descends to the benthos and everts the adult rudiment into a juvenile with a pentameric radial symmetry. In Mediterranean benthic communities they play a key role in the general functioning of ecosystems controlling the abundance and distribution of multicellular photosynthetic organisms and also as scavengers of decaying matter on the seafloor (Sala et al., 1998; Yorke et al., 2019). Between the algae forests and the sea urchins grazing activity there is a surprising succession of equilibrium states that alternate between copious algae forests and "barren habitat' " of relatively depleted sea urchins (Bulleri et al., 1999). In addition to their ecological relevance, the sea urchin *P. lividus* is known worldwide as seafood for its gonads (both male and female), generally referred to as "roe" in the fishery and sushi market, and this makes them the most exploited in the Mediterranean and Atlantic Europe. In particular, France is the second largest consumer of sea urchin roe in the world (100 tons of sea urchin per year) only after Japan. In Italy, even if there is a heterogeneous utilization in the southern regions, especially in the Sardinia island, the consumption of *P. lividus* has a significant social-economic impact with an annual pro-capita value of about 1.1 kg (about four times the Japanese consumption) (Carboni et al., 2012; Furesi et al., 2014). Human impact has compromised the abundance of *P. lividus* in different ways: not only declining wild stocks by reducing its abundance through harvesting (Addis et al., 2015) but also contributing to the collapse of *P. lividus* populations by altering the physical environment through direct and indirect introduction of

contaminants (Yeruham et al., 2015). In order to guarantee market demands and the protection of wild specimens, and promote the restoration of local populations, the interest in the aquaculture technologies for sea urchins increased over the years improving rearing methods, natural and artificial diets, and the selection and improvement of strains (Yokota et al., 2002). However, to date, the key challenges are to obtain an optimal gonadal state in terms of biomass and organoleptic properties through a highly nutritional and cost-effective diet (Grosso et al., 2021).

Anatomy

P. lividus is a regular sea urchin that shows a peculiar rounded and spiny skeletal structure with highly variable colour: black-purple, purple, red-brown, dark brown, yellow-brown, light brown or olive green (Boudouresque & Verlaque, 2020). Originating from spines, the pedicellariae are another type of appendage that covers the body of the sea urchins with various functions including cleaning processes and physical defence against parasites and predators (Coppard et al., 2012). The pentameric radial structure is characterized by five sectors called ambulacrum plates containing a row of tube feet which alternate with regions without it called inter-ambulacrum. The tube feet are the final part of the water vascular system (WSV), the distinctive feature of echinoderms and in particular of sea urchin. Indeed, the WSV confers to the sea urchin's unique properties as a semi-autonomous hydraulic system which is used for adhesion, locomotion, feeding and respiration. The sea water enters through a calcareous opening called madreporite, from which a series of channels start: first the stone canal, then the ring canal until it ends at the ampullae, cell-bulb like structures at the base of the tube feet. The contraction of the ampullae results in an increasing hydraulic pressure that protrudes the tube feet, provided that the valve is closed. The tube feet seem to be also involved in light sensitivity due to the presence of five ossicles in the terminal discs that act as photoreceptors (Lesser et al., 2011; Ullrich-Luter et al., 2011). At the lateral edge of the stone canal, there is the axial organ, a small sack conformation by as yet unknown functions. Recent evidence highlighted the axial organ as a site of coelomocyte proliferation and a centre for cellular removal and recycling (Golconda et al., 2019). In the oral side of the animal, there is the mouth, commonly known as Aristotle's Lantern. This particular structure consisting of penta-symmetric conical shape is a complex of interconnected plates (pyramids) that allow protraction and retraction of the teeth. Unlike other echinoderms, the digestive tract seems not to begin with the pharynx but with esophagus, which runs back down the outside of the lantern continuing with siphon and stomach running parallel to the gut at the beginning of the intestine (Holland, 2020). This latter ends with the rectum from which the faeces are then expelled through the anus which opens at periproct area. On this opposite aboral side around the madreporite, other plates are arranged in each of which there is a gonopore, that is the cavity through which the gametes (male and female) are spitted out during spawning. The gonads of the sea urchin

are five and disposed radially in the coelomic cavity along ambulacrum plates, each of which is characterized by a gonoduct that carries the gametes up to the gonopore (Figure 5). Although the sea urchins are not cephalized, they show a hardly organized nervous systems composed of 5 segmented radial nerves forming a nerval ring and appendages that appear to have an independent sensory–interneuron–motor system (Cobb et al., 1988; Burke et al., 2006).
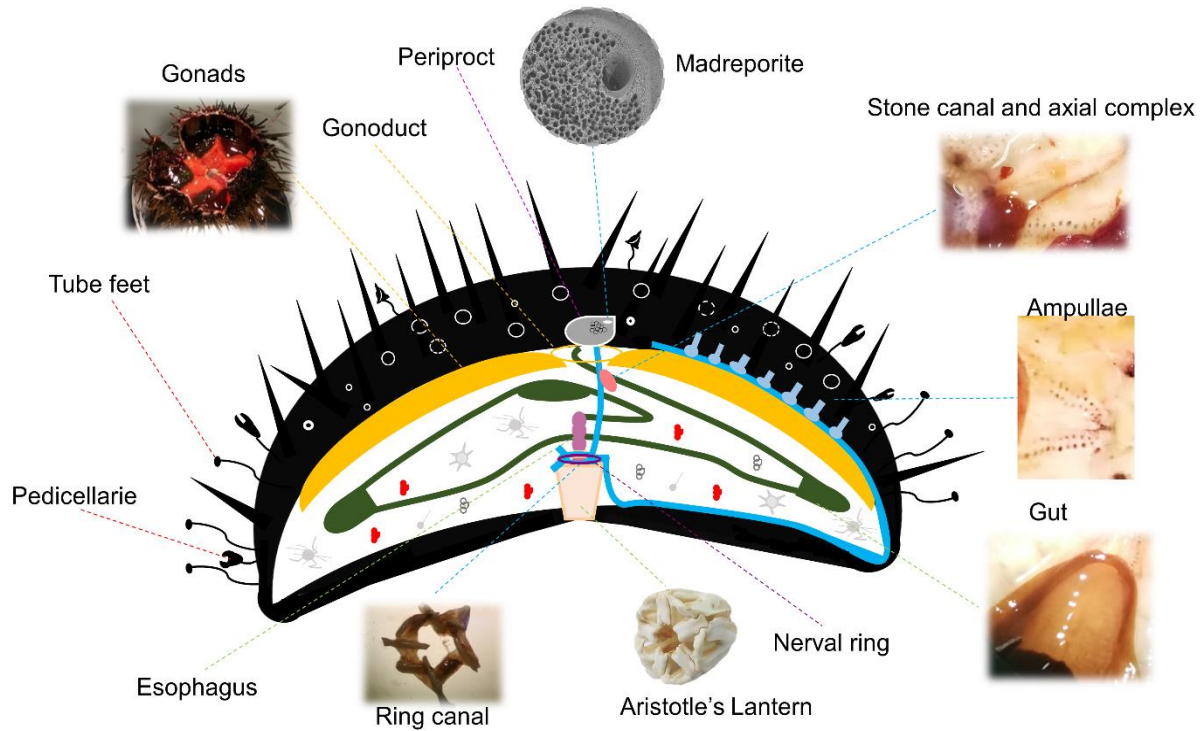
Figure 5. Schematic illustration of sea urchin anatomy.

Immune system

Sea urchins exhibit a peculiar immune system whose functions are very similar to the non-adaptive system or the innate system of vertebrates and can be considered the baseline of the original deuterostome ancestor (Smith & Davidson, 1992; Pancer et al., 1999). Like any other innate immunity system, the one of sea urchin is a very complex network based on cellular and humoral factors which together act to counteract pathogens, foreign substances and other kinds of environmental challenges (Smith et al., 2010). The humoral defence consists of various soluble factors such as lectins, opsonins, hemagglutinins, hemolysins, cytokines as well as molecules with antimicrobial properties (Chiaramonte & Russo, 2015). In the coelomic cavity, the immune cells of the sea urchin, named as coelomocytes, circulating freely in the coelomic fluid also reaching tissues and organs, control the cellular response (Buckley & Rast, 2019). Generally, these are classified simply on the basis of morphological characteristics distinguishing as follows: phagocytes, red and white amoebocytes and vibratile cells (Figure 6).
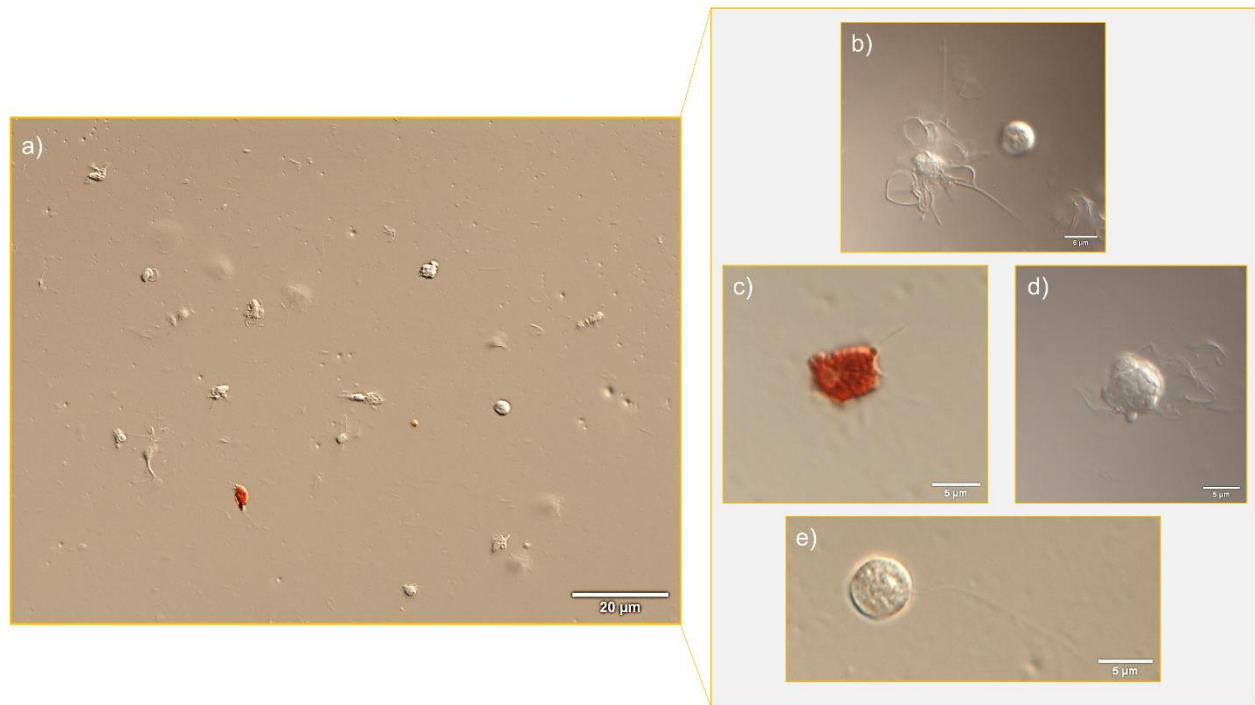
Figure 6. Immune cells of *Paracentrotus lividus* under optical microscope diluted 1:2 with anticoagulant (a). Scale bar: 20 µm. (b) phagocytes; (c) red amoebocytes;(d) white/colourless amoebocytes; (e) vibratile cells. Scale bar: 5 µm.

Being the main effector of the sea urchin immune system, phagocytes represent the most abundant morphological type (about 80%). Specifically, they are involved in the main functions of cellular response such as phagocytosis, encapsulation and rejection of foreign materials and cytolytic and cytotoxic activities. In detail, there are two different morphotypes of phagocytes that are involved in two main different pathways: petaloid phagocytes widely implicated in phagocytosis and in migration toward the sites of injury and filopodial phagocytes which are involved in clotting formation (Pinsino & Matranga, 2015). As a matter of fact, osmotic changes, differences in calcium concentration and coelomocytes handling could result in transformation of large petaloid phagocytes to a filopodial morphology (Smith et al., 2019). The vibratile cells of sea urchins constitute about 7.5 % of the total cell population (Matranga et al., 2006). Thanks to a long flagellum, they are able to move in a helicoidally pattern and for this reason they are thought to be involved in cellular homeostasis. Although their function is still poorly understood, they seem to be involved in the release of clotting proteins following degranulation of their body (Smith et al., 2016). Red and white amoebocytes compose 13% of the total cell population. The amoebocytes, so called for their fast change of shape, regulate the first phase of pathogen immobilization. They are also referred as "spherule cells" since they show a granulated body while white spherule granules differ in the electron density from the red ones, probably are the same cell type in different cell division stage (Branco et al., 2014; Deveci et al., 2015). The distinctive red colour of amoebocytes is due to the presence of cytoplasmic granules

containing 1,4-napthoquinone pigment known as Echinochrome A, a substance with high bactericidal activity due to their iron-chelating properties, that might play a role in innate immune defence (Smith et al., 2006). Specifically, red spherules are able to respond to pathogen associated patterns (such as PAMP and LPS) by undergoing exocytosis through a mechanism most likely involving Ca^{2+} influx (Coates et al., 2017). Interestingly, the ratio between red and white amoebocytes is widely recognized as the healthy status index of sea urchins (Matranga et al., 2005; Pinsino et al., 2008). Indeed, an increased incidence of red cells is related to wound healing, the loss of spine and defense against bacterial or fungal infections (Arizza et al., 2007; Branco et al., 2014). In recent years, sea urchin's immune cells generated great interest as a prominent biosensor for environmental monitoring not only for their features but also for the sea urchin's strategic phylogenetic position. Indeed, thanks to the availability of the full sea urchin genome sequence (Sea Urchin Genome Sequencing Consortium, 2006), an extraordinary and also unexpected relationship to humans was disclosed. In particular, these strong similarities between sea urchin and humans mainly involve the immune system in terms of alternative adaptive and anticipatory immune functions (Hibino et al., 2006; Rast et al., 2006).

Being recognized as sensitive tools for investigating sea urchin health status, coelomocytes have been used for studying environmental status, such as ocean acidification, marine pollution including emerging contaminants as NPs (Falugi et al., 2012; Pinsino et al., 2015; Marques-Santos et al., 2018; Migliaccio et al., 2019; Alijagic et al., 2020; Milito et al., 2020). Despite the growing interest in MPs/ nanoplastics pollution and the ecological relevance of the sea urchin as well as its high commercial value, no studies have been performed on sea urchin adults and very few papers appeared in literature on the effect on sea urchin immune cells and embryo's development (Della Torre et al., 2014; Pinsino et al., 2017; Marques-Santos et al., 2018; Messinetti et al., 2018). These studies highlight that both nanoplastics and MPs are able to strongly interfere with the sea urchin embryos development in terms of accumulation and modulating protein/gene profile (Della Torre et al., 2014; Pinsino et al., 2017) as well as of immune cell function (Marques-Santos et al., 2018; Messinetti et al., 2018). Moreover, the percentage of papers documenting the ingestion of plastic debris from 1988 to August 2019 in the Mediterranean Sea concerns only 3% of Echinodermata, among which only sea cucumber has been explored (Alomar et al., 2016; Anastasopoulou & Fortibuoni, 2019). Representing a native sensitive species, the sea urchin *P. lividus* might be expected to be gradually damaged by extreme anthropogenic pressures related to temperature rise, ocean acidification, predator hyper-abundance, toxic algae bloom and pollution (Yeruham et al., 2015). Therefore, all these observations suggest the clear requirement of in-depth investigations on the interactions between MPs/nanoplastics and benthic species such as the sea urchin, especially in relation to its key role in the structure of benthic communities and in the balance of ecosystem dynamics.

Objectives of the PhD thesis

Up to now, there are still several scientific issues to be addressed in understanding MP and nanoplastic toxicity for marine benthic species such as sea urchin. Translating this knowledge-gap on the biological impacts of both MPs/nanoplastics on one of the key species of the Mediterranean Sea, this PhD project aims to explore the impacts of MPs/nanoplastics on the sea urchin *P. lividus* by investigating mechanisms of uptake, biodisposition and clearance, toxicological outcomes in different organs and cells and concerning the nanosize fraction (<100 nm) the bio-nano interactions occurring at the base of the observed toxic effects.

The present thesis aimed to achieve the following objectives:

1. Assess the uptake and tissue distribution of MPs in adult specimens of *P. lividus* and their potential impact on immune cells according to their size
2. Evaluate how naturally occurring biofilm processes (plastisphere) could affect the toxicological responses of MPs in adult specimen of *P. lividus*
3. Investigate the occurrence of MPs in wild adult specimen of *P. lividus* caught in the Mediterranean regions
4. Evaluate the role of surface charges of polymeric NPs as PS NPs as proxy for nanoplastics in the observed toxicity towards *P. lividus* immune cells

The first step was to analyze the sea urchin's capabilities to internalize MPs, to establish if there was a size-dependent effect and if internalization could cause immunological alterations by exposing adults sea urchin to PS-MPs (10 and 45 μm, 10 MPs/ mL) for 72h (Chapter 1).

In Chapter 2 the hypothesis that biofilms naturally occurring on PS-MPs could affect uptake, biodistribution, organ, and immunological responses was tested. In this case, adult specimens of sea urchin were exposed to colonized-PS-MPs and virgin-PS-MPs (45 μm, 10 MPs mL^{-1}) and to only NSW (control) for 48h. After exposure, uptake of PS-MPs, egestion rate, digestive system stress status, and immune response were assessed. Furthermore, to get an overview of what happens in the marine environment, a preliminary study was conducted to evaluate the MPs occurrence in wild sea urchin specimens collected from the Gulf of Naples (Tyrrhenian Sea) (Chapter 3). In particular, four distinct points (Rocce Verdi, Capo Miseno, Ischia, Nisida) were selected for the sampling of the sea urchins, to evaluate the MPs content in gonads, coelomic fluid and digestive system.

Last but not least, Chapter 4 concerned the evaluation of the cellular-trafficking of negatively charged PS-NPs-COOH (0, 5, 25 μg mL^{-1}) and subsequent effects on immune cell functions (cell viability, lysosomal destabilization and phagocytic activity) after acute *in vitro* exposure (4h).

As a proxy to study MPs and bio-nano interactions, in this work PS MPs/nanoplastics were employed. In detail, as MPs we used fluorescent-labelled polystyrene microbeads (micro-PS) (441excitation/486 emission) of 10 - 45 µm while as NPs we used PS-NPs with positive (-NH$_2$) and negative surface charge (-COOH) of 50 and 60 nm, respectively. See Table 1 for furthers details.

Table 1. PS MPs/nanoplastics employed in this thesis. The information reported here were provided by the manufacturers and are also available at https://www.polysciences.com/default/catalog-products/microparticles-particles/fluorescent-microspheres (micro-PS 10 and 45 µm) and at https://www.bangslabs.com/products/polystyrene-microspheres/functionalized-polystyrene (PS-COOH and PS- NH$_2$).

	micro-PS	micro-PS	PS-NH$_2$	PS-COOH	PS-COOH
Catalog ID	18140-2	18242-2	PA02N	PC02N	FCDG001
Diameter (µm)	10	43.2	0.050	0.060	0.050
Density (g/cm^3)	1.03	1.03	1.05	1.06	1.06
Solid Content (%)	2.5	2.5	10	10.1	1
Number particles/mL	4.55 x 10^7	4.99x 10^5	1.46x 10^{15}	7.68x 10^{14}	1.46x 10^{14}
Suspension	milliQ only	milliQ only	milliQ only	MilliQ 0.1% SDS 0.05% NaN$_3$	MilliQ 2Mm NaN$_3$ 0.01%Tween20
Fluorescence	Yellow green (441, 486)	Yellow green (441, 486)	-	-	Dragon Green (480,520)

References

Abidli, S., Antunes, J.C., Ferreira, J.L., Lahbib, Y., Sobral, P., Trigui El Menif, N., 2018. Microplastics in sediments from the littoral zone of the north Tunisian coast (Mediterranean Sea). *Estuarine, Coastal and Shelf Science* 205, 1–9. https://doi.org/10.1016/j.ecss.2018.03.006

Addis, P., Moccia, D., Secci, M., 2015. Effect of two different habitats on spine and gonad colour in the purple sea urchin *Paracentrotus lividus*. *Marine Ecology* 36, 178–184. https://doi.org/10.1111/maec.12133

Alijagic, A., Gaglio, D., Napodano, E., Russo, R., Costa, C., Benada, O., Kofroňová, O., Pinsino, A., 2020. Titanium dioxide nanoparticles temporarily influence the sea urchin immunological state suppressing inflammatory-relate gene transcription and boosting antioxidant metabolic activity. *Journal of Hazardous Materials* 384, 121389. https://doi.org/10.1016/j.jhazmat.2019.121389

Alomar, C., Estarellas, F., Deudero, S., 2016. Microplastics in the Mediterranean Sea: Deposition in coastal shallow sediments, spatial variation and preferential grain size. *Marine Environmental Research* 115, 1–10. https://doi.org/10.1016/j.marenvres.2016.01.005

Al-Thawadi, S., 2020. Microplastics and Nanoplastics in Aquatic Environments: Challenges and Threats to Aquatic Organisms. *Arabian Journal for Science and Engineering* 45, 4419–4440. https://doi.org/10.1007/s13369-020-04402-z

Anastasopaulou, A., Fortiboni, T., 2019. Impact of Plastic Pollution on Marine Life in the Mediterranean Sea. *The Handbook of Environmental Chemistry*, 1-62. https://doi.org/10.1007/698_2019_421

Andrady, A.L., 2017. The plastic in microplastics: A review. *Marine Pollution Bulletin* 119, 12–22. https://doi.org/10.1016/j.marpolbul.2017.01.082

Andrady, A.L., Neal, M.A., 2009. Applications and societal benefits of plastics. *Philosophical Transactions of the Royal Society B: Biological Sciences* 364, 1977–1984. https://doi.org/10.1098/rstb.2008.0304

Arizza, V., Giaramita, F.T., Parrinello, D., Cammarata, M., Parrinello, N., 2007. Cell cooperation in coelomocyte cytotoxic activity of Paracentrotus lividus coelomocytes. *Comparative Biochemistry and Physiology Part A: Molecular & Integrative Physiology*, Issue includes papers from a presentation at a Memorial Symposium in honor of Dr. Peter Lutz held at Florida Atlantic University on September 23rd, 2005 147, 389–394. https://doi.org/10.1016/j.cbpa.2007.01.022

Baini, M., Fossi, M.C., Galli, M., Caliani, I., Campani, T., Finoia, M.G., Panti, C., 2018. Abundance and characterization of microplastics in the coastal waters of Tuscany (Italy): The application of the MSFD monitoring protocol in the Mediterranean Sea. *Marine Pollution Bulletin* 133, 543–552. https://doi.org/10.1016/j.marpolbul.2018.06.016

Barboza, L.G.A., Cózar, A., Gimenez, B.C.G., Barros, T.L., Kershaw, P.J., Guilhermino, L., 2019. Chapter 17 - Macroplastics Pollution in the Marine Environment, in: Sheppard, C. (Ed.), World Seas: An Environmental Evaluation (Second Edition). *Academic Press*, 305–328. https://doi.org/10.1016/B978-0-12-805052-1.00019-X

Bellas, J., Martìnez-Armental, J., Martìnez-Camàra, A., Besada, V., Martìnez-Gòmez, C., 2016. Ingestion of microplastics by demersal fish from the Spanish Atlantic and Mediterranean coasts. *Marine Pollution Bulletin* 109 (1), 55-60. https://doi.org/10.1016/j.marpolbul.2016.06.026

Bergami, E., Krupinski Emerenciano, A., González-Aravena, M., Cárdenas, C.A., Hernández, P., Silva, J.R.M.C., Corsi, I., 2019. Polystyrene nanoparticles affect the innate immune system of the Antarctic sea urchin *Sterechinus neumayeri*. *Polar Biology* 42, 743–757. https://10.1007/s00300-019-02468-6

Besseling, E., Redondo-Hasselerharm, P., Foekema, E., Koelmans, A.A., 2018. Quantifying ecological risks of aquatic micro- and nanoplastic. *Critical Reviews in Environmental Science and Technology,* 1547-6537. https://doi.org/10.1080/10643389.2018.1531688

Boudouresque, C.F., Verlaque, M., 2020. *Paracentrotus lividus*, in: Developments in Aquaculture and Fisheries Science. *Elsevier,* 447–485. https://doi.org/10.1016/B978-0-12-819570-3.00026-3

Branco, P., Figueiredo, D., 2014. New insights into innate immune system of sea urchin: coelomocytes as biosensors for environmental stress. *OA Biology* 18, 2(1), 2.

Brandts, I., Teles, M., Gonçalves, A.P., Barreto, A., Franco-Martinez, L., Tvarijonaviciute, A., Martins, M.A., Soares, A.M.V.M., Tort, L., Oliveira, M., 2018. Effects of nanoplastics on *Mytilus galloprovincialis* after individual and combined exposure with carbamazepine. *Science of The Total Environment* 643, 775–784. https://doi.org/10.1016/j.scitotenv.2018.06.257

Browne, M.A., Dissanayake, A., Galloway, T.S., Lowe, D.M., Thompson, R.C., 2008. Ingested Microscopic Plastic Translocates to the Circulatory System of the Mussel, *Mytilus edulis* (L.). *Environmental Science & Technology 42*, 5026–5031. https://doi.org/10.1021/es800249a

Buckley, K.M., Rast, J.P., 2019. Immune activity at the gut epithelium in the larval sea urchin. *Cell Tissue Research* 377, 469–474. https://doi.org/10.1007/s00441-019-03095-7

Bulleri, F., Benedetti-Cecchi, L., Cinelli, F., 1999. Grazing by the sea urchins *Arbacia lixula* L. and *Paracentrotus lividus* Lam. in the Northwest Mediterranean. *Journal of Experimental Marine Biology and Ecology* 241, 81–95. https://doi.org/10.1016/S0022-0981(99)00073-8

Bulleri, F., Ravaglioli, C., Anselmi, S., Renzi, M., 2021. The sea cucumber *Holothuria tubulosa* does not reduce the size of microplastics but enhances their resuspension in the water column. *Science of the Total Environment* 248, 146650. https://doi.org/10.1016/j.scitotenv.2021.146650

Burke, R.D., Angerer, L.M., Elphick, M.R., Humphrey, G.W., Yaguchi, S., Kiyama, T., Liang, S., Mu, X., Agca, C., Klein, W.H., Brandhorst, B.P., Rowe, M., Wilson, K., Churcher, A.M., Taylor, J.S., Chen, N., Murray, G., Wang, D., Mellott, D., Olinski, R., Hallböök, F., Thorndyke, M.C., 2006. A genomic view of the sea urchin nervous system. *Developmental Biology, Sea Urchin Genome: Implications and Insights* 300, 434–460. https://doi.org/10.1016/j.ydbio.2006.08.007

Canesi, L., Corsi, I., 2016. Effects of nanomaterials on marine invertebrates. *Science of The Total Environment* 565, 933-940. https://doi.org/10.1016/j.scitotenv.2016.01.085

Capolupo, M., Gunaalan, K., Booth, A.M., Sørensen, L., Valbonesi, P., Fabbri, E., 2021. The sub-lethal impact of plastic and tire rubber leachates on the Mediterranean mussel *Mytilus galloprovincialis*. *Environmental Pollution* 283, 117081. https://doi.org/10.1016/j.envpol.2021.117081

Carboni, S., Vignier, J., Chiantore, M., Tocher, D.R., Migaud, H., 2012. Effects of dietary microalgae on growth, survival and fatty acid composition of sea urchin *Paracentrotus lividus* throughout larval development. *Aquaculture* 324–325, 250–258. https://doi.org/10.1016/j.aquaculture.2011.10.037

Carpenter, E.J., Anderson S.J., Harvey, G.R., Miklas, H.P., Peck, B.B., 1972. Polystyrene Spherules in Coastal Waters. *Science* 178 (4062), 749-750. https://10.1126/science.178.4062.749

Chiaramonte, M., Russo, R., 2015. The echinoderm innate humoral immune response. *Italian Journal of Zoology* 82, 300–308. https://doi.org/10.1080/11250003.2015.1061615

Chen, X., Gu, X., Bao, L., Ma, S., Mu, Y., 2021. Comparison of adsorption and desorption of triclosan between microplastics and soil particles. *Chemosphere* 263, 127947. https://doi.org/10.1016/j.chemosphere.2020.127947

Choy, C.A., Robison, B.H., Gagne, T.O., Erwin, B., Firl, E., Halden, R.U., Hamilton, J.A, Katja, K., Lisin, S.E., Rolsky, C., von Houtan, K.S., 2019. The vertical distribution and biological transport of marine microplastics across the epipelagic and mesopelagic water column. *Scientific Report* 9, 7843. https://doi.org/10.1038/s41598-019-44117-2

Chua, E.M., Shimeta, J., Nugegoda, D., Morrison, P.D., Clarke, B.O., 2014. Assimilation of Polybrominated Diphenyl Ethers from Microplastics by the Marine Amphipod, *Allorchestes Compressa*. *Environmental Science & Technology* 48, 14, 8127–8134. https://doi.org/10.1021/es405717z

Cincinelli, A., Martellini, T., Guerranti, C., Scopetani, C., Chelazzi, D., Giarrizzo, T., 2019. A potpourri of microplastics in the sea surface and water column of the Mediterranean Sea. *TrAC Trends in Analytical Chemistry* 110, 321–326. https://doi.org/10.1016/j.trac.2018.10.026

Coates, C.J., McCulloch, C., Betts, J., Whalley, T., 2018. Echinochrome A Release by Red Spherule Cells Is an Iron-Withholding Strategy of Sea Urchin Innate Immunity. *JIN* 10, 119–130. https://doi.org/10.1159/000484722

Cobb, J.L.S., 1988. Neurohumors and neurosecretion in echinoderms: A review. *Comparative Biochemistry and Physiology Part C: Comparative Pharmacology* 91, 151–158. https://doi.org/10.1016/0742-8413(88)90181-8

Cole, M., Liddle, C., Consolandi, G., Drago, C., Hird, C., Lindeque, P.K., Galloway, T.S., 2020. Microplastics, microfibres and nanoplastics cause variable sub-lethal responses in mussels (*Mytilus* spp.). *Marine Pollution Bulletin* 160, 111552. https://doi.org/10.1016/j.marpolbul.2020.111552

Compa, M., Alomar, C., Wilcox, C., van Sebille, E., Lebreton, L., Hardesty, B.D., Deudero, S., 2019. Risk assessment of plastic pollution on marine diversity in the Mediterranean Sea. *Science of The Total Environment* 678, 188-196. https://doi.org/10.1016/j.scitotenv.2019.04.355

Compa, M., Ventero, A., Iglesias, M., Deudero, S., 2018. Ingestion of microplastics and natural fibres in *Sardina pilchardus* (Walbaum, 1972) and *Engraulis encrascicolus* (Linnaeus, 1758). *Marine Pollution Bulletin* 128, 89-96. https://doi.org/10.1016/j.marpolbul.2018.01.009

Coppard, S.E., Kroh, A., Smith, A.B., 2012. The evolution of pedicellariae in echinoids: an arms race against pests and parasites. *Acta Zoologica* 93, 125–148. https://doi.org/10.1111/j.1463-6395.2010.00487.x

Corsi, I., Bergami, E., Grassi, G., 2020. Behaviour and bio-interactions of anthropogenic particles in marine environment for a more realistic ecological risk assessment. *Frontiers in Enviromental Science* 8. https://doi.org/10.3389/fenvs.2020.00060

Courtene-Jones, W., Quinn, B., Gary, S.F., Mogg, A.O.M., Narayanaswamy, B.E., 2017. Microplastic pollution identified in deep-sea water and ingested by benthic invertebrates in the Rockall Trough, North Atlantic Ocean. *Environmental Pollution* 231, 271–280. https://doi.org/10.1016/j.envpol.2017.08.026

Cózar, A., Echevarria, F., Gonzalez-Gordillo, J.I., Irigoien, X., Ubeda, B., Hernandez-Leon, S., Palma, A.T., Navarro, S., Garcia-de-Lomas, J., Ruiz, A., Fernandez-de-Puelles, M.L., Duarte, C.M., 2014. Plastic debris in the open ocean. *Proceedings of the National Academy of Sciences* 111, 10239–10244. https://doi.org/10.1073/pnas.1314705111

Cózar, A., Sanz-Martín, M., Martí, E., González-Gordillo, J.I., Ubeda, B., Gálvez, J.Á., Irigoien, X., Duarte, C.M., 2015. Plastic Accumulation in the Mediterranean Sea. *PLOS ONE* 10, e0121762. https://doi.org/10.1371/journal.pone.0121762

da Costa, J.P., Santos, P.S.M., Duarte, A.C., Rocha-Santos, T., 2016. (Nano)plastics in the environment – Sources, fates and effects. *Science of The Total Environment* 566–567, 15–26. https://doi.org/10.1016/j.scitotenv.2016.05.041

Danovaro, R., 2003. Pollution threats in the Mediterranean Sea: An overview. *Chemistry and Ecology* 19, 15–32. https://doi.org/10.1080/0275754031000081467

Della Torre, C., Bergami, E., Salvati, A., Faleri, C., Cirino, P., Dawson, K. A., Corsi, I., 2014. Accumulation and Embryotoxicity of Polystyrene Nanoparticles at Early Stage of Development of Sea Urchin Embryos *Paracentrotus lividus*. *Environmental Science & Technology* 48, 12302–12311. https://doi.org/10.1021/es502569w

Deudero, S., Alomar, C., 2015. Mediterranean marine biodiversity under threat: Reviewing influence of marine litter on species. *Marine Pollution Bulletin* 98, 58–68. https://doi.org/10.1016/j.marpolbul.2015.07.012

Deveci, R., Şener, E., İzzetoğlu, S., 2015. Morphological and ultrastructural characterization of sea urchin immune cells. *Journal of Morphology* 276, 583–588. https://doi.org/10.1002/jmor.20368

Digka, N., Tsangaris, C., Torre, M., Anastasopoulou, A., Zeri, C., 2018. Microplastics in mussels and fish from the Northern Ionian Sea. *Marine Pollution Bulletin* 135, 30-40. https://10.1016/j.marpolbul.2018.06.063

Duncan, E.M., Arrowsmith, J., Bain, C., Broderick, A.C., Lee, J., Metcalfe, K., Pikesley, S.K., Snape, R.T.E., van Sebille, E., Godley, B.J., 2018. The true depth of the Mediterranean plastic problem: extreme microplastic pollution on marine turtle nesting beaches in Cyprus. *Marine Pollution Bulletin* 136, 334-340. https://doi.org/10.1016/j.marpolbul.2018.09.019

Eliso, M.C., Bergami, E., Manfra, L., Spagnuolo, A., Corsi, I., 2020. Toxicity of Nanoplastics during the Embryogenesis of the Ascidian *Ciona robusta* (Phylum *Chordata*). *Nanotoxicology* 14, 1415–1431, https://10.1080/17435390.2020.1838650

Eriksen, M., Lebreton, L.C.M., Carson, H.S., Thiel, M., Moore, C.J., Jose C. Borerro, J.C., Galgani, F., Ryan, P.G., Reisser, J., 2014. Plastic Pollution in the World's Oceans: More than 5 Trillion Plastic Pieces Weighing over 250,000 Tons Afloat at Sea. *PLOS ONE* 9 (12), e111913. https://doi.org/10.1371/journal.pone.0111913

Everaert, G., De Rijcke, M., Lonneville, B., Janssen, C.R., Backhaus, T., Mees, J., van Sebille, E., Koelmans, A.A., Catarino, A.I., Vandegehuchte, M.B., 2020. Risks of floating microplastic in the global ocean. *Environmental Pollution* 267, 115499. https://doi.org/10.1016/j.envpol.2020.115499

Falugi, C., Aluigi, M.G., Chiantore, M.C., Privitera, D., Ramoino, P., Gatti, M.A., Fabrizi, A., Pinsino, A., Matranga, V., 2012. Toxicity of metal oxide nanoparticles in immune cells of the sea urchin. *Marine Environmental Research* 76, 114–121. https://doi.org/10.1016/j.marenvres.2011.10.003

Fossi, M.C., Panti, C., Guerranti, C., Coppola, D., Giannetti, M., Marsili, L., Minutoli, R., 2012. Are baleen whales exposed to the threat of microplastics? A case study of the Mediterranean fin whale (*Balaenoptera physalus*). *Marine Pollution Bulletin* 54 (11), 2374-2379. https://doi.org/10.1016/j.marpolbul.2012.08.013

Fossi, M.C., Pedà, C., Compa, M., Tsangaris, C., Alomar, C., Claro, F., Ioakeimidis, C., Galgani, F., Hema, T., Deudero, S., Romeo, T., Battaglia, P., Andaloro, F., Caliani, I., Casini, S., Panti, C., Baini, M., 2018. Bioindicators for monitoring marine litter ingestion and its impacts on Mediterranean biodiversity. *Environmental Pollution* 237, 1023-1040. https://doi.org/10.1016/j.envpol.2017.11.019

Fotopoulou, K.N., Karapanagioti, H.K., 2012. Surface properties of beached plastic pellets. *Marine Environmental Research* 81, 70–77. https://doi.org/10.1016/j.marenvres.2012.08.010

Fries, E., H. Dekiff, J., Willmeyer, J., Nuelle, M.-T., Ebert, M., Remy, D., 2013. Identification of polymer types and additives in marine microplastic particles using pyrolysis-GC/MS and scanning electron microscopy. *Environmental Science: Processes & Impacts* 15, 1949–1956. https://doi.org/10.1039/C3EM00214D

Furesi, R., Madau, F.A., Palomba, A., Pulina, P., 2014. Stated Preferences for Consumption of Sea Urchin: A Choice Experiment in Sardinia (Italy). *Internationa Journal Food System Dynamics* 5 (3), 111-119. https://10.22004/ag.econ.198961

Gago, J., Galgani, F., Maes, T., Thompson, C.R., 2016. Microplastics in Seawater: Recommendations from the Marine Strategy Framework Directive Implementation Process. *Frontiers in Marine Science* 3, 219. https://10.3389/fmars.2016.00219

Galgani, F., Hanke, G., Werner, S., De Vrees, L., 2013. Marine litter within the European Marine Strategy Framework Directive. *ICES Journal of Marine Science* 70, 1055–1064. https://doi.org/10.1093/icesjms/fst122

Gallo, F., Fossi, C., Weber, R., Santillo, D., Sousa, J., Ingram, I., Nadal, A., Romano, D., 2018. Marine litter plastics and microplastics and their toxic chemicals components: the need for urgent preventive measures. *Environmental Sciences Europe* 30, 13. https://doi.org/10.1186/s12302-018-0139-z

Galloway, T.S., Cole, M., Lewis, C., 2017. Interactions of microplastic debris throughout the marine ecosystem. *Nature Ecology & Evolution* 1, 0116. https://doi.org/10.1038/s41559-017-0116

Giani, D., Baini, M., Galli, M., Casini, S., Fossi, M.C., 2019. Microplastics occurrence in edible fish species (*Mullus barbatus* and *Merluccius merluccius*) collected in three different geographical sub-areas of the Mediterranean Sea. *Marine Pollution Bulletin* 140, 129–137. https://doi.org/10.1016/j.marpolbul.2019.01.005

Gigault, J., Halle, A. ter, Baudrimont, M., Pascal, P.Y., Gauffre, F., Phi, T.-L., El Hadri, H., Grassl, B., Reynaud, S., 2018. Current opinion: What is a nanoplastic?. *Environmental Pollution* 235, 1030–1034. https://doi.org/10.1016/j.envpol.2018.01.02

Gigault, J., Pedrono, B., Maxit, B., Halle, A.T., 2016. Marine plastic litter: the unanalyzed nano-fraction. *Environmental Science: Nano* 3, 346–350. https://doi.org/10.1039/C6EN00008H

Golconda, P., Buckley, K.M., Reynolds, C.R., Romanello, J.P., Smith, L.C., 2019. The Axial Organ and the Pharynx Are Sites of Hematopoiesis in the Sea Urchin. *Frontiers in Immunology* 10. https://doi.org/10.3389/fimmu.2019.00870

Griffiths, J.R., Kadin, M., Nascimento, F.J.A., Tamelander, T., Törnroos, A., Bonaglia, S., Bonsdorff, E., Brüchert, V., Gårdmark, A., Järnström, M., Kotta, J., Lindegren, M., Nordström, M.C., Norkko, A., Olsson, J., Weigel, B., Žydelis, R., Blenckner, T., Niiranen, S., Winder, M., 2017. The importance of benthic–pelagic coupling for marine ecosystem functioning in a changing world. *Global Change Biology* 23, 2179–2196. https://doi.org/10.1111/gcb.13642

Grosso, L., Rakaj, A., Fianchini, A., Morroni, L., Cataudella, S., Scardi, M., 2021. Integrated Multi-Trophic Aquaculture (IMTA) system combining the sea urchin *Paracentrotus lividus*, as primary species, and the sea cucumber *Holothuria tubulosa* as extractive species. *Aquaculture* 534, 736268. https://doi.org/10.1016/j.aquaculture.2020.736268

Guerranti, C., Perra, G., Martellini, T., Giari, L., Cincinelli, A., 2020. Knowledge about Microplastic in Mediterranean Tributary River Ecosystems: Lack of Data and Research Needs on Such a Crucial Marine Pollution Source. *Journal of Marine Science and Engineering* 8, 216. https://doi.org/10.3390/jmse8030216

Güven, O., Gökdağ, K., Jovanović, B., Kıdeyş, A.E., 2017. Microplastic litter composition of the Turkish territorial waters of the Mediterranean Sea, and its occurrence in the gastrointestinal tract of fish. *Environmental Pollution* 223, 286-294. https://doi.org/10.1016/j.envpol.2017.01.025

Hartmann, N.B., Hüffer, T., Thompson, R.C., Hassellöv, M., Verschoor, A., Daugaard, A.E., Rist, S., Karlsson, T., Brennholt, N., Cole, M., Herrling, M.P., Hess, M.C., Ivleva, N.P., Lusher, A.L., Wagner, M., 2019. Are We Speaking the Same Language? Recommendations for a Definition and Categorization Framework for Plastic Debris. *Environmental Science & Technology* 53, 1039–1047. https://doi.org/10.1021/acs.est.8b05297

Hibino, T., Loza-Coll, M., Messier, C., Majeske, A.J., Cohen, A.H., Terwilliger, D.P., Buckley, K.M., Brockton, V., Nair, S.V., Berney, K., Fugmann, S.D., Anderson, M.K., Pancer, Z., Cameron, R.A., Smith, L.C., Rast, J.P., 2006. The immune gene repertoire encoded in the purple sea urchin genome. *Developmental Biology, Sea Urchin Genome: Implications and Insights* 300, 349–365. https://doi.org/10.1016/j.ydbio.2006.08.065

Horton, A.A, Dixon, S.J., 2017. Microplastics: An introduction to environmental transport processes. *WIREs Water* 5, e1268. https://doi.org/10.1002/wat2.1268

Holland, N.D., 2020. Digestive system in regular sea urchins, in: Developments in Aquaculture and Fisheries Science. *Elsevier*, 147–163. https://doi.org/10.1016/B978-0-12-819570-3.00008-1

Hu, M., Palic, D., 2020. Micro- and nano-plastics activation of oxidative and inflammatory adverse outcome pathways. *Redox Biology* 37, 101620. https://doi.org/10.1016/j.redox.2020.101620

Jambeck, J.R., Geyer, R., Wilcox, C., Siegler, T.R., Perryman, M., Andrady, A., Narayan, R., Law, K.L., 2015. Plastic waste inputs from land into the ocean. *Science* 347, 768–771. https://doi.org/10.1126/science.1260352

Klaine, S.J., Koelmans, A.A., Horne, N., Carley, S., Handy, R.D., Kapustka, L., Nowack, B., von der Kammer, F., 2012. Paradigms to assess the environmental impact of manufactured nanomaterials. *Environmental Toxicology and Chemistry* 31, 3–14. https://doi.org/10.1002/etc.733

Koelmans, A.A., 2019. Proxies for nanoplastic. *Nature Nanotechnoogy* 14, 307–308. https://doi.org/10.1038/s41565-019-0416-z

Kihara, S., Ashenden, A., Kaur, M., Glasson, J., Ghosh, S., van der Heijden, N., Brooks, A.E.S., Mata, J.P., Holt, S., Domigan, L.J., Köper, I., McGillivray, D.J., 2021. Cellular interactions with polystyrene nanoplastics—The role of particle size and protein corona. *Biointerphases* 16, 041001. https://doi.org/10.1116/6.0001124

Koelmans, A.A., Besseling, E., Sim, J.W., 2015. Nanoplastics in the Aquatic Environment. Critical Review. *Marine Anthropogenic Litter*, Chapter 12. https://10.1007/978-3-319-16510-3_12

Kooi, M., van Nes, E.H., Scheffer, M., Koelmans, A.A., 2017. Ups and Downs in the Ocean: Effects of Biofouling on Vertical Transport of Microplastics. Environmental Science & Technology 51, 7963–7971. https://doi.org/10.1021/acs.est.6b04702

Koutsodendris, A., Papatheodorou, G., Kougiourouki, O., Georgiadis, M., 2008. Benthic marine litter in four Gulfs in Greece, Eastern Mediterranean; abundance, composition and source identification. *Estuarine, Coastal and Shelf Science* 77, 501–512. https://doi.org/10.1016/j.ecss.2007.10.011

Kvale, K., Prowe, A.E.F., Chien, CT., Landolfi, A., Oschlies, A., 2020.The global biological microplastic particle sink. *Scientific Report* 10, 16670. https://doi.org/10.1038/s41598-020-72898-4

Lambert, S., Wagner, M., 2016. Characterisation of nanoplastics during the degradation of polystyrene. *Chemosphere* 145, 265–268. https://doi.org/10.1016/j.chemosphere.2015.11.078

Lebreton, L., Slat, B., Ferrari, F., Sainte-Rose, B., Aitken, J., Marthouse, R., Hajbane, S., Cunsolo, S., Schwarz, A., Levivier, A., Noble, K., Debeljak, P., Maral, H., Schoeneich-Argent, R., Brambini, R., Reisser, J., 2018. Evidence that the Great Pacific Garbage Patch is rapidly accumulating plastic. *Scientific Report* 8, 4666. https://doi.org/10.1038/s41598-018-22939

Lee, H., Shim, W.J., Kwon, J.-H., 2014. Sorption capacity of plastic debris for hydrophobic organic chemicals. *Science of The Total Environment* 470–471, 1545–1552. https://doi.org/10.1016/j.scitotenv.2013.08.023

Lefebvre, C., Saraux, C., Heitz, O., Nowaczyk, A., Bonnet, D., 2019. Microplastics FTIR characterization and distribution in the water column and digestive tracts of small pelagic fish in the Gulf of Lions. *Marine Pollution Bulletin*, 142, 510–519. https://doi.org/10.1016/j.marpolbul.2019.03.025

Lesser, M.P., Carleton, K.L., Böttger, S.A., Barry, T.M., Walker, C.W., 2011. Sea urchin tube feet are photosensory organs that express a rhabdomeric-like opsin and PAX6. *Proceedings of the Royal Society B: Biological Sciences* 278, 3371–3379. https://doi.org/10.1098/rspb.2011.0336

Lots, F.A.E., Behrens, P., Vijver, M.G., Horton, A.A., Bosker, T., 2017. A large-scale investigation of microplastic contamination: Abundance and characteristics of microplastics in European beach sediment. *Marine Pollution Bulletin* 123, 219–226. https://doi.org/10.1016/j.marpolbul.2017.08.057

Macias, D., Cózar, A., Garcia-Gorriz, E., González-Fernández, D., Stips, A., 2019. Surface water circulation develops seasonally changing patterns of floating litter accumulation in the Mediterranean Sea. A modelling approach. *Marine Pollution Bulletin* 149, 110619. https://doi.org/10.1016/j.marpolbul.2019.11061

Magni, S., Gagné, F., André, C., Della Torre, C., Auclair, J., Hanana, H., Parenti, C.C., Bonasoro, F., Binelli, A., 2018. Evaluation of uptake and chronic toxicity of virgin polystyrene microbeads in freshwater zebra mussel *Dreissena polymorpha* (Mollusca: Bivalvia). *Science of The Total Environment* 631–632, 778-788. https://doi.org/10.1016/j.scitotenv.2018.03.075

Marques-Santos, L.F., Grassi, G., Bergami, E., Faleri, C., Balbi, T., Salis, A., Damonte, G., Canesi, L., Corsi, I., 2018. Cationic polystyrene nanoparticle and the sea urchin immune system: biocorona formation, cell toxicity, and multixenobiotic resistance phenotype. *Nanotoxicology* 12, 847–867. https://doi.org/10.1080/17435390.2018.1482378

Martellini, T., Guerranti, C., Scopetani, C., Ugolini, A., Chelazzi, D., Cincinelli, A., 2018. A snapshot of microplastics in the coastal areas of the Mediterranean Sea. *TrAC Trends in Analytical Chemistry* 109, 173-179. https://doi.org/10.1016/j.trac.2018.09.028

Matranga, V., Pinsino, A., Celi, M., Bella, G.D., Natoli, A., 2006. Impacts of UV-B radiation on short-term cultures of sea urchin coelomocytes. *Marine Biology* 149, 25–34. https://doi.org/10.1007/s00227-005-0212-1

Matranga, V., Pinsino, A., Celi, M., Natoli, A., Bonaventura, R., Schröder, H.C., Müller, W.E.G., 2005. Monitoring Chemical and Physical Stress Using Sea Urchin Immune Cells, in: Matranga, Valeria (Ed.), *Echinodermata, Progress in Molecular and Subcellular Biology*. Springer, Berlin, Heidelberg, 85–110. https://doi.org/10.1007/3-540-27683-1_5

Messinetti, S., Mercurio, S., Parolini, M., Sugni, M., Pennati, R., 2018. Effects of polystyrene microplastics on early stages of two marine invertebrates with different feeding strategies. *Environmental Pollution* 237, 1080-1087. https://doi.org/10.1016/j.envpol.2017.11.030

Migliaccio, O., Pinsino, A., Maffioli, E., Smith, A.M., Agnisola, C., Matranga, V., Nonnis, S., Tedeschi, G., Byrne, M., Gambi, M.C., Palumbo, A., 2019. Living in future ocean acidification, physiological adaptive responses of the immune system of sea urchins resident at a CO_2 vent system. *Science of The Total Environment* 672, 938–950. https://doi.org/10.1016/j.scitotenv.2019.04.005

Milito, A., Murano, C., Castellano, I., Romano, G., Palumbo, A., 2020. Antioxidant and immune response of the sea urchin *Paracentrotus lividus* to different re-suspension patterns of highly polluted marine sediments. *Marine Environmental Research* 160, 104978. https://doi.org/10.1016/j.marenvres.2020.104978

Navarro, J., Jordá, G., Compa, M., Alomar, C., Fossi, M.C., Deudero, S., 2021. Impact of the marine litter pollution on the Mediterranean biodiversity: A risk assessment study with focus on the marine protected areas. *Marine Pollution Bulletin* 165, 112169. https://doi.org/10.1016/j.marpolbul.2021.112169

Nuelle, M.-T., Dekiff, J.H., Remy, D., Fries, E., 2014. A new analytical approach for monitoring microplastics in marine sediments. *Environmental Pollution* 184, 161–169. https://doi.org/10.1016/j.envpol.2013.07.027

Pancer, Z., Rast, J.P., Davidson, E.H., 1999. Origins of immunity: transcription factors and homologues of effector genes of the vertebrate immune system expressed in sea urchin coelomocytes. *Immunogenetics* 49, 773–786. https://doi.org/10.1007/s002510050551

Paul, M., Stock, V., Cara-Carmona, J., Lisicki, E., Shopova, S., Fessard, V., Braeuning, A., Sieg, H., Böhmert, L., 2020. Micro- and nanoplastics – current state of knowledge with the focus on oral uptake and toxicity. *Nanoscale Advances* 2, 4350–4367. https://doi.org/10.1039/D0NA00539H

Paul-Pont, I., Lacroix, C., Gonzàaìlez Fernàndez, C., Hègaret, H., Lambert, C., Le Goïc, N., Frére, L., Cassone, A.L., Sussarellu, R., Fabioux, C., Guyomarch, J., Albentosa, M., Huvet, A., Soudant, P., 2016. Exposure of marine mussels *Mytilus spp*. to polystyrene microplastics: Toxicity and influence on fluoranthene bioaccumulation. *Environmental Pollution* 216, 724-737. http://dx.doi.org/10.1016/j.envpol.2016.06.039

Pasquini, G., Ronchi, F., Strafella, P., Scarcella, G., Fortibuoni, T., 2016. Seabed litter composition, distribution and sources in the Northern and Central Adriatic Sea (Mediterranean). *Waste Management* 58, 41–51. https://doi.org/10.1016/j.wasman.2016.08.038

Pedà, C., Caccamo, L., Fossi, M.C., Gai, F., Andaloro, F., Genovese, L., Perdichizzi, A., Romeo, T., Maricchiolo, G., 2016. Intestinal alterations in European sea bass *Dicentrarchus labrax* (Linnaeus, 1758) exposed to microplastics: Preliminary results. *Environmental Pollution* 212, 251–256. https://doi.org/10.1016/j.envpol.2016.01.083

Peeken, I., Primpke, S., Beyer, B., Gütermann, J., Katlein, C., Krumpen, T., Bergmann, M., Hehemann, L., Gerdts, G., 2018. Arctic sea ice is an important temporal sink and means of transport for microplastic. *Nature Communication* 9, 1505. https://doi.org/10.1038/s41467-018-03825-5

Phuong, N.N., Zalouk-Vergnoux, A., Kamari, A., Mouneyrac, C., Amiard, F., Poirier, L., Lagarde, F., 2018. Quantification and characterization of microplastics in blue mussels (*Mytilus edulis*): protocol setup and preliminary data on the contamination of the French Atlantic coast. *Environmental Science and Pollution Research* 25, 6135–6144. https://doi.org/10.1007/s11356-017-8862-3

Pinsino, A., Bergami, E., Della Torre, C., Vannuccini, M. L., Addis, P., Secci, M., Dawson, K.A., Matranga, V., Corsi, I., 2017. Amino-modified polystyrene nanoparticles affect signalling pathways of the sea urchin (*Paracentrotus lividus*) embryos. *Nanotoxicology* 11, 201–209. https://10.1080/17435390.2017.1279360

Pinsino, A., Della Torre, C., Sammarini, V., Bonaventura, R., Amato, E., Matranga, V., 2008. Sea urchin coelomocytes as a novel cellular biosensor of environmental stress: a field study in the Tremiti Island Marine Protected Area, Southern Adriatic Sea, Italy. *Cell Biology & Toxicology* 24, 541–552. https://doi.org/10.1007/s10565-008-9055-0

Pinsino, A., Matranga, V., 2015. Sea urchin immune cells as sentinels of environment al stress. *Developmental & Comparative Immunology* 49, 198–205. https://doi.org/10.1016/j.dci.2014.11.013

Pinsino, A., Russo, R., Bonaventura, R., Brunelli, A., Marcomini, A., Matranga, V., 2015. Titanium dioxide nanoparticles stimulate sea urchin immune cell phagocytic activity involving TLR/p38 MAPK-mediated signalling pathway. *Scientific Report* 5, 14492. https://doi.org/10.1038/srep14492

Porter, A., Lyons, B.P., Galloway, S.T., Lewis, C., 2018. Role of Marine Snows in Microplastic Fate and Bioavailability. *Environmental Science & Technology* 52, 12, 7111–7119. https://doi.org/10.1021/acs.est.8b01000

Plastic Europe, 2020. Plastics - the Facts 2020. An analysis of European plastics production, demand and waste data. https://www.plasticseurope.org/en/resources/publications/4312-plastics-facts-2020

Purcell, S.W., 2019. Evaluating the impacts of improving postharvest processing of sea cucumbers in the Western Pacific region. *ACIAR Final Reports* No.FR2019/49, 41.

Rist, S., Baun, A., Almeda, R., Hartmann, N.B., 2019. Ingestion and effects of micro- and nanoplastics in blue mussel (*Mytilus edulis)* larvae. *Marine Pollution Bulletin 140*, 423–430. https://doi.org/10.1016/j.marpolbul.2019.01.069

Rast, J.P., Smith, L.C., Loza-Coll, M., Hibino, T., Litman, G.W., 2006. Genomic Insights into the Immune System of the Sea Urchin. *Science* 314, 952–956. https://doi.org/10.1126/science.1134301

Romeo, T., Pietro, B., Pedà, C., Consoli, P., Andaloro, F., Fossi, M.C., 2015. First evidence of presence of plastic debris in stomach of large pelagic fish in the Mediterranean Sea. *Marine Pollution Bulletin* 95 (1), 358-361. https://doi.org/10.1016/j.marpolbul.2015.04.048

Sala, E., Ribes, M., Hereu, B., Zabala, M., Alvà, V., Coma, R., Garrabou, J., 1998. Temporal variability in abundance of the sea urchins *Paracentrotus lividus* and *Arbacia lixula* in the northwestern Mediterranean: comparison between a marine reserve and an unprotected area. *Marine Ecology Progress Series* 168, 135-145. https://10.3354/meps168135

Schirinzi, G.F., Llorca, M., Seró, R., Moyano, E., Barceló, D., Abad, E., Farré, M., 2019. Trace analysis of polystyrene microplastics in natural waters. *Chemosphere* 236, 124321. https://doi.org/10.1016/j.chemosphere.2019.07.052

Schmid, C., Cozzarini, L., Zambello, E., 2021. A critical review on marine litter in the Adriatic Sea: Focus on plastic pollution. *Environmental Pollution* 273, 116430. https://doi.org/10.1016/j.envpol.2021.116430

Sea Urchin Sequencing Consortium, 2006. The sequence of the sea urchin genome. *Science* 314, 941. https://10.1126/science.1133609

Sebille, E. van, Wilcox, C., Lebreton, L., Maximenko, N., Hardesty, B.D., Franeker, J.A. van, Eriksen, M., Siegel, D., Galgani, F., Law, K.L., 2015. A global inventory of small floating plastic debris. *Environmental Research Letter* 10, 124006. https://doi.org/10.1088/1748-9326/10/12/124006

Sendra, M., Carrasco-Braganza, M. I., Yeste, P. M., Vila, M., and Blasco, J., 2020. Immunotoxicity of polystyrene nanoplastics in different hemocyte subpopulations of *Mytilus galloprovincialis*. *Scientific Report* 10, 8637. https://10.1038/s41598-020-65596-8

Sharma, V.K., Ma, X., Guo, B., Zhang, K., 2021. Environmental factors-mediated behavior of microplastics and nanoplastics in water: A review. *Chemosphere* 271, 129597. https://doi.org/10.1016/j.chemosphere.2021.129597

Simon-Sánchez, L., Grelaud, M., Garcia-Orellana, J., Ziveri, P., 2019. River Deltas as hotspots of microplastic accumulation: The case study of the Ebro River (NW Mediterranean). *Science of The Total Environment* 687, 1186–1196. https://doi.org/10.1016/j.scitotenv.2019.06.168

Singh, B., Sharma, N., 2008. Mechanistic implications of plastic degradation. *Polymer Degradation and Stability* 93, 561–584. https://doi.org/10.1016/j.polymdegradstab.2007.11.008

Smith, L.C., 2010. Diversification of innate immune genes: lessons from the purple sea urchin. *Disease Models & Mechanisms* 3, 274–279. https://doi.org/10.1242/dmm.004697

Smith, L.C., Davidson, E.H., 1992. The echinoid immune system and the phylogenetic occurrence of immune mechanisms in deuterostomes. *Immunology Today* 13, 356–362. https://doi.org/10.1016/0167-5699(92)90172-4

Smith, L.C., Hawley, T.S., Henson, J.H., Majeske, A.J., Oren, M., Rosental, B., 2019. Chapter 15 - Methods for collection, handling, and analysis of sea urchin coelomocytes, in: Foltz, K.R., Hamdoun, A. (Eds.), *Methods in Cell Biology, Echinoderms, Part A. Academic Press*, 357–389. https://doi.org/10.1016/bs.mcb.2018.11.009

Smith, L.C., Rast, J.P., Brockton, V., Terwilliger, D.P., Nair, S.V., Buckley, K.M., Majeske, A.J., 2006. The sea urchin immune system. *ISJ-Invertebrate Survival Journal*, 25–39. ISSN 1824-307X

Suaria, G., Avio, C.G., Mineo, A., Lattin, G.L., Magaldi, M.G., Belmonte, G., Moore, C.J., Regoli, F., Aliani, S., 2016. The Mediterranean Plastic Soup: synthetic polymers in Mediterranean surface waters. *Scientific Report* 6, 37551. https://doi.org/10.1038/srep37551

Suaria, G., Perold, V., Lee, J.R., Lebouard, F., Aliani, S., Ryan, P.G., 2020. Floating macro- and microplastics around the Southern Ocean: Results from the Antarctic Circumnavigation Expedition. *Environment International* 136, 105494. https://doi.org/10.1016/j.envint.2020.105494

Sussarellu, R., Suquet, M., Thomas, Y., Lambert, C., Fabioux, C., Pernet, M.E.J., Le Goïc, N., Quillien, V., Mingant, C., Epelboin, Y., Corporeau, C., Guyomarch, J., Robbens, J., Paul-Pont, I., Soudant, P., Huvet, A., 2016. Oyster reproduction is affected by exposure to polystyrene microplastics. *Proceedings of the National Academy of Sciences*, USA 113 (9), 2430–2435. https://doi.org/10.1073/pnas.1519019113

Tallec, K., Huvet, A., di Poi, C., González-Fernández, C., Lambert, C., Petton, B., le Goïc, N., Berchel, M., Soudant, P., Paul-Pont, I., 2018. Nanoplastics impaired oyster free living stages, gametes and embryos. *Environmental Pollution* 242, 1226–1235. https://10.1016/j.envpol.2018.08.020

Ter Halle, A., Jeanneau, L., Martignac, M., Jardé, E., Pedrono, B., Brach, L., Gigault, J., 2017. Nanoplastic in the North Atlantic Subtropical Gyre. *Environmental Science & Technology* 51, 13689–13697. https://doi.org/10.1021/acs.est.7b03667

Ullrich-Luter, E.M., Dupont, S., Arboleda, E., Hausen, H., Arnone, M.I., 2011. Unique system of photoreceptors in sea urchin tube feet. *Proceedings of the National Academy of Sciences* 108, 8367–8372. https://doi.org/10.1073/pnas.1018495108

Wang, L., Cho, D.-W., Tsang, D.C.W., Cao, X., Hou, D., Shen, Z., Alessi, D.S., Ok, Y.S., Poon, C.S., 2019. Green remediation of As and Pb contaminated soil using cement-free clay-based stabilization/solidification. *Environment International* 126, 336–345. https://doi.org/10.1016/j.envint.2019.02.057

Wong, C.S., Green, D.R., Cretney, W.J., 1974. Quantitative Tar and Plastic Waste Distributions in the Pacific Ocean. *Nature* 247, 30–32. https://doi.org/10.1038/247030a0

WWF, 2018. Out of the plastic trap. https://www.wwf.org.uk/sites/default/files/2018-06/WWF_Plastics_MED_WEB.pdf

Yeruham, E., Rilov, G., Shpigel, M., Abelson, A., 2015. Collapse of the echinoid *Paracentrotus lividus* populations in the Eastern Mediterranean—result of climate change? *Scientific Report* 5, 13479. https://doi.org/10.1038/srep13479

Yokota, Y., 2002. Fishery and consumption of the sea urchin in Japan. In: Y. Yokota, V. Matranga & Z. Smolenicka. The sea urchin: from basic biology to aquaculture. *Lisse, The Netherlands: Swets & Zeitlinger*, 129–138.

Yorke, C.E, Page, M.E., Miller, R.J., 2019. Sea urchins mediate the availability of kelp detritus to benthic consumers. *Proceedings of the Royal Society* B 286. https://doi.org/10.1098/rspb.2019.0846

Yu, F., Yang, C., Zhu, Z., Bai, X., Ma, J., 2019. Adsorption behavior of organic pollutants and metals on micro/nanoplastics in the aquatic environment. *Science of The Total Environment* 694, 133643. https://doi.org/10.1016/j.scitotenv.2019.133643

Zettler, E.R., Mincer, T.J., Amaral-Zettler, L.A., 2013. Life in the "Plastisphere": Microbial Communities on Plastic Marine Debris. *Environmental Science & Technology* 47, 7137–7146. https://doi.org/10.1021/es401288x

Chapter 1

"How sea urchins face microplastics: uptake, tissue distribution and immune system response"

Abstract

Plastic pollution represents one of the major threats to the marine environment. A wide range of marine organisms has been shown to ingest microplastics due to their small dimensions (less than 1 mm). This negatively affects some biological processes, such as feeding, energy reserves and reproduction. Very few studies have been performed on the effect of microplastics on sea urchin development and virtually none on adults. The aim of this work was to evaluate the uptake and distribution of fluorescent labelled polystyrene microbeads (micro-PS) in the Mediterranean Sea urchin *Paracentrotus lividus* and the potential impact on circulating immune cells. Differential uptake was observed in the digestive and water vascular systems as well as in the gonads based on microbeads size (10 and 45 μm in diameter). Treatment of sea urchins with particles of both sizes induced an increase of the total number of immune cells already after 24h. No significant differences were observed among immune cell types. However, the ratio between red and white amoebocytes, indicative of sea urchin healthy status, increased with both particles. This effect was detectable already at 24h upon exposure to smaller micro-PS (10 μm). An increase of intracellular levels of reactive oxygen and nitrogen species was observed at 24h upon both micro-PS exposure, whereas at later time these levels became comparable to those of controls. A significant increase of total antioxidant capacity was observed after treatment with 10 μm micro-PS. Overall data provide the first evidence on polystyrene microbeads uptake and tissue distribution in sea urchins, indicating a stress-related impact on circulating immune cells.

Main findings

The uptake and distribution of polystyrene microbeads was found to be size dependent in adult sea urchins with stress-related impacts on circulating immune cells

Keywords: Coelomocytes, microplastics, nitrosative stress, oxidative stress, sea urchin

1.1 Introduction

Over the last decade, the anthropogenic pressure on the marine environment has resulted in the widespread occurrence, distribution and accumulation of mismanaged plastic waste in both abiotic and biotic compartments leading to a growing concern on their ecological impact (Còzar et al., 2014; Eriksen et al., 2014; Geyer et al., 2017). According to recent model-based projections, large rivers (>100 Km^2) represent the major sources of plastic (91%) into the sea, thus marine species living in coastal areas could be more at risk than those living in the open-sea (Lebreton & Andrady, 2019). Semi-enclosed basins as the Mediterranean Sea are considered among the most polluted areas with estimates of a range between 873 and 2576 tons of plastic particles floating on sea surface, among which between 3.2×10^{12} and 28.2×10^{12} items of a small dimension, i.e. microplastics (<1mm, Hartmann et al., 2019) (Còzar et al., 2015; van Sebille et al., 2015; Suaria et al., 2016). Recent plastic fate models show that the distribution of micro- and nanoplastics (<1µm) on the sea surface, water column, and sediment is driven partly by polymers size and density, which affect their sinking or floating behavior/capacity (Kooi et al., 2017). Once in natural waters, biofouling, chemicals adsorption (including contaminants) and incorporation into fecal pellets, and marine aggregates can significantly affect their buoyancy or precipitation to seafloor (Qian et al., 2007; Lobelle & Cunliffe, 2011; Rochman, 2015; Cole et al., 2016). Moreover, due to environmental conditions, polymer type and weathering, fragmentation of plastic can originate smaller particles, down to nanometer (nm) size (nanoplastics), as those recently detected in seawater below the North Atlantic sub-tropical gyre (Andrady, 2017; Ter Halle et al., 2017; Ekvall et al., 2019).

Microplastic exposure could pose a high risk to marine species, according to their ecological and behavioural traits (home range and feeding strategies), as well as their position in the food web (pelagic, demersal or benthic). Microplastic-associated effects on marine biota have been increasingly investigated, especially for what concerns the mechanism of interaction at the cellular level (Prinz & Korez, 2020). Size-dependent effects have been reported in different organisms such as *Danio rerio* (Lu et al., 2016), *Brachionus koreanus*, (Jeong et al., 2016), *Mus musculus* (Deng et al., 2017), *Paracyclopina nana* (Jeong et al., 2017), *Caenorhabditis elegans* (Lei et al., 2018) in terms of uptake, oxidative damage and neurotoxicity. Several impairments have been associated with microplastic ingested both in larvae (development and survival) (Sussarellu et al., 2016) and in adult stages (inflammation, growth and fecundity) (Lee et al., 2013; Besseling et al., 2014; Cole et al., 2015). Species living in highly urbanized sites in which domestic and industrial sewages exist together with other local sources (tourism, fishery, aquaculture) are likely more threatened by both micro- and nanoplastics. In particular, Mediterranean coastal species are considered at higher risk of microplastic ingestion than those living in the open sea according to the model of Compa and co-authors (2018),

based on data on plastic ingestion, species distribution, and plastic dispersion. Small home range species are more exposed to plastic closer to their habitat, while long-range migrating species will catch those more highly distributed in the environment.

Mediterranean benthic marine species have been overlooked for plastic ingestion compared to filter-feeders, fish, and large mammals (Fossi et al., 2012; Romeo et al., 2015; Bellas et al., 2016; Güven et al., 2017; Compa et al., 2018; Digka et al., 2018; Duncan et al., 2018; Phuong et al., 2018; Giani et al., 2019; Lefebvre et al., 2019). The few available studies reported the presence of plastics in biota from a Norwegian fjord and in deep sea invertebrates, belonging to different phyla, including cnidarians, echinoderms, arthropods and molluscs (Taylor et al., 2016; Bour et al., 2018; Cau et al., 2019; Courtene-Jones et al., 2019).

Among the benthic species, sea urchins are key grazers structuring kelp forest ecosystems and represent an important element of trophic cascade (Steneck, 2013). In fact, when sea urchin predators are scarce, the number of sea urchins greatly increased forming the so called "urchin barrens", thus limiting the extent of seagrass beds (Sala et al., 1998; Eklöf et al., 2008). Recently, sea urchins have been shown to act also as shredders, in capturing and converting the coarse kelp litter to fine fragments utilized by benthic detritivores (Yorke et al., 2019).

The abundance of *P. lividus* has been reported in Northwestern Mediterranean Sea, in the area around Corsica and Tuscany (Palacin et al., 1998; Sala et al., 1998; Jacinto et al., 2013; Duchaud et al., 2018). The growing demand and market values of gonads as food significantly affect both sea urchin abundance and population size in the Gulf of Naples, that receives terrestrial inputs from a highly urbanized area, with over 2 million inhabitants. Urban, industrial and agricultural discharges exert a strong pressure on the coastal area, including the contribution of the Sarno river, one of the most polluted rivers in Europe (Montuori et al., 2013). Therefore, *P. lividus* population living in the area is continuously threatened by a variety of pressures, acting alone or simultaneously, including microplastics. Data on floating microplastic concentrations in the Gulf of Naples are scarce. In 2017, a cruise along the Italian coasts sampled at coastal (Portici) and offshore (Punta Campanella) stations, reporting 3.56 and 0.26 items per m^3 (CNR-ISMAR, 2017). Distribution appears to be strongly affected by the general water circulation and residency times, being strongly spatially and seasonally variable. These concentrations lie within those reported from other areas of the Mediterranean Sea, ranging from 0.15 to 7.68 items m^3 (Cincinelli et al., 2019), and are strongly influenced by hydrodynamic features such as currents, vertical movements, gyres and fronts. However, thus these data refer to microplastics greater than 200 -780 μm depending on the mesh net used for sampling (Cincinelli et al., 2019). A few papers have hitherto reported the effects of microplastics on sea urchin embryo development. However, no studies have been performed on adults. Contrasting results have

been reported on sea urchin embryo development probably due to differences in the type, concentration and size of the polymers as well as in the developmental stage chosen for the treatment (Kaposi et al., 2014; Martínez-Gómez et al., 2017; Trifuoggi et al., 2019). The possible toxicity of microplastics has been related to different processes like larval ejection, the absorption of contaminants, or the release of plastic additives (Kaposi et al., 2014; Nobre et al., 2015; Martínez-Gómez et al., 2017; Beiras & Tato, 2019).

Adult sea urchins could accumulate microplastics via at least two different pathways, food ingestion and water vascular system, with putative differential impacts on the animal physiology and on the highly sensitive immune system, known as a sentinel of environmental stress (Pinsino & Matranga 2015). In addition, sea urchin *P. lividus* show distinctive features for macro-plastic fragmentation producing smaller plastic pieces (Porter et al., 2019). The aim of the present study was to investigate the uptake and tissue distribution of polystyrene microplastics of different size in *P. lividus* adults and their potential impact on immune cells.

1.2 Materials and Methods

1.2.1 Sea Urchins collection and maintenance

Adult specimens of *P. lividus* (Lamark 1816) (diameter 4.68 ± 0.46 cm) were collected in in the Gulf of Naples from sites (40°46'50" N 14°12'03" E) that are not privately-owned nor protected in any way, according to the authorization of Marina Mercantile (DPR 1639/68, 09/19/1980, confirmed on 01/10/2000). Sea urchins were acclimated for two weeks in glass tanks filled with circulating natural seawater (temperature 18 ± 1°C; salinity 38 ± 1; dissolved O_2 7 mg/L; pH 8.1; all the parameters remained constant during the experiment) and fed ad libitum with *Ulva lactuca*. Although no authorization is required for sea urchins, all procedures were performed according to the European Directive 2010/63/EU on the protection of animals used for scientific purposes by reducing at minimum the number of specimens used and any pain or distress of animals during exposure.

1.2.2 Sea urchins *in vivo* exposure

1.2.2.1 Morphology of *P. lividus* madreporite

Before starting uptake experiments, the pore size of sea urchins madreporite was determined using scanning electron microscopy available at the Advanced Microscopy Center (AMC), at Stazione Zoologica Anton Dohrn of Naples. The madreporite was removed using scissors from three sea urchins with same dimensions of those used for the experiments. Madreporite specimens were washed two times in deionized water and then placed overnight in a NaClO solution (1:4 in deionized water) (Tamori et al., 1996). After further washing in deionized water, they were placed in a 70% ethanol, air dried, sputter coated with gold, using a Leica ACE200 vacuum coater (Leica Microsystems, Inc. Buffalo Grove, IL. Observations were performed with a SEM JSM-6700F (JEOL USA, Inc. Peabody, MA).

1.2.2.2 Polystyrene microbeads

Fluorescent-labelled polystyrene microbeads (micro-PS) (441 excitation/ 485 emission) of 10 μm and 45 μm were purchased from Polysciences (Warrington, PA, U.S.A.). According to the supplier, the particles were packaged as 2.5% aqueous suspension without biocides or stabilizers. Besides, the fluorophore was embedded inside the particles, thus providing the fluorescent beads high stability and resistance. Micro-PS working solutions (10^4 particles mL^{-1}) were prepared in deionized water and then added to filtered natural sea water (0.22 μm) to reach the final concentration of 10 particles mL^{-1}. Stock and working solutions were vortexed for 3 minutes prior to use. Size and shape of micro-PS was further confirmed by light microscopy (Supplementary data, Figure S1.1).

1.2.2.3 Experimental design

Control and micro-PS exposed treatments (10 particles mL^{-1}) were set up by placing sea urchins in 4L experimental glass tanks (1 specimen per liter) supplied with natural filtered seawater (0.22 μm) in a closed flow-through system, constantly aerated. Waters were renewed every 24h. Sea urchins were exposed for 72h and not fed. Experiments were run three times. In absence of reliable data on the environmental levels of MPs in the size range, 10 μm and 45 μm, we chose to expose the animals to 10 particles mL^{-1}, on the base of the micro-PS concentrations used in the last 5 years in similar ecotoxicological studies (see Supplementary data, Table S1.1). This concentration also ensures that detectable MP amounts could be resolved following uptake and organ distribution by sea urchins.

1.2.3 Extraction and quantification of microplastics from sea urchin tissues

After 72h, the abundance of micro-PS was examined in various organs, including the digestive system (esophagus and gut), the vascular system (ring canal, stone canal and ampullae), and the whole gonads. Sea urchins were sacrificed by cutting off the peristomal membrane. Digestive system, water vascular system and gonads were removed, weighed and kept at 4°C until further processing. Microplastics were extracted from organs according to the method of Kühn et al. (2017) by placing fresh tissue in KOH 1M (1:20, w: v) at room temperature for two days under continuous orbital shacking (IKA KS250). After 48h, the obtained solution was filtered on cellulose acetate membrane filters (0.45 μm) and then analysed under optical microscopy to quantify micro-PS (Supplementary data, Figure S1.2 and S1.3). As quality control of measures, a recovery test of the extraction method was performed as follows: a known aliquot of the working micro-PS solution (equivalent to 200 particles) was added to KOH 1M, and treated as the tissue extracts; at the end the micro-PS quantified on the filter.

1.2.4 Coelomic fluid collection and analysis

Every 24h, 1mL of the coelomic fluid was withdrawn from each specimen (control and treated) through a puncture (needle 26 gauge) in the peristomial membrane using anticoagulant solution CCM 2X (NaCl 1M, MgCl$_2$ 10 mM, EGTA 2mM, Hepes 40 mM, pH 7.2) at a ratio of 1:1 (anticoagulant: coelomic fluid) (Pinsino & Matranga, 2015; Migliaccio et al., 2019). Coelomocytes were immediately counted. Aliquots of the coelomic fluid was used to measure ROS and RNS, according to protocols described below. At the end of the exposure period (72h), coelomic fluid was again withdrawn from each specimen (control and treated) and observed under a fluorescence microscope to assess the presence of micro-PS (Zeiss Axioscope). An aliquot of coelomic fluid was washed twice in CCM 1X and the pellet was stored at -80°C until total antioxidant capacity analysis.

1.2.4.1 Coelomocytes counts

Coelomocytes were then counted using Neubauer chamber (Bright-Line Hemacytometer) under optical microscope (Zeiss) and cells were morphologically identified according to Pinsino & Matranga (2015) as phagocytes, vibratile cells, white and red amoebocytes.

1.2.4.2 Reactive Oxygen Species (ROS) and Nitrogen Species (RNS)

Intracellular levels of ROS and RNS were determined using a specific fluorescent probe: DCFH-DA (2′,7′-dichlorohydro-fluoresceindiacetate) and DAF-DA (4-amino-5-methylamino-2',7'-difluororescein diacetate), respectively. Sea urchin coelomocytes (about $1.5 \cdot 10^6$) were incubated for 1h in the dark at room temperature with 20 µM DCFH-DA or 20 µM DAF-DA in 1mL of CCM anticoagulant. Control samples ($1.5 \cdot 10^6$ coelomocytes) were incubated with DMSO. After incubation, cells were collected by centrifugation at 8000 rcf for 10 min at +4 °C, briefly rinsed twice with CCM1x without DCFH-DA/ DAF-DA and stored at -80°C. An aliquot of coelomocytes suspended in CCM1X was used in order to verify the specificity of the intracellular signal through observation with a fluorescence microscope (Zeiss Axioscope). Frozen cells were suspended in 0.5mL Tris–HCl buffer 40 mM, pH 7.0, vortexed for 1 min, and finally centrifuged for 10min at 8000 rcf at +4 °C. The supernatant was harvested, and the fluorescence was measured using the spectrofluorometer (Tecan) at ex 488/em 525nm for DCFH-DA and at ex 495/em 515 nm for DAF-DA. Fluorescence values were normalized by subtracting the auto-fluorescence of unlabeled extracts (DMSO). For the detection of ROS and RNS 16 organisms were used for each experimental group and triplicate measurements for each sample were performed. Results are expressed as fluorescence intensity referred to $1.5 \cdot 10^6$ cells.

1.2.4.3 Total antioxidant capacity (TAC)

TAC was determined according to our previous study (Milito et al., 2020) evaluating the decolorization of 2,2′-azinobis-3-ethylbenzothiazoline-6-sulfonic acid (ABTS) radical cation (ABTS•+), generated by oxidation of ABTS with hydrogen peroxide in the presence of horseradish peroxidase, by scavenging ability of antioxidants in the samples. The TAC is quantified by measuring the absorbance at 730 nm using as a reference standard curve of ascorbic acid (1- 15 µM) and then the values were normalized versus total protein content. Total proteins were measured at 595nm according to Bradford (1976) using a Tecan spectrometer and bovine serum albumin as standard. Also in this case, 16 organisms were used for each experimental group and triplicate measurements for each sample were performed.

1.2.5 Statistical Analysis

The data on qualitative and qualitative analysis of coelomocytes were analyzed by two-way analysis of variance ANOVA followed by Bonferroni's multiple comparisons test. Intracellular levels of ROS/RNS and TAC were analyzed by two-way analysis of variance (ANOVA) (*p-value* < 0.05) followed by Tukey's multiple comparison test. Data are presented as mean ± SD and statistics was performed using GraphPad Prism version 7.00 for Windows.

1.3 Results

1.3.1 Madreporite pores size

SEM analysis performed on three madreporite samples revealed that the mean diameter of pores is between 65μm and 70μm (Figure 1.1). Therefore, the micro-PS selected for the study were of 10 μm and 45 μm, thus able to pass through pores.
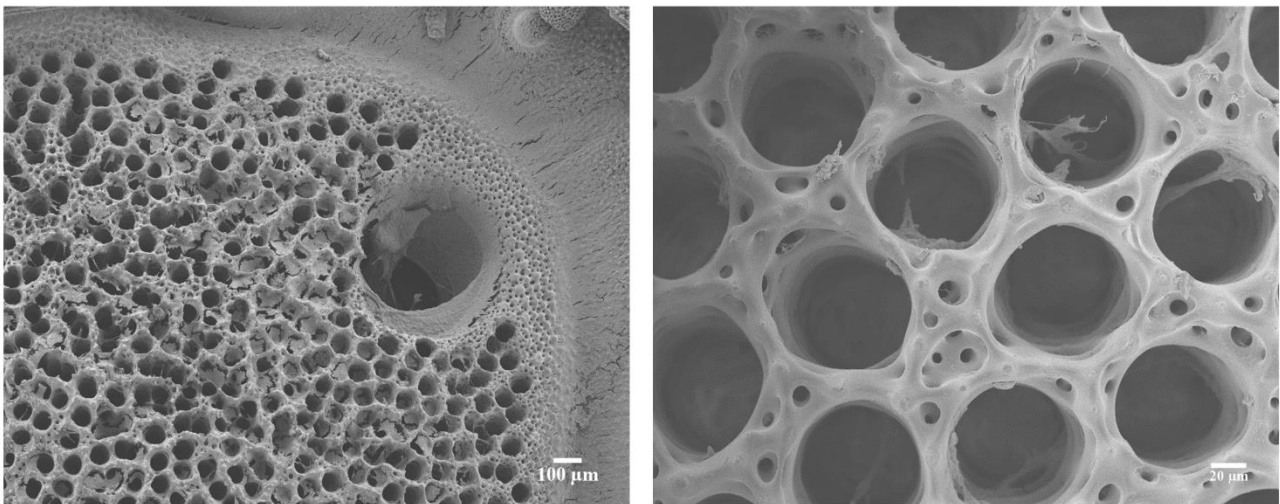
Figure 1.1 Aboral views of *Paracentrotus lividus* madreporite examined with scanning electron microscope (SEM).

1.3.2 Uptake and accumulation of microplastics in sea urchin tissues

Micro-PS content analysis in sea urchin organs showed a size-dependent uptake and a different distribution among tissues (Figure 1.2 and Table 1.1). A greater abundance of micro-PS was found in sea urchins exposed to 45 μm PS-MPs (104.05 ± 43.3 particles g^{-1} whole fresh tissue) than in those exposed to 10 μm micro-PS (86.1 ± 23.4 particles g^{-1} whole fresh tissue) (Table 1.1).

Table 1.1 Abundance of micro-PS (10 µm and 45 µm) in the organs of *P. lividus* upon waterborne exposure (72h). Data shown as mean ± SE.

	particles/ g	
	10 µm	**45 µm**
Esophagus	8.25±2.24	3.86±1.76
Digestive system	13.5±3.67	61.39±27.9
Ring Canal	28±7.34	15.09±6.81
Stone Canal	33±8.98	0±0
Ampullae	2.14±0.64	5.54±2.57
Gonads	1.24±0.57	18.17±8.27

The bigger micro-PS (45 µm) resulted highly present in the digestive system (mainly in the gut 67.5 %), followed by the ring canal, the ampullae of the vascular system (20.3 %) and finally in the gonads (12.2 %) (Figure 1.2). No 45 µm particles were found in the stone canal. By contrast, smaller micro-PS (10 µm) were mostly found in the ring and stone canal of the water vascular system (74.1%) than in the digestive system (24.8%) in which they were equally distributed between esophagus and gut. Very low amount of 10 µm micro-PS was found in the gonads (1.0 %). Apparently, no particles were found in the coelomic fluid after 72h of exposure to both micro-PS (10 and 45 µm). The recovery-effectiveness of particles using the KOH microplastics extraction method was about 75.25 ± 6 %.
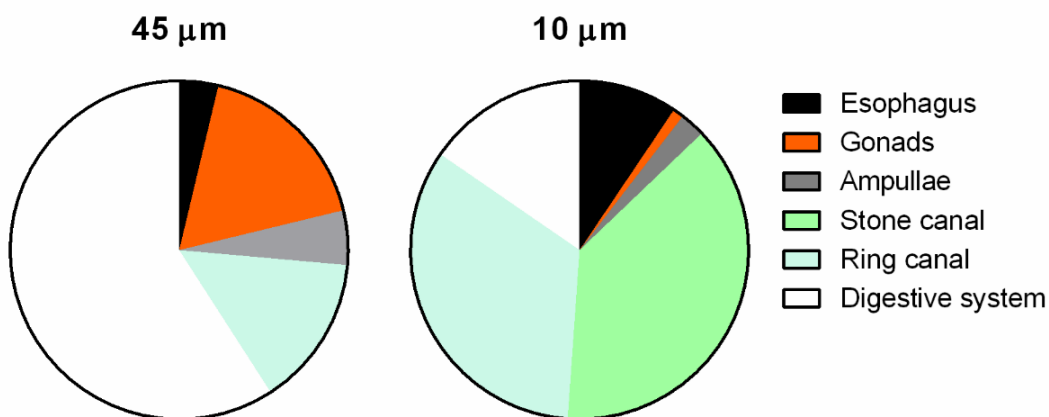
Figure 1.2 Abundance of PS-MPs in different tissues of sea urchins after 72h of exposure. The results are expressed as percentage of particles found in tissues normalized by the weight of fresh tissue.

1.3.3 Sea urchin's immune cells response

Coelomocytes total count showed a significant increase already after 24h of exposure in both treatments compared to controls regardless the micro-PS size (45μm and 10μm) (Figure 1.3).
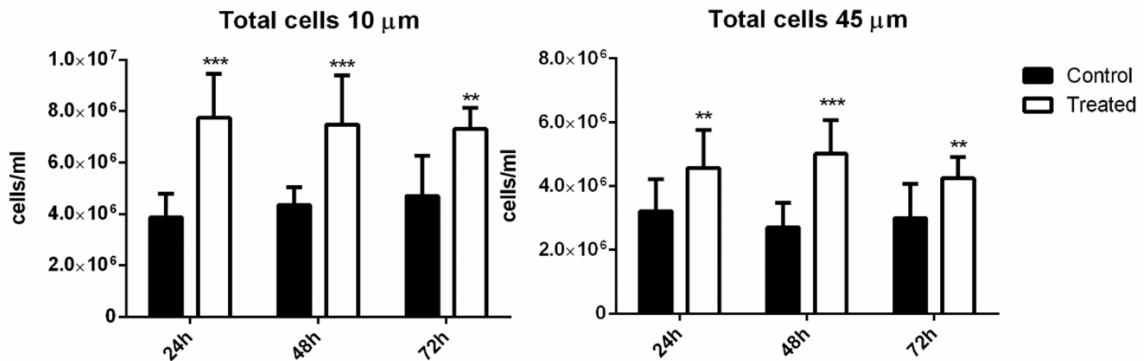
Figure 1.3 Total immune cells count of sea urchin at different time of exposure to a PS-MPs (10 μm and 45 μm). All data were analyzed by Two-way ANOVA followed by Bonferroni post-test compared with the respective control. Bars represent mean ±SD. Asterisks indicate values that are significantly different from the control, $**P < 0.01$, $***P < 0.001$.

Phagocytes resulted the most abundant immune cells in both micro-PS and controls (Figure 1.4). No significant differences were detected among immune cell types, except for an increase of red amoebocytes, more evident in sea urchins exposed to smaller micro-PS (10 μm). Indeed, the ratio between red and white amoebocytes (R/W) was significantly higher in specimens exposed to the 10μm micro-PS at all experimental times compared to controls (Figure 1.5). This increase was detectable after 48 and 72h of exposure also in sea urchins exposed to PS-MPs-45 μm (Figure 1.5).
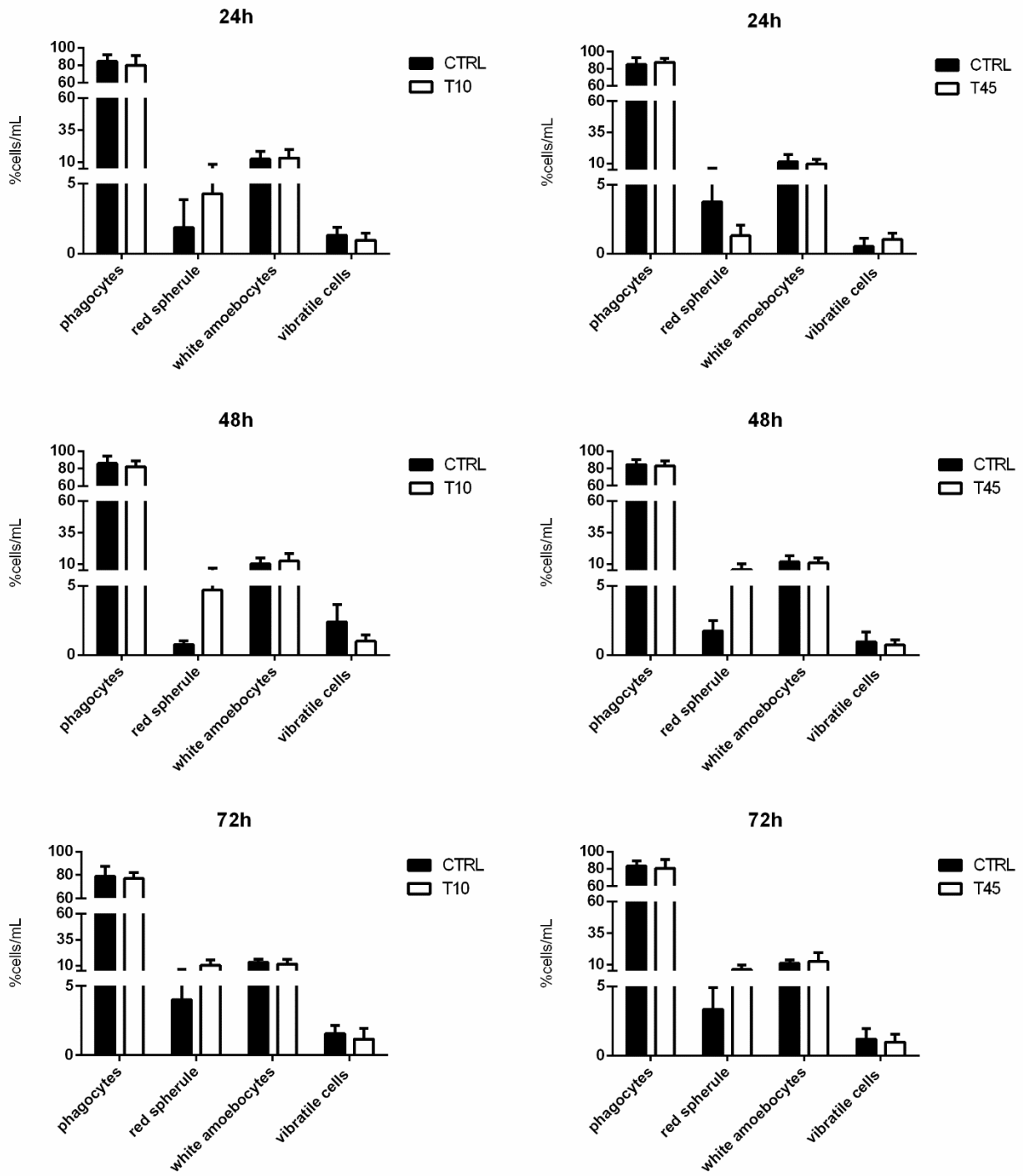
Figure 1.4. Immune cells morphology of sea urchin at different time of exposure to a PS-MPs (10 and 45 mm). Bars represent mean ± SD.
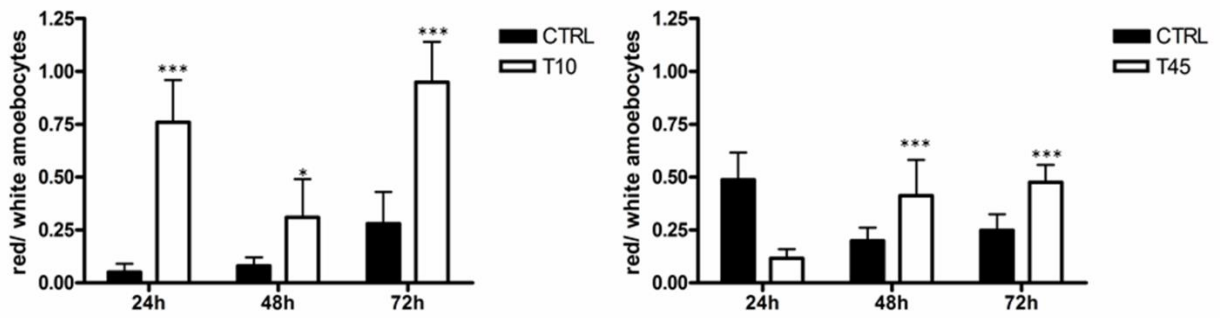
Figure 1.5. Ratio between red (%) and white amoebocytes (%) of sea urchin at different time of exposure to a PS-MPs (10 and 45μm). All data were analyzed by Two-way ANOVA followed by Bonferroni post-test compared with the respective control. Bars represent mean ±SD. Asterisks indicate values that are significantly different from the control, *P < 0.05, ***P < 0.001.

1.3.4 Intracellular levels of ROS and RNS

An increase of intracellular levels of ROS and RNS in coelomocytes was observed after 24h exposure to micro-PS regardless to their size. At 48h and 72h, the levels of both ROS and RNS in coelomocytes were comparable in control and micro-PS treated animals (Figure 1.6, Supplementary data Figure S1.4 and S1.5).
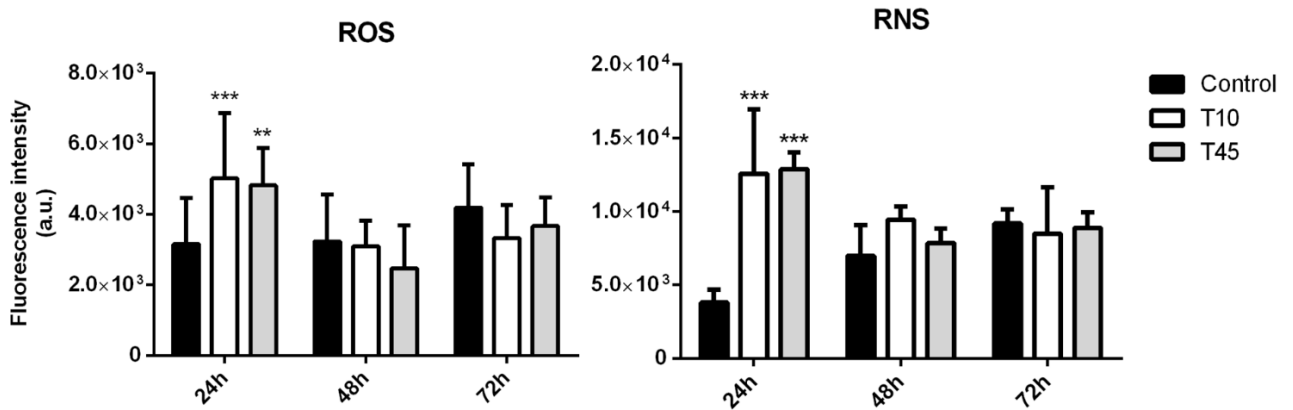
Figure 1.6 Intracellular ROS and RNS levels at different time of exposure to a PS-MPs (10 μm and 45 μm). All data were analyzed by Two-way ANOVA followed by Tukey's post-test compared with the respective control, **P<0.01, ***P < 0.001. Bars represent mean ±SD.

1.3.5 Total antioxidant capacity

Upon exposure to smaller micro-PS (10 μm), coelomocytes showed a significant increase of total antioxidant capacity compared to the controls. No effect was observed with micro-PS-45μm treatment (Figure 1.7).
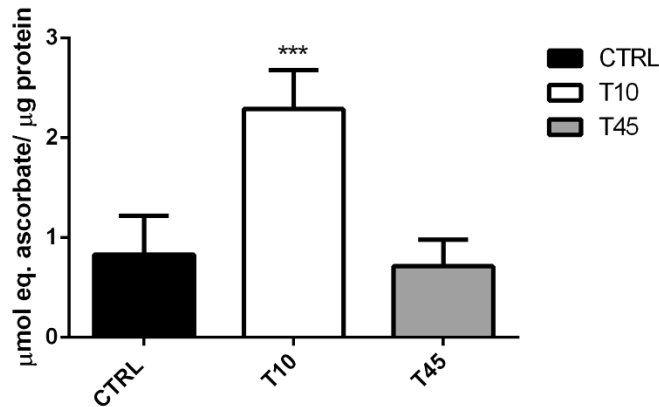
Figure 1.7 Total antioxidant activity of coelomocytes after 72h of exposure to PS-MPs (10 μm and 45 μm). All data were analyzed by Two-way ANOVA followed by Tukey's post-test compared with the respective control, ***$P < 0.001$. Bars represent mean ±SD.

1.4 Discussion

The results reported in this study highlighted for the first time a size-dependent uptake and distribution of micro-PS in the adult sea urchin *P. lividus* and their impact on circulating immune cells through *in vivo* exposure.

The different localization of micro-PS of different size is striking. While the 45 μm micro-PS were particularly abundant in the digestive system, more than 70% of the smaller micro-PS (10 μm) were found in the water vascular system. An important observation regards the higher amount of bigger micro-PS (45 μm) in the sea urchin' gonads compared to smaller ones (10 μm). These differences could be due to a potential sorting action of the madreporite, facilitating the penetration, as well as the consequent excretion, of the smaller micro-PS. However, also the dynamics of the micro-PS retention and egestion processes as well as the capability of organs to retain the particles of different size could play a significant role in the observed differential uptake. The presence of micro-PS in the sea urchin' aquifer system may affect important functions such as movement, feeding and breathing, although the continuous influx/efflux of seawater may reduce longer retention. Nevertheless, sea urchins in comparison with other echinoderms show relatively slow circulation in the aquifer system and therefore might be more affected by potential particles retention (Ferguson, 1996). As far as

digestive system, a longer retention time could be predicted based on the estimates by Lawrence et al. (1989) which are between 8 and 40h. No micro-PS was detected in the coelomic fluid after 72h of exposure suggesting that translocation across sea urchin tissues is unlikely. The ability of 10 μm micro-MPs to penetrate biological barriers and to move in different tissues has been already described in both freshwater and marine mussels as *Dreissena polymorpha* (Magni et al., 2018) and *Mytilus edulis* (Browne et al., 2008). On the opposite, no translocation has been reported in the shore crab *Carcinus maenas* upon waterborne exposure to micro-PS of same size (Watts et al., 2014). Despite limited information, such processes appear to be species-specific and uptake and translocation dynamics might significantly affect micro-PS distribution.

Despite the sea urchin is a benthic grazer and not a filter-feeder, the micro-PS retention inside different organs clearly highlights potential ecological impacts (through trophic transfer) as well as human risks associated for instance to predation and the high consumption of sea urchins' gonads in the Mediterranean area (Carbery et al., 2018). The comparison of sea urchin micro-PS retention with what reported in other marine organisms (sea cucumbers, copepods, bivalves, crustaceans) is challenging due to differences in feeding strategies, exposure scenarios, particles concentration and size (Browne et al., 2008; Graham & Thompson., 2009; Cole et al., 2013, 2015; Setälä et al., 2015; Sussarellu et al., 2016; Welden & Cowie, 2016; Sun et al., 2017). On the other hand, our results showed that sea urchin has a good ability to accumulate micro-PS, considering that the total number of micro-PS for each gram of tissue ranged between 0.46 – 1.65 % initial concentration. This is still relevant, even though it is less than what reported in other organisms such as shore crab gills (0.39 – 7.7% initial concentration) (Watts et al., 2014). The higher amount of the larger micro-PS (45 μm) in the gonads compared to the smaller micro-PS (10 μm) may significantly affect the reproductive success of sea urchin in analogy to what is reported in oysters, which showed negative effects on the reproductive health indices, quality and quantity of gametes, and fecundity (Sussarellu et al., 2016).

Our study showed for the first time the ability of adult sea urchins to accumulate micro-PS from sea water and distribute them to various organs according to their size. Although no data are currently available on the occurrence of microplastics in sea urchin specimens from the Gulf of Naples and generally from the Mediterranean Sea, such findings clearly suggest potential risk scenarios for sea urchin's local population. In fact, coastal areas of the Mediterranean Sea have been recently identified as hot spots of microplastic pollution (Compa et al., 2019). In the coastal environments *P. lividus* controls the dynamic, structure and composition of shallow macroalgal assemblages through its grazing activity and represents also a food source for fishes and other animals, including humans. Sea urchin predators which include gastropods, shore crabs, fish and star fish will then receive microplastics from their prey and then transfer them along the trophic food web allowing

bioaccumulation and biomagnification (Boudouresque & Verlaque, 2001).

The presence of MPs in the seafood might represent a further threat to human health due to their consumption (van Cauwenberghe & Janssen, 2014). Although sea urchin eggs consumption is heterogeneously distributed along the Mediterranean countries, it has been reported for instance an annual pro-capita consumption of about 1.1 kg in the Island of Sardinia, NW Mediterranean (Carboni et al., 2012). Based on our findings (see paragraph 1.3.2) on the micro-PS occurrence in sea urchin' gonads (about 12% of the 45 µm internalized particles/g fresh tissue), one year based consumption of sea urchin eggs could be around 5.5-19 particles g^{-1} fresh gonads. These findings are comparable to similar estimates for shrimp annual consumption of about 175 microplastic particles per person per year (considering scenario that 90% of microplastics will be removed) (Devriese et al., 2015). Van Cauwenberghe & Janssen (2014) estimated that in Europe molluscs consumers ingest up to 11,000 microplastics per year, a larger quantity compared to results obtained in this study considering only the edible part of the sea urchin without considering ejection mechanisms. Nevertheless, an annual dietary exposure based on species of high commercial value in the Mediterranean Sea, such as mussels and gonads of sea urchins, raises the issue of the impact of microplastics on seafood quality, even though it is still early for a proper risk assessment on human health. Field measurements of the presence of MPs inside sea urchin wild specimens collected from Mediterranean coastal areas, more densely populated as the Southern Thyrrenian coasts (i.e. the Gulf of Naples), will elucidate the real exposure scenarios and will allow to assess any potential risk for sea urchin populations and human health. Considering model-based projections, the coastal areas could be more impacted by MPs, reaching up higher levels than predicted due to specific regional and local input (Jambeck et al., 2015). For this reason, although egestion has not been investigated in the present study, we cannot disregard that the observed accumulation and toxicological effects might describe a real scenario under chronic exposure conditions.

An important outcome of this study is the analysis of the impact of MPs on immune cells. In sea urchins, cell-mediated immune response is played by heterogeneous free circulating cells, coelomocytes (Smith, 2010). The three cell types of coelomocytes, phagocytes, vibratile cells and red and white amoebocytes, have been recognized to perform functions similar to those of the vertebrate blood cells (Ito et al., 1992; Smith et al., 1995; Pinsino & Matranga, 2015). Sea urchin immune cells have been proposed as biosensors of several environmental stressors such as temperature shock, sea water acidification, UV-B radiation, and more recently nanoplastics (Matranga et al., 2000; Matranga et al., 2006; Marquez-Santos et al., 2018; Migliaccio et al., 2019). The major findings on the impact of micro-PS on sea urchin's immune cells underlined a stress syndrome as outlined below.

Although micro-PS were not found in the coelomic fluid, the number of immune cells increased after 24h compared to the control for both micro-PS suggesting the induction of proliferation. The increase in the number of coelomocytes has been also reported for the sea urchin *S. purpuratus*, as due to cell release from hematopoietic tissues in response to specific immune challenges and to a lesser extent, about 10%, to cell proliferation (Golconda et al., 2019). The higher increase of coelomocytes in *P. lividus* adults exposed to the smaller micro-PS (10 µm) than to the larger ones (45 µm) could be due to their presence in the stone canal which could stimulate coelomocytes production by an unknown mechanism. Indeed, the stone canal is located at the lateral edge of the axial organ which is recognized as one of the potential coelomocyte production site (Ramírez-Gómez and García-Arrarás, 2010; Golconda et al., 2019). A significant increase in the ratio of red to white amoebocytes compared to the controls was also observed after 24h of exposure to micro-PS 10 µm and after 48h and 72h to 45 µm micro-PS. These results are in line with previous studies showing an increase in the percentage of red amoebocytes under stress conditions even though the total number of coelomocytes remain constant (Matranga et al., 2005; Pinsino et al., 2008). The significant increase of ROS and RNS levels in coelomocytes after 24h and their subsequent recovery to control values upon exposure to both micro-PS 10 and 45 µm suggest that coelomocytes can cope with micro-PS mitigating the concentration of these reactive species. Levels of ROS and RNS play an important role as regulatory mediators in signalling processes (Gonzàles et al., 2015; Di Meo et al., 2016). Although it is widely known that MPs can induce ROS generation (Jeong et al., 2016, 2017; Prinz & Korez, 2019), this is the first report of an increase in RNS levels following micro-PS exposure. Increased levels of ROS have been also reported in haemocytes of *M. edulis* treated with micro-PS (2 – 6 µm) (Paul-Pont et al., 2016). Similar results were reported for haemocytes of the blue mussel *Mytilus* spp. after exposure to a mixture of micro polyethylene and polypropylene (20 µm) at different concentrations (Revel et al., 2019).

Generally, oxidative damage is the result of the imbalance between the formation of free radicals, including ROS and RNS, and the production of antioxidants (Ghiselli et al., 2000; de Almeida et al., 2007). When ROS and RNS are overproduced, they induce lipid oxidation/nitration and damage to proteins and DNA (Lesser, 2006; Gonzàles et al., 2015). The observed differential increase in total antioxidant capacity levels in coelomocytes of sea urchins exposed to 10 µm micro-PS than in those exposed to 45µm micro-PS suggests a size-dependent reaction, with smaller particles inducing a greater production of antioxidants than bigger ones. This could be due to the higher capacity of smaller particles to interact or aggregate with other cellular or extra-cellular components. The antioxidant capacity has a dynamic profile with increases or decreases depending on the time exposure and concentration of the stressors (Lushchak, 2011). Indeed, increased antioxidant

enzymatic activities have been reported after exposure to micro-PS in gills and digestive gland of *Scrobicularia plana* (Ribeiro et al., 2017), in the whole body of *Brachionus koreanus* (Jeong et al., 2016), and *Paracyclopina nana* (Jeong et al., 2017). By contrast, a decrease in the antioxidant enzyme activities has been reported in the digestive system of mussels after exposure to micro-PS (Avio et al., 2015; Paul-Pont et al., 2016).

Overall our results on ROS/RNS and total antioxidant capacity suggest that the sea urchin is able to restore basal redox homeostasis at the level of coelomocytes after 72 hours of PS-MPs exposure.

1.5 Conclusions

Although microplastic pollution has received considerable attention in recent years, no study has been carried out on their potential effects on adult sea urchins. In this context, this study acts as a pivotal investigation to understand the key factors that determine microplastics accumulation in sea urchin, thus providing also the necessary background for future biomonitoring campaigns. Precisely, the present study shows for the first time how sea urchin may represent suitable model organisms to highlight different uptake routes and toxic effects caused by the exposure to micro-PS of different sizes. The outcomes of this work provide first insights into the effects of MPs on marine benthic grazers with potential implications at ecological and human health levels. Also, these results will provide the basis for future studies to investigate how other particle sizes, polymers, and the biofilm may influence the uptake and biodistribution as well as immune-reactivity in *P. lividus*.

Chapter 1-Supplementary material

Polystyrene microbeads

Working solutions (10^4 particles mL^{-1}) of micro-PS (10 µm and 45µm) were prepared in deionized water and then added to exposure sea water to reach the final concentration of 10 particles mL^{-1}. Stock and working solution were vortexed for 3 minutes prior to use. The shape and size of microplastics stated by the supplier were confirmed by microscopy analysis. In Figure S1.1, fluorescent labelled micro-PS images obtained by using ApoTome Axio Cam Bright-field (left) and 503-GFP filter (right) were used for further confirmation of their dimension (45 **(A)** and 10µm **(B)**) and fluorescence (441 excitation/ 485 emission) as declared by company.
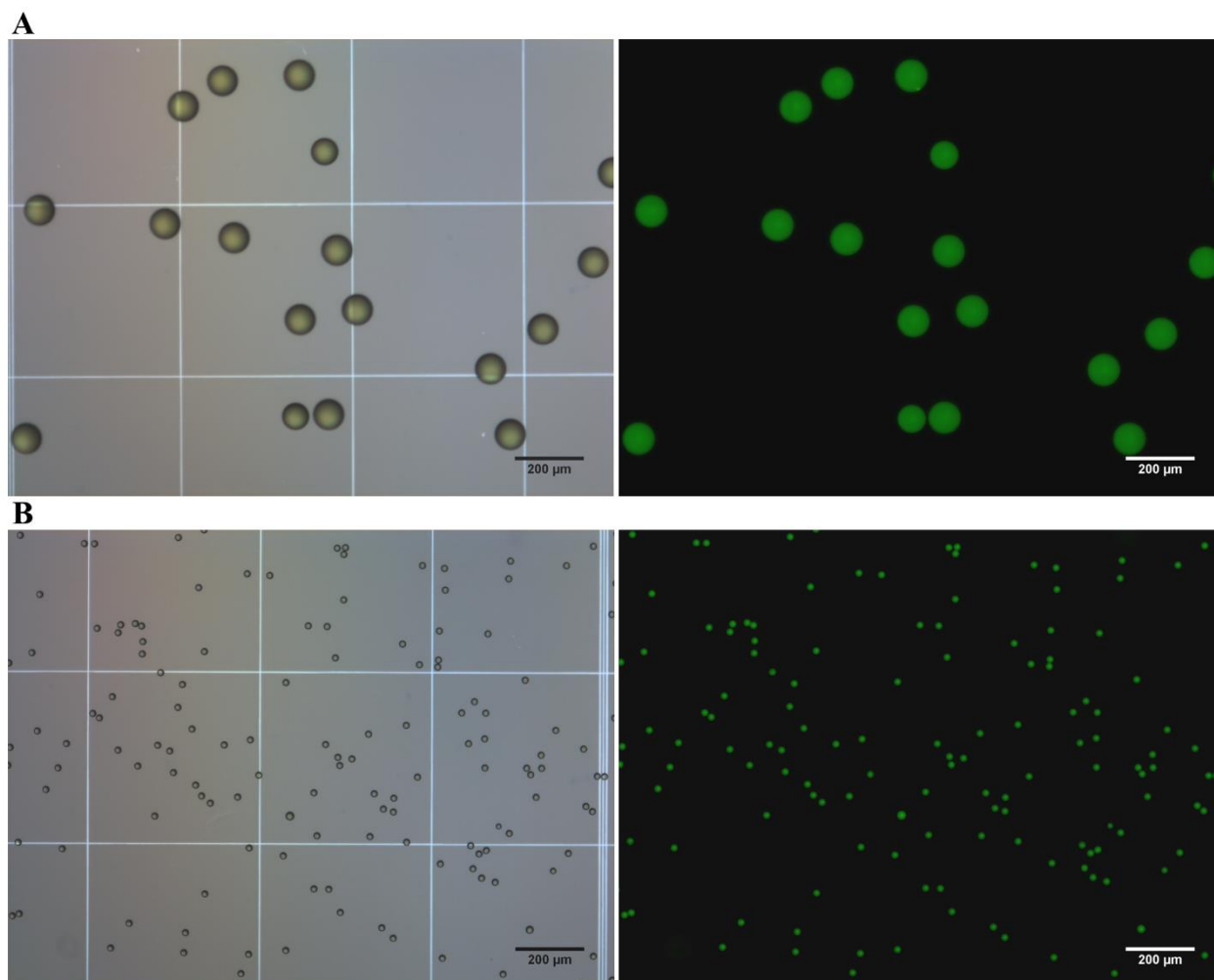
Figure S1.1. Fluorescent-labelled polystyrene microbeads (441 excitation/ 485 emission) of 45 **(A)** and 10µm **(B).** Images were captured using ApoTome Axio Cam Bright-field (left) and 503-GFP filter (right).
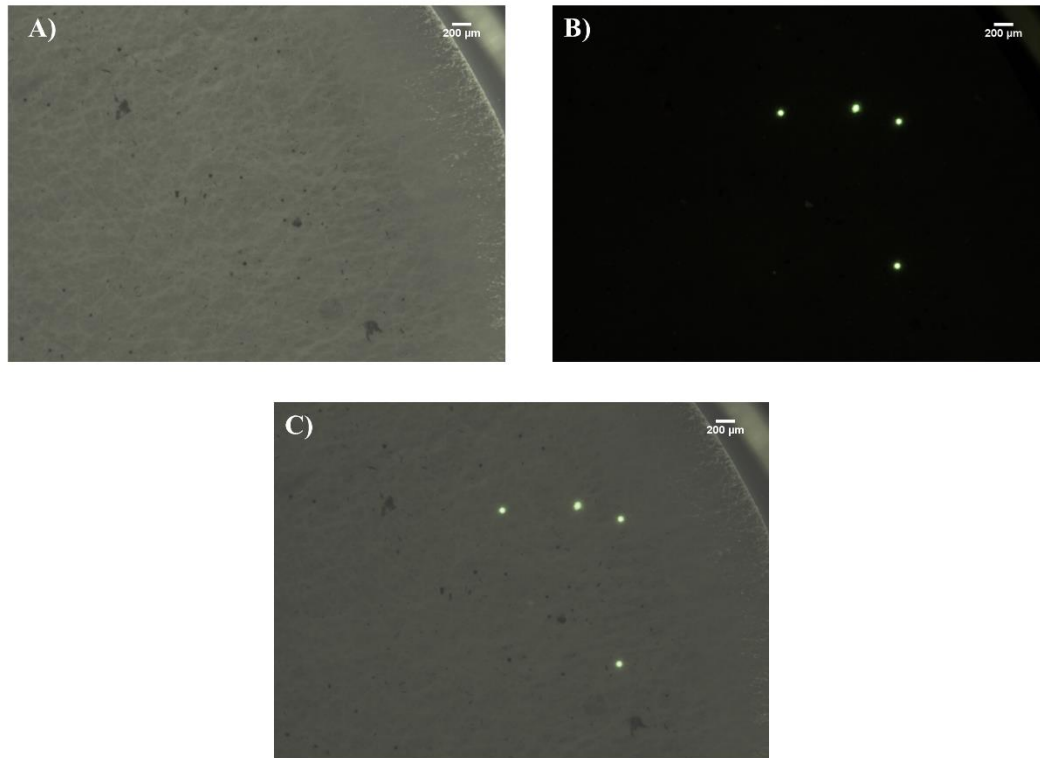
Figure S1.2. Representative images of fluorescent-labelled polystyrene microbeads (45µm) on cellulose acetate membrane filters (0.45 µm) after digestion process. Images were captured using ApoTome Axio Cam Bright-field (A), 503-GFP filter (B), merge channels (C).
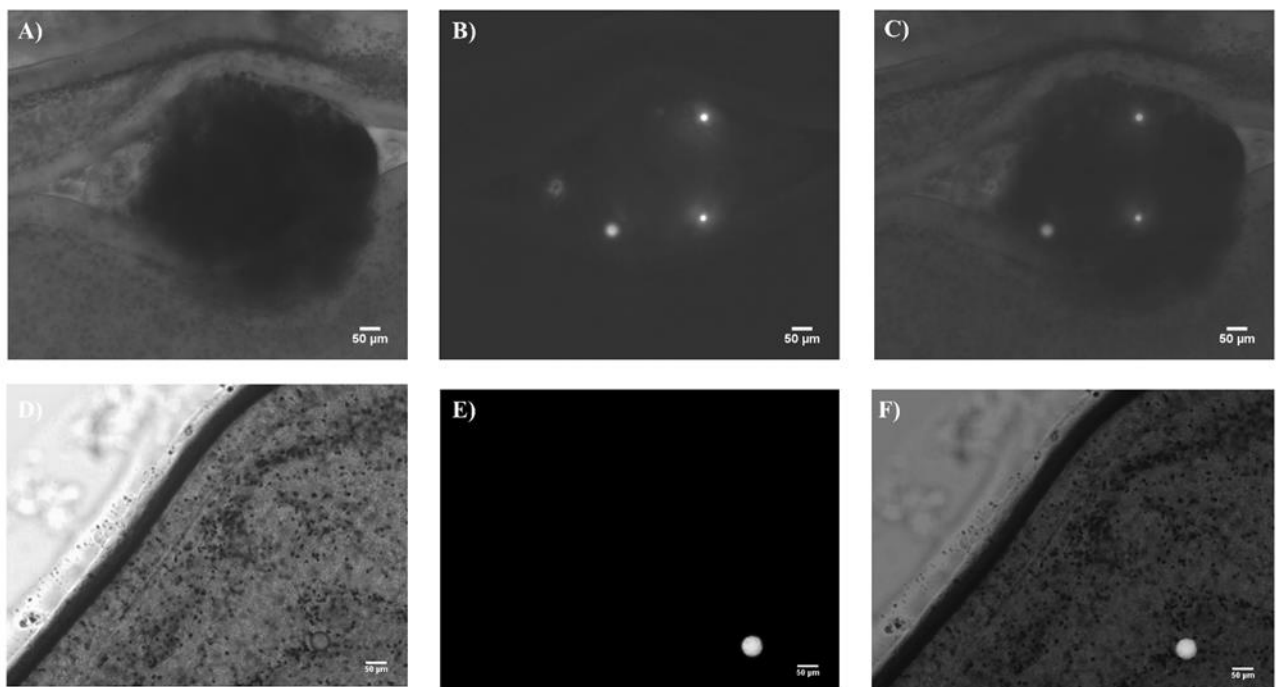
Figure S1.3. Representative images of fluorescent-labelled polystyrene microbeads (45µm) on cellulose acetate membrane filters (0.45 µm) after digestion process. Images were captured using ApoTome Axio Cam Bright-field (A), 506-mono filter (B), merge channels (C).

Table S1. MPs concentration used in ecotoxicological studies performed in the last 5 years using different aquatic model organisms.

| Model system	Polymer	Size	Concentration	Reference
Danio rerio	PS	5 μm and 20 μm	20 mg/L (2.9×10^5 MPs mL^{-1} for 5-μm, 4.5×10^3 MPs mL^{-1} for 20-μm)	Lu et al., 2016
Mytilus edulis	PS	10, 30 and 90 μm	MiX: 10 μm (50 MPs mL^{-1}), 30 μm (50 MPs mL^{-1}) 90 μm (10 MPs mL^{-1}), Final: 110 MPs mL^{-1}	Van Cauwenberghe et al., 2015
Mytilus spp.	PS	2 μm and 6 μm	32 μg/L (1800 MPs mL^{-1} for 2 μm, 200 MPs mL^{-1} for 6 μm, final: 2×10^3 MPs mL^{-1})	Paul-Pont et al., 2016
Eriocheir sinensis	PS	5 μm	40μg/L (5.4×10^2 MPs mL^{-1}), 400μg/L (5.4×10^3 MPs mL^{-1}), 4000μg/L (5.4×10^4 MPs mL^{-1}) 40000μg/L (5.4×10^5 MPs mL^{-1})	Yu et al., 2018
Coastal invertebrate community	PS	10 μm	5,50, 250 MPs mL^{-1}	Setälä et al., 2015
Xenopus tropicalis	PS	1 and 10 μm	10,10^3, 10^5 MPs mL^{-1} for 1 μm; 0.1, 10, 10^3 MPs mL^{-1} for 10 μm	Hu et al., 2016
Artemia parthenogenetica,	PS	10 μm	1 and 10 MPs mL^{-1}	Wang et al., 2019
Chlamys farreri	PS	2 μm	125 μg L^{-1}	Xia et al., 2019
Paracyclopina nana	PS	0.05-, 0.5-, and 6-μm	10 μg mL^{-1}	Jeong et al., 2017
Cladocopium goreaui	PS	1 μm	9.0×10^9 MPs L^{-1}	Su et al., 2020
Neomysis japonica	PS and PS-COOH	5 μm	10, 50, 250, 1250, 6250 μg L^{-1}	Wang et al.,2020
Mytilus galloprovincialis	PS and PE	<100 μm	1.5 g L^{-1}	Avio et al., 2015
Danio rerio	PS and HDPE	90% <90 μm; 50% <50 μm; 10% <25 μm	100 μg L^{-1},1000 μg L^{-1}	Limonta et al., 2019
Mytilus edulis	HDPE	< 50 μm = 35−45%, < 63 μm = 60−80%, < 80 μm	2.5 g mL^{-1}	Von moos et al., 2018
Ostrea edulis	PE and PLA		low (0.8 μg L^{-1}) high (80 μg L^{-1})	Green, 2016
Mytilus edulis	PE and PHB	10–90 μm	1000 MPs mL^{-1}	Magara et al., 2019
Crassostrea gigas	PE and PP	<400 μm	0, 0.008, 10, 100 μg L^{-1}	Revel et al., 2020
Danio rerio	PE,PA,PS,PVC, PP	PA, PE, PVC, PP (<200 μm) PS (0.1, 1, 5 μm)	0.001, 0.01, 0.1, 1.0, 10 mg L^{-1}	Lei et al., 2017
Calanus helgolandicus	LDPE, Nylon, PET	LDPE (10-20, 20-27, 27- 32 μm); Nylon (20, 10x40, 23 x100 μm); PET(17x60; 23x 70 μm)	100 MPs mL^{-1}	Coppock et al., 2019
Dicentrarcus labrax	PET	1–5 μm diameter	0.26 mg L^{-1} (MPs-low) and 0.69 mg L^{-1} (MPs-high)	Barboza et al., 2018
Mytilus edulis	PVC	1 to 75 μm	20 MPs mL^{-1}	Li et al., 2020

ROS production in immune cells

A)
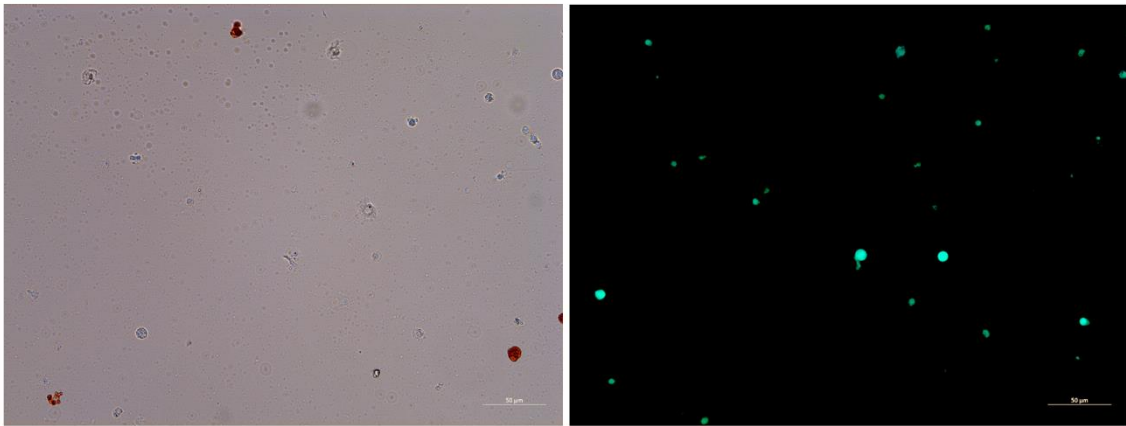
B)
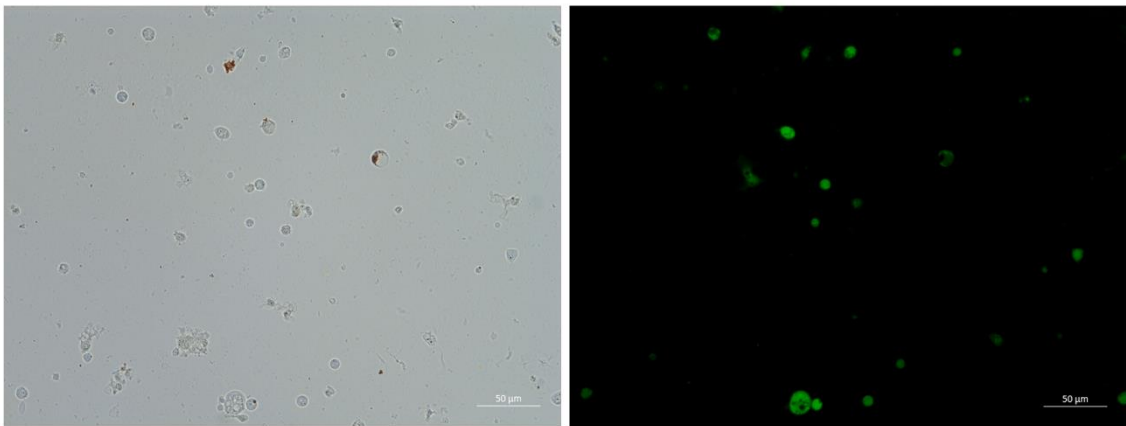
C)

Figure S1.4. ROS production in immune cells of sea urchins. Representative images of immune cells after 24h sea urchin exposure to PS-MPs: (A) Control group, (B) PS-MPs 10 µm treatment, (C) PS-MPs 45 µm treatment. Detection by the ROS sensitive dye DCF-DA. Images were captured using ApoTome Axio Cam Bright-field (left) and 503-GFP filter (right).

RNS production in immune cells

A)

B)

C)

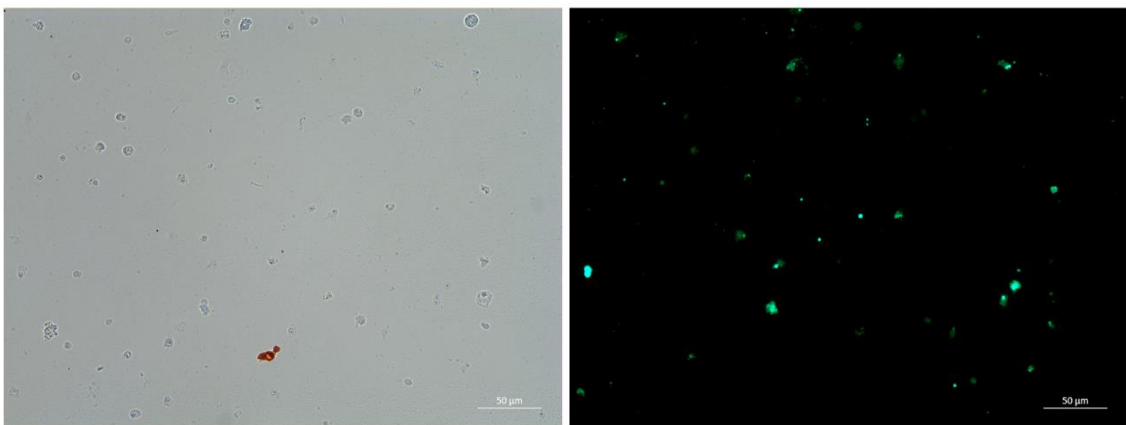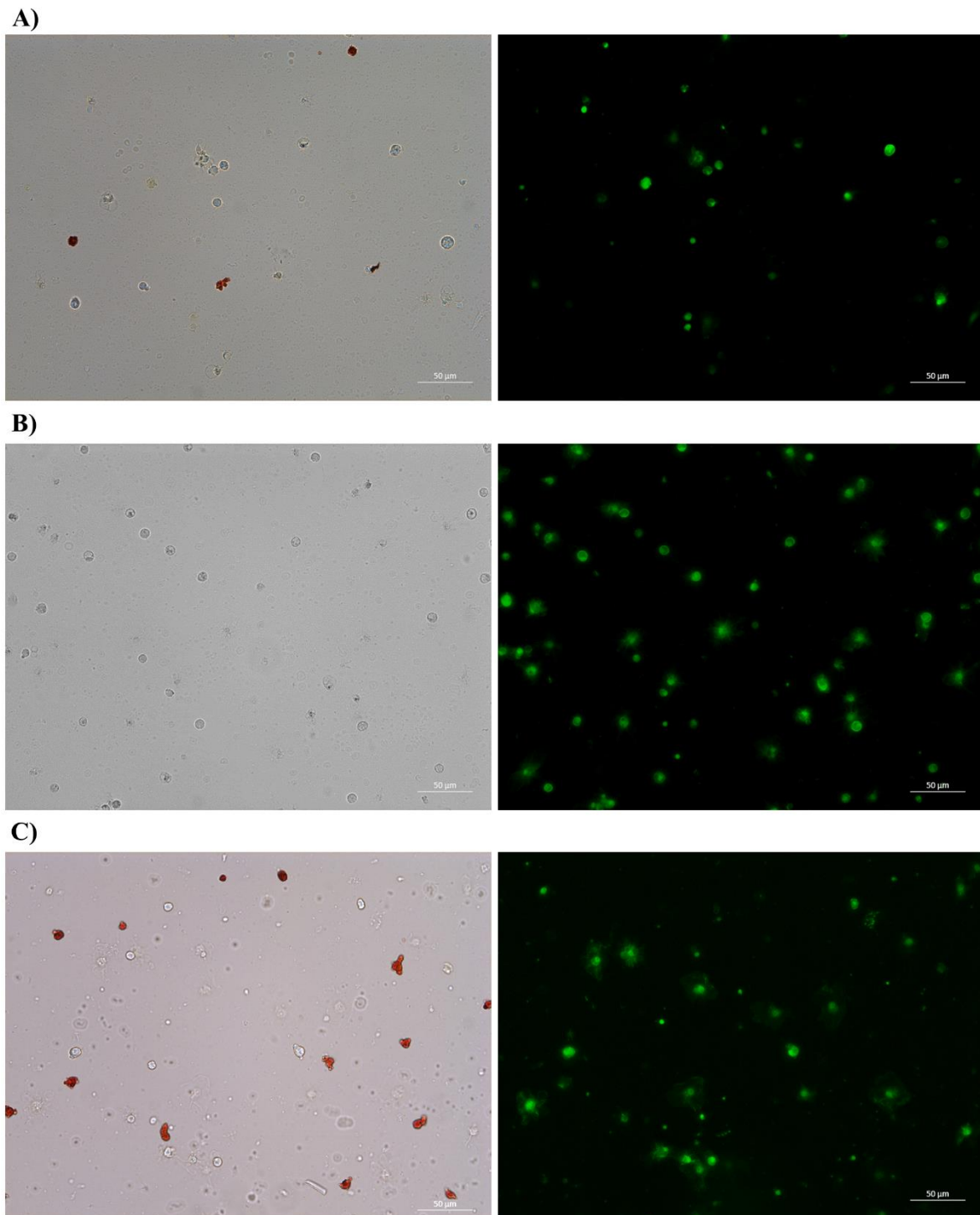**Figure S1.5** RNS production in immune cells of sea urchins. Representative images of immune cells after 24h sea urchin exposure to PS-MPs: (A) Control group, (B) PS-MPs 10 µm treatment, (C) PS-MPs 45 µm treatment. Detection by the RNS sensitive dye DAF-DA. Images were captured using ApoTome Axio Cam Bright-field (left) and 503-GFP filter (right).

References

Andrady, A.L., 2017. The plastic in microplastics: a review. *Marine Pollution Bulletin 119*, 12-22. https://doi.org/10.1016/j.marpolbul.2017.01.08 2

Avio, C.G., Gorbi, S., Milan, M., Benedetti, M., Fattorini, D., d'Errico, G., Bargelloni, L., Regoli, F., 2015. Pollutants bioavailability and toxicological risk from microplastics to marine mussels. *Environmental Pollution* 198, 211-222. http://dx.doi.org/10.1016/j.envpol.2014.12.021

Barboza, L. G. A., Viera, L. G., Guilhermino, L., 2018. Single and combined effects of microplastics and mercury on juveniles of the European seabass (*Dicentrarchus labrax*): Changes in behavioural responses and reduction of swimming velocity and resistance time. *Environmental Pollution* 236, 1014-1019. https://doi.org/10.1016/j.envpol.2017.12.082

Beiras, R., Tato, T., 2019. Microplastics do not increase toxicity of a hydrophobic organic chemical to marine plankton. *Marine Pollution Bulletin* 138, 58-62. https://doi.org/10.1016/j.marpolbul.2018.11.029

Bellas, J., Martìnez-Armental, J., Martìnez-Camàra, A., Besada, V., Martìnez-Gòmez, C., 2016. Ingestion of microplastics by demersal fish from the Spanish Atlantic and Mediterranean coasts. *Marine Pollution Bulletin* 109 (1), 55-60. https://doi.org/10.1016/j.marpolbul.2016.06.026

Besseling, E., Wang, B., Lürling, M., Koelmans, A.A., 2014. Nanoplastic affects growth of S. obliquus and reproduction of *D. magna*. *Environmental Science & Technology* 48 (20), 2336-12343. https://doi.org/10.1021/es503001d

Boudouresque, C.F., Verlaque, M., 2001. Ecology of *Paracentrotus lividus*. In: Lawrence JM (ed) Edible sea urchins: biology and ecology. *Elsevier*, Amsterdam, Chapter 13, 177–216. https://doi.org/10.1016/S0167-9309(07)80077-9

Bour, A., Avio, C.G., Gorbi, S., Regoli, F., Hylland, K., 2018. Presence of microplastics in benthic and epibenthic organisms: Influence of habitat, feeding mode and trophic level. *Environmental Pollution 243Part B,* 1217-1225. https://doi.org/10.1016/j.envpol.2018.09.115

Browne, M.A., Dissanayake, A., Galloway, T.S., Lowe, D.W., Thompson, R., 2008. Ingested microscopic plastic translocates to the circulatory system of the mussel, *Mytilus edulis* (L.). *Environmental Science & Technology* 42, 5026–5031. https://doi.org/10.1021/es800249a

Carbery, M., O' Connor, W., Palanisami, T., 2018. Trophic transfer of microplastics and mixed contaminants in the marine food web and implications for human health. *Environ International* 115, 400-409. https://doi.org/10.1016/j.envint.2018.03.007

Carboni, S., Addis, P., Cau, A., Atack, T., 2012. Aquaculture could enhance Mediterranean Sea urchin fishery, expand supply. *The Global Aquaculture Advocate* 15, 3: 44–4.

Cau, A., Avio, C.G., Dessì, C., Follesa, M.C., Moccia, D., Regoli, F., Pusceddu, A., 2019. Microplastics in the crustaceans *Nephrops norvegicus* and *Aristeus antennatus*: Flagship species for deep-sea environments?. *Environmental Pollution* 255 *Part* 1, 113107. https://doi.org/10.1016/j.envpol.2019.113107

Cincinelli, A., Martellini, T., Guerranti, C., Scopetani, C., Chelazzi, D., Giarrizzo T., 2019. A potpourri of microplastics in the sea surface and water column of the Mediterranean Sea. *Trends in Analytical Chemistry* 110, 321- 326. https://doi.org/10.1016/j.trac.2018.10.026

CNR-ISMAR Activity Report, 2017. "Microplastic investigation in water and trophic chain along the Italian coast 06/24/2017– 07/15/2017", 25.

Cole, M., Lindeque, P., Fileman, E., Clark, J., Lewis, C., Halsband, C., Galloway, T.S., 2016. Microplastics alter the properties and sinking rates of zooplankton fecal pellets. *Environmental Science & Technology* 50, 3239-3246. https://doi.org/10.1021/acs.est.5b05905

Cole, M., Lindeque, P., Fileman, E., Halsband, C., Galloway, T.S., 2015. The impact of polystyrene microplastics on feeding, function and fecundity in the marine copepod *Calanus helgolandicus*. *Environmental Science & Technology* 49 (2), 1130-1137. https://doi.org/10.1021/es504525u

Cole, M., Lindeque, P., Fileman, E., Halsband, C., Goodhead, R., Moger, J., Galloway, T.S., 2013. Microplastic ingestion by Zooplankton. *Environmental Science & Technology* 47, https://doi.org/12.10.1021/es400663f

Compa, M., Alomar, C., Wilcox, C., van Sebille, E., Lebreton, L., Hardesty, B.D., Deudero, S., 2019. Risk assessment of plastic pollution on marine diversity in the Mediterranean Sea. *Science of The Total Environment* 678, 188-196. https://doi.org/10.1016/j.scitotenv.2019.04.355

Compa, M., Ventero, A., Iglesias, M., Deudero, S., 2018. Ingestion of microplastics and natural fibres in *Sardina pilchardus* (Walbaum, 1972) and *Engraulis encrasicolus* (Linnaeus, 1758). *Marine Pollution Bulletin* 128, 89-96. https://doi.org/10.1016/j.marpolbul.2018.01.009

Coppock, R. L., Galloway, T. S., Cole, M., Fileman, E. S., Queirós, A. M., Lindeque, P. L., 2019. Microplastics alter feeding selectivity and faecal density in the copepod, *Calanus helgolandicus*. *Science of The Total Environment* 687, 780-789. https://doi.org/10.1016/j.scitotenv.2019.06.009

Courtene-Jones, W., Quinn, B., Ewins, C., Gary, S.F., Narayanaswamy, B.E., 2019. Consistent microplastic ingestion by deep-sea invertebrates over the last four decades (1976-2015), a study from the North East Atlantic. *Environmental Pollution* 244, 503-512. https://doi.org/10.1016/j.envpol.2018.10.090

Còzar, A., Echevarrìa, F., Gonzàlez-Gordillo, J.I., Irigoien, X., Úbeda, B., Hernàndez-Leòn, S., Palma, Á.T., Navarro, S., Garcìa-de-Lomas, J., Ruiz, A., Fernàndez-de-Puelles, M.L., 2014. Plastic debris in the open ocean. *Proceedings of the National Academy of Sciences*, USA 111, 10239-10244. https://doi.org/10.1073/pnas.1314705111

Còzar, A., Sanz-Martìn, M., Martì, E., Gonzàlez-Gordillo, J.I., Úbeda, B., Gàlvez, J.A., Irigoien, X., Duarte, C.M., 2015. Plastic accumulation in the Mediterranean Sea. *PLoS One* 10 (4), 0121762. https://doi.org/10.1371/journal.pone.0121762

De Almeida, E.A., Bainy, A.C.D., de Melo Loureiro, A.P., Martinez, G.R., Miyamoto, S., Onuki, J., Barbosa, L.F., Machado Garcia, C.C., Prado, F.M., Ronsein, G.E., Sigolo, C.A., Barbosa Brochini, C., Gracioso Martins, A.M., de Medeiros, M.H.G., Di Mascio, P., 2007. Oxidative stress in *Perna perna* and other bivalves as indicators of environmental stress in the Brazilian marine environment: Antioxidants, lipid peroxidation and DNA damage. *Comparative Biochemistry and Physiology* 146, 588-600. https://doi.org/10.1016/j.cbpa.2006.02.040

Deng, Y., Zhang, Y., Lemos, B., Ren, H., 2017. Tissue accumulation of microplastics in mice and biomarker responses suggest widespread health risks of exposure. *Scientific Reports* 7, 46687. https://10.1038/srep46687

Devriese, L.I., Van de Meulen, M.D., Maes, T., Bekaert, K., Paul-Pont, I., Frère, L., Robbens, J., Vethaak, A.D., 2015. Microplastic contamination in brown shrimp (*Crangon crangon*, Linnaeus 1758) from coastal waters of the southern North Sea and channel area. *Marine Pollution Bulletin* 98, 179-187. https://doi.org/10.1016/j.marpolbul.2015.06.051

Di Meo, S., Reed, T.T., Venditti, P., Victor, M., 2016. Role of ROS and RNS Sources in Physiological and Pathological Conditions. *Oxidative Medicine and Cellular Longevity* 2016, 1245049. https://doi.org/10.1155/2016/1245049

Digka, N., Tsangaris, C., Torre, M., Anastasopoulou, A., Zeri, C., 2018. Microplastics in mussels and fish from the Northern Ionian Sea. *Marine Pollution Bulletin* 135, 30-40. https://doi.org/10.1016/j.marpolbul.2018.06.063

Duchaud, S., Durieux, E.D.H., Coupe, S., Pasqualini, V., Ternengo, S., 2018. Spatio-temporal patterns based on demographic and genetic diversity of the purple sea urchin *Paracentrotus lividus* in the area around Corsica (Mediterranean Sea). *Mediterranean Marine Science* 19, 620-641. http://dx.doi.org/10.12681/mms.14184

Duncan, E.M., Arrowsmith, J., Bain, C., Broderick, A.C., Lee, J., Metcalfe, K., Pikesley, S.K., Snape, R.T.E., van Sebille, E., Godley, B.J., 2018. The true depth of the Mediterranean plastic problem: extreme microplastic pollution on marine turtle nesting beaches in Cyprus. *Marine Pollution Bulletin* 136, 334-340. https://doi.org/10.1016/j.marpolbul.2018.09.019

Eklöf, J.S., de la Torre-Castro, M., Gullström, M., Uku, J., Muthiga, N., Lyimo, T., Bandeira, S.O., 2008. Sea urchin overgrazing of seagrasses: a review of current knowledge on causes, consequences, and management. *Estuarine, Coastal and Shelf Science* 79 (4), 569–580. https://doi.org/10.1016/j.ecss.2008.05.005

Ekvall, M., Ludquist, M., Kelpsiene, E., Sileikis, E., Gunnarsson, S.B., Cedervall, T., 2019. Nanoplastics formed during the mechanical breakdown of daily-use polystyrene products. *Nanoscale Advances* 1, 1055-1061. https://doi.org/10.1039/C8NA00210J

Eriksen, M., Lebreton, L.C.M., Carson, H.S., Thiel, M., Moore, C.J., Borerro, J.C., Galgani, F., Ryan, P.G., Reisser, J., 2014. Plastic pollution in the world's oceans: more than 5 trillion plastic pieces weighing over 250,000 tons afloat at sea. *PLoS One* 9 (12),111913. https://doi.org/10.1371/journal.pone.0111913

Ferguson J.C., 1996. Madreporite function and fluid volume relationships in sea urchins. *Biology Bullettin* 191, 431-440.

Fossi, M.C., Panti, C., Guerranti, C., Coppola, D., Giannetti, M., Marsili, L., Minutoli, R., 2012. Are baleen whales exposed to the threat of microplastics? A case study of the Mediterranean fin whale (*Balaenoptera physalus*). *Marine Pollution Bulletin* 54 (11), 2374-2379. https://doi.org/10.1016/j.marpolbul.2012.08.013

Geyer, R., Jambeck, J.R., Lavender, K., 2017. Production, use, and fate of all plastics ever made. *Science Advances* 3 (12), 1700782. https://10.1126/sciadv.1700782

Ghiselli, A., Serafini, M., Natella, F., Scaccini, C., 2000. Total antioxidant capacity as a tool to assess redox status: critical view and experimental data. *Free Radical Biology & Medicine* 29, 1106-1114. https://doi.org/10.1016/S0891-5849(00)00394-4

Giani, D., Baini, M., Galli, M., Casini, S., Fossi, M.C., 2019. Microplastics occurence in edible fish species (*Mullus barbatus* and *Merluccius merluccius*) collected in three different geographical sub-areas of the Mediterranean Sea. *Marine Pollution Bulletin* 140, 129–137. https://doi.org/10.1016/j.marpolbul.2019.01.005

Golconda, P., Buckley, K.M., Reynolds, C.R., Romanello, J.P., Smith, L.C., 2019. The Axial Organ and the Pharynx are sites of hematopoiesis in the Sea Urchin. *Frontiers in Immunology* 10, 870. https://doi.org/10.3389/fimmu.2019.00870

González, P.M., Malanga, G., Puntarulo, S., 2015. Cellular Oxidant/Antioxidant Network: update on the environmental effects over marine organisms. *The Open Marine Biology Journal* 9, 1-13. https://doi.org/10.2174/1874450801509010001

Graham, E.R., Thompson, J.T., 2009. Deposit- and suspension-feeding sea cucumbers (*Echinodermata*) ingest plastic fragments. *Journal of Experimental Marine Biology and Ecology* 368 (1), 22-29. https://doi.org/10.1016/j.jembe.2008.09.007

Green, D. S., 2016. Effects of microplastics on European flat oysters, *Ostrea edulis* and their associated benthic communities. *Environmental Pollution* 216, 95-103. https://doi.org/10.1016/j.envpol.2016.05.043

Güven, O., Gökdağ, K., Jovanović, B., Kıdeyş, A.E., 2017. Microplastic litter composition of the Turkish territorial waters of the Mediterranean Sea, and its occurrence in the gastrointestinal tract of fish. *Environmental Pollution* 223, 286-294. https://doi.org/10.1016/j.envpol.2017.01.025

Hartmann, N.B., Hüffer, T., Thompson, R.C., Hassellöv, M., Verschoor, A., Daugaard, A.S., Rist, S., Karlsson, T., Brennholt, N., Cole, M., Herrling, M.P., C. Hess, M.C., Ivleva, N.P., Lusher, A.L., Wagner, M., 2019. Are we speaking the same language?. Recommendations for a definition and categorization framework for plastic debris. *Environmental Science & Technology* 53, 1039-1047. https://doi.org/10.1021/acs.est.8b05297

Hu, L., Su, L., Xue, Y., Mu, J., Zhu, J., Xu, J., Shi, H., 2016. Uptake, accumulation and elimination of polystyrene microspheres in tadpoles of *Xenopus tropicalis*. *Chemosphere* 164, 611-617. http://dx.doi.org/10.1016/j.chemosphere.2016.09.002

Ito, T., Matsutani, T., Mori, K., Nomura, T., 1992. Phagocytosis and hydrogen peroxide production by phagocytes of the sea urchin *Strongylocentrotus nudus*. *Developmental and Comparative Immunology* 16, 272-294. https://doi.org/10.1016/0145-305X(92)90003-U

Jacinto, D., Bulleri, F., Benedetti-Cecchi, L., Cruz, T., 2013. Patterns of abundance, population size structure and microhabitat usage of *Paracentrotus lividus* (Echinodermata: *Echinoidea*) in SW Portugal and NW Italy. *Marine Biology* 160, 1135–1146.
https://doi.org/10.1007/s00227-013-2166-z

Jambeck, J.R., Geyer, R., Wilcox, C., Siegler, T. R., Perryman, M., Andrady, A., Narayan, R., Lavender, K., 2015. Plastic waste inputs from land into the ocean. *Science* 347 (6223), 768-771.
https://doi.org/10.1126/science.1260352

Jeong, C.B., Won, E.J., Kang, H.M., Lee, M.C., Hwang D.S., Hwang, U.K., Zhou, B., Souissi, S., Lee, S.J., Lee J.S., 2016. Microplastic Size-Dependent Toxicity, Oxidative Stress Induction, and p-JNK and p-p38 Activation in the Monogonont Rotifer (*Brachionus koreanus*). *Environmental Science & Technology 50* (16), 8849-8857. https://doi.org/10.1021/acs.est.6b01441

Jeong, C.B., Kang, H.M., Lee, M.C., Kim, D.H., Han, J., Hwang, D.S., Souissi, S., Lee, S.J., Shin, K.H., Park, H.G., Lee, J.S., 2017. Adverse effects of microplastics and oxidative stress-induced MAPK/Nrf2 pathway-mediated defense mechanisms in the marine copepod *Paracyclopina nana*. *Scientific Reports* 7, 41323. https://doi.org/10.1038/srep41323

Kaposi, K.L., Mo s, B., Kelaher, B.P., Dworjanyn, S.A., 2014. Ingestion of microplastic has limited impact on a marine larva. *Environmental Science & Technology* 48 (3), 1638−1645.
https://doi.org/10.1021/es404295e

Kooi, M., van Nes, E.H., Scheffer, M., Koelmans, A.A., 2017. Ups and downs in the ocean: Effects of biofouling on vertical transport of microplastics. *Environmental Science & Technology* 51,7963-7971. https://doi.org/10.1021/acs.est.6b04702

Kühn, S., van Werven, B., van Oyenc, A., Meijboom, A., Bravo Rebolledo, E. L.; van Franeker, J.A., 2017. The use of potassium hydroxide (KOH) solution as a suitable approach to isolate plastics ingested by marine organisms. *Marine Pollution Bulletin* 115, 86–90.
http://dx.doi.org/10.1016/j.marpolbul.2016.11.034

Lawrence, J., Régis, M. B., Delmas, P., Gras, G., Klinger, T., 1989. The effect of quality of food on feeding and digestion in *Paracentrotus lividus* (Lamarck) (Echinodermata: *Echinoidea*). *Marine Behaviour and Physiology* 15, 137-144. https://doi.org/10.1016/S0167-9309(07)80071-8

Lebreton, L., Andrady, A., 2019. Future scenarios of global plastic waste generation and disposal. *Palgrave Communications* 5, 6. https://doi.org/10.1057/s41599-018-0212-7

Lee, K.W., Shim, W.J., Kwon, O.Y., Kang, J.H., 2013. Size-dependent effects of micro-polystyrene particles in the marine copepod Tigriopus japonicas. *Environmental Science & Technology* 47, 11278-11282. https://doi.org/10.1021/es401932b

Lei, L., Liu, M., Song, Y., Lu, S., Hu, J., Cao, C., Xie, B., Shic, H., He, D., 2018. Polystyrene (nano)microplastics cause size-dependent neurotoxicity, oxidative damage and other adverse effects in *Caenorhabditis elegans*. *Environmental Science: Nano* 5, 2009-2020. https://doi.org/10.1039/C8EN00412A

Lefebvre, C., Saraux, C., Heitz, O., Nowaczyk, A., Bonnet, D., 2019. Microplastics FTIR characterization and distribution in the water column and digestive tracts of small pelagic fish in the Gulf of Lions. *Marine Pollution Bulletin*, 142, 510–519. https://doi.org/10.1016/j.marpolbul.2019.03.025

Lesser, M.P., 2006. Oxidative stress in marine environments: Biochemistry and Physiological Ecology. *Annuual Review Physiology* 68, 253–78. https://doi.org/10.1146/annurev.physiol.68.040104.110001

Li, J., Chapman, E.C., Shi, H., Rotchell, J., 2020. PVC Does Not Influence Cadmium Uptake or Effects in the Mussel (*Mytilus edulis*). *Bullettin Environmental Contamination & Toxicology* 104, 315–320. https://doi.org/10.1007/s00128-020-02789-x

Lobelle, D., Cunliffe, M., 2011. Early microbial biofilm formation on marine plastic debris. *Marine Pollution Bulletin* 62, 197-200. https://doi.org/10.1016/j.marpolbul.2010.10.013

Lu, Y., Zhang, Y., Deng, Y., Jiang, W., Zhao, Y., Geng, J., Ding, L., Ren, H., 2016. Uptake and accumulation of polystyrene microplastics in zebrafish (*Danio rerio*) and toxic effects in liver. *Environmental Science & Technology* 50 (7), 4054-6. https://doi.org/10.1021/acs.est.6b00183

Lushchak, V.I., 2011. Environmentally induced oxidative stress in aquatic animals. *Aquatic Toxicology* 101 (1), 13-30. https://doi.org/10.1016/j.aquatox.2010.10.006

Magni, S., Gagnè, F., Andrè, C., Della Torre, C., Auclair, J., Hanana, H., Parenti, C.C., Bonasoro, F., Binelli, A., 2018. Evaluation of uptake and chronic toxicity of virgin polystyrene microbeads in freshwater zebra mussel *Dreissena polymorpha* (Mollusca: *Bivalvia*). *Science of Total Environment* 637, 778-788. https://doi.org/10.1016/j.scitotenv.2018.03.075

Marques-Santos, L. F., Grassi, G., Bergami, E., Faleri, C., Balbi, T., Salis, A., Damonte, G., Canesi, L., Corsi, I., 2018. Cationic polystyrene nanoparticle and the sea urchin immune system: biocorona formation, cell toxicity, and multixenobiotic resistance phenotype. *Nanotoxicology* 12 (8), 847-867. https://10.1080/17435390.2018.1482378

Martínez-Gómez, C., León, V.M., Calles, S., Gomáriz-Olcina, M., Vethaak, A.D., 2017. The adverse effects of virgin microplastics on the fertilization and larval development of sea urchins. *Marine Environment Research* 130, 69-76. https://doi.org/10.1016/j.marenvres.2017.06.016

Matranga, V., Pinsino, A., Celi, M., Bonaventura, R., Natoli, A., Schröder, H.G., Müller, W.E.G., 2005. Monitoring Chemical and Physical Stress Using Sea Urchin Immune Cells. *Progress in molecular and subcellular biology* 39, 85-110. https://doi.org/10.1007/3-540-27683-1_5

Matranga, V., Pinsino, A., Celi, M., Di Bella, G., Natoli, A., 2006. Impacts of UV-B radiation on short-term cultures of sea urchin coelomocytes. *Marine Biology* 149, 25-34. https://doi.org/10.1007/s00227-005-0212-1

Matranga, V., Toia, G., Bonaventura, R., Muller, W., 2000. Cellular and biochemical responses to environmental and experimentally induced stress in sea urchin coelomocytes. *Cell Stress & Chaperones* 5, 113-120. https://doi.org/10.1379/1466-1268(2000)005<0113:cabrte>2.0.co;2

Milito, A., Murano, C., Castellano, I., Romano, G., Palumbo, A., 2020. Antioxidant and immune response of the sea urchin *Paracentrotus lividus* to different re-suspension patterns of highly polluted marine sediments. *Marine Environmental Research* 160, 104978. https://doi.org/10.1016/j.marenvres.2020.104978

Migliaccio, O., Pinsino, A., Maffioli, E., Smith, A.M., Agnisola, C., Matranga, V., Nonnis, S., Tedeschi, G., Byrne, M., Gambi, M.C., Palumbo, A., 2019. Living in feature ocean acidification, physiological adaptive responses of the immune system of sea urchins resident at CO_2 vent system. *Science of Total Environment* 672, 938-950. https://doi.org/10.1016/j.scitotenv.2019.04.005

Montuori, P., Lama, P., Aurino, S., Naviglio, D., Triassi, M., 2013. Metals loads into the Mediterranean Sea: Estimate of Sarno River inputs and ecological risk. *Ecotoxicology* 22 (2), 295-307. https://doi.org/10.1007/s10646-012-1026-9

Nobre, C.R., Santana, M.F.M., Maluf, A., Cortez, F.S., Cesar, A., Pereira, C.D.S., Turra, A., 2015. Assessment of microplastic toxicity to embryonic development of the sea urchin *Lytechinus variegatus* (Echinodermata: *Echinoidea*). *Marine Pollution Bulletin* 92, 99-104. https://doi.org/10.1016/j.marpolbul.2014.12.050

Palacin, C., Giribet, G., Carner, S., Dantart, L., Turin, X., 1998. Low density of sea urchins influence the structure of algal assemblages in the western Mediterranean. *Journal of Sea Research* 38 (3-4), 281–290. https://doi.org/10.1016/S1385-1101(97)00061-0

Paul-Pont, I., Lacroix, C., Gonzàaìlez Fernàndez, C., Hègaret, H., Lambert, C., Le Goïc, N., Frére, L., Cassone, A.L., Sussarellu, R., Fabioux, C., Guyomarch, J., Albentosa, M., Huvet, A., Soudant, P., 2016. Exposure of marine mussels *Mytilus* spp. to polystyrene microplastics: Toxicity and influence on fluoranthene bioaccumulation. *Environmental Pollution* 216, 724-737. http://dx.doi.org/10.1016/j.envpol.2016.06.039

Phuong, N.N., Zalouk-Vergnoux, A., Kamari, A., Mouneyrac, C., Amiard, F., Poirier, L., Lagarde, F., 2018. Quantification and characterization of microplastics in blue mussels (*Mytilus edulis*): protocol setup and preliminary data on the contamination of the French Atlantic coast. *Environmental Science and Pollution Research* 25, 6135–6144. https://doi.org/10.1007/s11356-017-8862-3

Pinsino, A., Della Torre, C., Sammarini, V., Bonaventura, S., Matranga, V., 2008. Sea urchin coelomocytes as a novel cellular biosensor of environmental stress: a field study in the Tremiti Island Marine Protected Area, Southern Adriatic Sea, Italy. *Cell Biology and Toxicology* 24, 541-552. https://doi.org/10.1007/s10565-008-9055-0

Pinsino, A., Matranga, V., 2015. Sea urchin immune cells as sentinels of environmental stress. *Developmental and Comparative Immunology* 49 (1), 198-205. https://doi.org/10.1016/j.dci.2014.11.013

Porter, A., Smith, K.E., Lewis, C., 2019. The sea urchin *Paracentrotus lividus* as a bioeroder of plastic. *Science of the Total Environment* 693, 133621. https://doi.org/10.1016/j.scitotenv.2019.133621

Prinz, N., Korez, S., 2020. Understanding How Microplastics Affect Marine Biota on the Cellular Level Is Important for Assessing Ecosystem Function: A Review. *YOUMARES 9 - The Oceans: Our Research, Our Future*; 101-120. https://doi.org/10.1007/978-3-030-20389-4_6

Qian, P.Y., Lau, S.C.K., Dahms, H.U., Dobretsov, S., Harder, T., 2007. Marine Biofilms as mediators of colonization by marine macroorganisms: implications for antifouling and aquaculture. *Marine Biotechnology* 9, 399-410. https://doi.org/10.1007/s10126-007-9001-9

Ramírez-Gómez, F., García-Arrará, J.E., 2010. Echinoderm immunity. *Invertebrate Survival Journal* 211-220. ISJ 7: 211-220, 2010

Revel, M., Lagarde, F., Perrein-Ettajani, H., Bruneau1, M., Akcha, F., Sussarellu, R., Rouxel, J., Costil, K., Decottignies, P., Cognie, B., Châtel, A., Mouneyrac, C., 2019. Tissue-Specific biomarker responses in the Blue Mussel *Mytilus* spp. exposed to a mixture of microplastics at environmentally relevant concentrations. *Frontiers in Environmental Science* 7, 33. https://doi.org/10.3389/fenvs.2019.00033

Ribeiro, F., Garcia, A.R., Pereira, B.P., Fonseca, M., Mestre, N.C., Fonseca, T.G., Ilharco, L.M., Bebianno, M.J., 2017. Microplastics effects in *Scrobicularia plana*. *Marine Pollution Bulletin* 122 (1–2), 379-391. https://doi.org/10.1016/j.marpolbul.2017.06.078

Rochman, C.M., 2015. The complex mixture, fate and toxicity of chemicals associated with lastic debris in the marine environment. In M. Bergmann, L. Gutow, & M. Klages (Eds), *Marine anthropogenic litter*, 117-140. https://doi.org/10.1007/978-3-319-16510-3_5

Romeo, T., Pietro, B., Pedà, C., Consoli, P., Andaloro, F., Fossi, M.C., 2015. First evidence of presence of plastic debris in stomach of large pelagic fish in the Mediterranean Sea. *Marine Pollution Bulletin* 95 (1), 358-361. https://doi.org/10.1016/j.marpolbul.2015.04.048

Sala, E., Boudouresque, C.F., Harmelin-Vivien, M.L., 1998. Fishing, trophic cascades, and the structure of algal assemblages: evaluation of an old but untested paradigm. *Oikos* 82 (3), 425–439. https://doi.org/10.2307/3546364

Setälä, O., Norkko, J., Lehtiniemi, M., 2015. Feeding type affects microplastic ingestion in a coastal invertebrate community. *Marine Pollution Bulletin* 102 (1), 95-101. http://dx.doi.org/10.1016/j.marpolbul.2015.11.053

Smith, L.C., 2010. Diversification of innate immune genes: Lessons from the purple sea urchin. *Disease Models and Mechanisms*, 1-6. https://10.1242/dm m.004697

Smith, L.C., Britten, R.J., Davidson, E.H., 1995. Lipopolysaccharide activates the sea urchin immune system. *Developmental and Comparative Immunology* 10 (3), 217-224. https://doi.org/10.1016/0145-305X(95)00009-I

Steneck, R.S., 2013. Sea urchins as drivers of shallow benthic marine community structure, Developments in aquaculture and fisheries science. *Sea urchins: biology and ecology, third edition, Ed Lawrence JM, chapter* 14, 195-212. https://doi.org/10.1016/B978-0-12-396491-5.00014-9

Suaria, G., Avio, C.G., Mineo, A., Lattin, G.L., Magaldi, M.G., Belmonte, G., Moore, C.J., Regoli, F., Aliani, S., 2016. The Mediterranean Plastic Soup: Synthetic Polymers in Mediterranean Surface Waters. *Scientific Report* 23 (6), 37551. https://doi.org/10.1038/srep3755

Sun, X., Li, Q., Zhu, M., Liang, Z.J., Zheng S., Zhao, Y., 2017. Ingestion of microplastics by natural zooplankton groups in the northern South China Sea. *Marine Pollution Bullettin* 115, 217-224. https://doi.org/10.1016/j.marpolbul.2016.12.004

Sussarellu, R., Suquet, M., Thomas, Y., Lambert, C., Fabioux, C., Pernet, M.E.J., Le Goïc, N., Quillien, V., Mingant, C., Epelboin, Y., Corporeau, C., Guyomarch, J., Robbens, J., Paul-Pont, I., Soudant, P., Huvet, A., 2016. Oyster reproduction is affected by exposure to polystyrene microplastics. *Proceedings of the National Academy of Sciences*, USA 113 (9), 2430–2435. https://doi.org/10.1073/pnas.1519019113

Tamori, M., Matsuno, A., Takahashi, K., 1996. Structure and function of the pore canals of the sea urchin madreporite. *Philosophical Transactions of The Royal Society B Biological Sciences* 351(1340), 659-676. https://doi.org/10.1098/rstb.1996.0063

Taylor, M., Gwinnett, C., Robinson, L., Woodall, L.C., 2016. Plastic microfibre ingestion by deep-sea organisms. *Scientific Report* 30 (6), 33997. https://doi.org/10.1038/srep33997

Ter Halle, A., Jeannau, L., Martignac, M., Jardé, E., Predono, B., Brach, L., Gigault, J., 2017. Nanoplastic in the North Atlantic Subtropical Gyre. *Environmental Science & Technology* 51(23), 13689-13697. https://doi.org/10.1021/acs.est.7b03667

Trifuoggi, M., Pagano, G., Oral, R., Pavičić-Hamer, D., Burić, P., Kovačić, I., Siciliano, A., Toscanesi, M., Thomas, P.J., Paduano, L., Guida, M., Lyons, D.M., 2019. Microplastic-induced damage in early embryonal development of sea urchin *Sphaerechinus granularis*. *Environmental Research* 179 Part A, 108815. https://doi.org/10.1016/j.envres.2019.108815

van Cauwenberghe, L., Janssen, C.R., 2014. Microplastics in bivalves cultured for human consumption. *Environmental Pollution* 193, 65-70. https://doi.org/10.1016/j.envpol.2014.06.010

van Cauwenberghe, L., Claessens, M., Vandegehuchte, M.B., Janssen, C.R., 2015. Microplastics are taken up by mussels (*Mytilus edulis*) and lugworm (*Arenicola marina*) living in natural habitats. *Environmental Pollution* 199, 10-17. http://dx.doi.org/10.1016/j.envpol.2015.01.008

van Sebille, E., Wilcox, C., Lebreton, L., Maximenko, N., Hardesty, B.D., van Franeker, J.A., Eriksen, M., Siegel, D., Galgani, F., Law, K.L., 2015. A global inventory of small floating plastic debris. *Environmental Research Letters* 10, 124006. https://doi.org/10.1088/1748-9326/10/12/124006

Yorke, C.E., Page, H.M., Miller, R.J., 2019. Sea urchins mediate the availability of kelp detritus to benthic consumers. *Proceedings of the Royal Society B: Biological Sciences* 286, 20190846. https://doi.org/10.1098/rspb.2019.0846

Watts, A.W. J., Lewis, C., Goodhead, R.M., Beckett, S.J., Moger, J., Tyler, C.R., Galloway, T.S., 2014. Uptake and Retention of Microplastics by the Shore Crab *Carcinus maenas*. *Environmental Science &Technology* 48 (15), 8823-8830. https://doi.org/10.1021/es501090

Welden, N. A.C., Cowie, P. R., 2016. Long-term microplastic retention causes reduced body condition in the langoustine, *Nephrops norvegicus*. *Environmental Pollution* 218, 895 - 900. https://doi.org/10.1016/j.envpol.2016.08.020

Chapter 2

"Impact of microbial colonization of polystyrene microbeads on the toxicological responses in the sea urchin *Paracentrotus lividus*"

Abstract

The sea urchin *Paracentrotus lividus* was exposed to either virgin or biofilm-covered polystyrene microbeads (micro-PS, 45µm) in order to test the effect of microbial colonization on the uptake, biodistribution and immune response. The biofilm was dominated by bacteria, as detected by Scanning Electron Microscopy and 16S rRNA sequencing. A higher internalization rate of colonized micro-PS inside sea urchins compared to virgin ones was detected, suggesting a role of the plastisphere in the interaction. Colonized and virgin micro-PS showed the same biodistribution pattern by accumulating mainly in the digestive system with higher levels and faster egestion rates for colonized. However, a significant increase of catalase and total antioxidant activity was observed only in the digestive system of colonized micro-PS exposed individuals. Colonized micro-PS induced also a significant decrease in the number of coelomocytes with a significant increase in vibratile cells, compared to control and virgin micro-PS exposed animals. Moreover, a general time-dependent increase in red/white amoebocytes ratio and reactive oxygen species and decrease in nitrogen ones was observed upon exposure to both colonized and virgin micro-PS. Overall, micro-PS colonization clearly affected uptake and toxicological responses of the Mediterranean sea urchin *P. lividus* in comparison to virgin micro-PS.

Main findings

The naturally occurring colonization of polystyrene microplastics affects uptake, biodistribution and the organ and immune cells response in the Mediterranean sea urchin *Paracentrotus lividus*

Keywords: biofilm; coelomocytes; microplastics; plastisphere; sea urchin

2.1 Introduction

The widespread occurrence of microplastics (<5 mm, MPs) in the marine environment from the coast to offshore, from surface to the deep sea, from most urbanized to remote regions is the result of their continuous production, dispersal and long persistence (Bergmann et al., 2017; Cincinelli et al., 2017; Lebreton & Andrady, 2019; Suaria et al., 2020). With its confined borders, tourist attractions and extremely populated coastlines, the Mediterranean Sea is recognized as the sixth great accumulation zone for marine litter worldwide and consequently a hotspot for MP pollution (Pedrotti et al., 2016; Suaria et al., 2016; Còzar et al., 2017; Cincinelli et al., 2019). In particular, the Mediterranean seafloor is considered a long-term sink for MPs and coastal areas the most affected by plastic pollution (Pham et al., 2014; Clark et al., 2016). The interactions between the hydrophobic surface of MPs and the seawater significantly affect their properties, density, size and their position along the water column and enhance their bioavailability to benthic organisms (Andrady, 2011; Galloway et al., 2017). These interactions lead to the formation of the so-called "corona", a dynamic layer covering the particles surface which for nanoparticles is formed by proteins or metabolites and for larger particles is represented by microbial biofilm (Chetwynd et al., 2020; Tan et al., 2020). As a matter of fact, as soon as MPs enter the sea their surface is immediately colonized by microbes (heterotrophs, autotrophs, predators, and symbionts) which together form the microbial members of the so-called "Plastisphere" (Zettler et al., 2013). The Plastisphere harbors distinct communities from the surrounding free-living representatives, thus representing a new marine niche (Lobelle et al., 2011; Zettler et al., 2013; Oberbeckmann et al., 2014, 2015). One of the key species of benthic Mediterranean habitats is the sea urchin *Paracentrotus lividus* in terms of its trophic peculiarities and ecological contribution to ecosystem functioning. Sea urchins possess an extraordinary immune system formed by a heterogeneous cell population, the coelomocytes, which mediate the effects of a variety of environmental stressors (Matranga et al., 2000, 2006; Pinsino & Matranga, 2015; Smith et al, 2018; Migliaccio et al., 2019; Milito et al., 2020). Moreover, due to their apostatic diet selection and intense grazing activity, sea urchins control the organization, structure and composition of shallow macroalgal assemblages (Boudouresque & Verlaque, 2020). This feeding behavior contributes to plastic fragmentation, also inducing the release of secondary MPs in the marine environment as observed for other benthic species (Cau et al., 2019; Porter et al., 2019). Up to now there is only a study showing MPs occurrence in wild specimens of some sea urchin species, in particular in the gut, coelomic fluid and gonads (Feng et al., 2020). In our previous work, we showed for the first time a size-dependent uptake of virgin microbeads (10 and 45 μm) in the digestive, water vascular systems and gonads of *P. lividus* and impact on immune cells (Murano et al., 2020). Although the growing attention to MPs pollution and the several investigations of microbial biofilm

are thriving (see Amaral-Zettler et al., 2020 for a review), its role in MPs uptake, biodisposition and impact on marine organisms, is barely known. Here, we tested the hypothesis that biofilm naturally occurring on micro-PS could affect uptake, biodistribution, organ and immunological responses in the sea urchin *P. lividus*. Colonized micro-PS (45 µm) were obtained upon incubation in natural sea water in order to resemble an environmental realistic colonization scenario. Microbial biofilm grown on micro-PS was characterized and their role in MP uptake, biodisposition and impact on sea urchin organ and immune cells investigated *in vivo* by comparison with virgin micro-PS exposure.

2.2 Material and Methods

2.1 Experimental design

The experimental design is summarized in Figure 2.1. Fluorescent-labeled polystyrene microbeads (441 excitation/485 emission, micro-PS) of 45 µm in diameter were purchased from Polysciences (Warrington, PA, U.S.A). To confirm the polystyrene core composition and particle size the fourier transformed infrared spectroscopy (FT-IR) and Scanning Electron Microscopy (SEM) analyses were performed (see Supporting Information). Colonized micro-PS were obtained by one-week incubation (7 days) in unfiltered natural sea water (NSW) collected from a coastal site in the Gulf of Naples and microbial colonization of micro-PS was verified by SEM (Figure 2.2 A, B). Microbial communities on colonized micro-PS were analyzed by DNA sequencing.

Sea urchin *in vivo* exposure was performed by using working solutions of virgin micro-PS (45µm) in distilled water from the manufacturer.

Adult specimens of *P. lividus* were exposed to 10 particles mL^{-1} of (i) virgin micro-PS, (ii) colonized micro-PS and to (iii) NSW (control). Micro-PS uptake and egestion were assessed at day 2. The following biochemical markers, such as catalase (CAT) and glutathione-S-transferase (GST) activities and nitric oxide (NO) levels and total antioxidant capacity (TAC) were measured in the digestive system. Effect on the immune system was assessed on coelomocytes by the total cell counts, morphology and oxidative stress analyses (reactive oxygen species, reactive nitrogen species and TAC) (For further details see Supporting Information). Each experiment was run at least three times. For each experimental condition, 16 specimens of sea urchins were used.

2.2 Micro-PS colonization and SEM

Both virgin and colonized micro-PS were fixed in paraformaldehyde 4% (final concentration) and then dehydrated in a series of solutions with different percentages of ethanol: 10 min each in 70%, 85%, 95%, followed by 3×15 min in 100% ethanol. Samples were then immediately critical point dried using a Leica EM CPD300 (Leica Microsystems Inc., Wetzlar, Germany) and then sputter-coated with 15 nm of platinum using a Polaron SC7640 (Thermo Scientific, Waltham, MA, USA). Samples on stubs were visualized and imaged using a JEOL 6700F microscope (JEOL Ltd, Tokyo, Japan).

2.3 Microbial communities: DNA extraction and sequencing

DNA was extracted from colonized micro-PS beads using a modified glass bead-beating approach in combination with the Puregene Tissue DNA extraction kit (Qiagen, Valencia, CA). The sizes of DNA extraction products were checked on 0.8% agarose gel electrophoresis. The extracted DNA was sent to the CGBM Sequencing Facility of the Dalhousie University, Canada, for Illumina MiSeq

sequencing of V4/V5 hypervariable region of the 16SrDNA gene (Richa et al., 2017) and processed as in Comeau et al., (2017) (For further details see the Supporting Information). All sequences are deposited in the European Nucleotide Archive (ENA) under primary succession number PRJEB40656.

2.4 Uptake and egestion

After 48 h of exposure, sea urchins were sacrificed and organs processed for extraction and quantification of micro-PS by following the procedure previously described in Murano et al. (2020). To assess egestion, each specimen was placed in a beaker filled with filtered NSW (0.22 μm) and every 24h water was collected and stored at 4°C. Quality control and assurance detailed experiments were run including fluorophore leaching (see the Supporting Information).

2.5 Stress markers and immune cells response

In the cytosolic fraction of the sea urchin digestive system the following markers were analyzed: NO levels, TAC, CAT and GST activities (For further details see the Supporting Information). At 12h, 24h and 48h, coelomic fluid was withdrawn from each specimens following protocols described and levels of Reactive Oxygen Species (ROS), Reactive Nitrogen Species (RNS) and TAC measured in immune cells (coelomocytes) (Murano et al., 2020) (For further details see the Supporting Information).

2.6 Statistical Analyses

Dissimilarity matrix, Non-metric multidimensional scaling (NMDS), Alpha diversity indexes, Venn diagrams and Linear Discriminant Analyses were performed using Venny open-source online website (Oliveros, J.C., 2007-2015) and Linear discriminant analysis (LDA) effect size (LefSe) (For further details, see the Supporting Information). Data on coelomocytes were analyzed by two-way ANOVA followed by Bonferroni's multiple comparisons test (n= 48). Intracellular levels of ROS/RNS were analyzed by two-way ANOVA (*p-value* < 0.05) followed by Tukey's multiple comparison test (n= 48). NO levels, TAC, catalase and GST activities were analyzed by one-way ANOVA (*p-value* <0.05) followed by Dunnett's multiple comparisons test (n= 48). Data are presented as mean ± SD and statistics were performed using GraphPad Prism version 7.00 for Windows.

2.3 Results and Discussion

2.3.1 Microbial biofilm characterization grown on micro-PS

The infrared absorption spectrum of micro-PS confirmed the manufacturer's claim polystyrene as reported in Figure S2.1. The average micro-PS size distribution was also confirmed as 43 μm (Figure S2.2). Micro-PS incubated for 1 week in NSW from a coastal site in the Gulf of Naples (micro-PS-colonized) exhibited a consistent growth of a microbial community, mainly composed by bacteria (Figure 2.2 A, B). Microbial diversity increased in micro-PS both in virgin and colonized beads after incubation with the sea urchins for 48h (micro-PS-virgin-post and micro-PS-colonized-post) (Figure 2.2 C). Only <1% of the operational taxonomic units (OTUs) were shared by all bacteria in the three conditions and the highest number of shared OTUs (6.4%) occurred between the micro-PS, virgin and colonized, collected from the two tanks at the end of the experiment (Figure 2.2 D).
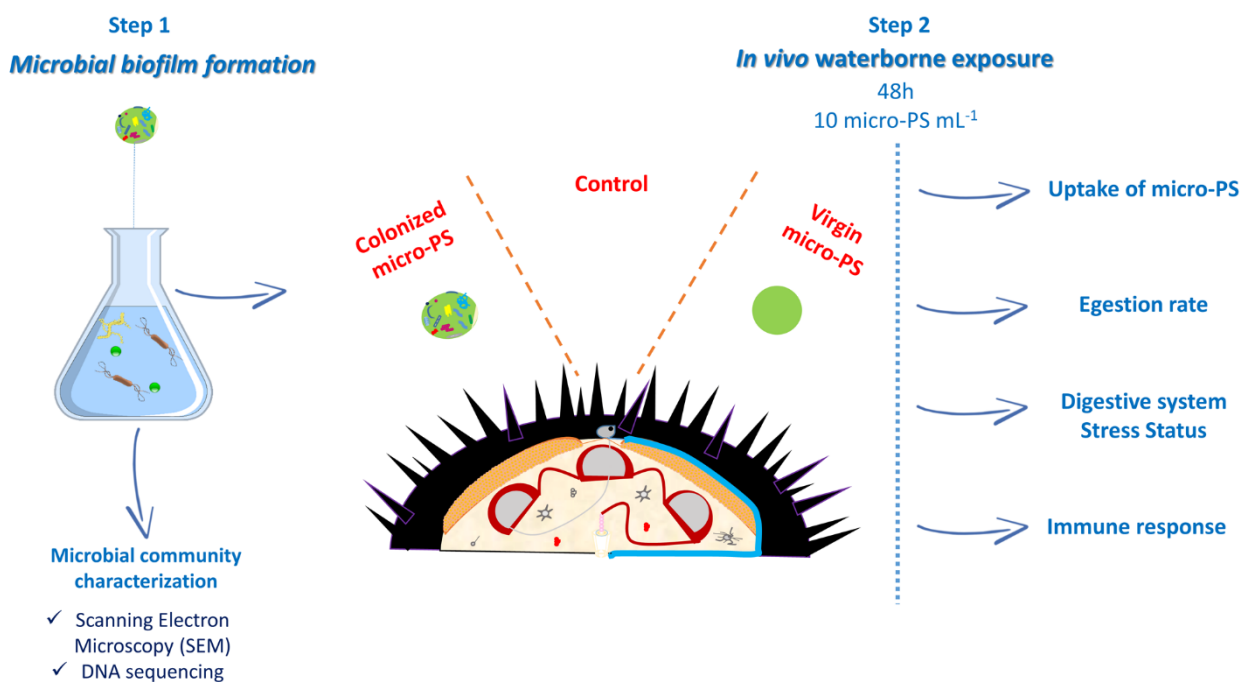
Figure 2.1. Schematic representation of the experimental design. Step 1 involved the formation of the microbial biofilm. Step 2 consisted of in vivo waterborne exposure of sea urchins to colonized and virgin micro-PS (10 micro-PS mL^{-1}) and to only NSW (control) for 48h. After exposure, uptake of micro-PS, egestion rate, digestive system stress status and immune response were assessed.
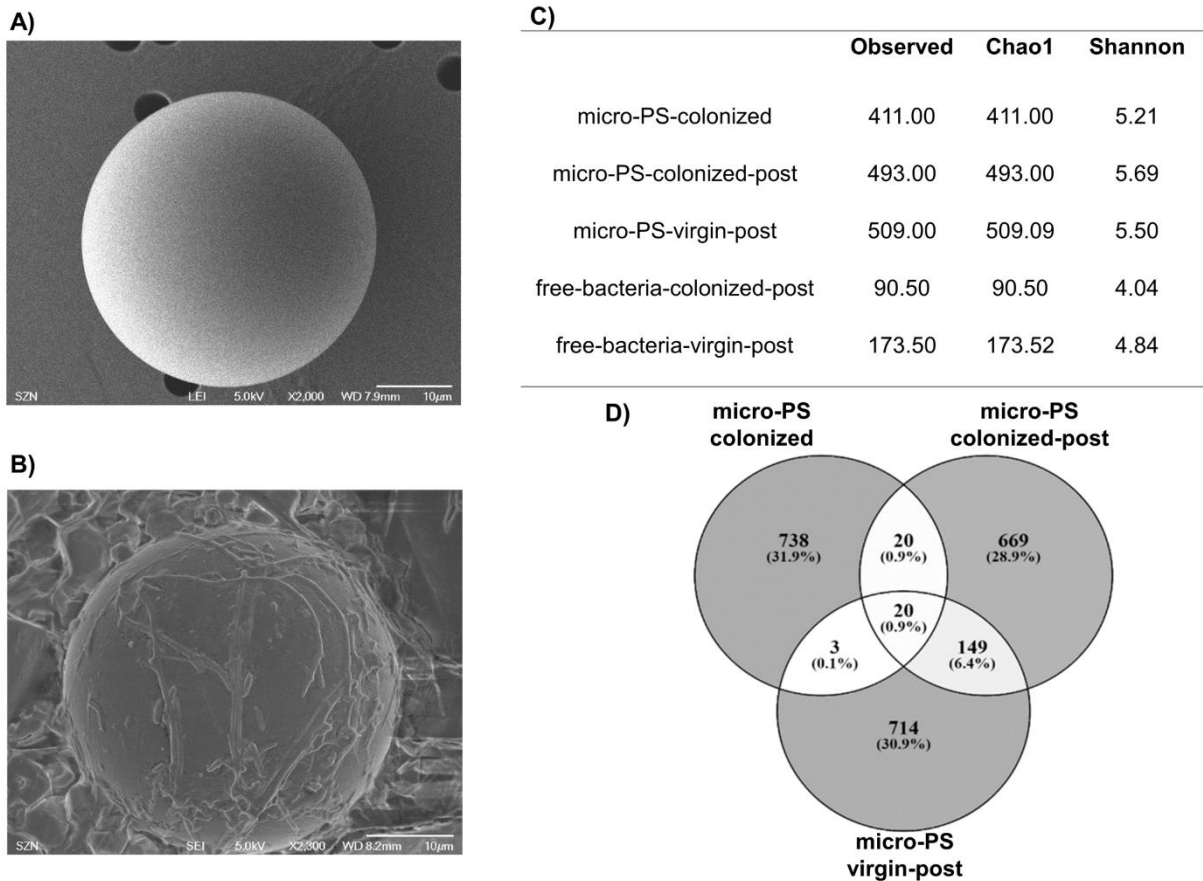
Figure 2.2. Microbial biofilm formation on micro-PS. (A) SEM images of micro-PS beads with no biofilm colonization and (B) after 1 week in NSW from a coastal site, in a temperature and light-controlled chamber. (C) Diversity indexes, Observed, Chao and Shannon of bacterial communities. (D) Venn's diagrams showing the number and percentages (in brackets) of OTUs shared by bacterial communities under the three conditions. Micro-PS-colonized are beads incubated for 1 week in NSW from a coastal site under controlled conditions. Micro-PS-colonized-post and micro-PS-virgin-post are the beads recovered after 48 h exposure of sea urchins to colonized or virgin micro-PS, respectively.

At the same time, the free-living bacteria present in the tanks showed similar composition in terms of dominant phyla (*Bacteroidetes* and *Proteobacteria*), but very little number of OTU shared with attached communities (Figure S2.3). Biofilm bacteria showed also higher alpha diversity and higher number of OTUs compared to free bacteria (Figure 2.2 C). Micro-PS-colonized beads were dominated by *Bacteroidetes* (68%) and *Proteobacteria* (30%), with a minor contribution of *Planctomycetes* (1%). After incubation with sea urchins, the community of micro-PS-colonized-post shifted to 45% *Bacteroidetes*, 46% *Proteobacteria*, and 2% *Planctomycetes*. The micro-PS-virgin-post showed a bacterial community formed by 52% of *Bacteroidetes*, 30% of *Proteobacteria* and 1.8% of *Planctomycetes* (Figure 2.3 A). Both post-treatment bacterial communities showed over 5 to 7 times more OTUs belonging to *Firmicutes* than the ones colonized before treatment. When analyzed at the family level, the bacterial community on micro-PS incubated in NSW from a coastal site in the Gulf of Naples showed lower evenness, with *Saprospiraceae*, *Rhodobacteraceae* and

Flavobacteriaceae dominating, together with *Alteromonadaceae* and *Cryomorphaceae*, and *Haliaeaceae* and *Sphingomonadaceae* (1.9% each family) as minor contributors. Instead, *Marinilabiliaceae* emerged consistently as components of the bacteria incubated in presence of the sea urchins, also with *Saprospiraceae*, *Rhodobacteraceae*, *Flavobacteraceae* and the uncultured family of *Bacteroidetes* VC 2.1_Bac22 (Figure 2.3 B). Although they were not dominant, it is noteworthy that representatives of the genera *Arcobacter*, *Vibrio*, and *Colwellia*, hosting potential human pathogenic strains, were observed in the post-experiment attached communities, even though they were not detected among the initially attached bacteria (or the free-living ones – Figure 2.3 B). The use of different approaches allowed us to demonstrate and characterize bacterial colonization on micro-PS beads. Alpha diversity values together with SEM analysis revealed bacterial biofilm formation on beads incubated for 1 week in NSW from a coastal site in the Gulf of Naples. The similarity of the diversity values reported in this study between virgin and colonized micro-PS collected after incubation with sea urchins were consistent with the highest number of shared OTUs (6.4%) under these conditions. By contrast, the very low value of <1% of the OTUs shared by all bacteria in the three conditions indicated little overlap in bacteria in the different treatments. The diversity values of our samples were similar to those reported in literature for, e.g. MPs retrieved at sea (Zettler et al., 2013) or incubation experiments with pellets (Oberbeckmann et al., 2018). The observed changes in the bacterial community after incubation with sea urchins could derive from the passage through the digestive system, suggesting that the animals and their released organic compounds may promote the proliferation of specific taxa. This is supported by the increased presence of OTUs belonging to *Firmicutes*, one of the most abundant phylum belonging to the sea urchin internal microbiome (Laport et al., 2018), supporting the hypothesis of sea urchins' microbiome contribution to the beads community as for instance originating from the contact of free micro-PS with faeces in the exposure medium. As a further confirmation, the richness of families in post-treatment micro-PS compared to the ones pre-treatment was consistent with previous observations that the bacterial plastisphere offers favorable growth conditions to members of the so-called "rare biosphere" which are usually found in very low amounts in NSW. This confirms that micro-PS represent new niches allowing an adaptive advantage for specific some bacteria over some others. Whether this is simply due by mechanical support or interactions within the plastisphere (increased nutrient availability, competition or mutualism) or if there is any chemical interaction with the different polymers, is still under debate (Amaral-Zettler et al., 2020). Among colonizing bacteria there were some genus related to human pathogenic strains, e.g. *Colwellia*, which is also responsible for the infection called "*bald sea urchin disease*", known to turn to green some affected areas and the loss of spines and other appendages (Girard et al., 2012; Boudouresque &Verlaque, 2020). Therefore,

in peculiar conditions, such as in the presence of high dissolved organic matter, also combined with substrate specificity, potential pathogens might find favorable conditions for growth (Wright et al., 2020). A possible threat for marine species originating from it cannot be excluded as well as hazard for human being due to their consumption.
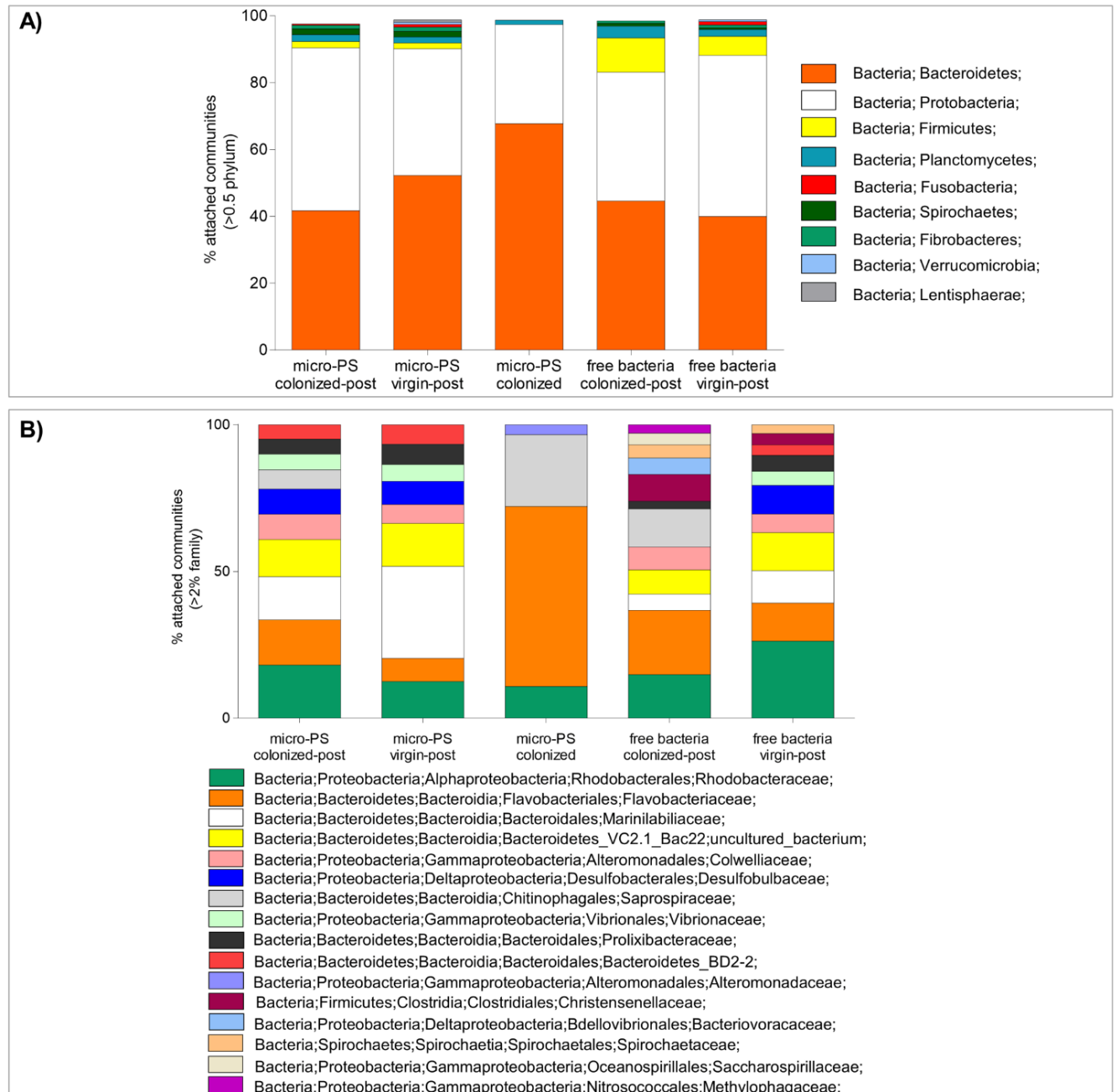
Figure 2.3. Composition of the bacterial community grown on micro-PS or present in the seawater. (A) Phylum and (B) Family composition. Micro-PS-colonized were incubated for 1 week in NSW from a coastal site under controlled conditions. Micro-PS-colonized-post and micro-PS-virgin-post are the beads recovered after 48 h exposure of sea urchins to colonized or virgin micro-PS, respectively. The free bacteria were the bacteria present in the seawater of the tanks after 48 h.

2.3.2 Colonized micro-PS accumulation in the digestive system and egestion

After 48h of exposure, the total number of internalized micro-PS, was higher for colonized beads compared to virgin ones, resulting in 156.5 ± 16.3 *vs* 34.0 ± 1.0 particles, respectively (Figure 4A). The digestive system contained a higher number of micro-PS (95.05 % colonized *vs* 81.80 % virgin) (Figure S4), followed by the ampullae of the aquifer system (2.38 % colonized *vs* 10.00 % virgin), the gonads (1.67 % colonized *vs* 7.10 % virgin) and the esophagus (0.90% colonized *vs* 1.10 % virgin). No beads were found in other parts of the aquifer system (e.g. the stone and ring canal) and in the coelomic fluid (Figure 2.4 A) in agreement with our previous observation also regardless of micro-PS size (Murano et al., 2020). However, the shape of both micro-PS (virgin and colonized) resulted significantly affected by incubation with the sea urchins: the regular spherical shape (see Figure 2.2) turns into a hexagonal prism morphology (Figure 2.4 B). In terms of micro-PS egestion, after 24h reaching 60% of micro-PS were ejected from the digestive system and up to 90% at 48h (Figure 2.4 C). By contrast, a higher number of virgin micro-PS was still found in the digestive system after 24h which decreased at 48h (approx. 30%) (Figure 2.4 C). The number of micro-PS found in NSW after 24h was higher in specimens exposed to colonized beads compared to virgin ones (45% *vs* 11%, respectively) with a time dependent increase at 48h (80% *vs* 50 % respectively) (Figure 2.4 D). The time dependent increase was also observed in virgin beads although to a lesser extent (about 50%) (Figure 2.4 D). Although the use of fluorescent labeled particles (both of micro and nanoscale dimension) was highly debated for translocation studies, unless specific protocols to avoid biases are used (Catarino et al., 2019; Shur et al., 2019), here we further confirmed the suitability of our stock to track both uptake and distribution of micro-PS in sea urchin *in vivo*. The fluorophore was demonstrated with no leaching of the dye as well as the efficiency of the extraction method from sea urchin tissues and organs (Figure S2.5).
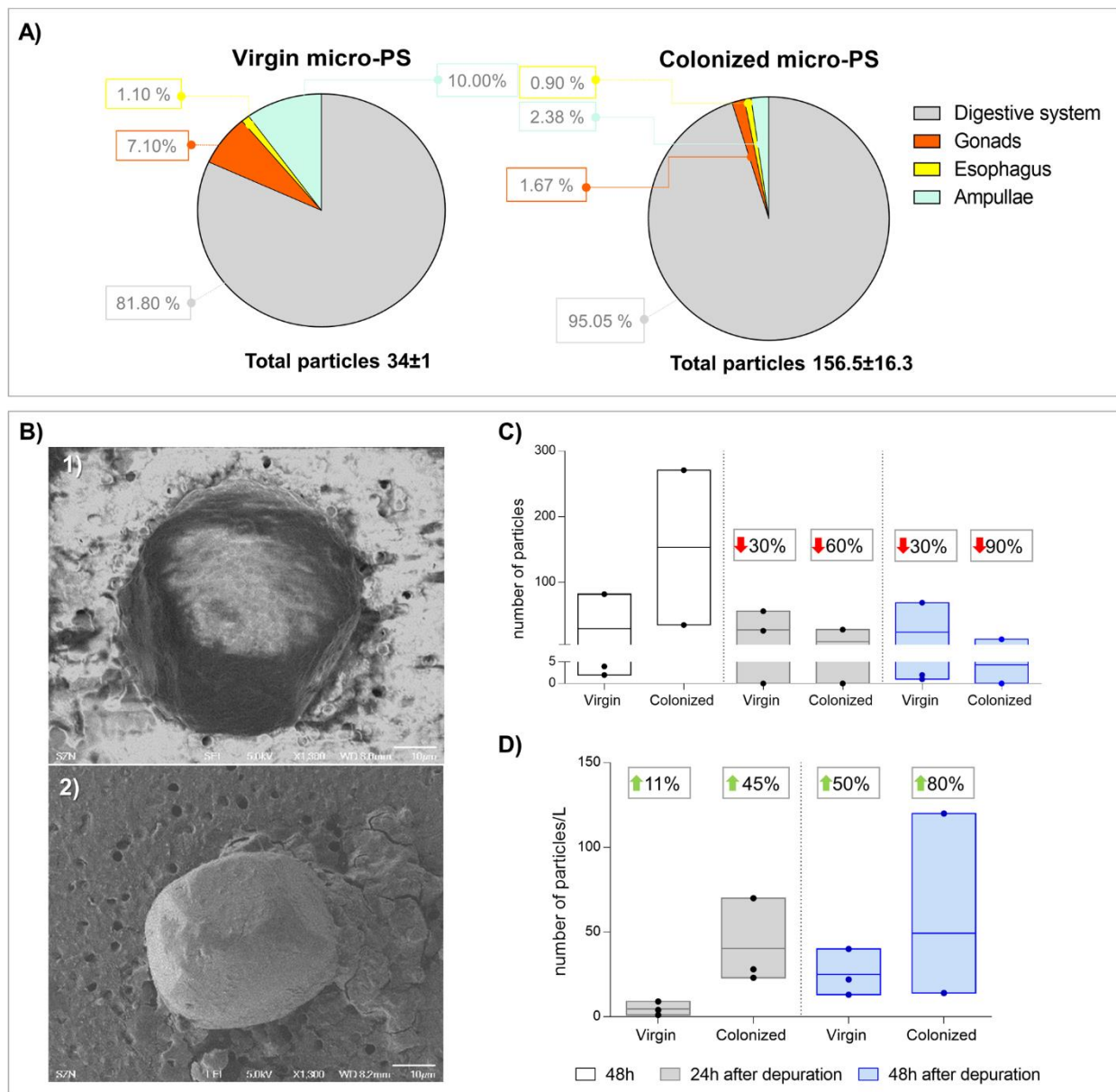
Figure 2.4. Uptake and egestion of virgin and colonized micro-PS. (A) Abundance of micro-PS (virgin and colonized) in different organs of sea urchins after 48h of incubation, expressed as percentage of micro-PS found normalized by the weight of fresh organs. (B) SEM images of virgin (1) and colonized micro-PS (2) after 48h of sea urchin's exposure. (C-D) Egestion experiment. After 48h of exposure to virgin or colonized micro-PS, the abundance of particles was assessed after 24h and 48h of depuration inside the sea urchin's digestive system (C) and in sea water (D) Box-plot represents median, mean, upper and lower quartile. For each box-plot, is indicated the % of micro-PS eliminated (C) or micro-PS found in sea water (D) 24 and 48h of depuration compared to the particles found at 48h after exposure.

The main outcome of our study is to have demonstrated a higher uptake of colonized micro-PS to virgin ones by sea urchin and therefore the possible role played by the plastisphere. The use of chemodetection to find and eat particles has been already shown by zooplanktonic grazers with a preference towards aged beads over pristine ones (Vroom et al., 2017). While virgin particles maintained a spherical size distribution, here we showed that the biofilm formation changed their shape and perhaps those properties (e.g. density, shape and aggregation) which could have made them more palatable (Lobelle et al., 2016; Rummel et al., 2017). Porter et al. (2019) also reported that biofouling of the MP surface increased its fragmentation by sea urchin. Therefore, the presence of biofilm and prey seems to determine the choice of the sea urchin towards the assimilation of colonized particles *vs* virgin ones. The digestive system showed the highest abundance of micro-PS with a higher percentage of colonized beads over virgin ones in agreement with previous studies (Watts et al., 2014; Lu et al., 2016; Murano et al., 2020). By contrast, ampullae and gonads showed a prevalence of virgin ones suggesting a different micro-PS distribution based on their surface properties. The absence of virgin or colonized micro-PS in the coelomic fluid further confirmed our previous findings in which only smaller micro-PS (10 µm) were able to translocate among tissues (Browne et al., 2008; Farrel et al., 2013; Watts et al., 2014). In terms of micro-PS egestion, colonized seemed to be faster egested than virgin ones, suggesting low risk of their trophic transfer to predators including humans by their consumption. In details, the excretion of virgin and colonized microbeads was observed already at the end of experiments, after 48h of depuration according to the estimated time of *P. lividus* gut-clearance and 90% of fecal pellets production, reported to be between 21 and 33 h (Lawrance et al., 1989). The gut-retention time reported in this study for sea urchins was lower compared to the time required by *Aurelia sp. ephyrae* (up to 72 h), *Carcinus maenas* (3 weeks), *Seriolella violacea* (up to 7 weeks) (FArrel et al., 2013; Ory et al., 2018; Costa et al., 2020) but very similar to what reported for *Magallana gigas*, *Gasterosteus aculeatus* (about 48-72h) (Graham et al., 2019; Bour et al., 2020). However, as reported for bivalves, rejection, ingestion, and egestion of plastic particles were strongly affected by particles properties and food abundance, making it difficult to predict the real rates in realistic exposure scenarios and the possible environmental consequences (Fernandéz et al., 2019). Since the sea urchin's gut processes the food particles as membrane-surrounded food pellets in a relatively rapid continuous flow, even MPs may follow the same route (Lawrence, 2020). In fact, micro-PS SEM images (Figure 2.4 B) confirm the change in particle shape after exposure, probably as a consequence of their interaction with sea urchins' digestive system. While the virgin micro-PS are wrapped in a layer resembling the marine algae *Ulva lactuca* signature (used to feed sea urchin during acclimation before experiments) (Postma et al., 2018), the colonized micro-PS are covered with a thick mucus layer. Such differences suggest the stimulation of production of mucus

by colonized micro-PS by the sea urchin's digestive tract. The overproduction of mucus is recognized as a defensive response against stressors including pollutants (Groh et al., 2017; Liberti et al., 2020) and therefore it could have facilitated the rapid egestion of colonized micro-PS by sea urchins. Our preliminary findings support future studies aimed to underline the interactions, even mechanical, that might occur between micro-PS and the sea urchin's digestive system.

2.3.3 Micro-PS impact on digestive system and immune system

As a further confirmation of a higher interaction between colonized micro-PS and the sea urchin digestive system over virgin ones, higher levels of TAC (*p-value*= 0.015) and CAT activities (*p-value* = 0.044) were found in the digestive system of sea urchins exposed to colonized micro-PS compared to virgin ones and controls (Figure S2.6). No changes were found in the endogenous NO levels and GST activity. The greater accumulation in the digestive tract of colonized micro-PS *vs* virgin ones may have resulted in the observed higher total antioxidant capability and CAT activities. Another possibility, which requires further investigation, is that the biofilm itself interact with the gut microbiome by stimulating an oxidative response. Altogether, our findings suggest that, after 48h, colonized micro-PS are apparently counteracted by the activation of defense systems, involving CAT, a direct ROS-scavenging enzyme, and the antioxidant cellular pool. These results are in line with the literature in which the formation of ROS is recognized as a molecular initiating event of MPs toxicity (Hu & Palic, 2020). In invertebrate species, the innate immune system plays a key role in protecting the organism from the excessive generation of ROS triggered by MPs and the scavenging system (CAT, SOD, GPx, vitamins and other enzymes) is involved to avoid any damage in cells and tissues. Since the digestive system is recognized as an active site in the immune response in sea urchins and it plays a fundamental role in modulating the response towards various stressors (Buckley et al., 2019), a close interplay with the immune system towards MP exposure is assumed (Rast et al., 2006). In the sea urchin, the physiological homeostasis towards multiple stressors is maintained by immune cells, known as coelomocytes, a heterogeneous population composed of phagocytes, vibratile cells, and colorless and red spherule cells (Pinsino & Matranga, 2015). They mediate immune responses through phagocytosis, encapsulation of foreign particles, and production of diffusible factors including antimicrobial molecules (Smith et al., 2018). In this study, we investigate their responses towards the exposure virgin and colonized micro-PS by measuring several parameters. Only specimens exposed to colonized micro-PS already after 24h showed a significant decrease in the total number of coelomocytes ($2.4 \cdot 10^6 \pm 7.4 \cdot 10^5$ cells mL^{-1}) compared to the control ($3.50 \cdot 10^6 \pm 6.2 \cdot 10^5$ cells mL^{-1}), (Figure 2.5 A) while no changes were observed in those exposed to virgin ones. No significant changes in the amount of immune cell types were found, except for the red, white amoebocytes and vibratile cells depending on time and treatment (Figure 2.5 C). Vibratile cells

increased in specimens exposed to colonized micro-PS, compared to control and those exposed to virgin micro-PS (Figure 2.5 C).
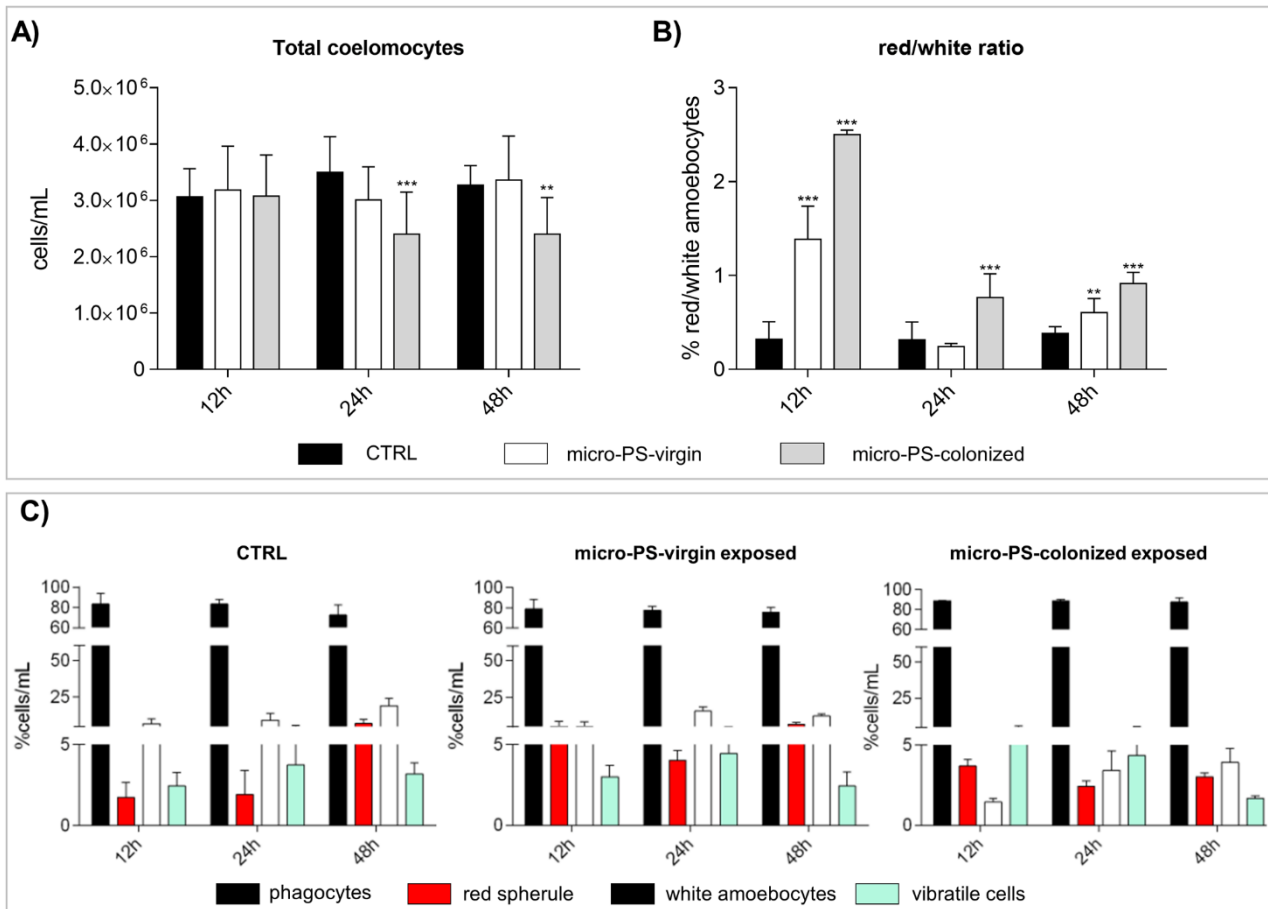
Figure 2.5. Morphological analysis of coelomocytes in sea urchins exposed at different times to virgin and colonized micro-PS. (A) Total coelomocytes count. (B) Red to White amoebocytes ratios and (C) Percent distribution of cell types. Bars represent mean± SD. Asterisks indicate values that are significantly different from the control, **p-value* < 0.01, ***p-value*< 0.001 (n=48).

Moreover, the ratio between red and white amoebocytes (R/W) was significantly higher in individuals exposed to both micro-PS particles compared to the controls, except at 24h for virgin beads-exposed animals (0.24 ± 0.03 *vs* control 0.31 ± 0.19) (Figure 2.5 B). Specifically, specimens exposed to colonized micro-PS showed a number of red amoebocytes about 2.5 times higher than whites ones at 12h, while virgin micro-PS 1.4 times and the control group 0.4 times higher.
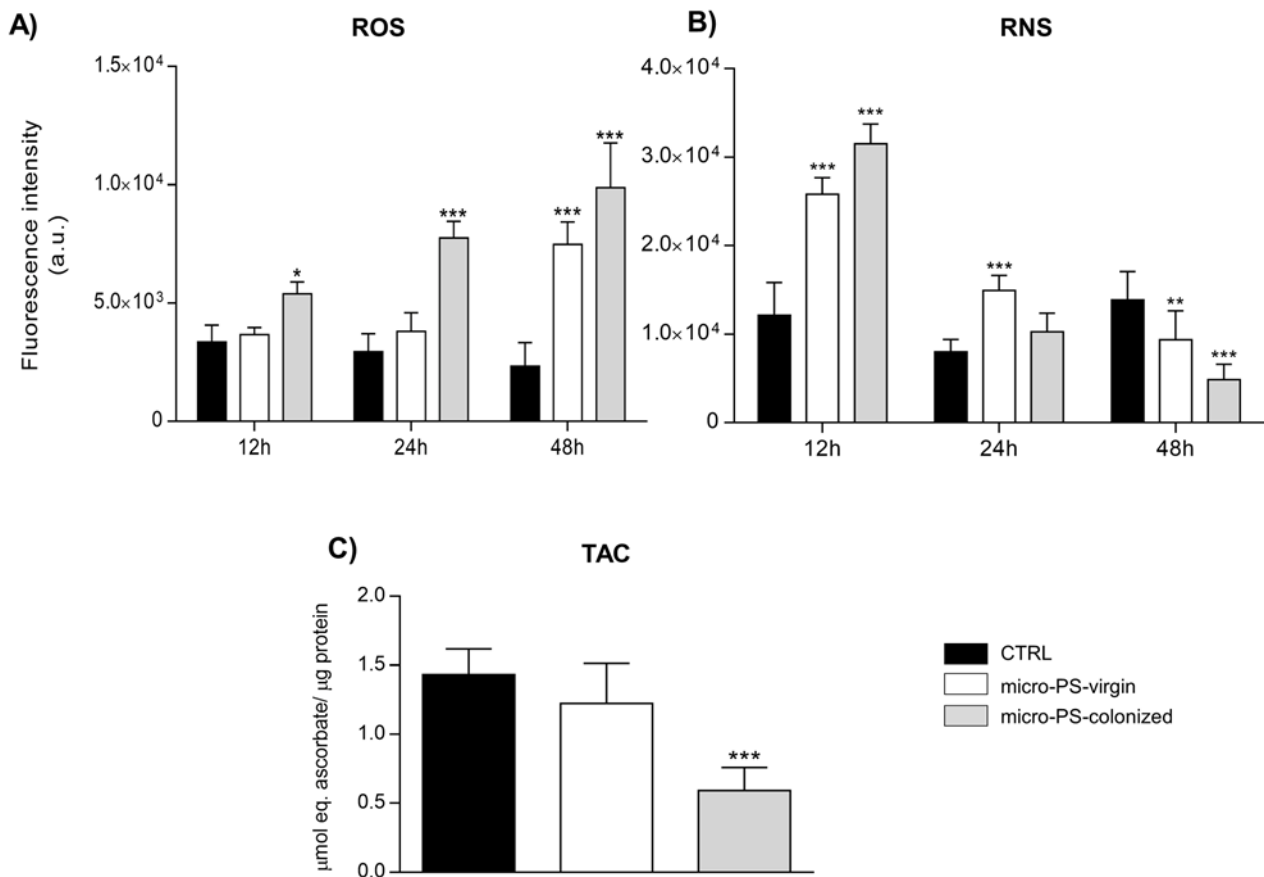
Figure 2.6. Intracellular redox state in coelomocytes of sea urchins exposed at different times to virgin and colonized micro-PS. (A) Reactive oxygen species (ROS) and (B) Reactive nitrogen species (RNS) levels at 12h, 24h and 48h of treatment. (C) Total antioxidant activity (TAC) at 48h of treatment. Bars represent mean ± SD. Asterisks indicate values that are significantly different from the control, *p-value <0.05, **p-value < 0.01, ***p-value < 0.001 (n=48).

ROS and RNS, as further indicators of immune cell stress response were also monitored (Coteur et al., 2005). In sea urchins exposed to colonized micro-PS intracellular levels of ROS showed a time-dependent increase starting from 5397 ± 500 a.u. (*vs* control 3359 ± 713 a.u.) (12h) up to 9884 ± 1883 a.u. (*vs* control 2328 ± 997 a.u.) at 48h (Figure 2.6 A). The same trend was observed only after 48h for virgin beads-treated animals (7485 ± 943 a.u.). Coelomocytes of specimens exposed to virgin micro-PS exhibited higher levels of RNS compared to controls at 12h and 24h (*p-value* < 0.0001), whereas the increase was observed only at 12h for those exposed to colonized particles (31530 ± 2232 *vs* control 12039 ± 3703 a.u.). At 48h decreased levels of RNS were observed for both beads (control: 13884± 3210, virgin: 9383 ± 3267, colonized: 4869 ± 1739 a.u.) (Figure 2.6 B). The total antioxidant activity significantly decreased after 48h in animals treated with colonized micro-PS (*p-value* < 0.0001) (Figure 2.6 C). The observed changes in the total number of immune cells upon exposure to MPs is in agreement with previous findings in marine invertebrates, leading to an increase (Murano

et al., 2020) or a decrease (Sun et al., 2020). The significant decrease observed only in specimens exposed to colonized micro-PS could be related to the presence of bacterial component such as LPS, already reported to be able to reduce the total number of immune cells in sea urchin as well in other invertebrates' species (Lorenzon et al., 1999; Renwrantz et al., 2013; Chiaramonte et al., 2020). Our findings also revealed that the presence of biofilm markedly affected the coelomocytes profile resulting in increased number of vibratile cells and in higher ratio red-white cells soon after 12h of exposure. Such changes have been already described as a marker of the sea urchins' health status (Matranga et al., 2005; Pinsino et al., 2008) and significantly affected upon exposure to stressful conditions (Arizza et al., 2007; Branco et al., 2014). The higher number of red amoebocytes in specimens exposed to colonized micro-PS is associated with the presence of a cytoplasmic red pigment, the echinochrome A, which is reported to bear a high bactericidal activity. Therefore, the presence of bacteria on the surface of colonized micro-PS could have stimulated such immunological responses with an increased production of the red pigment. Similar findings have been already reported in our previous study upon exposure to only virgin micro-PS regardless of their size (Murano et al., 2020) while no changes in coelomocyte sub-populations including red *vs* white amoebocytes were observed by short-term *in vitro* exposure of coelomocytes to PS nanoparticles (60-50 nm) (Kirsh et al., 2000). In agreement with previous findings in other biological systems, the increasing trend of ROS over time together and with the concomitant decrease of RNS found in coelomocytes of specimens exposed to colonized micro-PS suggested NO scavenging by ROS through the formation of peroxynitrite by reaction between NO and superoxide anion (Kirsh et al., 2000; Tafalla et al., 2003; Gallina et al., 2014). ROS levels increase in larvae, tissues and immune cells of some marine invertebrate species upon MPs exposure (Lu et al., 2016; Jeong et al., 2016; Jeong et al., 2017). On the other hand, NO is also reported to increase upon exposure to several stress was shown to be produced by immune cells or developing embryos or tissues of different marine invertebrates in response to stress agents (Ottaviani et al., 1993; Gourdon et al., 2001; Tafalla et al., 2003; de Barros et al., 2009; Romano et al., 2011; Migliaccio et al., 2014; Migliaccio et al., 2016). The observed decrease of TAC in specimens exposed to colonized micro-PS after 48h of exposure suggest their inability to mitigate the oxidizing effects through regulation of coelomocytes metabolism. However, we cannot exclude a potential compensatory effect and therefore activation of antioxidant response during the first hours of exposure, followed by a decrease in antioxidant activity afterwards, in agreement to what has been reported in the bivalve mussel *Mytilus sp* (Paul-Pont et al., 2016).

2.4 Conclusions

In conclusion, the results of this study show, for the first time, that naturally occurring colonization of micro-PS in NSW is able to affect uptake, biodisposition and the organ and immune cells response in the Mediterranean sea urchin *P. lividus*. Microbial colonization of micro-PS targets immune cell count and their morphology as well as their redox status. The greater accumulation in the sea urchin digestive system of colonized micro-PS *vs* virgin could be related to their greater palatability due to the presence of biofilm which is also to affect the antioxidant system of the organ. However, although the sea urchin showed extraordinary ability to internalize micro-PS compared to other marine species, their fast egestion regardless of biofilm formation indicates that micro-PS might not be transferred along food chains up to humans due to their consumption. However, the presence of potential pathogens in the biofilm of colonized micro-PS cannot exclude potential harmful implication in terms of food security and aquaculture purposes. Concerning the Mediterranean Sea in terms of realistic exposure scenarios, currently projections suggest that in coastal areas concentration could reach higher levels than predicted causing an exceeding of the toxicity thresholds for marine organisms (Jambeck et al., 2015; Compa et al., 2019; Lebreton et al., 2019). In this contest, the outcomes of this work provides the basis for future investigations on MPs ecotoxicity, encouraging the use of colonized rather than virgin plastics, considering that colonization occurs as soon as plastics enter the marine environment and are therefore their most realistic form.

Chapter 2- Supplementary material

Methods

Fourier-transform infrared analysis

FTIR spectrum of MPs sample were recorded at room temperature by means of a Perkin Elmer Spectrum 100 FTIR spectrometer, equipped with an attenuated total reflectance accessory (ATR). MPS dispersion was cast at room temperature on a KBr disk, the disk surface was kept in contact with the ATR crystal. The scanned wavenumber range was 4000–650 cm^{-1}. The spectrum was recorded at a resolution of 4 cm^{-1}, and 16 scans were averaged for each sample.

Polystyrene microbeads

Colonized micro-PS was obtained incubating a dispersion solution of 4 x10^4 fluorescent particles L^{-1} for 10 days in unfiltered sea water (one-liter glass flasks) from a coastal site (40° 49'13.8" N, 14° 18'09.7" E) in the Gulf of Naples. Incubations were performed in a temperature-controlled culture cabinet chamber (Angelantoni, Italy), at 18±1°C, light 100 µmol; LD 12:12 cycle on an orbital shaker in order to promote microbial biofilm formation. Aliquots of colonized micro-PS were taken for scanning electron microscopy (SEM), sequence analysis and incubation experiments with sea urchins. In this case, colonized beads were added to the tanks (final concentration 10 particles mL^{-1}). For virgin micro-PS, the working solution (10^4 particles mL^{-1}) was prepared in deionized water from the manufacturer's vial, vortexed for 3 minutes and then directly added to the tank to reach the final concentration of 10 particles mL^{-1}.

Post-sequencing processing

For the analyses chloroplastic, mitochondrial, eukaryotic and unknown sequences were removed. Bacterial and archaeal sequences were randomly resampled in the Operational taxonomic unit (OTU) file to enable comparison between samples, by normalizing the number of sequences between the samples to the smallest number of sequences in one sample (n=2578), using R software (RCore Team, 2017). Dissimilarity matrix was computed (by vegdist functioning vegan in R) using the Bray–Curtis analysis and used for subsequent analyses (clustering, ordination). Non-metric multidimensional scaling (NMDS) was performed using the metaNMDS function in vegan and the dendrograms presenting hierarchically organized samples were built with hclust and average method. Alpha diversity indexes (Observed, Chao and Shannon) were calculated using R software. Venn diagrams were obtained using the Venny open-source online website (Oliveros, 2007-2015). Linear discriminant analysis (LDA) effect size was performed with a standard LDA score (log 10) of 3.5. Significance of different abundances was tested using Wilcoxon test by R software.

Sea urchin's collection, maintenance and exposure

Adult individuals of *Paracentrotus lividus* (Lamark 1816) (diameter 4.75 ± 0.56 cm) were collected in the Gulf of Naples according to the authorization of Marina Mercantile (DPR 1639/68, 09/19/1980, confirmed on 01/10/2000), from a specific site (40° 42.031' N, 13°57.254'E) that is not privately-owned nor protected in any way. Although no authorization is required for sea urchins, all procedures were performed according to the European Directive 2010/63/ EU on the protection of animals used for scientific purposes by reducing at minimum the number of specimens used and any pain or distress of animals during treatments. Sea urchins were acclimated for two weeks in glass tanks filled with circulating NSW (temperature 18 ± 1°C, salinity 38 ± 1, dissolved O_2 7 mg/L, pH 8.1) and were fed ad libitum with the green algae *Ulva lactuca*. Specimens of adult sea urchin were placed in 4L glass tanks (ratio of 1 specimen per liter) supplied with filtered NSW (0.22 μm) from the coastal site in the Gulf of Naples (see above) in a closed flow-through system constantly aerated. They were incubated in presence of either colonized micro-PS or virgin micro-PS, both at concentration of 10 mL^{-1} or only sea water (control) for 48h. Sea urchins were not fed during the experiments, and each treatment was repeated at least three times. Temperature, salinity, pH and dissolved O_2 of NSW remained constant during the experiments.

Coelomic fluid collection and analysis

After 12, 24 and 48 h from incubation, the coelomic fluid from all sea urchins (controls and treated) was collected from the coelomic cavity using a sterile syringe (5 mL, needle 26 gauge) containing the anticoagulant solution CCM 2X at a ratio of 1:1 (anticoagulant: coelomic fluid) as reported in Murano et al. (2020). Heterogeneous coelomocytes were counted using a Neubauer counting chamber (Bright-Line Hemacytometer) under light microscope (ZEISS Apotome.2) At the end of the experiment (48 h) the coelomic fluid of sea urchins exposed to micro-PS was visualized under an epifluorescence microscope (ZEISS Apotome.2) to assess the presence of micro-PS. At different times, aliquots of the coelomic fluid were washed twice in CCM 1X and the pellet was stored at -80 °C until levels of Reactive Oxygen Species (ROS), Reactive Nitrogen Species (RNS) and Total Antioxidant Capacity (TAC) were assessed.

Digestive system extraction and analysis

The cytosolic fraction of the digestive system was prepared by following the method of Regoli et al. (2002). The homogenization buffer (50 mM K_2HPO_4, 0.75 M sucrose, 1 mM EDTA, 0.5 mM DTT, 400 μM PMSF, 10 μM leupeptin, 1 μM pepstatin A, 1 mg L^{-1} aprotinin) was added to the sample in

1:2 (w/v) ratio. The solution was homogenized with an ultra-turrax T-25 (IKA®-Werke GmbH & Co. KG, DE) and the homogenate was centrifuged at 9,300 x g for 25 min at +4°C. The supernatant, which represents the cytosolic fraction, was collected and then stored at -80 °C for subsequent analyses, including determination of NO levels and TAC, as well as catalase and glutathione-S-transferase activities. Total proteins were measured according to Bradford (1976) using a Tecan spectrophotometer (Infinite M100 Pro) and bovine serum albumin as standard at 595 nm.

Extraction and quantification of micro-PS in sea urchin organs

After 48 h incubation, the individual sea urchins were killed by cutting off the peristomal membrane. The digestive system (separating the esophagus from the remaining stomach and gut, collected together), the water vascular system and the gonads were dissected using a stereomicroscope with GFP filter (LEICA M205C Microscope), weighed and then kept at 4°C before processing (Fig. S3). A small portion of the digestive system (stomach and gut together), was kept at -80°C until biochemical analyses were performed. Micro-PS was extracted from tissues according the method of Kuhn et al., 2017. All fresh organs were added to 20 mL of KOH 1M (1:20, w: v) at room temperature for 48 h under continuous orbital shaking (IKA KS250, IKA®-Werke GmbH & Co. KG, DE). Successively, the so-obtained solution was filtered through cellulose acetate membrane filters (GVC, 47 mm CA 0.45 μm) and the filters observed with an epifluorescence microscope (ZEISS Apotome.2) equipped with GFP-filter set in order to detect and count micro-PS beads.

Control experiments for the extraction method and fluorophore leaching

To test the efficiency of the extraction method an aliquot of known concentration (200 micro-PS) was added to 20 mL KOH 1M and then particles were quantified on the filter, obtaining a recovery of about 75.25 ±6%. For analysis of fluorophore leaching, 10^3 micro-PS was added to 1 mL KOH 1M and NSW for 48h and then centrifuged in centrifugal sample clarification units (Microcon®- 10 kDa) to check if the KOH digestion and NSW would damage the beads causing the leaching of the fluorophore. The fluorescence intensity of the resulting solutions was recorded through Tecan spectrofluorometer (Infinite M1000 Pro) (λ_{em}=441nm/λ_{ex}=485nm). After 48h through 10 kDa filters, no detection of fluorescence in the filtrates was assessed, indicating the absence of leaching of the fluorophore beads in KOH and NSW (Figure S4).

Determination of intracellular levels of ROS and RNS

Intracellular levels of ROS and RNS in coelomocytes were determined at 12, 24, 48h using the fluorescence dyes DCFH-DA (2′,7′-dichlorohydro-fluoresceindiacetate, λ_{ex} = 488/ λ_{em} = 525 nm)

and DAF-DA (4-amino-5-methylamino-2',7'-difluororescein diacetate, $\lambda_{ex} = 495$/ $\lambda_{em} = 515$ nm), respectively, as reported in Murano et al. (2020)[4]. Fluorescence values were normalized by subtracting the autofluorescence of unlabeled extracts (DMSO). Results are expressed as fluorescence intensity of $1.5 \cdot 10^6$ cells.

Determination of NO levels

The endogenous NO levels in the digestive system were measured by monitoring nitrite formation by Griess reaction. An aliquot of 150 µL of cytosolic fraction of the digestive system (stomach and gut), diluted 1:6 in the homogenization buffer, was incubated for 1h with 150 µL of mix reaction (NADPH 0.6 mM, nitrate reductase 1U mL^{-1}, FAD 100 µM). The sample was then incubated for 10 min with sulphanilamide 1% (w/v) in 5% phosphoric acid. Subsequently, the solution was incubated for 10 min with N-(1-naphthyl) ethylenediamine (NED) 0.1% (w/v) in deionized water. The absorbance was determined at 540 nm using a spectrophotometer (Agilent, 8453) and the molar concentration of nitrite in the sample was calculated from a standard curve generated using known concentrations of sodium nitrite (0–100 µM).

Determination of TAC

After 48 h of exposure, TAC in coelomocytes was determined according to Murano et al. (2020). Aliquots of immune cells, collected in CCM as described above, were centrifuged at 8000 rcf for 10 min at + 4 °C, briefly rinsed twice in CCM and stored at -80°C. Frozen cells, suspended in PBS 1x (1:2; w: v), were centrifuged at 14000 rcf for 30 min at +4°C and the supernatant was used for the assay. For the digestive system, the cytosolic fraction prepared as described above was used. The reaction mixture contained 0.1 mM ABTS, 20 µM hydrogen peroxide and 0.25 mM horseradish peroxidase type II (Sigma) in 50 mM glycine-HCl buffer (pH 4.5). The ability of the extract from coelomocytes or the digestive system to discolor the solution of 2,2′-azinobis-3-ethylbenzothiazoline-6-sulfonic acid (ABTS) radical cation (ABTS•+), generated by oxidation of ABTS with hydrogen peroxide in the presence of horseradish peroxidase, was measured by following the absorbance at 730 nm (Agilent). The TAC was quantified according to a standard curve of ascorbic acid (1- 15 µM) and normalized to protein content by Bradford (1976) using a Tecan spectrophotometer (Infinite M100 Pro) and bovine serum albumin as standard at 595 nm.

Catalase Activity

Catalase activity was measured by a spectrophotometric method evaluating the peroxidase activity due to the dismutation of H_2O_2 ($\varepsilon = 40$ M^{-1} cm^{-1}) at 240 nm according to Regoli et al. (2014). Aliquots of 10 µl of cytosolic fraction of the digestive system (diluted 1:10 in homogenization buffer) were

added to 100 mM of phosphate buffer (pH=7) and 150 mM H_2O_2 (in phosphate buffer). The kinetics of hydrogen peroxide decomposition was recorded using an Agilent spectrophotometer (Agilent, 8453). The activity was expressed as µmol of H_2O_2 min^{-1} µg $protein^{-1}$.

Glutathione-S-transferase activity (GST)

GST activity was evaluated according to Habig et al. (1974). The formation of dinitrophenyl thioether, formed by reaction between reduced glutathione (GSH) and CDNB (1-chloro-2,4-dinitrobenzene), was detected spectrophotometrically at 340 nm, using a Tecan spectrophotometer with a microplate reader. The reaction mixture contained CDNB 1.74 mM (190 µl), GSH 33 mM (10 µL), GST assay buffer, 0.1 M phosphate pH 7.42, and 20 µL of cytosolic fraction of the digestive system. The increase in absorbance at 340 nm was measured before and after 3 min of incubation at + 20 °C. The activity was expressed in µmol CDNB-GSH conjugated min^{-1} µg $prot^{-1}$.
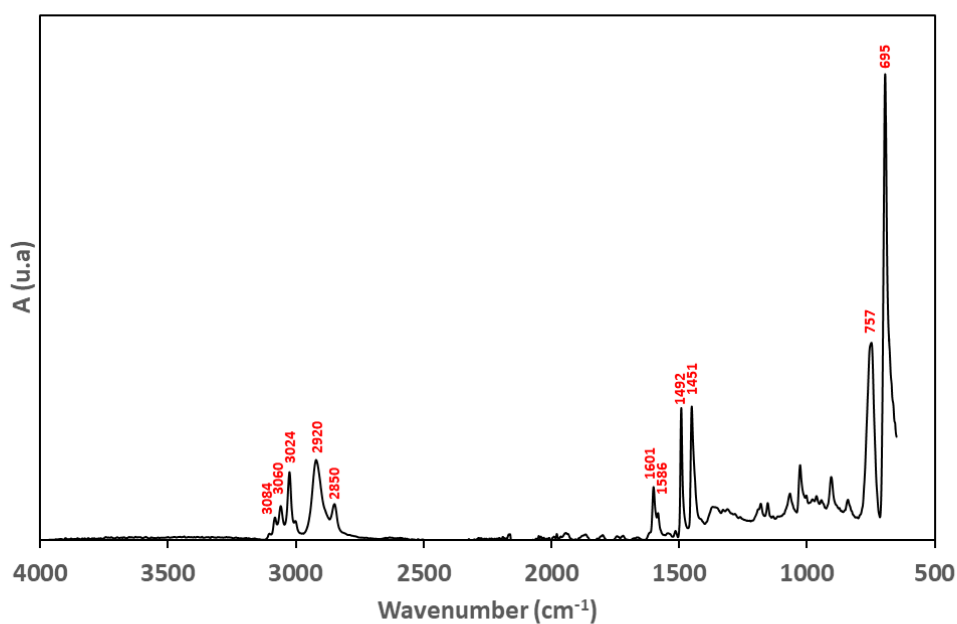
Figures

Figure S2.1 Fourier transform infrared spectra of fluorescent-labeled polystyrene microbeads (441 excitation/485 emission, micro-PS) from Polysciences (Warrington, PA, U.S.A) cast on KBr disk. The absorption bands at 3084, 3060 and 3024 cm^{-1} are assigned to aromatic C–H stretching vibrations, while the bands at 2920 and 2850 cm^{-1} are due to asymmetric and symmetric stretching vibrations of methylene groups –CH$_2$. The bands at 1601 and 1586 cm^{-1} are ascribed to the in-plane ring breathing modes of carbon–carbon stretches in the aromatic. The absorptions at 1492 cm^{-1} and 1451 cm^{-1} are also due to carbon–carbon stretching vibrations in the aromatic ring. At 1069 and 1028 cm^{-1} there are the in-plane C–H bending of the phenyl ring. The pattern of the out-of-plane (oop) C–H bending bands in the region 900–675 cm^{-1} is also characteristic of the aromatic substitution pattern, being intense at 695 and 757 cm^{-1} respectively.
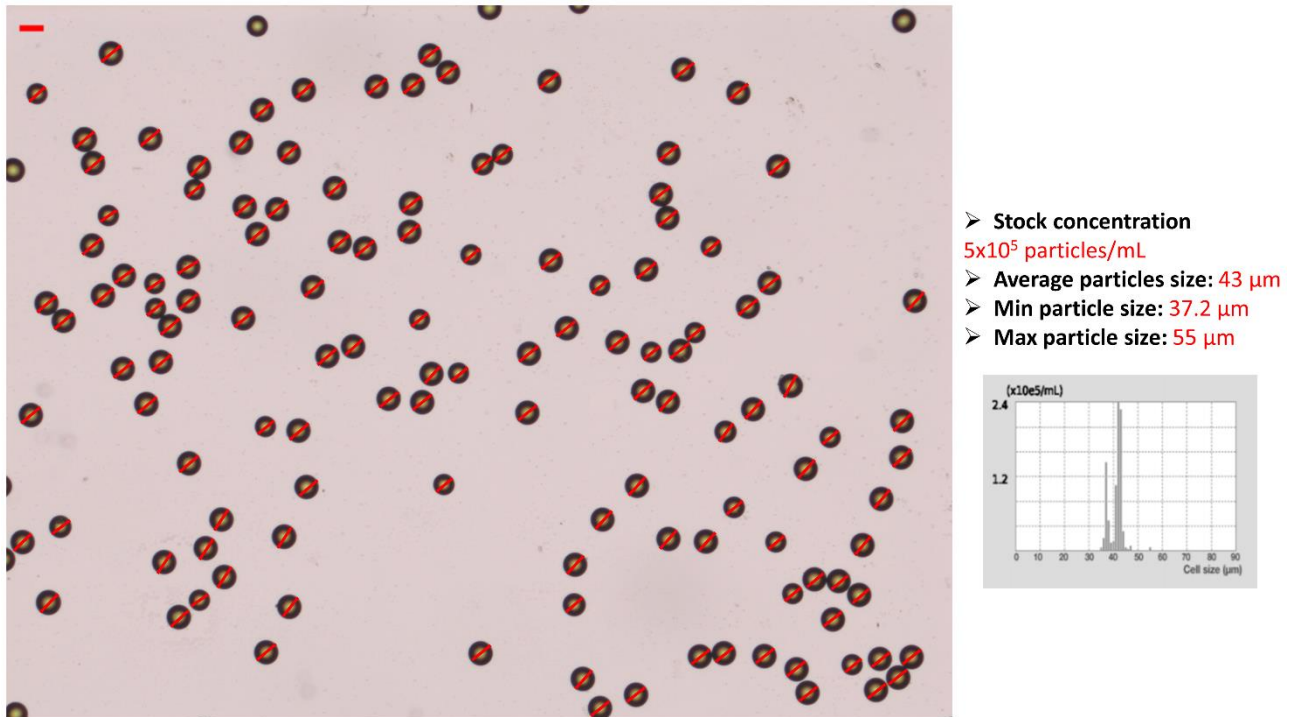
Figure S2.2 Analysis of size distribution of fluorescent-labeled micro-PS beads (441 excitation/ 485 emission). Images were captured using ApoTome Axio Cam Bright-field and processed with ImageJ software. Scale bar 45 µm. The beads size is in agreement with the data sheet provided by the manufacturer (https://www.polysciences.com/german/fluoresbrite-yg-microspheres-450m).
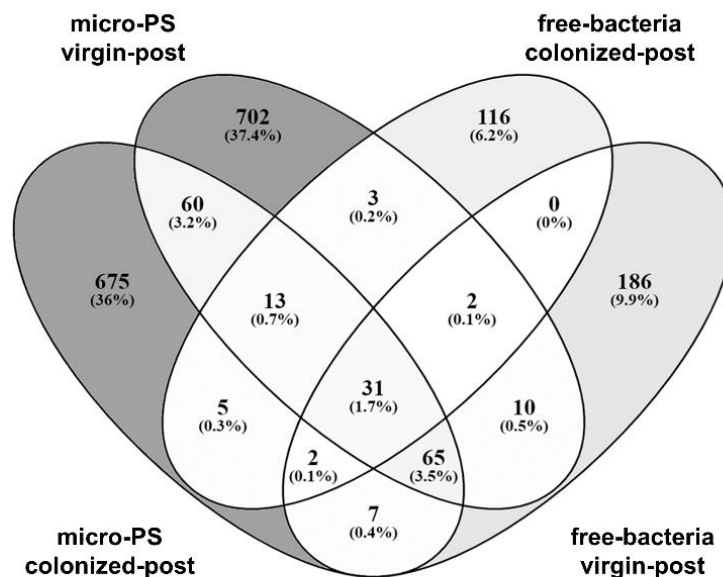
Figure S2.3 Venn's diagrams showing the number and percentages (in brackets) of OTUs shared by bacterial communities. Micro-PS-colonized-post and micro-PS-virgin-post are the beads recovered after 48 h exposure of sea urchins to colonized or virgin micro-PS, respectively. Free-bacteria-colonized post and free-bacteria-virgin-post are the corresponding bacterial OTUs present free in the seawater of the corresponding tanks.
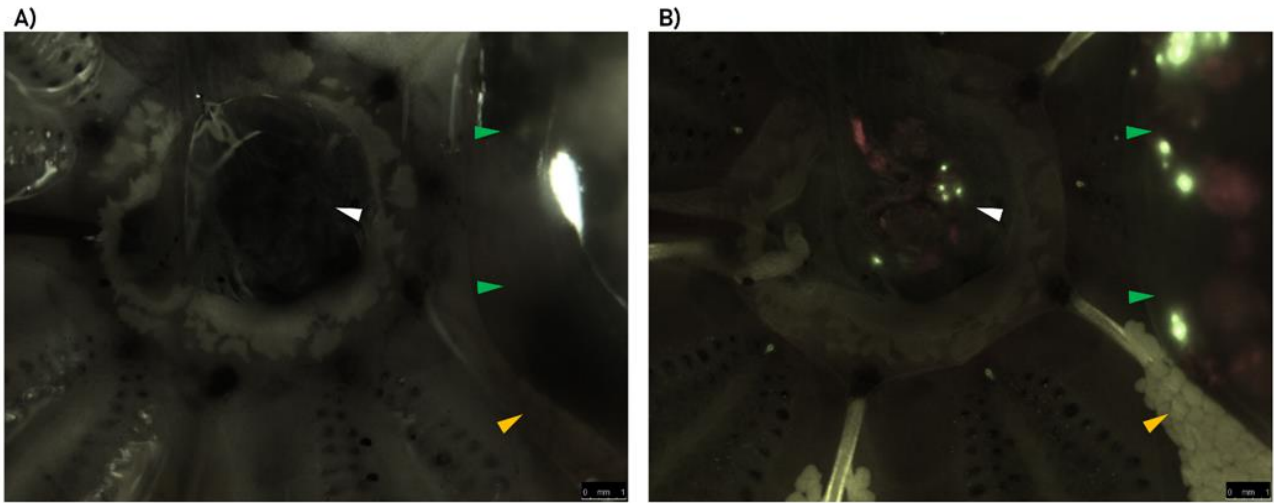
Figure S2.4 Representative images of fluorescent-labeled polystyrene microbeads (45µm) inside the digestive system of sea urchin *P. lividus.* Images were captured using Leica M205C Bright-field (A), 503-GFP filter (B). Orange arrow indicates the gonads, the green and the white arrows indicate the middle and the final parts of the digestive system, respectively.
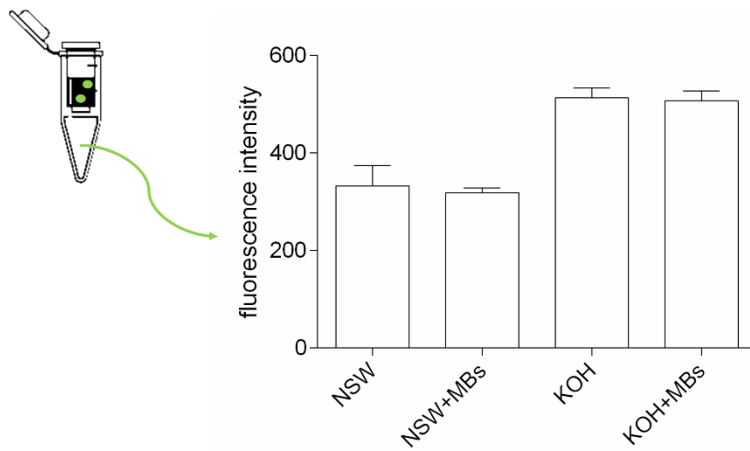
Figure S2.5 Fluorescence intensity of the filtrates after centrifugation of NSW-micro-PS and KOH-micro-PS in centrifugal sample clarification units of 10 kDa.
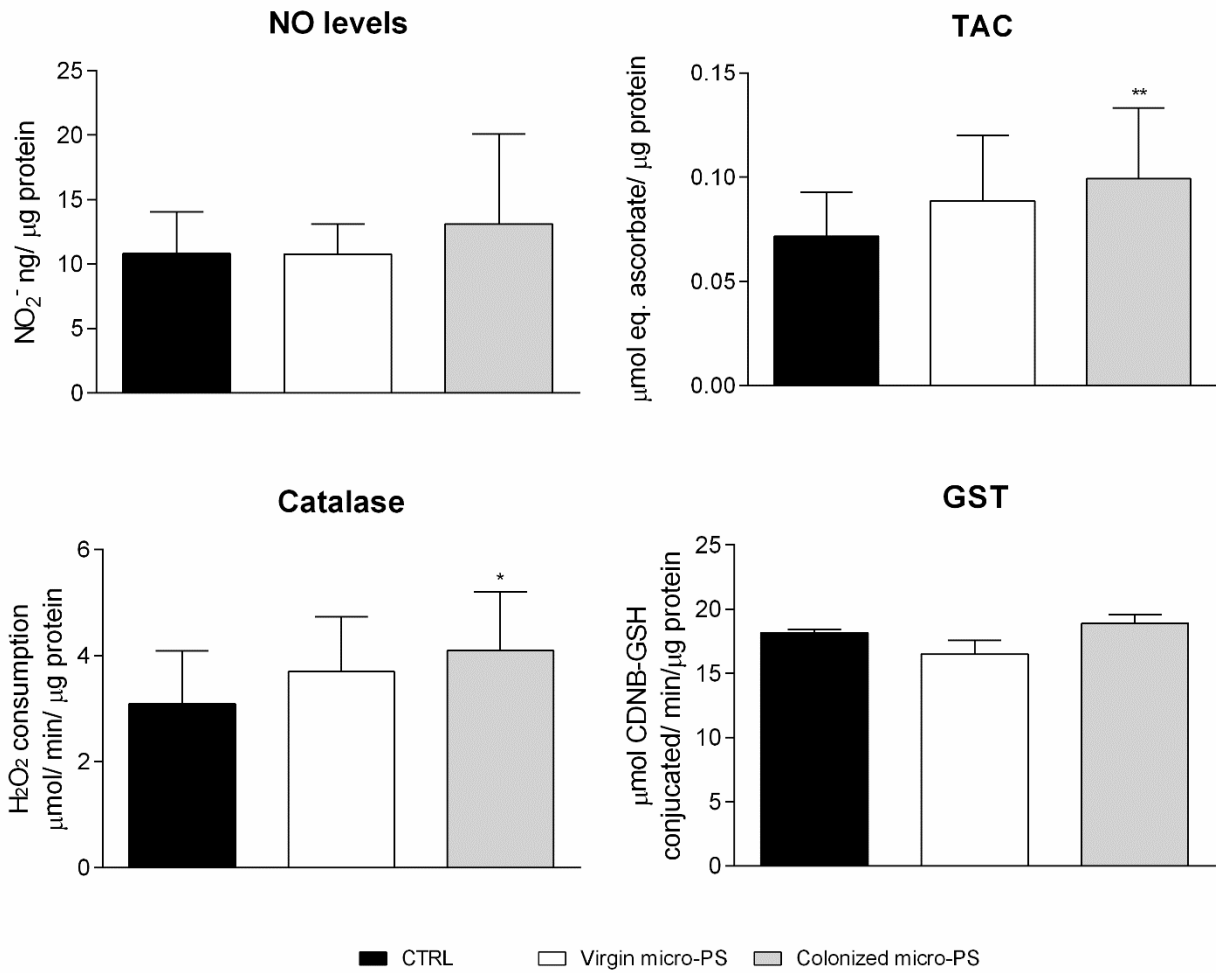
Figure S2.6. Nitric oxide (NO) levels, total antioxidant capacity (TAC), catalase and glutathione-S-transferase (GST) activities in the digestive system of sea urchins after 48h of exposure to virgin and colonized micro-PS. Bars represent mean ± SD. Asterisks indicate values that are significantly different from the control, *p-value*<0.05; **p-value*<0.01 (n=48).

References

Amaral-Zettler, L.A., Zettler, E.R., Mincer, T.J., 2020. Ecology of the plastisphere. *Nature Review Microbiology* 18(3), 139-151. https://doi.org/10.1038/s41579-019-0308-0

Andrady, A.L., 2011. Microplastics in the marine environment. *Marine Pollution Bullettin* 62, 1596-1605. https://doi.org/10.1016/j.marpolbul.2011.05.030

Arizza, V., Giaramita, T.Z., Parrinello, D., Cammarata, M., Parrinello, N., 2007. Cell cooperation in coelomocyte cytotoxic activity of *Paracentrotus lividus* coelomocytes. *Comparative Biochemistry Physiology A Molecular Integrative Physiology* 147(2), 389-394. https://doi.org/10.1016/j.cbpa.2007.01.022

Bergmann, M., Wirzberger, V., Krumpen, T., Lorenz, C., Primpke, S., Tekman, M.B., Gerdts G., 2017. High quantities of microplastic in Arctic deep-sea sediments from the HAUSGARTEN Observatory. *Environmental Science & Technology* 51 (19), 1000-11010. https://doi.org/10.1021/acs.est.7b03331

Boudouresque, C.F., Verlaque, M., 2013. *Paracentrotus lividus*. *In Lawrence, J.M. (ed) Sea Urchins: Biology and Ecology*. Third Edition, 297–327.

Boudouresque, C.F., Verlaque, M., 2020. *Paracentrotus lividus*. *In Lawrence, J.M. (ed) Sea Urchins: Biology and Ecology*. Fourth Edition 43, 447-485. https://doi.org/10.1016/B978-0-12-819570-3.00026-3

Bour, A., Sturve, J., Höjesjö, J., Carney Almroth B., 2020. Microplastic vector effects: are fish at risk when exposed via the trophic chain?. *Frontiers Environmental Science* 8, 90. https://doi.org/10.3389/fenvs.2020.00090

Branco, P.C., Figueiredo, D.A.L., da Silva, J.R.M.C., 2014. New insights into innate immune system of sea urchin: coelomocytes as biosensors for environmental stress. *OA Biology* 2(1), 2.

Browne, M.A., Dissanayake, A., Galloway, T.S., Lowe, D.W., Thompson, R., 2008. Ingested microscopic plastic translocates to the circulatory system of the mussel, *Mytilus edulis* (L.). *Environmental Science & Technology* 42, 5026-5031. https://10.1021/es800249a

Buckley, K.M., Rast, J.P., 2019. Immune Activity at the Gut Epithelium in the Larval Sea Urchin. *Cell Tissue Research* 377 (3), 469–474. https://doi.org/10.1007/s00441-019-03095-7

Catarino, A., Frutos, A., Henry, T.B., 2019. Use of fluorescent-labelled nanoplastics (NPs) to demonstrate NP absorption is inconclusive without adequate controls. *Science Total Environment* 670, 915-920. https://doi.org/10.1016/j.scitotenv.2019.03.194

Cau, A., Avio, C.G., Dessì, C., Follesa, M.C., Moccia, D., Regoli, F., Pusceddu, A., 2019. Microplastics in the crustaceans *Nephrops norvegicus* and *Aristeus antennatus*: Flagship species for deep-sea environments?. *Environmental Pollution* 255 (1), 113107. https://doi.org/10.1016/j.envpol.2019.113107

Chetwynd, A.J., Lynch, I., 2020. The rise of the nanomaterial metabolite corona, and emergence of the complete corona. *Environment Science: Nano* 7, 1041-1060. https://doi.org/10.1039/C9EN00938H

Chiaramonte, M., Arizza, V., La Rosa, S., Queiroz, V., Mauro, M., Vazzana, M., Inguglia, L., 2020. Allograft Inflammatory Factor AIF-1: Early Immune Response in the Mediterranean Sea Urchin *Paracentrotus Lividus*. *Zoology* 142, 125815. https://doi.org/10.1016/j.zool.2020.125815

Cincinelli, A., Martellini, T., Guerranti, C., Scopetani, C., Chelazzi, D., Giarrizzo, T., 2019. A potpourri of microplastics in the sea surface and water column of the Mediterranean Sea. *TrAC Trends in Analytical Chemistry* 110, 321-326. https://doi.org/10.1016/j.trac.2018.10.026

Cincinelli, A., Scopetani, C., Chelazzi, D., Lombardini, E., Martellini, T., Katsoyiannis, A., Fossi, M.C., Corsolini, S., 2017. Microplastic in the surface waters of the Ross Sea (Antarctica): Occurrence, distribution and characterization by FTIR. *Chemosphere* 175, 391-400. https://doi.org/10.1016/j.chemosphere.2017.02.024

Clark, J.R., Cole, M., Lindeque, P.L., Fileman, E., Blackford, J., Lewis, C., Lenton, T.M., Galloway, T.S., 2016. Marine microplastic debris: a targeted plan for understanding and quantifying interactions with marine life. *Frontiers Ecology Environment* 14(6), 317-324. https://doi.org/10.1002/fee.1297

Comeau, A.M., Douglas, G.M., Langille, M.G.I., 2017. Microbiome helper: a custom and streamlined workflow for microbiome research systems. *American Society of Microbiology Journal* 2 (1), e00127-16. https://doi.org/10.1128/mSystems.00127-16

Compa, M., Alomar, C., Wilcox, C., van Sebille, E., Lebreton, L., Hardesty, B.D., Deudero, S., 2019. Risk assessment of plastic pollution on marine diversity in the Mediterranean Sea. *Science Total Environment* 678, 188-196. https://doi.org/10.1016/j.scitotenv.2019.04.3550048-9697

Costa, E., Gambardella, C., Piazza, V., Vassalli, M., Sbrana, F., Lavorano, S., Garaventa, F., Faimali, M., 2020. Microplastics ingestion in the ephyra stage of *Aurelia* sp. triggers acute and behavioral responses. *Ecotoxicology Environmental Safety* 189, 109983. https://doi.org/10.1016/j.ecoenv.2019.109983

Coteur, G., Danis, B., Dubois, P., 2005. Echinoderm reactive oxygen species (ROS) production measured by peroxidase, luminol-enhanced chemiluminescence (PLCL) as an immunotoxicological tool. *Progress in Molecular and Subcellular Biology* 39, 71–83. https://doi.org/10.1007/3-540-27683-1_4

Cózar, A., Sanz-Martín, M., Martí, E., González-Gordillo, J.I., Ubeda, B., Gálvez, J.A., Irigoien, X., Duarte, C. M., 2015. Plastic accumulation in the Mediterranean Sea. *PloS One* 10 (4), e0121762. https://doi.org/10.1371/journal.pone.0121762

Farrel, P., Nelson, K., 2013. Trophic level transfer of microplastic: *Mytilus edulis* (L.) to *Carcinus maenas* (L.). *Environmental Pollution* 177, 1-3. https://doi.org/10.1016/j.envpol.2013.01.046

Feng, Z., Wang, R., Zhang, T., Wang, J., Huang, W., Li, J., Xu, J., Gao, G., 2020. Microplastics in specific tissues of wild sea urchins along the coastal areas of northern China. *Science Total Environment* 728, 138660. https://doi.org/10.1016/j.scitotenv.2020.138660

Fernández, B., Albentosa, M., 2019. Dynamic of small polyethylene microplastics ($\leq 10\,\mu m$) in mussel's tissues. *Marine Pollution Bullettin* 146, 493-501. https://doi.org/10.1016/j.marpolbul.2019.06.021

Gallina, A., Brunet, C., Palumbo, A., Casotti, R., 2014. The Effect of polyunsaturated aldehydes on *Skeletonema marinoi* (*Bacillariophyceae*): the involvement of reactive oxygen species and nitric oxide. *Marine Drugs* 12(7),4165-4187. https://doi.org/10.3390/md1207416

Galloway, T.S., Cole, M., Lewis, C., 2017. Interactions of microplastic debris throughout the marine ecosystem. *Nature Ecology & Evolution* 1, 116. https://doi.org/10.1038/s41559-017-0116

Girard, D., Clemente, S., Toledo-Guedes, K., Brito, A., Hernandez, J.C., 2012. A mass mortality of subtropical intertidal populations of the sea urchin *Paracentrotus lividus*: analysis of potential links with environmental conditions. *Marine Ecology* 33 (3), 377-385. https://doi.org/10.1111/j.1439-0485.2011.00491.x

Gourdon, I., Guérin, M.C., Torreilles, J., Roch, P., 2001. Nitric oxide generation by hemocytes of the mussel *Mytilus galloprovincialis*. *Nitric Oxide* 5 (1), 1-6. https://doi.org/10.1006/niox.2000.0327

Graham, P., Palazzo, L., de Lucia, G.A., Telfer, T.C., Baroli, M., Carboni, S., 2019. Microplastics uptake and egestion dynamics in Pacific oysters, *Magallana gigas* (Thunberg, 1793), under controlled conditions. *Environmental Pollution* 252(A),742-748. https://doi.org/10.1016/j.envpol.2019.06.002

Holland, 2020. *Paracentrotus lividus*. In Lawrence, J.M. (ed) Sea Urchins: Biology and Ecology. Fourth Edition, 43, 447-485. https://doi.org/10.1016/B978-0-12-819570-3.00026-3

Hu, M., Palić, D., 2020. Micro- and Nano-Plastics Activation of Oxidative and Inflammatory Adverse Outcome Pathways. *Redox Biology* 37, 101620. https://doi.org/10.1016/j.redox.2020.101620

Jambeck, J., Geyer, R., Wilcox, C., Siegler, T.R., Perryman, M., Andrady, A., Narayan, R., Law, K., 2015. Plastic waste inputs from land into the ocean. *Science* 347 (6223), 768-771. https://doi.org/10.1126/science.1260352

Jeong, C.B., Won, E.J., Kang, H.M., Lee, M.C., Hwang D.S., Hwang, U.K., Zhou, B., Souissi, S., Lee, S.J., Lee J.S., 2016. Microplastic size-dependent toxicity, oxidative stress induction, and p-JNK and p-p38 activation in the monogonont rotifer (*Brachionus koreanus*). *Environmental Science & Technology* 50 (16), 8849-8857. https://doi.org/10.1021/acs.est.6b01441

Jeong, C.B., Kang, H.M., Lee, M.C., Kim, D.H., Han, J., Hwang, D.S., Souissi, S., Lee, S.J., Shin, K.H., Park, H.G., Lee, J.S., 2017. Adverse effects of microplastics and oxidative stress-induced MAPK/Nrf2 pathway-mediated defense mechanisms in the marine copepod *Paracyclopina nana*. *Scientific Report* 7, 41323. https://doi.org/10.1038/srep41323

Kirsch, M., de Groot, H., 2000. Ascorbate is a potent antioxidant against peroxynitrite-induced oxidation reactions: evidence that ascorbate acts by re-reducing substrate radicals produced by peroxynitrite. *Journal Biological Chemistry* 275, 16702-16708. https://doi.org/10.1074/jbc.M909228199

Lebreton, L., Andrady, A., 2019. Future scenarios of global plastic waste generation and disposal. *Palgrave Communication* 5, 6. https://doi.org/10.1057/s41599-018-0212-7

Lobelle, D., Cunliffe, M., 2011. Early microbial biofilm formation on marine plastic debris. *Marine Pollution Bullettin* 62, 197-200. https://doi.org/10.1016/j.marpolbul.2010.10.013.

Lorenzon, S., de Guarrini, S., Smith, V.J., Ferrero, E.A., 1999. Effects of LPS Injection on Circulating Haemocytes in Crustaceans in Vivo. *Fish & Shellfish Immunology*, 9 (1), 31–50. https://doi.org/10.1006/fsim.1998.0168

Laport, M.S., Bauwens, M., Collard, M., George, I., 2018. Phylogeny and antagonistic activities of culturable bacteria associated with the gut microbiota of the sea urchin (*Paracentrotus lividus*). *Current microbiology* 75, 359–367. https://doi.org/10.1007/s00284-017-1389-5

Lu, Y., Zhang, Y., Deng, Y., Jiang, W., Zhao, Y., Geng, J., Ding, L., Ren, H., 2016. Uptake and accumulation of polystyrene microplastics in zebrafish (*Danio rerio*) and toxic effects in liver. *Environmental Science Technology* 50 (7), 4054-4056. https://doi.org/10.1021/acs.est.6b00183

Matranga, V., Toia, G., Bonaventura, R., Muller, W., 2000. Cellular and biochemical responses to environmental and experimentally induced stress in sea urchin coelomocytes. *Cell Stress & Chaperones* 5, 113-120. https://doi.org/10.1379/1466-1268(2000)005

Matranga, V., Pinsino, A., Celi, M., Bonaventura, R., Natoli, A., Schroder, H.G., Müller, W.E.G., 2005. Monitoring chemical and physical stress using sea urchin immune cells. *Progress in Molecular and Subcellular Biology* 39, 85-110. https://doi.org/10.1007/3- 540-27683-1_5

Matranga, V., Pinsino, A., Celi, M., Di Bella, G., Natoli, A., 2006. Impacts of UV-B radiation on short-term cultures of sea urchin coelomocytes. *Marine Biology* 149, 25-34. https://doi.org/10.1007/s00227-005-02121

Migliaccio, O., Pinsino, A., Maffioli, E., Smith, A.M., Agnisola, C., Matranga, V., Nonnis, S., Tedeschi, G., Byrne, M., Gambi, M.C., Palumbo, A., 2019. Living in feature ocean acidification, physiological adaptive responses of the immune system of sea urchins resident at CO_2 vent system. *Scientific Total Environment* 672, 938-950. https://doi.org/10.1016/j.scitotenv.2019.04.005

Migliaccio, O., Castellano, I., Romano, G., Palumbo, A., 2014. Stress response to cadmium and manganese in *Paracentrotus lividus* developing embryos is mediated by nitric oxide. *Aquatic Toxicology* 156, 125-134. https://doi.org/10.1016/j.aquatox.2014.08.007

Migliaccio, O., Castellano, I., Di Cioccio, D., Tedeschi, G., Negri, A., Cirino, P., Romano, G., Zingone, A., Palumbo, A., 2016. Subtle reproductive impairment through nitric oxide-mediated mechanisms in sea urchins from an area affected by harmful algal blooms. *Scientific Report* 6, 26086. https://doi.org/10.1038/srep26086

Milito, A., Murano, C., Castellano, I., Romano, G., Palumbo, A., 2020. Antioxidant and immune response of the sea urchin *Paracentrotus lividus* to different re-suspension patterns of highly polluted marine sediments. *Marine Environmental Research* 160, 104978. https://doi.org/10.1016/j.marenvres.2020.104978

Murano, C., Agnisola, C., Caramiello, D., Castellano, I., Casotti, R., Corsi, I., Palumbo, A., 2020. How sea urchins face microplastics: uptake, tissue distribution and immune system response. *Environmental Pollution* 264, 114685. https://doi.org/10.1016/j.envpol.2020.1146850269-7491

Murano, C., Bergami, E., Liberatori, G., Palumbo, A., Corsi, I., 2021. Interplay between polystyrene nanoparticles and immune system of the Mediterranean sea urchin *Paracentrotus lividus*. *Frontiers Marine Science* 8, 647394. https://doi.org/10.3389/fmars.2021.647394

Oberbeckmann, S., Löder, M.J.G., Gerdts, G., Osborn A.M., 2014. Spatial and seasonal variation in diversity and structure of microbial biofilms on marine plastics in Northern European waters. *FEMS Microbiology Ecology* 90(2), 478-492. https://doi.org/10.1111/1574-6941.12409

Oberbeckmann, S., Löder, M.G.J., Labrenz, M., 2015. Marine microplastic-associated biofilms – a review. *Environmental Chemistry* 12, 551-562. https://doi.org/10.1071/EN15069

Oberbeckmann, S., Bernd, K., Matthias, L., 2018. Environmental factors support the formation of specific bacterial assemblages on microplastics. *Frontiers Microbiology* 8, 2709. https://doi.org/10.3389/fmicb.2017.02709

Ottaviani, E., Paeman, L.R., Cadet, P., Stefano, G.B., 1993. Evidence for nitric oxide production and utilization as a bacteriocidal agent by invertebrate immunocytes. *European Journal Pharmacology: Environmental Toxicology Pharmacology* 248 (4), 319-324. https://doi.org/10.1016/09266917(93)90006-C

Paul-Pont, I., Lacroix, C., Gonzàaìlez Fernàndez, C., Hègaret, H., Lambert, C., Le Goïc, N., Frére, L., Cassone, A.L., Sussarellu, R., Fabioux, C., Guyomarch, J., Albentosa, M., Huvet, A., Soudant, P., 2016. Exposure of marine mussels *Mytilus* spp. to polystyrene microplastics: Toxicity and influence on fluoranthene bioaccumulation. *Environmental Pollution* 216, 724-737. http://dx.doi.org/10.1016/j.envpol.2016.06.039

Pedrotti, M.L., Petit, S., Elineau, A., Bruzaud, S., Crebassa, J.C., Dumontet, B., Martì, E., Gorsky, G., Còzar, A., 2016. Changes in the floating plastic pollution of the Mediterranean Sea in relation to the distance to land. *PloS One* 11(8), e0161581. https://doi.org/10.1371/journal.pone.0161581

Pham, C.K., Ramirez-Llodra, E., Alt, C.S.H., Amaro, T., Bergmann, M., 2014. Marine litter distribution and density in European seas, from the shelves to deep basins. *PloS One* 9(4), e95839. https://doi.org/10.1371/journal.pone.0095839

Pinsino, A., Della Torre, C., Sammarini, V., Bonaventura, S., Matranga, V., 2008. Sea urchin coelomocytes as a novel cellular biosensor of environmental stress: a field study in the Tremiti Island Marine Protected Area, Southern Adriatic Sea, Italy. *Cell Biology Toxicology* 24, 541-552. https://doi.org/10.1007/s10565-008-9055-0

Pinsino, A., Matranga, V., 2015. Sea urchin immune cells as sentinels of environmental stress. *Developmental & Comparative Immunology* 49 (1), 198-205. https://doi.org/10.1016/j.dci.2014.11.013

Porter, A., Smith, K.E., Lewis, C., 2019. The sea urchin *Paracentrotus lividus* as a bioeroder of plastic. *Science Total Environment* 693, 133621. https://doi.org/10.1016/j.scitotenv.2019.133621

Postma, P.R., Cerezo-Chinarro, O., Akkerman, R.J., Olivieri, G., Wijffels, R.H., Brandenburg, W. A., Eppink, M. H. M., 2018. Biorefinery of the Macroalgae Ulva Lactuca: Extraction of Proteins and Carbohydrates by Mild Disintegration. *Journal of Applied Phycology* 30 (2), 1281–1293. https://doi.org/10.1007/s10811-017-1319-8

Rast, J.P., Smith, L.C., Loza-Coll, M., Hibino, T., Litman, G.W., 2006. Genomic Insights into the Immune System of the Sea Urchin. *Science* 314 (5801), 952–956. https://doi.org/10.1126/science.1134301

Renwrantz, L., Siegmund, E., Woldmann, M., 2013. Variations in hemocyte counts in the mussel, *Mytilus edulis*: Similar reaction patterns occur in disappearance and return of molluscan hemocytes and vertebrate leukocytes. *Comparative Biochemistry Physiology A: Molecular Integrative Physiology* 164 (4), 629-637. https://doi.org/10.1016/j.cbpa.2013.01.021

Richa, K., Balestra, C., Piredda, R., Benes, V., Borra, M., Passarelli, A., Margiotta, F., Saggiomo, M., Biffali, E., Sanges, R., Scanlan, D.J., Casotti, R., 2017. Distribution, community composition, and potential metabolic activity of bacterioplankton in an urbanized Mediterranean Sea coastal zone. *Applied Environmental Microbiology* 83 (17), e00494-17. https://doi.org/10.1128/AEM.0049417

Romano, G., Costantini, M., Buttino, I., Ianora, A., Palumbo, A., 2011. Nitric oxide mediates the stress response induced by diatom aldehydes in the sea urchin *Paracentrotus lividus. PloS One* 6(10), e25980. https://doi.org/10.1371/journal.pone.0025980

Rummel, C.D., Jahnke, A., Gorokhova, E., Kühnel, D., Schmitt-Jansen, M., 2017. Impacts of biofilm formation on the fate and potential effects of microplastic in the aquatic environment. *Environmental Science Technology Letters* 4, 258-267. https://doi.org/10.1021/acs.estlett.7b00164

Shür, C., Rist, S., Baun, A., Mayer, P., Hartmann, N.B, Wagner, M., 2019. When fluorescence is not a particle: the tissue translocation of microplastics in *Daphnia magna* seems an artifact. *Environmental Toxicology & Chemistry* 38 (7), 1495-1503. https://doi.org/10.1002/etc.4436

Smith, L.C., Arizza, V., Hudgell, M.A.B., Barone, G., Bodnar, A.G., Buckley, K.M., Cunsolo, V., Dheilly, N.M., Franchi, N., Fugmann, S.D., Furukawa, R., Garcia-Arraras, J., Henson, J.H., Hibino, T., Irons, Z.H., 2018. Echinodermata: The Complex Immune System in Echinoderms. In: Cooper, E. (ed) Adv Comp Immunol. Springer, Cham. https://doi.org/10.1007/978-3-319-76768-0_13

Suaria, G., Perold, V., Lee, J.R., Lebouard, F., Aliani, S., Ryan, P.G., 2020. Floating macro- and microplastics around the Southern Ocean: results from the Antarctic Circumnavigation Expedition. *Environmental International* 136, 105494. https://doi.org/10.1016/j.envint.2020.105494

Suaria, G., Avio, C.G., Mineo, A., Lattin, G.L., Magaldi, M.G., Belmonte, G., Moore, C.J., Regoli, F., Aliani, S., 2016. The Mediterranean plastic soup: synthetic polymers in Mediterranean surface waters. *Scientific Report* 23 (6), 37551. https://doi.org/10.1038/srep37551

Sun, S., Shi, W., Tang, Y., Han, Y., Du, X., Zhou, W., Hu, Y., Zhou, C., Liu, G., 2020. Immunotoxicity of petroleum hydrocarbons and microplastics alone or in combination to a bivalve species: Synergic impacts and potential toxication mechanisms. *Science Total Environment* 728, 138852. https://doi.org/10.1016/j.scitotenv.2020.1388520048-9697

Tafalla, C., Gómez-León, J., Novoa, B., Figueras, A., 2003. Nitric oxide production by carpet shell clam (*Ruditapes decussatus*) hemocytes. *Developmental & Comparative Immunology* 27(3), 197-205. https://doi.org/10.1016/S0145-305X(02)00098-8

Tan, T., Zhu, T., Wu, D., Song, E., Song, T., 2020. Compromised autophagic effect of polystyrene nanoplastics mediated by protein corona was recovered after lysosomal degradation of corona. *Environmental Science & Technology* 54, 11485−11493. https://doi.org/10.1021/acs.est.0c04097

Vroom, R.J.E., Koelmans, A.A., Besseling, E., Halsband, C., 2017. Aging of microplastics promotes their ingestion by marine zooplankton. *Environmental Pollution* 231, 987-996. http://dx.doi.org/10.1016/j.envpol.2017.08.088

Watts, A.W.J., Lewis, C., Goodhead, R.M., Beckett, S.J., Moger, J., Tyler, C.R., Galloway, T.S., 2014. Uptake and retention of microplastics by the shore crab *Carcinus maenas*. *Environmental Science Technology* 48 (15), 8823-8830. https://doi.org/10.1021/es501090

Wright, R., Erni-Cassola, G., Zadjelovic, V., Latva, M., Christie-Oleza, J.A., 2020. Marine Plastic Debris: a new surface for microbial colonization. *Environmental Science & Technology* 54(19), 11657–11672. https://doi.org/10.1021/acs.est.0c02305

Zettler, E.R., Mincer, T., Amaral- Zettler, L., 2013. Life in the "Plastisphere": Microbial communities on plastic marine debris. *Environmental Science & Technology* 47(13), 7137–7146. https://doi.org/10.1021/es401288x

Chapter 3

"Microplastics occurrence in the Mediterranean sea urchin

Paracentrotus lividus along the Gulf of Naples (Italy)"

Abstract

Nowadays, it is well established that plastic pollution has become a problem of global concern. Serious questions remain still unexplored regarding the interaction between living organisms and plastic debris including MPs (< 5mm). Here, the aim of this study was to assess the presence of MPs in sea urchins *Paracentrotus lividus* from a coastal area of Southern Italy, the Gulf of Naples, to monitor the extent of MP contamination in local sea urchin's populations and assess the potential risks for the species as well as for humans due to their consumption. The data revealed the occurrence of MPs, mostly MFs (>90%), in adult sea urchin specimens sampled in four sites in the Gulf of Naples (Ischia, Rocce Verdi, Capo Miseno, Nisida). MFs were found both in gonads, coelomic fluid and digestive system, although the latter is more affected in all sampling sites. Altogether the 100 sea urchin specimens collected and analyzed for the 4 collection sites of the Gulf of Naples, showed a total of 260 fibers with an average of 2.6 items/ individual. The highest number of fibers was found in those retrieved from Rocce Verdi (4.88 items/ individual) followed by those from Nisida (3.28 items/ individual), while the lowest in those from Ischia (0.60 items/ individual). The most representative MFs colours were: black, grey and blu, but red, green and transparent fibers were also found in smaller quantities. Fourier Transform Infrared spectroscopy (µ-FTIR) analysis revealed that both polyester and cotton-based fibers were found. The origin of such polymers could be mainly attributable to fragmentation of fishing lines and/or release of sewages discharges from municipal sewage treatment plants. This study acts as a pivotal investigation to unravel the occurrence of MPs in wild-caught sea urchins from Mediterranean coastal areas, thus providing the key elements for future biomonitoring investigations. Overall, the sea urchins represent a suitable bioindicator to easily monitor the presence of MPs and in particular MFs in a benthic ecosystem.

Main findings: MF were found in the soft body of wild-caught sea urchins collected along various sites of the Gulf of Naples. Either of synthetic (polyester) and natural origin (cellulose) they showed a different disposition with digestive system keeping the highest amount compared to gonads and coelomic fluid.

3.1 Introduction

The interaction of plastic debris with marine organisms can occur through different routes either in single cell organisms or through contact with gills and body. It is widely recognized that the main route having a significant impact on marine life is represented by ingestion (Anastasopoulou & Fortibuoni, 2019). Since the first scientific observations reported by Kenyon & Kridler (1969) and Carpenter (1972) in wildlife, evidence has exponentially increased, and the presence of more than 90 species which have ingested plastic items has been documented in critical areas, such as the Mediterranean Sea (Deudero & Alomar, 2015; Fossi et al., 2018). The highest amount of plastic was found in species that mainly populate benthic and benthopelagic habitats, therefore recognized as being at greater risk of MP contamination. This is amplified even more in coastal areas, where the presence of river and land runoffs make them hotspot areas for cumulative anthropogenic impacts (Compa et al., 2019; Navarro et al., 2021). Field observation and bench-scale studies documented that the most commonly reported harmful implications in marine organisms upon ingestion of plastic items (mostly MPs) include predator avoidance, satiety-induction, intestinal blockage, inflammation and physical damages (Pedà et al., 2016; Alomar et al., 2017; Jovanović et al., 2018; Giani et al., 2018; Chan et al., 2019; Solomando et al., 2020; Chenet et al.,2021). In point of fact, not only MPs thus represent a threat by themselves as "plastic" but the presence of polymer additives (e.g. bisphenols, phthalates), adsorbed contaminants and pathogens on MPs (e.g. heavy metals, persistent organic pollutant, *vibrio*) could contribute to their ecological risks (Rochmann et al., 2013; Zettler et al., 2013, Koelmans et al., 2016; Oberbeckmann, et al., 2018). Moreover, the transfer and accumulation of contaminants and pathogens along food webs from prey to predators up to humans is of greater concern (Carbery et al., 2018; Ribeiro et al., 2019).

In this framework, the shellfish consumption appears to be greater compared to that of fish (Garrigo et al., 2020). Indeed, while shellfish (including various species of molluscs, crustaceans, and echinoderms) are usually eaten as whole soft body without gut removal (e.g. oysters, mussels, clams), the digestive tract of fishes, commonly recognized as the organ mostly affected by the internalization of plastic items, is discharged. Moreover, while fish of high commercial value such as *Sardina pilchardus*, *Mullus barbatus* and *Merluccius merluccius* contain less than 3 MPs/individual (Compa et al., 2018; Digka, 2018; Giani et al., 2018), the concentrations found in Mediterranean shellfish can range from 2 up to 12 MPs/individual (Avio et al., 2017; Bordbar et al., 2018; Cau et al., 2019; Wakkaf et al., 2020). Seafood is an important part of the Mediterranean diet and shellfish consumption in some area, for example in Italy, is expected to exceed 45 g/day per capita (EFSA,2014). According to estimates by Van Cauwenberghe & Janssen (2014), the European shellfish consumers can ingest from 1,800 to 11,000 MPs per year although it is not yet regulated

(Ziccardi et al., 2016). Globally, the estimated average number of MP intake from shellfish ranged from 2602 to 16288 items/capita/year (Senathirajah et al., 2021).

In the Mediterranean coastal areas, sea urchin's gonad roe of *P. lividus* is among the most consumed seafood products, mostly in France and Southern Italy (Stefánsson et al., 2017). Annual global production is estimated at 60,000-70,000 tonnes per year (FAO, 2016). It is not surprising that among shellfish for human consumption, sea urchin is one of the species highly subjected to intensive harvesting by official and recreational fishermen during last year's thus contributing to the continuous depletion of natural stocks (Pais et al., 2021; Furesi et al., 2016). Sea urchin plays a key role in benthic communities in the organization and structure of shallow macroalgal assemblages (Boudouresque & Verlaque, 2020). Being a voracious herbivore, sea urchin ingests daily large amounts of algal biomass and it represents also an important energetic link from shallow water macroalgae to benthic communities (Dethier et al., 2019). Despite its high ecological relevance and its importance as a sea food, the interaction between plastic debris and sea urchins *P. lividus* are overlooked. Based on the current knowledge, *in vivo* and *in vitro* laboratory studies reported the first indications of the harmful effects of the MPs and nanoplastics exposure in sea urchin from the early stages of development up to adults (Pinsino et al., 2017; Beiras et al., 2019; Murano et al., 2020; Bertucci & Bellas, 2021; Murano et al., 2021). However, up to now, few data are available on MP's occurrence in wild caught specimens of the Mediterranean sea urchin *P. lividus*. Recently, MPs concentration in the sea urchin *P. lividus* from Aegean Sea (Greece) was reported to be $1.95 \pm 1.70 \ g^{-1}$ (Hennicke et al., 2021). However, this quantification could have overestimated the real MPs concentration because the polymer characterization was not performed.

In light of the limited data available and the importance to assess the occurrence of MPs in wild caught specimens of *P. lividus*, the aim of this study was to assess the presence of MPs in *P. lividus* from a coastal area of Southern Italy, the Gulf of Naples, to monitor the extent of MP contamination in local sea urchin's populations and assess the potential risks for the species as well as for humans due to their consumption.

3.2 Materials and methods

3.2.1. Sampling area

The Gulf of Naples (Campania Region, Italy) is located in the south-eastern Tyrrhenian Sea (western Mediterranean Sea) with a coverage of 870 km² and an average depth of 170 m (Carrada et al., 1980). It is widely recognized as a biodiversity hotspot and hosts a large marine protected area (1128 ha) "Punta Campanella" located in the Sorrento Peninsula. From a hydrological point of view, the Gulf of Naples showed typical features of both oligotrophic and eutrophic systems (Cianelli et al., 2012). Here, the sciaphilic hard bottom habitats show the highest biophysical and economic value in terms of marine natural capital stocks (Buonocore et al., 2020). On the external side of the Gulf are located the 3 most important islands of the Campania Region: Ischia, Procida and Capri. Between Ischia and Capri, there is the main opening of the Gulf named "Bocca Grande " which guarantees the largest exchanges between the Gulf and the Southern Tyrrhenian Sea. By contrast, the communication with other neighbouring basins, Gulf of Salerno and Gulf of Gaeta, occurs along "Bocca Piccola " and also Ischia and Procida channels. Despite the relatively small extension of the Gulf of Naples, this area is known as one of the most strongly anthropized urban areas in South Italy with over 1 million inhabitants living along its coasts (Alberico et al., 2018). Different inputs co-existing the area thus having a strong pressure including plastic pollution from various sources (e.g., extensive touristic, maritime and commercial activities and urban, industrial and agricultural wastewaters) (Cianelli et al., 2012). In particular, the North-Eastern part of the Gulf is considered the mosst affected by anthropic pollution due to a considerable presence of industries linked to the sectors of food preservation, textile-clothing production and leather tannery (Tornero & Ribera d'Acalà, 2014). In the area flows the Sarno river, one of the most polluted rivers in Europe, which collects not only the spill of tannery and canning factories but also a large amount of plastic from land run-off (Montuori et al., 2013).

3.2.1.1 Sea urchin sampling

Within the Gulf of Naples, four sampling sites representative of the common habitats of *P. lividus* were chosen: Rocce Verdi (RV), Nisida (NS), Capo Miseno (CM) and Ischia (I) (Figure 3.1, Table 3.1). The sampling period was between July and December 2020 thanks to the precious support of all the scuba diving staff of the Stazione Zoologica Anton Dohrn of Naples.
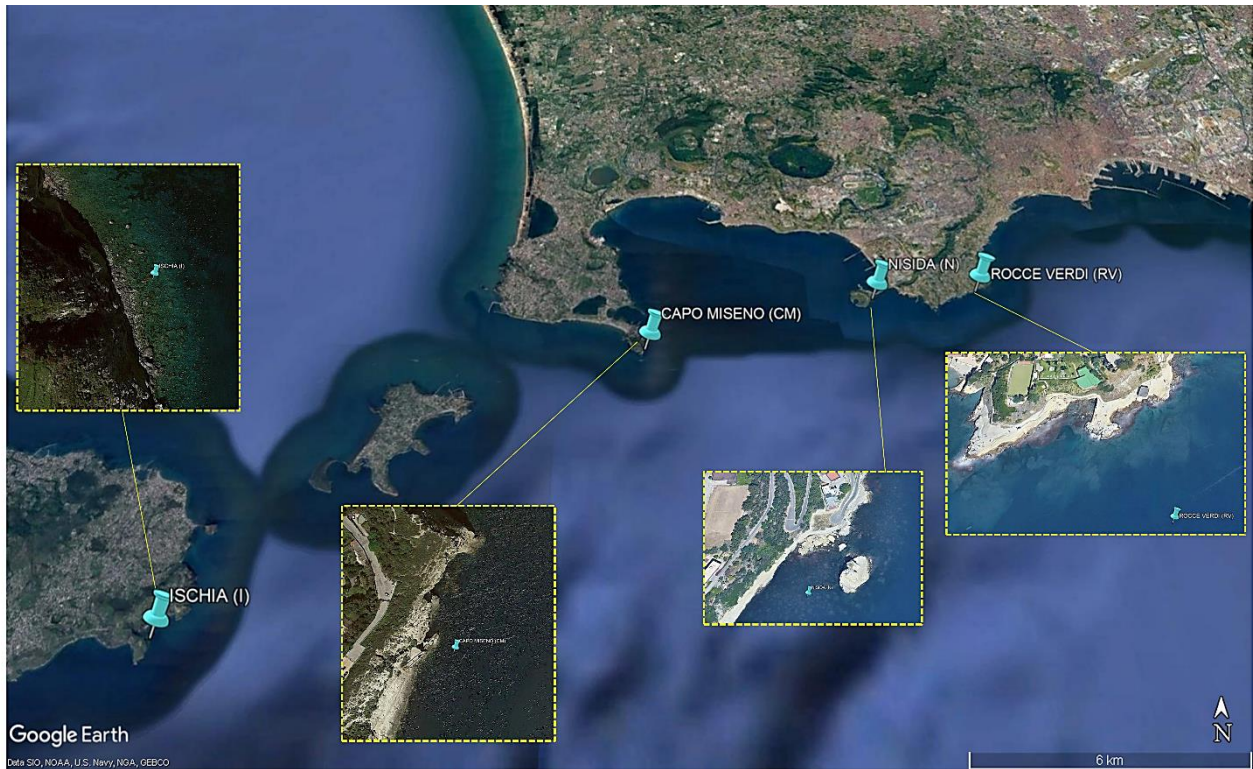
Figure 3.1. Sea urchin's sampling sites in the Gulf of Naples, Tyrrhenian Sea, Italy: Ischia (I), Capo Miseno (CM), Nisida (NS) and Rocce Verdi (RV). Scale bar: 6 km.

In each site, 25 adult specimens of *P. lividus* (>4 cm size, shell diameter without the spines) were collected manually, stored in a cool box covered with aluminium foil and immediately transferred to the Palumbo's laboratory of Stazione Zoologica.

Shell diameter (cm, without the spines) and whole body weight (g) were recorded individually (Table 3.1) before dissection and the following tissues and organs were removed under stereomicroscope Zeiss (KL1500 LCD): coelomic fluid, gonads and digestive system. Sex was determined only when the organism was sacrificed by observing the color of the gonoducts under the stereomicroscope.

The coelomic fluid was immediately filtered on Whatman filter papers (41, Ashless, 47 mm), the gonads and the digestive system were wrapped in aluminium foil and kept at −20 °C until further processing for MPs isolation and analysis

Table 3.1. Geographical coordinates of sampling sites and parameters of sea urchin specimens (weight, diameter and sex).

Area	ID	Coordinates	Depth (m)	Weight (g)	Diameter (cm)	Sex
Rocce Verdi	RV	40°47.809' N 14°12.065' E	7-12	44 ± 9.48	4.8 ±0.47	13 F 12 M
Capo Miseno	CM	40°46.726' N 14°5.418' E	6-10	40 ± 4.8	4.1 ± 0.33	14 F 11 M
Ischia	I	40°42.335' N 13°57.351' E	5-7	60 ± 12.3	6.3 ± 1.44	14 F 11 M
Nisida	NS	40°47.667' N 14°9.971' E	6-9	52.6 ± 15	4.9 ± 0.71	11 F 14 M

3.2.2 MPs analysis

Tissue and organs digestion

Sea urchin's tissues (coelomic fluid) and organs (digestive system and gonads) were processed according to the digestion method of Li et al. (2016) with some modifications. Fresh gonads and digestive system were inserted into a glass flask and pre-treated with 0.3% Trypsin (25 mL) at 45°C for 1h. Subsequently, tissue samples (1–10 g) were digested with 50 mL of H_2O_2 (10%) added to each sample and placed in an oscillator batch at 65°C for 48h. The digestion process was considered complete only when the solution appeared clear with no traces of tissue. After 48h only for gonads, 100% ethanol (previously filtered on 0.45 glass filters) was added in the ratio 1: 2 to avoid lipid saponification according to the protocol reported by Dawson et al. (2020). A further step with saturated NaCl flotation technique was performed, adding 350 mL of NaCl (1.2 g cm^{-3} filtered 0.45 μm) overnight. Soon after, the entire solution was filtered on Whatman filter papers (41, Ashless, 47 mm) to avoid the loss of potential plastic items. All filters were observed and photographed using a stereomicroscope LEICA M205FA with image analysis system Leica Application Suite (LAS) software.

Items isolation and recovery

As reported in Bessa et al. (2019), the retrieved items were recorded according to their shape (fibers, fragments, films, beads), colour (black, grey, red/pink, blue, green, white/translucent) and size according to the following criteria taking into account the size limits commonly used for sub-micron, micro- and meso-plastics (<1 mm; 1-5 mm; >5mm, respectively). A subset of 20 filters was used in order to perform Nile Red staining (stock solution in acetone 5 mg L^{-1}) according to Shim et al., (2016). Filters are embedded in the Nile Red solution (1:100 in acetone) in a glass petri dish at room temperature for 4h. All the suspected items were then removed to be further identified by Fourier transform infrared microscopy (μ-FTIR).

MFs characterization

The current COVID-19 pandemic situation and related mitigation measures only allowed us to carry out a preliminary characterization of the fibers found in wild specimens of *P. lividus*. The attention was focused on representative fibers samples (mostly found) and not present in laboratory blanks. The measurements were carried out by Dr. Lisa Vaccari and Dr. Giovanni Birarda at the Synchrotron Infrared Source for Spectroscopy and Imaging (SISSI) laboratories of the ELETTRA Synchrotron in Trieste. MF samples (n = 4) (Figure 3.5) were identified under a stereomicroscope, isolated, rinsed in ultrapure water and analyzed individually by microscope-coupled Fourier Transformed Infrared spectroscopy (µ-FTIR). For the measurements, the individual MFs were compressed on a diamond cell (Diamond EXPress Compression Cell, ST-Japan) and examined under the Hyperion 3000 microscope, connected to the Vertex 70v interferometer (Bruker Optics) and to a Mercury-Cadmium-Tellurium detector. To determine the homogeneity of the sample, measurements were made at different points in the sample. Each measurement corresponds to 256 scans made at a frequency of 40 KHz and a resulting spectrum. As a reference, a reference spectrum was acquired in a region of the diamond cell without the sample prior to each measurement. The polymeric composition of the MFs was determined by the analysis of the spectra acquired through µ-FTIR thanks to the experience of the operators and a reference library on the instrument (BioRad KnowItAll software).

Quality assurance and quality control

During all phases of this study the operators worked under controlled conditions to reduce the interference from laboratory contamination (e.g., air) or other inputs. The most critical phase for possible contamination concerns all the steps starting from the dissection to visual identification. For this reason, the air circulation in the laboratory has been minimized from this point. All surfaces, dissecting equipment and instruments were washed with ethanol (70% filtered 0.45 µm) and no synthetic and coloured clothing was worn during the experiment. All glassware used for digestions was washed first in distilled water then in hydrochloric acid (2%) and again in distilled water and stored, covered by aluminium foil in places free of contaminants. Procedural blanks (run in parallel) and recovery test using PE fragments as briefly described in Table 3.2 according to recent literature (Prata et al., 2021) were run. The sample digestion took place following the recurring pattern: 6 samples, 3 blanks, 3 controls were processed for each batch (Table 3.2).

Table 3.2. Quality Assurance Procedures Applied during Sample Processing

Type		Action	Replicates	Total numbers
Control	Clean filter exposed to air of laboratory during sample filtration	Atmospheric contamination	32	3 black fibers
Blanks	Reagents used for tissue digestion processed at same way of the samples	Reagents contamination	32	4 black fibers
Internal Standards	30 PE fragments treated in same way of samples	Recovery	8	98% recovery

3.2.3 Data Analysis

The Shapiro-test was first used to assess data distribution. Since the data did not conform to the normality distribution assumptions, a non-parametric analysis of the data was performed using the One-way analysis of variance (ANOVA) (Kruskal-Wallis) (*p-value* < 0.05) followed by Dunn's multiple comparison test. Data on plastic abundance are presented as mean, min and max. All statistics analysis and Pearson correlation were performed using GraphPad Prism version 7.00 for Windows.

3.3 Results

3.3.1 Morphological characteristics and plastic items abundance

A total of 260 fibers and 1 fragment was found with an average of 2.6 items/individual in the 100 specimens of sea urchin collected and analysed for the 4 collection sites of the Gulf of Naples, (Table 3.3). For a better representation of the results obtained, the corresponding background values (control/blank) for each site have been subtracted from the samples. The recovery-effectiveness of MPs using the extraction method previously described confirms the validity of the method with a recovery greater than 98% (Table 3.2).

Table 3.3 Shape and abundance of plastic items in coelomic fluid (CF), digestive system (DG) and gonads (G) of sea urchins.

Area	Shape	Items (CF)	Items (DG)	items (G)	Total number of items	Total number of items/individual
Rocce Verdi	99.2% fibres 0.8 % fragment	9	69	44	122	4.88
Capo Miseno	100% fibres	17	12	13	42	1.68
Ischia	100% fibres	3	8	4	15	0.60
Nisida	100% fibres	29	31	22	82	3.28
Total	-	58	120	83	261	2.61

By looking at MPs in specimens site by site, the highest number of fibers was found in those retrieved from Rocce Verdi (4.88 items/individual) followed by those from Nisida (3.28 items/individual),

Capo Miseno (1.68 items/individual) and the lowest in those from Ischia (0.60 items/individual). The highest amount of fibers is found in the digestive system, containing 46% of all the fibers retrieved. The gonads also presented a fairly high number 31.8% while the coelomic fluid was the lowest 22.2%. Figure 3.2 shows the individual variations in the number of fibers found in tissue/organs and among sampling sites. As for the coelomic fluid, specimens from Nisida showed the highest amount of fibers with an average of 1.16 items/individual while the lowest were retrieved in those from Ischia where only 3 fibers were found, ($p<0.05$). In the case of the digestive system, the highest individual average was reported in the Rocce Verdi (2.76 items/individual) and Nisida sites (1.24 items/individual) and in both cases the maximum number of fibers per individual was n = 8. In fact, the internalization differences in the digestive system of the specimens sampled in the Rocce Verdi is statistically significant compared to the others. Instead, in the gonads, only the Rocce Verdi site reported a high average and with individuals internalizing up to n = 10 fibers. Also specimens from Ischia showed the lowest number of fibers.
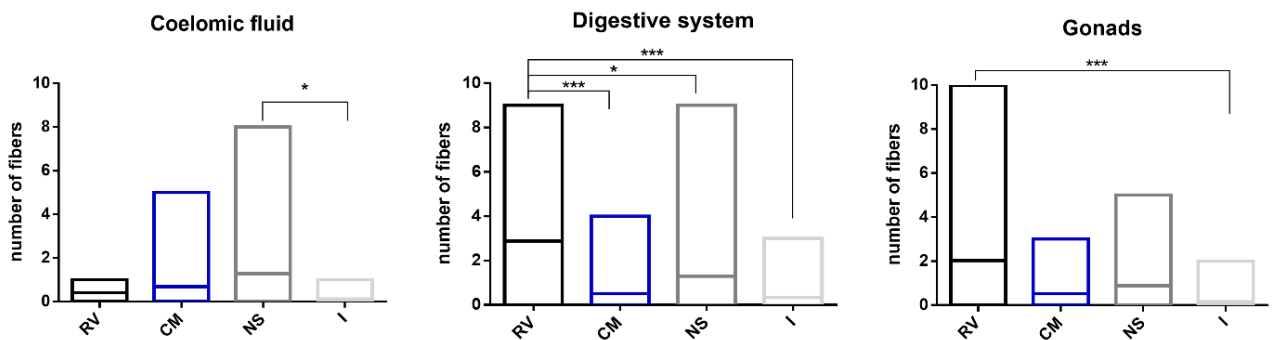
Figure 3.2 Number of fibers retrieved in the 25 individuals from each sampling site (RV, CM, NS, I in the coelomic fluid, digestive systems and gonads. Data are represented as floating bars (min, max and mean). Asterisks indicate values that are significantly different from each other, *p-value* < 0.05, *** *p-value* < 0.001.

In addition, from the Pearson correlation analysis between the numbers of fibers found in the different samples comparing the different tissues, it emerged that there was a very strong positive correlation between the number of fibers found in the digestive system and those in the coelomic fluid of specimens from Nisida ($r^2=0.98$). A positive correlation ($r^2 =0.60$) was also found between fibers found in the coelomic fluid and those in gonads in specimens from Capo Miseno and Ischia sites (Figure S.3.1). Finally, in the Rocce Verdi site, no statistical correlation was found between internalized fibers and the gonads, coelomic fluid and digestive system.

3.3.2 Size and color of plastic items in sea urchins

Examples of the most common fibers retrieved in sea urchin specimens from the Gulf of Naples are shown in Figure 3.3 and Figure S 3.2. The fibers showed an irregular shape with a structure similar to bundles of filaments and in some cases these appear to be knotted together. In terms of size, the half of ingested plastics were in the micron category <5 mm (53.4%) followed by meso and macro (>5 mm) (46.6%) (Figure S.3.3). The color classification highlights an important factor: the color pattern was preserved in the different organs of the same site (Figure 3.4). By contrast, in the same organs there was a clear difference among the sampling sites. In detail, the most representative colours in the Rocce Verdi site are: black (37-60%) and blue (20-33%). Similarly, Capo Miseno showed a pattern in which black (46-58.9 %), blue (5.8- 34%) but also grey (8-23.5 %) were the most abundant colors. Nisida, instead, presented more grey (36-57%) and blue fibers (20-36 %). Ischia was a particular case due to the few fibers found which are mainly black (62.5%-100%) and green (25%). Green colour was found in very low percentages also in the digestive system of sea urchin from Rocce Verdi (3%) and in the coelomic fluid-digestive system of sea urchin from Nisida.
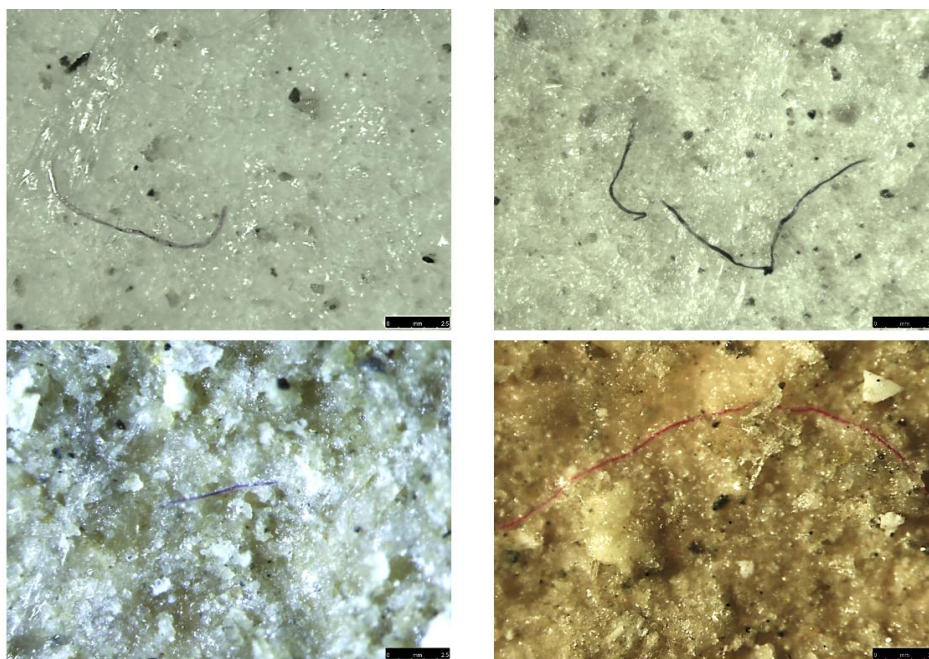
Figure 3.3. Examples of fibers found in sea urchin adult specimens retrieved from 4 sites located in the Gulf of Naples. Scale bar: 2.5 mm. Images were obtained using a stereomicroscope LEICA M205FA with image analysis system Leica Application Suite (LAS).
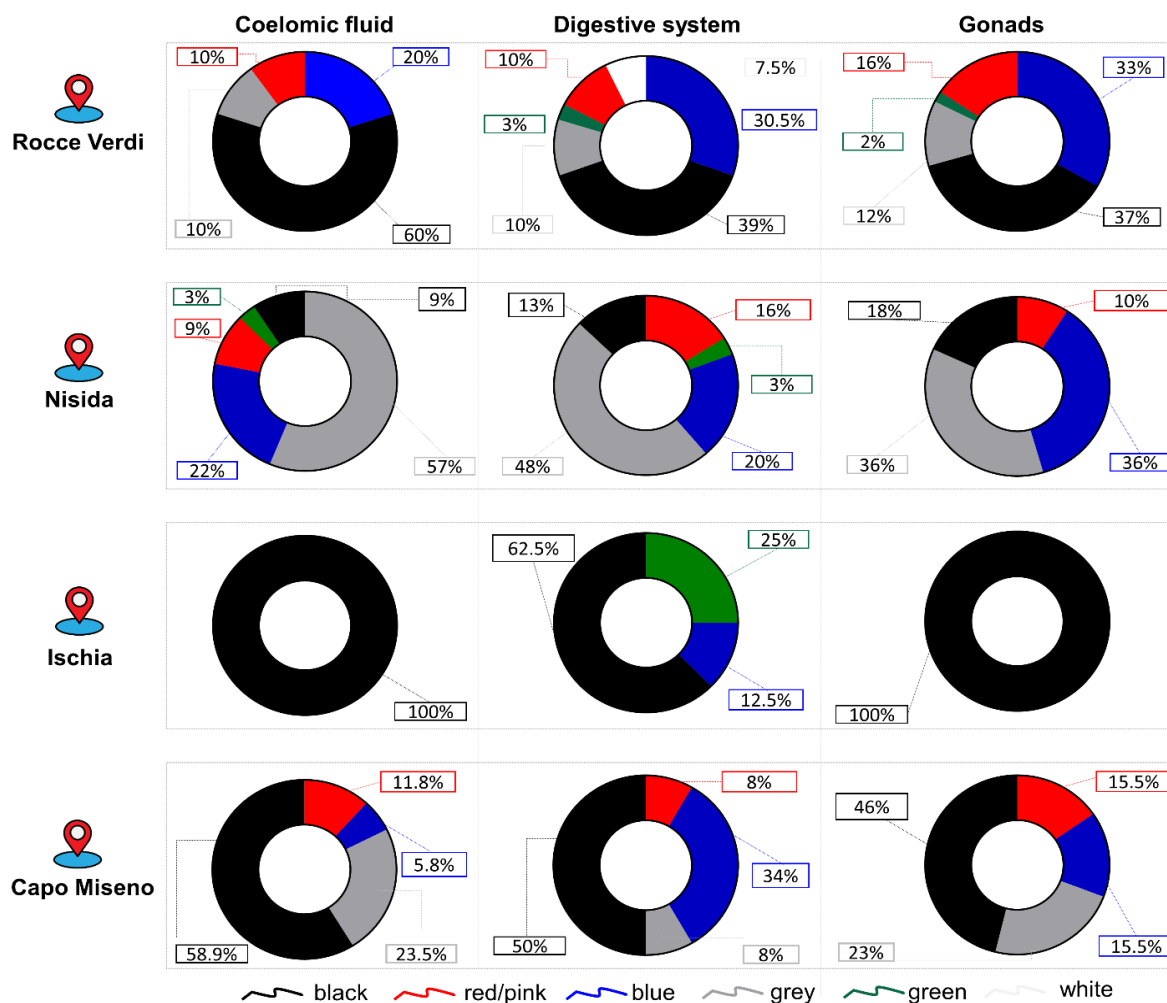
Figure 3.4. Percentage fibers colour in coelomic fluid, gonads and digestive systems at different sampling points.

3.3.3 Chemical composition of fibers

FT-IR analysis of a representative subsample of MF retrieved from wild-caught sea urchins from the 4 sites revealed the presence of polymers of either natural and synthetic origin. In detail, the analysis revealed polyester-based MFs as the most abundant (synthetic) (Figure 3.5 A) and cellulose-based MFs presumably of natural origin (Figure 3.5B).
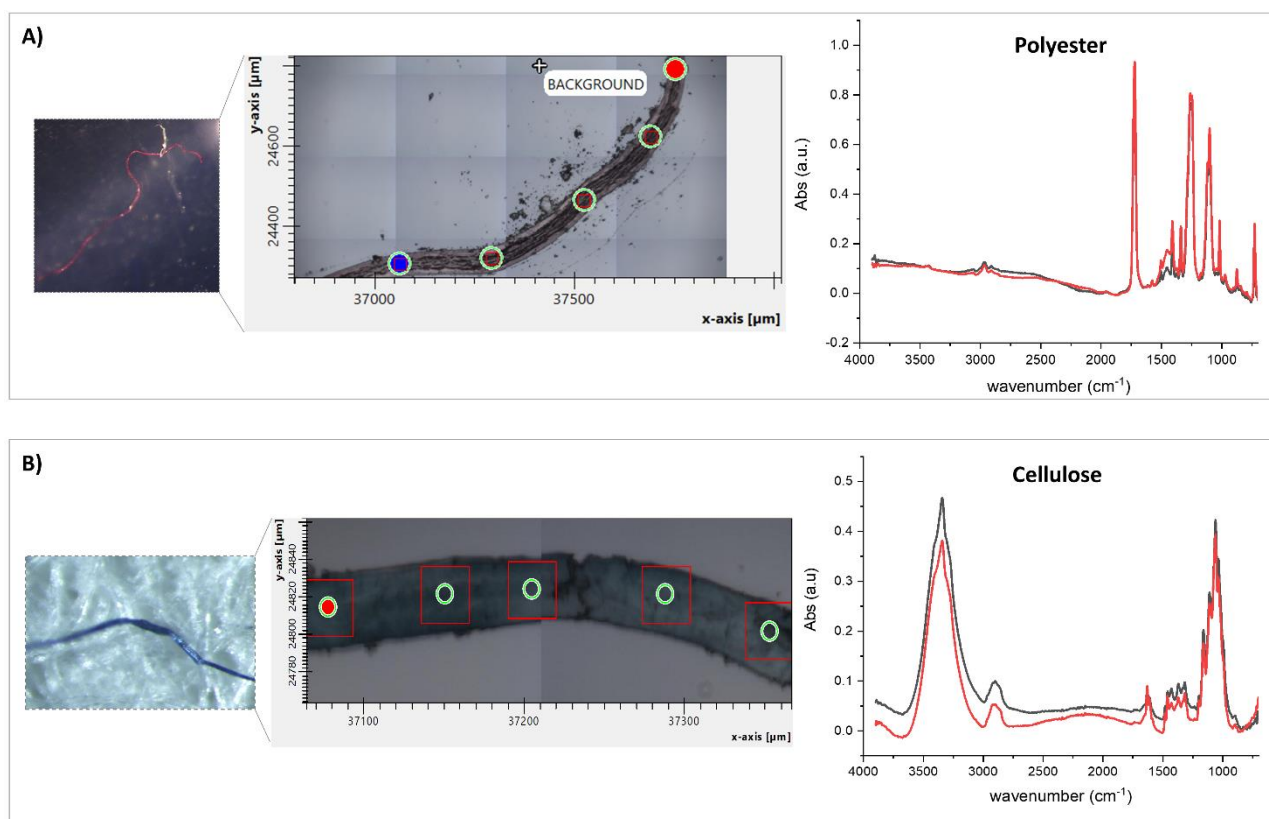
Figure 3.5. Fourier transform infrared (FT-IR) spectra of dominant MFs: A) example of red fibers identified as polyester-based; B) example of blue fibers identified as cellulose-based. The spectra are compared with their respective reference spectra.

3.4 Discussion

The present study, to the best of our knowledge, represents the first insight on the presence of MPs, in particular MFs, in wild specimens of the sea urchins *P. lividus* caught in different sites of the Gulf of Naples. MFs were found in gonads, digestive system and coelomic fluid of the sea urchins. Not surprisingly, the organ most affected in terms of the presence of MFs was the digestive system with a total of 120 fibers found in 100 specimens analyzed. The MFs overall average was of 2.6 items/individual ranging from 0.60 items/individual (Ischia site) up to about 5 items/individual (Rocce Verdi site). Cross- contamination during dissection and digestion of the biological samples was negligible since substantial differences were found between of the number of items retrieved in the sea urchins samples (260 fibers) and in control/blanks (7 fibers), respectively (Table 3.2)

A subsample of ingested fibers was analyzed through μ-FTIR revealing a predominance of polyester-based MFs and cellulose-based MFs consisting in dyed natural cellulose (cotton). The presence of this type of synthetic and non-synthetic fibers was in line with the fibers most recently found in the sediments of the Mediterranean Sea (Sànchez-Vìdal et al., 2018). Data available in the scientific literature reported that fibers are the majority of MPs (> 80%) found in other Mediterranean species

as demersal and pelagic fish (*Mullus barbatus*; *Sardina pilchardus; Engraulis encrasicolus; Zeus faber; Lepidopus caudatus*) (Bottari et al., 2019; Compa et al., 2018), green crab (*Carcinus aestuarii*) (Piarulli et al.,2019), the most commonly. In particular, the majority of fiber were made of cotton, polyester, polyacrylamide and polypropylene. Interestingly, Feng and co-authors (2020) highlighted the presence of polyester/polyethylene MFs (>90%) in the digestive system of four different species of sea urchins collected along the coast of China (*Hemicentrotus pulcherrimus, Temnopleurus reevesii, Strongylocentrotus intermedius, Temnopleurus hardwickii*).

By comparing the number of MF found in our study with other field studies using wild-caught sea urchins, they resulted significantly lower in number (our study 261 fibers in 100 specimens vs 1038 in 210 specimens by Feng et al. (Feng et al., 2020) According to Feng and co-authors, MFs are internalized by sea urchins through the peristiomal membrane and then pass into the fluid and gonads: therefore, it cannot exclude that MFs will enter through the madreporite itself as we showed for PS MPs (see chapter 1). Indeed, the madreporite is formed by pores large about 60- 70 µm (Murano et al., 2020) which would still allow the entry of MFs below this diameter as shown in other echinoderms such as holothurians (Iwalaye et al., 2020; Mohsen et al., 2021). Conversely, in the heart urchin (*Brissopsis lyrifera*), a very low number of MP was found (1 per each individual) and 90% as flakes and the remaining 10% as fibers (Bour et al. 2018).

Considering the amount of MFs internalized reported in this study, the sea urchin being a benthic grazer has retained less than expected considering the average amount of MPs found in the sea surface and sediments of the Mediterranean Sea. respectively in the range from 0.15 to 7.68 items m^{-3} (Cincinelli et al., 2019) and from 10 and 15 MFs per 50 mL (Woodal et al., 2015). More recent data reported 34.8 ± 18.3 per 50 mL (equivalent to 6.965 ± 3.669 microfibres m^{-2}) confirming the deep environment as the major MFs sink (Sanchez-Vidal et al., 2018).

The low number of MFs found in specimens analyzed in our study could be explained by spatio-temporal factors, hydrodynamism of marine coastal areas features and above all it reflects the low risk posed by them to the sea urchins living in those (Woodal et al., 2015). A high elimination rate of MFs by the urchins can be thus be hypothesized since based on our previous findings at bench-scale level *P. lividus* showed a marked capacity to egest MPs (microbeads like naturally occurring) up to 90% after 48 h (Murano et al., 2021). However, it cannot be ruled out that a rough surface, length-aspect-ratio and non-spherical shape of MFs could increase intestinal retention time with higher probability of causing harmful effects (Welden & Cowie, 2016; Gray et al., 2017). High MFs retention time not only could cause greater toxicity but also increase the possibility of transfer along the trophic chain (Mishra et al., 2019). Among the most common predators of the sea urchin there are two demersal fish species, sea bream (*Diplodus vulgaris)* and rainbow wrasse (*Coris julis)* both

actively controlling by predation sea urchin populations and in turn represent species of high commercial value (Sala & Zabala, 1996; Guidetti & Mori, 2005). Regarding the risk associated with the direct consumption of the sea urchin gonads, low risk can be assumed for human consumption. Indeed, taking into account that the average value of MFs found in the gonads was 0.83 items/individual and that mature urchin's gonads weigh was about 4-5 g/individual, 1 kg of sea urchin gonads consumed per year may transfer about 166-207 fibers/per year. This quantity is very low if compared with the quantities found in other types of sea food or other shellfish such as Mediterranean mussels (*M. galloprovincialis*) for which about 20.8 ± 8.88 MFs per individual are reported (Avio et al., 2020) corresponding to 1500-2600 fibers/per year (if a consumer eats 1kg of mussels). However, overall results, do not take into account neither the elimination of the MFs nor the possible difference of any seasonal changes in MF exposure concentrations. Although it is currently impossible to establish the exact amount of MPs/MFs ingested through seafood consumption, human exposure is certainly undeniable.

Currently, both synthetic and non-synthetic MFs are the contaminants of major concerns (Gago et al., 2018). In spite of the fact that non-synthetic items may be less persistent than synthetic ones, both are manipulated similarly with additives or dyes which may interact negatively with biota in aquatic environments (Compa et al., 2018). Owing to their small size, natural fibers like synthetic fibers can adsorb chemicals as well as bacteria (pathogens) onto their surface (Remy et al., 2015; Compa et al., 2018). Globally, the total production of textile fibers is about 60% of synthetic fibers, followed by 30% of cotton and 10% of other materials. Among the synthetic ones, the polyester fibers sale accounts for approximately half of the total global fiber market (Carr, 2017). As a matter of fact, the wastewaters discharged by textile industries and domestic laundering are the main pathways that allow MFs to enter the oceans making it the most common contaminant in sediment and sea water (Liu et al., 2021; Oldenburg et al., 2021). As revealed in a recent study, the pathway of synthetic MFs from atmospheric fallout and domestic wash to the wastewater treatment plant contribute the entry of $2.6 \times 10^3 - 3.7 \times 10^4$ MFs/m^3 in Mediterranean Sea (Pedrotti et al.,2021). Remarkably, MFs like those reported in our study showed a density greater than sea water (cotton and flax, 1.5 g/cm^3; polyester, 1.4 g/cm^3), thus suggesting their movements towards the bottom and their availability in the benthic environments.

In our study, Rocce Verdi and Nisida resulted the sites where the urchins presented the highest amount of MFs in their soft tissues. Interestingly, these two sites are very close to each other and are also close to Bagnoli-Coroglio area, an area heavily exposed to pollution for over a century due to the presence of the industrial district for metallurgical production (Giglioli et al., 2020). Rocce Verdi is an area highly interested by tourism, seaside activities and densely populated, while Nisida is a

circumscribed area (a sort of appendage of the gulf) interested mostly by residential activities. However, both sites are affected by the presence urban discharges one linked to the Wastewater Lift Station outflow (Nisida) and Rocce verdi to a sewer overflow (that elude the wastewater treatment) (https://www.arpacampania.it/web/guest/database-georeferenziato-scarichi-costieri). By contrast, Capo Miseno coastlines display only drain discharges. Interesting is the case of the Ischia site, in which sea urchins showed the lowest amount of MFs. The perimeter of the island is covered by submarine outfalls and natural thermal vents. These drainage points are far from the coast (or where the sea urchins usually reside) and the presence of special diffusers in these pipes favour the dilution in sea water of any contaminants, including MFs (Sinopoli et al., 2020). All these observations suggest that the MFs presence in sea urchins may strongly depend on the presence of these discharges that convey these MFs into the sea water, in particular at the Rocce Verdi and Nisida sites. However, since their lower density (in comparison to grain of sand for example) as well as the physical/ structural characteristics, the MFs are presumably subjected to both water and wind transport in longer range and larger scale (Brahney et al. 2021). Therefore, the presence of fibers could also derive from non-local but more dispersed sources.

3.5 Conclusions

Our study provided the first insight on the occurrence of MF in wild specimens of the sea urchin *P. lividus* collected from the Gulf of Naples. The results revealed that the sea urchin internalized mainly MFs in gonads, coelomic fluid, and digestive system, averaging about 2.6 MFs / individuals. Through a preliminary µ-FTIR analysis, these fibers were polymers either of natural (cellulose) and synthetic origin (polyester)The presence of such MFs suggest a common origin from urban wastewaters and fishing lines. Given the presence of MFs in wild sea urchins suggest that other benthic species including small pelagic fish can be exposed to them. Although the low amount of MFs found in the gonads of the sea urchin may pose a low risk to human health, the data presented in this study confirm that MFs currently may affect seafood quality.

Chapter 3- Supplementary material

	Coelomic fluid	Gonads	Digestive system
Coelomic fluid	1	0.12	-0.20
Gonads	0.12	1	-0.11
Digestive system	-0.20	-0.11	1

Rocce Verdi

	Coelomic fluid	Gonads	Digestive system
Coelomic fluid	1	-0.15	0.95
Gonads	-0.15	1	-0.24
Digestive system	0.95	-0.24	1

Nisida

	Coelomic fluid	Gonads	Digestive system
Coelomic fluid	1	0.66	0,19
Gonads	0.66	1	-0.69
Digestive system	0.19	-0.69	1

Ischia

	Coelomic fluid	Gonads	Digestive system
Coelomic fluid	1	0.60	0.29
Gonads	0.60	1	-0.34
Digestive system	0.29	-0.34	1

Capo Miseno

Figure S3.1. Results of the Pearson correlation between the match of fibers and the different organs in the different sampling sites. In the blue boxes the cases of high positive correlation are highlighted while in the yellow ones the negative correlation.

A)

B)
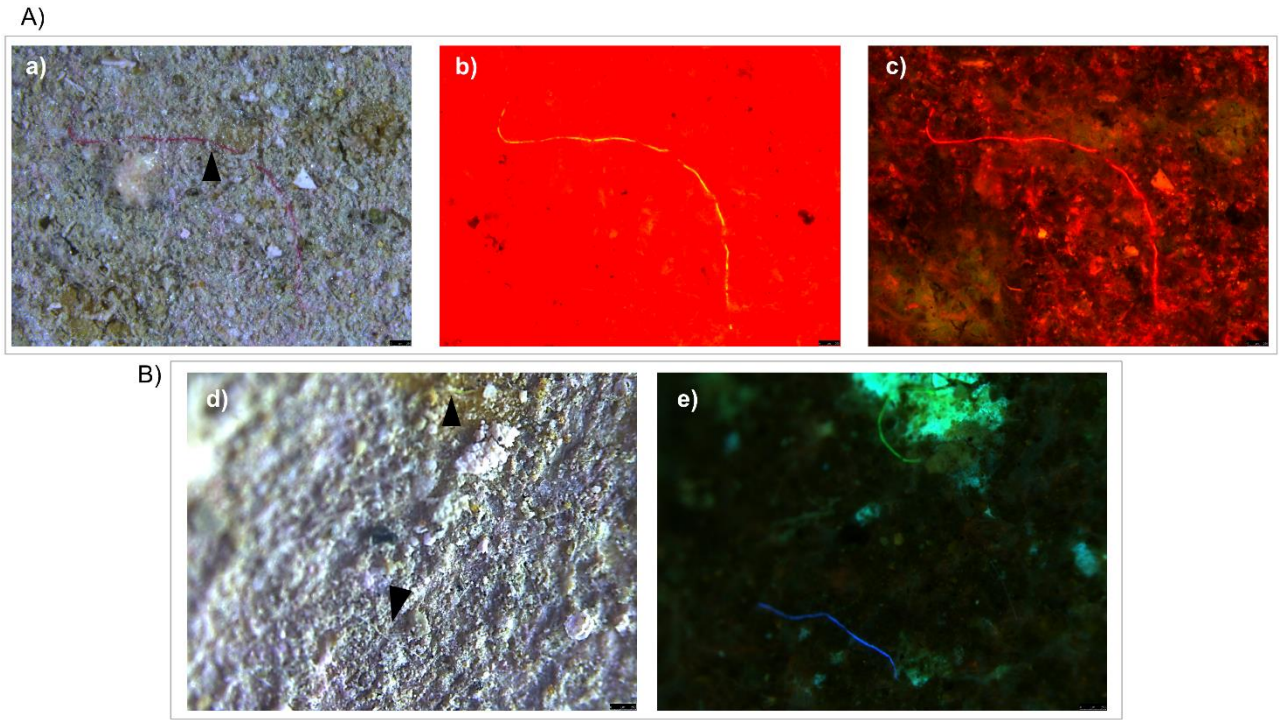
Figure S3.2. Examples of fibers treated with Nile red. In the upper box A was reported a red fiber in bright-field indicated by a black arrow (a), under red (b) and green (c) fluorescence. In the B box, instead, were represented two translucent fibers in bright-field indicated by a black arrow (d) and blue fluorescence (e). Scale bar 250 um.
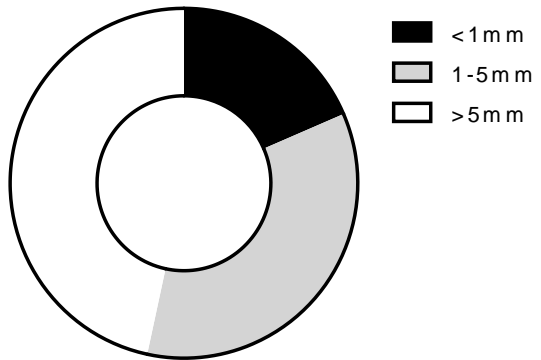
Figure S3.3. Representation of the average length of the fibers expressed as a percentage referring to 3 length classes: <1mm; 1-5 mm; >5 mm.

References

Alberico, I., Budillon, F., Casalbore, D., Di Fiore, V., Iavarone, R., 2018. A critical review of potential tsunamigenic sources as first step towards the tsunami hazard assessment for the Napoli Gulf (Southern Italy) highly populated area. *Nature Hazards* 92, 43–76. https://doi.org/10.1007/s11069-018-3191-5

Anastasopaulou, A., Fortiboni, T., 2019. Impact of Plastic Pollution on Marine Life in the Mediterranean Sea. *The Handbook of Environmental Chemistry*, 1-62. https://doi.org/10.1007/698_2019_421

Avio, C.G., Pittura, L., d'Errico, G., Abel, S., Amorello, S., Marino, G., Gorbi, S., Regoli, F., 2020. Distribution and characterization of microplastic particles and textile microfibers in Adriatic food webs: General insights for biomonitoring strategies. *Environmental Pollution* 258, 113766. https://doi.org/10.1016/j.envpol.2019.113766

Beiras, R., Muniategui-Lorenzo, S., Rodil, R., Tato, T., Montes, R., López-Ibáñez, S., Concha-Graña, E., Campoy-López, P., Salgueiro-González, N., Quintana, J.B., 2019. Polyethylene microplastics do not increase bioaccumulation or toxicity of nonylphenol and 4-MBC to marine zooplankton. *Science of The Total Environment* 692, 1–9. https://doi.org/10.1016/j.scitotenv.2019.07.106

Bertucci, J.I., Bellas, J., 2021. Combined effect of microplastics and global warming factors on early growth and development of the sea urchin (*Paracentrotus lividus*). *Science of The Total Environment* 782, 146888. https://doi.org/10.1016/j.scitotenv.2021.146888

Bessa, F., Frias, J., Kögel, T., Lusher, A., Andrade, J.M., Antunes, J., Sobral, P., Pagter, E., Nash, R., O'Connor, I., Pedrotti, M.L., Kerros, M.E., León, V., Tirelli, V., Suaria, G., Lopes, C., Raimundo, J., Caetano, M., Gago, J., Viñas, L., Carretero, O., Magnusson, K., Granberg, M., Dris, R., Fischer, M., Scholz-Böttcher, B., Muniategui, S., Grueiro, G., Fernández, V., Palazzo, L., de Lucia, A., Camedda, A., Avio, C.G., Gorbi, S., Pittura, L., Regoli, F., Gerdts, G., 2019. Harmonized protocol for monitoring microplastics in biota. Deliverable 4.3. (Report). *JPI-Oceans BASEMAN Project*. https://doi.org/10.13140/RG.2.2.28588.72321/1

Bordbar, L., Kapiris, K., Kalogirou, S., Anastasopoulou, A., 2018. First evidence of ingested plastics by a high commercial shrimp species (*Plesionika narval*) in the eastern Mediterranean. *Marine Pollution Bulletin* 136, 472–476. https://doi.org/10.1016/j.marpolbul.2018.09.030

Bottari, T., Savoca, S., Mancuso, M., Capillo, G., GiuseppePanarello, G., MartinaBonsignore, M., Crupi, R., Sanfilippo, M., D'Urso, L., Compagnini, G., Neri, F., Romeo, T., Luna, G.M., Spanò, N.,

Fazio, E., 2019. Plastics occurrence in the gastrointestinal tract of *Zeus faber* and *Lepidopus caudatus* from the Tyrrhenian Sea. *Marine Pollution Bulletin* 146, 408–416. https://doi.org/10.1016/j.marpolbul.2019.07.003

Bour, A., Avio, C.G., Gorbi, S., Regoli, F., Hylland, K., 2018. Presence of microplastics in benthic and epibenthic organisms: Influence of habitat, feeding mode and trophic level. *Environmental Pollution* 243, 1217–1225. https://doi.org/10.1016/j.envpol.2018.09.115

Brahney, J., Mahowald, N., Prank, M., Cornwell, G., Klimont, Z., Matsui, H., Prather, K.A., 2021. Constraining the atmospheric limb of the plastic cycle. *PNAS* 118. https://doi.org/10.1073/pnas.2020719118

Buonocore, E., Appolloni, L., Russo, G.F., Franzese, P.P., 2020. Assessing natural capital value in marine ecosystems through an environmental accounting model: A case study in Southern Italy. *Ecological Modelling* 419, 108958. https://doi.org/10.1016/j.ecolmodel.2020.108958

Carbery, M., O'Connor, W., Palanisami, T., 2018. Trophic transfer of microplastics and mixed contaminants in the marine food web and implications for human health. *Environment International* 115, 400–409. https://doi.org/10.1016/j.envint.2018.03.007

Carr, S.A., 2017. Sources and dispersive modes of micro-fibers in the environment. *Integrated Environmental Assessment and Management* 13, 466–469. https://doi.org/10.1002/ieam.1916

Carrada, G.C., Hopkins, T.S., Bonaduce, G., Ianora, A., Marino, D., Modigh, M., Ribera, D.M., Scotto, C.B., 1980. Variability in the Hydrographic and Biological Features of the Gulf of Naples. *Marine Ecology* 1, 105–120. https://doi.org/10.1111/j.1439-0485.1980.tb00213.x

Chenet, T., Mancia, A., Bono, G., Falsone, F., Scannella, D., Vaccaro, C., Baldi, A., Catani, M., Cavazzini, A., Pasti, L., 2021. Plastic ingestion by Atlantic horse mackerel (*Trachurus trachurus*) from central Mediterranean Sea: A potential cause for endocrine disruption. *Environmental Pollution* 284, 117449. https://doi.org/10.1016/j.envpol.2021.117449

Cho, Y., Shim, W.J., Jang, M., Han, G.M., Hong, S.H., 2021. Nationwide monitoring of microplastics in bivalves from the coastal environment of Korea. *Environmental Pollution* 270, 116175. https://doi.org/10.1016/j.envpol.2020.116175

Cianelli, D., Uttieri, M., Buonocore, B., Falco, P., Zambardino, G., Zambianchi, E., 2012. Dynamics of a very special Mediterranean coastal area: The Gulf of Naples. In: Mediterranean Ecosystems: Dynamics, Management & Conservation Editor: Gina S. William. ISBN 978-1-61209-146-4.

Cincinelli, A., Martellini, T., Guerranti, C., Scopetani, C., Chelazzi, D., Giarrizzo, T., 2019. A potpourri of microplastics in the sea surface and water column of the Mediterranean Sea. *TrAC Trends in Analytical Chemistry* 110, 321–326. https://doi.org/10.1016/j.trac.2018.10.026

Compa, M., Ventero, A., Iglesias, M., Deudero, S., 2018. Ingestion of microplastics and natural fibres in *Sardina pilchardus* (Walbaum, 1792) and *Engraulis encrasicolus* (Linnaeus, 1758) along the Spanish Mediterranean coast. *Marine Pollution Bulletin 128*, 89–96. https://doi.org/10.1016/j.marpolbul.2018.01.009

Dawson, A.L., Motti, C.A., Kroon, F.J., 2020. Solving a Sticky Situation: Microplastic Analysis of Lipid-Rich Tissue. *Frontiers in Environmental Science* 8, 163. https://doi.org/10.3389/fenvs.2020.563565

Dethier, M.N., Hoins, G., Kobelt, J., Lowe, A.T., Galloway, A.W.E., Schram, J.B., Raymore, M., Duggins, D.O., 2019. Feces as food: The nutritional value of urchin feces and implications for benthic food webs. *Journal of Experimental Marine Biology and Ecology* 514–515, 95–102. https://doi.org/10.1016/j.jembe.2019.03.016

Deudero, S., Alomar, C., 2015. Mediterranean marine biodiversity under threat: Reviewing influence of marine litter on species. *Marine Pollution Bulletin* 98, 58–68. https://doi.org/10.1016/j.marpolbul.2015.07.012

Feng, Z., Wang, R., Zhang, T., Wang, J., Huang, W., Li, J., Xu, J., Gao, G., 2020. Microplastics in specific tissues of wild sea urchins along the coastal areas of northern China. *Science of The Total Environment* 728, 138660. https://doi.org/10.1016/j.scitotenv.2020.138660

Furesi, R., Madau, F.A., Pulina, P., Sai, R., Pinna, M.G., Pais, A., 2016. Profitability and sustainability of edible sea urchin fishery in Sardinia (Italy). *Journal Coastal Conservation* 20, 299–306. https://doi.org/10.1007/s11852-016-0441-0

Gago, J., Carretero, O., Filgueiras, A.V., Viñas, L., 2018. Synthetic microfibers in the marine environment: A review on their occurrence in seawater and sediments. *Marine Pollution Bulletin* 127, 365–376. https://doi.org/10.1016/j.marpolbul.2017.11.070

Garrido Gamarro, E., Ryder, J., Elvevoll, E.O., Olsen, R.L., 2020. Microplastics in Fish and Shellfish – A Threat to Seafood Safety? *Journal of Aquatic Food Product Technology* 29, 417–425. https://doi.org/10.1080/10498850.2020.1739793

Giglioli, S., Colombo, L., Contestabile, P., Musco, L., Armiento, G., Somma, R., Vicinanza, D., Azzellino, A., 2020. Source Apportionment Assessment of Marine Sediment Contamination in a Post-Industrial Area (Bagnoli, Naples). *Water* 12, 2181. https://doi.org/10.3390/w12082181

Gray, A.D., Weinstein, J.E., 2017. Size- and shape-dependent effects of microplastic particles on adult daggerblade grass shrimp (*Palaemonetes pugio*). *Environmental Toxicology and Chemistry* 36, 3074–3080. https://doi.org/10.1002/etc.3881

Guidetti, P., Mori, M., 2005. Morpho-functional defences of Mediterranean sea urchins, *Paracentrotus lividus* and *Arbacia lixula*, against fish predators. *Marine Biology* 147, 797–802. https://doi.org/10.1007/s00227-005-1611-z

Harvesting Effects on *Paracentrotus lividus* Population Structure: A Case Study from Northwestern Sardinia, Italy, before and after the Fishing Season, 2011. *Journal of Coastal Research* 28, 570. https://doi.org/10.2112/JCOASTRES-D-10-00119.1

Hennicke, A., Macrina, L., Malcolm-Mckay, A., Miliou, A., 2021. Assessment of microplastic accumulation in wild *Paracentrotus lividus*, a commercially important sea urchin species, in the Eastern Aegean Sea, Greece. *Regional Studies in Marine Science* 45, 101855. https://doi.org/10.1016/j.rsma.2021.101855

Iwalaye, O.A., Moodley, G.K., Robertson-Andersson, D.V., 2020. The possible routes of microplastics uptake in sea cucumber *Holothuria cinerascens* (Brandt, 1835). *Environmental Pollution* 264, 114644. https://doi.org/10.1016/j.envpol.2020.114644

Li, J., Qu, X., Su, L., Zhang, W., Yang, D., Kolandhasamy, P., Li, D., Shi, H., 2016. Microplastics in mussels along the coastal waters of China. *Environmental Pollution* 214, 177–184. https://doi.org/10.1016/j.envpol.2016.04.012

Liu, J., Liang, J., Ding, J., Zhang, G., Zeng, X., Yang, Q., Zhu, B., Gao, W., 2021. Microfiber pollution: an ongoing major environmental issue related to the sustainable development of textile and clothing industry. *Environmental Devlopment and Sustainability* 23, 11240–11256. https://doi.org/10.1007/s10668-020-01173-3

Mishra, S., Rath, C.C., Das, A.P., 2019. Marine microfiber pollution: A review on present status and future challenges. *Marine Pollution Bulletin* 140, 188-197. https://doi.org/10.1016/j.marpolbul.2019.01.039

Mohsen, M., Lin, C., Liu, S., Yang, H., 2022. Existence of microplastics in the edible part of the sea cucumber Apostichopus japonicus. *Chemosphere* 287, 132062. https://doi.org/10.1016/j.chemosphere.2021.132062

Murano, C., Agnisola, C., Caramiello, D., Castellano, I., Casotti, R., Corsi, I., Palumbo, A., 2020. How sea urchins face microplastics: Uptake, tissue distribution and immune system response. *Environmental Pollution* 264, 114685. https://doi.org/10.1016/j.envpol.2020.114685

Murano, C., Donnarumma, V., Corsi, I., Casotti, R., Palumbo, A., 2021. Impact of Microbial Colonization of Polystyrene Microbeads on the Toxicological Responses in the Sea Urchin *Paracentrotus lividus*. *Environmental Science & Technology* 55, 7990–8000. https://doi.org/10.1021/acs.est.1c00618

Oberbeckmann, S., Kreikemeyer, B., Labrenz, M., 2018. Environmental Factors Support the Formation of Specific Bacterial Assemblages on Microplastics. *Frontiers in Microbiology* 8, 2709. https://doi.org/10.3389/fmicb.2017.02709

Oldenburg, K.S., Urban-Rich, J., Castillo, K.D., Baumann, J.H., 2021. Microfiber abundance associated with coral tissue varies geographically on the Belize Mesoamerican Barrier Reef System. *Marine Pollution Bulletin* 163, 111938. https://doi.org/10.1016/j.marpolbul.2020.111938

Pedrotti, M.L., Petit, S., Eyheraguibel, B., Kerros, M.E., Elineau, A., Ghiglione, J.F., Loret, J.F., Rostan, A., Gorsky, G., 2021. Pollution by anthropogenic microfibers in North-West Mediterranean Sea and efficiency of microfiber removal by a wastewater treatment plant. *Science of The Total Environment 758*, 144195. https://doi.org/10.1016/j.scitotenv.2020.144195

Piarulli, S., Scapinello, S., Comandini, P., Magnusson, K., Granberg, M., Wong, J.X.W., Sciutto, G., Prati, S., Mazzeo, R., Booth, A.M., Airoldi, L., 2019. Microplastic in wild populations of the omnivorous crab Carcinus aestuarii: A review and a regional-scale test of extraction methods, including microfibres. *Environmental Pollution* 251, 117–127. https://doi.org/10.1016/j.envpol.2019.04.092

Prata, J.C., Reis, V., da Costa, J.P., Mouneyrac, C., Duarte, A.C., Rocha-Santos, T., 2021. Contamination issues as a challenge in quality control and quality assurance in microplastics analytics. *Journal of Hazardous Materials* 403, 123660. https://doi.org/10.1016/j.jhazmat.2020.123660

Remy, F., Collard, F., Gilbert, B., Compère, P., Eppe, G., Lepoint, G., 2015. When Microplastic Is Not Plastic: The Ingestion of Artificial Cellulose Fibers by Macrofauna Living in Seagrass

Macrophytodetritus. *Environmental Science & Technology* 49, 11158–11166. https://doi.org/10.1021/acs.est.5b02005

Ribeiro, F., O'Brien, J.W., Galloway, T., Thomas, K.V., 2019. Accumulation and fate of nano- and micro-plastics and associated contaminants in organisms. *TrAC Trends in Analytical Chemistry* 111, 139–147. https://doi.org/10.1016/j.trac.2018.12.010

Rochman, C.M., Hoh, E., Kurobe, T., Teh, S.J., 2013. Ingested plastic transfers hazardous chemicals to fish and induces hepatic stress. *Scientific Report* 3, 3263. https://doi.org/10.1038/srep03263

Sala, E., Zabala, M., 1996. Fish predation and the structure of the sea urchin *Paracentrotus lividus* populations in the NW Mediterranean. *Marine Ecology Progress Series* 140, 71–81. https://doi.org/10.3354/meps140071

Sanchez-Vidal, A., Thompson, R.C., Canals, M., de Haan, W.P., 2018. The imprint of microfibres in southern European deep seas. *PLoS ONE* 13, e0207033. https://doi.org/10.1371/journal.pone.0207033

Shim, W.J., Song, Y.K., Hong, S.H., Jang, M., 2016. Identification and quantification of microplastics using Nile Red staining. *Marine Pollution Bulletin* 113, 469–476. https://doi.org/10.1016/j.marpolbul.2016.10.049

Sinopoli, S., Bonora, M.A., Capano, G., Carini, M., Pantusa, D., Maiolo, M., 2020. Optimization of Submarine Outfalls with a Multiport Diffuser Design, in: Sergeyev, Y.D., Kvasov, D.E. (Eds.), Numerical Computations: Theory and Algorithms. Springer International Publishing, Cham, pp. 604–618.

Soto-Navarro, J., Jordá, G., Compa, M., Alomar, C., Fossi, M.C., Deudero, S., 2021. Impact of the marine litter pollution on the Mediterranean biodiversity: A risk assessment study with focus on the marine protected areas. *Marine Pollution Bulletin* 165, 112169. https://doi.org/10.1016/j.marpolbul.2021.112169

Tornero, V., Ribera d'Alcalà, M., 2014. Contamination by hazardous substances in the Gulf of Naples and nearby coastal areas: A review of sources, environmental levels and potential impacts in the MSFD perspective. *Science of The Total Environment* 466–467, 820–840. https://doi.org/10.1016/j.scitotenv.2013.06.106

Wakkaf, T., El Zrelli, R., Kedzierski, M., Balti, R., Shaiek, M., Mansour, L., Tlig-Zouari, S., Bruzaud, S., Rabaoui, L., 2020. Microplastics in edible mussels from a southern Mediterranean lagoon: Preliminary results on seawater-mussel transfer and implications for environmental protection and seafood safety. *Marine Pollution Bulletin* 158, 111355. https://doi.org/10.1016/j.marpolbul.2020.111355

Welden, N.A.C., Cowie, P.R., 2016. Long-term microplastic retention causes reduced body condition in the langoustine, *Nephrops norvegicus*. *Environmental Pollution* 218, 895–900. https://doi.org/10.1016/j.envpol.2016.08.020

Woodall, L.C., Gwinnett, C., Packer, M., Thompson, R.C., Robinson, L.F., Paterson, G.L.J., 2015. Using a forensic science approach to minimize environmental contamination and to identify microfibres in marine sediments. *Marine Pollution Bulletin* 95, 40–46. https://doi.org/10.1016/j.marpolbul.2015.04.044

Ziccardi, L.M., Edgington, A., Hentz, K., Kulacki, K.J., Kane Driscoll, S., 2016. Microplastics as vectors for bioaccumulation of hydrophobic organic chemicals in the marine environment: A state-of-the-science review: Role of microplastics in marine contaminant transfer. *Environmental Toxicology Chemistry* 35, 1667–1676. https://doi.org/10.1002/etc.3461

Chapter 4

"Interplay between nanoplastics and the immune system of the Mediterranean sea urchin *Paracentrotus lividus*"

Abstract

The present study highlights for the first time the interplay between model nanoplastics, such as the carboxyl-modified polystyrene nanoparticles (PS-COOH, 60 nm) NPs and the coelomocytes of the sea urchin *Paracentrotus lividus,* a benthic grazer widely distributed in Mediterranean coastal area, upon acute *in vitro* exposure (4 h) (5 and 25 µg mL^{-1}). Insight into PS-COOH trafficking (uptake and clearance) and effects on immune cell functions (i.e., cell viability, lysosomal membrane stability and phagocytosis) are provided. Dynamic Light Scattering analysis reveals that PS NP suspensions in CF undergo a quick agglomeration, more pronounced for PS-COOH (608.3 ± 43 nm) compared to PS-NH$_2$ (329.2 ± 5 nm). However, both PS NPs are still found as nano-scale agglomerates in CF after 4 h of exposure, as shown by the polydispersity index > 0.3 associated with the presence of different PS NP size populations in the CF. The observed changes in ζ-potential upon suspension in CF (-11.1 ± 3 mV and -12.1 ± 4 mV for PS-COOH and PS-NH$_2$, respectively) confirm the formation of a bio-corona on both PS NPs. Optical fluorescence microscopy and fluorimetric analyses using fluorescently labelled PS-COOH (60 nm) reveal a fast uptake of PS-COOH primarily by phagocytes within 1 h of exposure. Upon transfer to PS NP-free CF, a significant decrease in fluorescence signal is observed, suggesting a fast cell clearance. No effect on cell viability is observed after 4 h of exposure to PS-COOH, however a significant decrease in lysosomal membrane stability (23.7 ± 4.8%) and phagocytic capacity (63.43 ± 3.4%) is observed at the highest concentration tested. Similarly, a significant reduction in cell viability, lysosomal membrane stability and phagocytosis is found upon exposure to PS-NH$_2$ (25 µg mL^{-1}), which confirms the important role of surface charges in triggering immunotoxicity. Overall, our results show that, although being quickly internalized, PS-COOH can be easily eliminated by the coelomocytes but may still be able to trigger an immune response upon long-term exposure scenarios. Taking into account that sediments along Mediterranean coasts are a sink for micro- and nanoplastics, the latter can reach concentrations able to exceed toxicity-thresholds for marine benthic species.

Main findings: A fast uptake by phagocytes and sequestration into lysosomal compartments has been demonstrated, with associated low acute toxicity in comparison with their positively charged counterparts under worst-case scenarios

Keywords: sea urchin; nanoplastics; polystyrene; surface charge; immune cells; Mediterranean Sea

4.1 Introduction

Being a semi-enclosed and convective basin, the Mediterranean Sea is a high plastic accumulation region, from where plastic debris can hardly elude (Cózar et al., 2015; Suaria et al., 2016; Macias et al., 2019). One of the latest basin-scale surveys estimated that 11.5 million of plastic pieces are floating over the entire Mediterranean region (Lambert et al., 2020). Through weathering, these plastics undergo chemical, physical and biological transformations, breaking down into microplastics (MPs, size < 1 mm) and nanoplastics (size < 1 μm) (Andrady, 2017; Hartmann et al., 2019). Such physico-chemical changes dictate both horizontal and vertical transport of plastic pieces of different size, which eventually sink to the seafloor, where they may significantly affect benthic communities (Courtene-Jones et al., 2017; Kane et al., 2020). Estimates of marine litter density in the seafloor of the Mediterranean Sea range from 0.25 to 30 items $100\,m^{-2}$ with macroplastics representing up to 98% of the waste (Angiolillo et al., 2015; Macic et al., 2017; Consoli et al., 2018). In Mediterranean coastal sediments, MPs show a heterogeneous distribution, with abundances between 480 ± 9 and 2052 ± 746 MPs kg^{-1} of sediment (Alomar et al., 2016; Abidili et al., 2018; Simon-Sanchez et al., 2019). Spatial risk assessment studies highlighted that marine organisms living along the Mediterranean coasts are at higher risk of ingesting plastics, especially those with low motility and/or small home range, compared to open-sea species (Compa et al., 2019). However, despite the growing concern related to MPs presence in coastal seafloor, only few studies investigated MP ingestion in Mediterranean benthic species belonging to different phyla (i.e., Mollusca and Chordata) (Abidli et al., 2019; Vered et al. 2019). Avio and co-authors (2017) found synthetic microfibers in benthic organisms as the most abundant MPs, with a polymeric composition of polyethylene, polystyrene (PS) and nylon films. Nanoplastic contamination in Mediterranean marine ecosystems is still unknown, although a first study from Schirinzi et al. (2019) reported traces of nano-sized PS, in the range of $1.08 – 136.7$ ng L^{-1} in estuarine and surface waters of the West Mediterranean Sea. Such findings raise concern due to the unique nanoscale properties of nanoplastics (i.e., high surface-volume ratio associated with remarkable biological, chemical and physical reactivity) that allow them to interact with the cellular machinery (Hewitt et al., 2020). As a result of the weathering process of plastic debris, occurring once released in sea water (e.g., changes in crystallinity and surface oxidation), nanoplastics are expected to acquire oxygenated moieties, such as carboxylic groups (-COOH) and thus a negative surface charge (Fotopoulou and Karapanagioti, 2012; Gigault et al., 2016; Andrady, 2017). Therefore, the resulting behavior of nanoplastics in dynamic and stochastic systems, such as in seawater and in biological milieus, depends on nano-specific properties (e.g., surface charge, size, chemical composition, functionalization) and those of the receiving environment (e.g., pH, ionic strength, natural organic matter content and hydrodynamic conditions) (Corsi et al., 2020).

The combination of these conditions defines nanoplastic ecological and ecotoxicological outcomes (Lowry et al., 2012; Mattson et al., 2018). Specifically, functionalization and surface charge are responsible for the interfacial dynamics and thus the interactions with living systems (Corsi et al., 2020 and references within). In recent years, laboratory studies on nanoplastic impact assessment in marine species have investigated the effects of PS nanoparticles (PS NPs) as a proxy for nanoplastics. The most commonly tested ones are carboxyl-functionalized (–COOH) and amino-functionalized (–NH$_2$) PS NPs that exhibit a negative and positive surface charge, respectively. While PS-NH$_2$ display a striking toxicity in many marine models, leading to physiological alterations (Bergami et al., 2016, 2017; Varó et al., 2019), oxidative damage (Feng et al., 2019) and developmental impairments (Della Torre et al., 2014; Pinsino et al., 2017; Tallec et al., 2019; Eliso et al., 2020), the negatively charged counterpart (PS-COOH) is generally less harmful (Bergami et al., 2017; Manfra et al., 2017; Eliso et al., 2020). At first, the PS NP-biological interactions occur through the external surfaces of exposed organisms with potential routes that include ingestion, passage through gills, adsorption on body skin (Lead et al., 2018). At the cellular level, an interplay between PS NP surface charges and proteins and other biomolecules adsorbed onto NP surface has been elucidated, mainly focusing on the formation of the protein-corona, which is considered the bridge at the bio-nano interface (Grassi et al., 2019; Canesi and Corsi, 2016; Canesi et al., 2016). Grassi and co-authors (2019) identified the hard protein corona on surface charged PS NPs upon incubation in sea urchin CF. The authors showed that such bio-corona was dominated by the toposome precursor protein (TPP), a modified iron-less Ca^{2+} binding transferrin known as a biotic and environmental stress target (Castellano et al., 2018). This latest study has been conducted on the Mediterranean Sea urchin *Paracentrotus lividus*, a key species in the organization of benthic communities across Mediterranean coastal areas, controlling shallow macroalgal assemblages either as opportunistic generalist herbivore or as prey for various taxa (Barnes et al., 2002; Boudouresque and Verlaque, 2020). Thanks to its grazing activity, *P. lividus* has been identified as a bioeroder of plastic items, able to generate 92 ± 34 MPs over a 10 d period (Porter et al., 2019). Plastic ingestion has been reported in sea urchins collected along the coastal areas of northern China (Feng et al., 2020) as in other echinoderms such as holothurians and sand dollars (Graham & Thompson, 2009; Taylor et al., 2016; Plee & Pomory, 2020). However, to date no data are available on the presence of plastic debris in wild specimens of the sea urchin *P. lividus* in the Mediterranean Sea. The findings of our previous laboratory based research showed PS MPs (10-45 μm, 72 h) internalization and distribution in *P. lividus* organs (gonads, digestive and water vascular systems), together with changes in the total number of immune cells (coelomocytes), and an increase in reactive nitrogen species (RNS) and ROS (Murano et al., 2020). Sea urchins show a distinctive immune system governed by coelomocytes, which are considered as prominent biosensors

for environmental monitoring (Pinsino and Matranga, 2015) and for studying environmental and anthropogenic challenges, such as ocean acidification, disused industrial activities, plastic pollution and engineered NPs (Falugi et al., 2012; Della Torre et al., 2014; Pinsino et al., 2015; Marques-Santos et al., 2018; Migliaccio et al., 2019; Milito et al., 2020; Murano et al., 2020; Alijacic et al., 2020). Recent investigations addressed the immunotoxicity of positively charged PS–NH$_2$ on sea urchin coelomocytes, with apoptotic-like nuclear alterations, reduction in cell viability and destabilization of the lysosomal membranes (Marques-Santos et al., 2018). Although negatively charged nanoplastics are likely the most common ones found in marine waters, their toxicity towards marine benthic species has been overlooked. The aim of the present study is to investigate the interplay between negatively charged PS-COOH (60 nm), as a proxy for natural occurring nanoplastics, and *P. lividus* coelomocytes to unravel bio-nano interactions at cellular level and predict ecological damages. Positively charged PS-NH$_2$ (50 nm) at 25 µg mL^{-1} have been tested as a surface charge counterpart. Following short-term exposure (4 h), the results obtained revealed a low acute toxicity of PS-COOH in comparison with PS-NH$_2$, as well as a fast uptake of PS-COOH by phagocytes and their sequestration into lysosomal compartments.

4.2 Materials and methods

4.2.1 Polystyrene nanoparticles and physico-chemical characterization

Unlabelled (60 nm, FC02N) and yellow-green fluorescently labelled carboxyl-modified PS NPs (PS-COOH, 60 nm, PC02N) (480/520 ex/em) as well as un-labelled amino-modified PS NPs (PS-NH$_2$, 50 nm, PA02N) were purchased from Bangs Laboratories Inc., Fishers, IN. Un-labelled PS-NH$_2$ and PS-COOH were used for *in vitro* exposure, while fluorescently labelled PS-COOH were used only for uptake and translocation experiments. Details about PS NP stock composition, labeling and surfactants/stabilizers content are reported in the Supplementary Material. With this regard, a rebuttal to the study of Pikuda et al. (2019) regarding the presence of stabilizers in PS NP stocks used in the present and our previous studies (Bergami et al., 2016; 2017; Della Torre et al., 2014; Pinsino et al., 2017) is also provided in the Supplementary Material. PS NPs stocks were briefly bath sonicated (bath sonicator CEIA CP316, at 600W, 40 kHz, 3 min) and working suspensions (10 mg mL^{-1}) made in 0.22 μm milli-Q Water (mQW). In order to investigate PS NP behavior under the experimental conditions, hydrodynamic diameter (Z-average, nm) and polydispersity index (PdI, dimensionless) were determined by Dynamic Light Scattering (DLS), while ζ-potential (mV) was determined by electrophoretic mobility (EM), using a Zetasizer Nano ZS90 (Malvern Instruments). PS NP stock suspensions (25 mg mL^{-1}) were prepared in mQW and in immune cell exposure media (CF) and measurements carried out at 0 h and after 4 h at a constant temperature of 18°C.

4.2.2 Sea Urchin collection and immune cell culture

Fifty adult specimens of *P. lividus* were collected from the Tuscany coasts (42°26'10.99"N, 11°09'13.74"E, Italy), in an area not privately-owned nor protected, according to the authorization of Marina Mercantile (DPR 1639/68, 09/19/1980, confirmed on 01/10/2000). Specimens were acclimated without feeding for 10 days in glass tanks filled with circulating natural seawater (NSW, 39 ± 1‰ salinity, pH 8, 18°C).

In vitro primary cultures of sea urchin coelomocytes were obtained following the protocol reported in Marques-Santos et al. (2018) and as previously described in Matranga et al. (2002). CF, used as exposure medium, was collected following the procedure reported in Marques-Santos et al. (2018) from a pool of 8 individuals, displaying active movement and low number of red amoebocytes with respect to the whole coelomocyte population. Soon after collection, CF was stored in Protein LoBind® Eppendorf tubes kept on ice prior to centrifugation at 600 x g for 20 min at 4°C. The supernatant was then sterile-filtered with 0.22 μm cellulose acetate syringe filters and stored at -80°C until use. Sea urchin coelomocytes, were obtained by using a 1 mL sterile syringe preloaded with CMFSW-EH anticoagulant solution (calcium and magnesium free seawater with EDTA and HEPES)

at a ratio of 1:1 to prevent clotting (NaCl 460 mM; KCl 10.7 mM; EDTA 70 mM; Hepes 20 mM; Na_2SO_4 7 mM; $NaHCO_3$ 2.4 mM, pH 7.4) following the protocol of Smith et al. (2019). Cell suspension was obtained after CF centrifugation at 600 x g for 5 min at 4°C and suspension in 0.22 µm filtered CF, obtained as described above.

The composition of the heterogeneous coelomocyte population (i.e., phagocytes, vibratile cells, white and red amoebocytes), based on Pinsino & Matranga (2015) was evaluated using Luna II Automated cell counter (Logos Biosystems Inc., see SI for instrument settings) and further confirmed under optical microscopy using FastRead® 102 chamber.

Coelomocytes suspensions in CF ($1 \cdot 10^6$ cells mL^{-1}) were exposed to un-labelled PS-COOH (5 and 25 µg mL^{-1}) and PS-NH$_2$ (25 µg mL^{-1}) in sterile 24 well plates (final volume of 1 mL) at 18°C in the dark. PS-NH$_2$ was used as a positively charged counterpart (25 µg mL^{-1}), based on previous findings from Marques-Santos et al. (2018). After 4 h incubation, cells were collected for viability, lysosomal membrane stability and phagocytosis assays. Each experiment was run 3 times. The tested concentrations of PS NPs for acute exposure were chosen according to our previous studies with sea urchin coelomocytes (Bergami et al., 2019, Marques-Santos et al., 2018). Here, the acute exposure conditions tested can be predictive of worst-case scenarios in Mediterranean coastal areas and crucial to improve our knowledge of the effects of PS NPs for environmental risk assessment purposes.

4.2.3 Cell viability

The trypan blue exclusion test was performed following the protocol of Strober (2015). At each time-point (0 and 4 h), coelomocytes in CF were collected ($1 \cdot 10^6$ cells mL^{-1}), centrifuged at 600 x g for 10 min at 4°C and then incubated in trypan blue in PBS-1X (0.4%) for 4 min and examined after adhesion on glass slides under optical microscope (Olympus BX51, Tokyo, Japan). Percentage of viable cells in the whole coelomocyte population was calculated as the number of viable cells *vs* the number of total cells. For each experimental group, the assay was performed in triplicate and run three times.

4.2.4 Lysosomal membrane stability

Neutral red retention time (NRRT) assay (Lowe et al., 1995) was adapted to coelomocytes following the protocol described in Marques-Santos et al. (2018). The NRRT assay was carried out using the NR dye as a marker of phagosome acidification in phagocytes (Pinsino et al., 2015), but it also stains primary lysosomes of vibratile cells (Pinsino and Matranga, 2015), which were included in the assay. After 4 h of exposure to PS NPs, 200 µL of cell suspensions were placed on a glass coverslip (22 x 22 cm) and incubated for 1 h in a humid chamber at 18°C in the dark. Cells were then incubated for 30 min at 18°C with 200 µL of NR dye solution (final concentration of 40 µg mL^{-1} from a stock solution of 40 mg mL^{-1} NR in DMSO). The excess of the dye was removed using a buffer solution

(20 mM Hepes; 436 mM NaCl; 53 mM MgSO$_4$; 12 mM KCl; 12 mM CaCl$_2$, pH 7.5) and coverslips placed on slide and sealed. Slides were checked every 15 min under an optical microscope (40X, Olympus BX51, Tokyo, Japan) and the percentage of cells showing loss of NR dye into the cytosol was counted. An average of 100 cells were scored at each time-point and end-point set when 50% of the cells showed signs of lysosomal leaking (cytosol becoming red and cells rounded shaped). The assay was run in triplicate and three times.

4.2.5 Phagocytosis

The phagocytosis assay was run as described in Bergami et al., (2019) and following the protocol by Borges et al., (2002) with slight modifications, as reported below. Before the assay, fresh suspensions of the yeast (*Saccharomyces cerevisiae*) in 0.22-µm filtered NSW were prepared and yeast cells were counted using Luna II Automated cell counter (Logos Biosystems Inc., Figure S1). The assay was run using coelomocytes collected after 4 h of exposure, placing 200 µL of cell suspension on a coverslip and incubating with yeast cells suspension for 1 h in a ratio 1:10 (phagocytes: yeast) in a humid chamber at 18°C in the dark. Coverslips were then washed with filtered NSW, fixed in ice-cold methanol for 20 min, air-dried and then stained with Giemsa (6%). A minimum of 100 cells per experimental group was observed under an optical microscope (Olympus BX51, Tokyo, Japan). Phagocytosis-related parameters were calculated on the phagocyte sub-population according to Borges et al. (2002): phagocytic capacity (PC, %) and phagocytic index (PI, %) as the number of phagocytes internalizing yeast on the total phagocytes and the number of yeast cells internalized related to the number of phagocytes containing the yeast, respectively.

4.2.6 Cellular uptake of PS-COOH

In order to evaluate the uptake of PS-COOH in sea urchin phagocytes, yellow-green fluorescently labelled PS-COOH (Dragon green labelling ex/em 480/520) were used. The fluorophore of labelled PS-COOH was embedded within the polymer during synthesis (see Supplementary Material for further details), thus preventing any leaching of the dye during testing. However, as underlined by the most recent literature, the stability of PS NP fluorophore should also be proven prior to use to avoid artefacts when studying NP uptake and translocation by fluorescence imaging and confocal laser scanning microscopy (Catarino et al., 2019; Schür et al., 2019). Here we further confirmed the stability of PS-COOH fluorophore during the exposure study (4 h in CF) using the following protocol. Labelled PS-COOH (25 µg mL^{-1}) were suspended in CF and collected at time 0 and after 4 h, centrifuged using Microcon® (10 kDa) tubes at 7000 x g for 30 min at 18°C and the fluorescence signal measured using Tecan spectrophofluorotometer (Infinite M1000 Pro). CF alone was also analyzed to determine the background auto-fluorescence (see Figure S2).

For the uptake study, monolayers of coelomocytes in CF ($1 \cdot 10^6$ cells mL^{-1}) on a glass slide were exposed to fluorescently labelled PS-COOH (5 and 25 µg mL^{-1}) in the dark at 18°C in a humid chamber. At different time-points (0, 15 min, 30 min, 1 h, 4 h) cells were observed under an optical microscope (Olympus BX51, Tokyo, Japan) equipped with a fluorescence filter (488 λ_{ex}- 510 λ_{em}). Quantitative measurements of the fluorescence signal were also performed using fluorimetry. Prior to analysis, the fluorescence intensity signal of fluorescently labelled PS-COOH suspensions in CF (without cells) was measured by using a multi-plate spectrofluorimeter (Victor 3 Perkin Elmer 1420 Multilabel Counter) in PS-COOH (5 and 25 µg mL^{-1}) incubated in CF for 4 h. Fluorescence (arbitrary units, a.u.) was calculated subtracting the auto-fluorescence of CF alone.

Coelomocytes suspensions in CF (300 µL) were then incubated with fluorescently labelled PS-COOH (5 and 25 µg mL^{-1}) following the same procedure described above. After 4 h, suspensions were centrifuged at 600 x g for 10 min at 4°C, washed twice in CF, tip-sonicated (30 sec 100 w, 1 cycle) in an ice-cool bath at 4°C and centrifuged again at 13000 x g for 10 min at 4°C. The resulting supernatant was transferred in 96-well black plates and the fluorescence (a.u.) measured by a multi-plate spectrofluorimeter (Victor 3 Perkin Elmer 1420 Multilabel Counter). Cell suspensions of control groups (incubated in CF only) were processed alike. Each reading was run in triplicate. Fluorescence (a.u.) was calculated by subtracting the auto-fluorescence of the control group.

Confocal laser scanning microscopy was used to assess PS-COOH uptake by coelomocytes. Monolayers of coelomocytes suspensions in CF ($1 \cdot 10^6$ cells mL^{-1} on coverslips) were fixed in 4% paraformaldehyde (in PBS) for 1 h at room temperature, then washed three times with PBS and incubated with Hoechst 33342 dye (10 µg mL^{-1}) and Red Phalloidin- Alexa 555 dye (1:100 in PBS) for 30 min. Coverslips were then placed on glass slides and observed by a confocal laser scanning microscope (Leica TCS SP8X) and images analyzed by the LAS X Life Software and ImageJ Software (Wayne Rasband, Bethesda, MA). A control group of unexposed cells (in CF only) was also processed and analyzed. All images were acquired using the same gain and pinhole aperture in order to assess the differences among the treatments, in terms of signal intensity at the same spatial resolution, and to avoid the saturation or photodamage effects of the fluorescence signal (Pawley, 2006). A recovery experiment was also performed in order to estimate the clearance of PS-COOH from coelomocytes. Cell suspensions in CF (300 µL) were exposed to fluorescently labelled PS-COOH for 1 h (5 and 25 µg mL^{-1}), as described above. Cells were then centrifuged at 600 x g for 10 min at 4°C, resuspended in CF (without NPs). After 3 h exposure to CF only, cells were washed in CF and processed for the fluorimetry analysis as described above.

4.2.7 Scanning and Transmission electron microscopy

Coelomocytes ($1 \cdot 10^6$ cells mL^{-1}) were exposed to CF only and to 25 µg mL^{-1} of fluorescently labelled PS-COOH for 4 h. Coelomocytes (50 µL) were then transferred to a filter Swinex system$^®$ and then fixed with 1% glutaraldehyde in 0.1 M cacodylate buffer in NSW (pH 7.5) at 4°C overnight and post-fixed with 1% osmium tetroxide in cacodylate buffer. Cells were washed three times in 0.1 M cacodylate buffer in NSW, dehydrated through an ethanol series (25, 50, 75 and 100%), and dried in a sputter coated with gold, using a Leica ACE200 vacuum coater (Leica Microsystems, Inc. Buffalo Grove, IL). Observations were performed with a scanning electron microscope (SEM) JSM-6700F (JEOL USA, Inc. Peabody, MA). For transmission electron microscopy (TEM) analysis, coelomocytes were transferred to an Eppendorf tube (2 mL) and fixed with 3% glutaraldehyde in 0.1 M cacodylate buffer in NSW (pH 7.5) at 4°C overnight. Samples were then post-fixed overnight at 4°C with 1% osmium tetroxide in cacodylate buffer. Cells were then washed three times in cacodylate buffer and three times in distilled water, and embedded into 4% low-melt agarose. Samples were finally dehydrated through a graded ethanol series and embedded in epoxy resin (EPON 812). The ultrathin sections were performed with Leica Ultracut ultramicrotome, stained with uranyl-less (EMS Catalog #22409) and lead citrate solution and observed with a TEM LEO 912AB. All images were processed with ImageJ Software (Wayne Rasband, Bethesda, MA).

4.2.8 Statistical analysis

Statistical analyses were performed using GraphPad Prism version 7.00 for Windows. Distribution of the data set was evaluated using a Shapiro-Wilk test and transformed where suitable. Data obtained from the NRRT assay were analyzed by One-way analysis of variance ANOVA followed by Tukey's Post-test. Viability assay and phagocytic activity were analyzed by Kruskal-Wallis test followed by Dunn's post-test. All data were presented as mean ± SD and were considered statistically significant at *p-value* < 0.05.

4.3   Results

4.3.1 Agglomeration of polystyrene nanoparticles in *P. lividus* coelomic fluid

DLS and EM are widely recognized as suitable tools for the physico-chemical characterization of nanoscale particles in nanoecotoxicology (Corsi et al., 2020). They have been used to assess behavior and stability of PS NPs (PS-COOH and PS-NH$_2$) colloidal suspensions under conditions of optimal dispersion in mQW and under more environmentally-relevant experimental conditions, as those in sea urchin CF used for primary culture of coelomocytes. The DLS analysis revealed an optimal dispersion and stability of both PS NPs in mQW up to 4 h, with NP size-related parameters close to their nominal size (50-60 nm), as shown by Z-average and PdI values (Figure 4.1 A, B). EM analysis confirmed PS NP surface charge in mQW and over time (0-4 h), as indicated by ζ-potential (mV) negative values for PS-COOH (from -57.4 ± 1.3 to -42.5 ± 3.7 mV) and positive ones for PS-NH$_2$ (from +39.7± 2.1 to +45.8 ± 0.7 mV) (Figure 4.1). A different behavior was observed for PS NPs in CF (i.e., the exposure medium), as indicated by the presence of large agglomerates (in the size range of 300-600 nm) shown by DLS analysis, even soon after the preparation of the suspension (at 0 h). PS-COOH suspensions in CF were characterized by a heterogeneous size distribution (PdI values > 0.5), forming large agglomerates with an average size of 600 nm at 0 and 4 h. Differently, PS-NH$_2$ suspensions presented two main peaks in the size distribution (PdI values > 0.3), corresponding to two size populations at approximately 80 and 500 nm, thus forming smaller agglomerates (average size of 330 nm) in CF and still stable up to 4 h. The EM analysis showed a general lower stability of PS NPs in CF compared to mQW. PS-COOH still maintained their negative surface charge over time (0-4 h) (from -11.1 ± 2.7 to -9.0 ± 1.2 mV), while PS-NH$_2$ acquired a new negative charge (from -12.1 ± 3.9 to -9.3 ± 2.1 mV) similar to the one of PS-COOH in CF.

Overall, DLS and SEM analyses confirmed the nanoscale properties of either anionic and cationic functionalized PS NPs when suspended in mQW, with narrow size distributions centered in their hydrodynamic diameter and preserved their negative (PS-COOH) and positive (PS-NH$_2$) surface charge. Such features, indicating an optimal dispersion, were lost once PS NPs were suspended in sea urchin CF in which, regardless NP surface charges, they show an unstable multimodal size distribution mostly related to their known interplay with inorganic and organic molecules of the CF (Marques-Santos et al., 2018; Grassi et al., 2019).
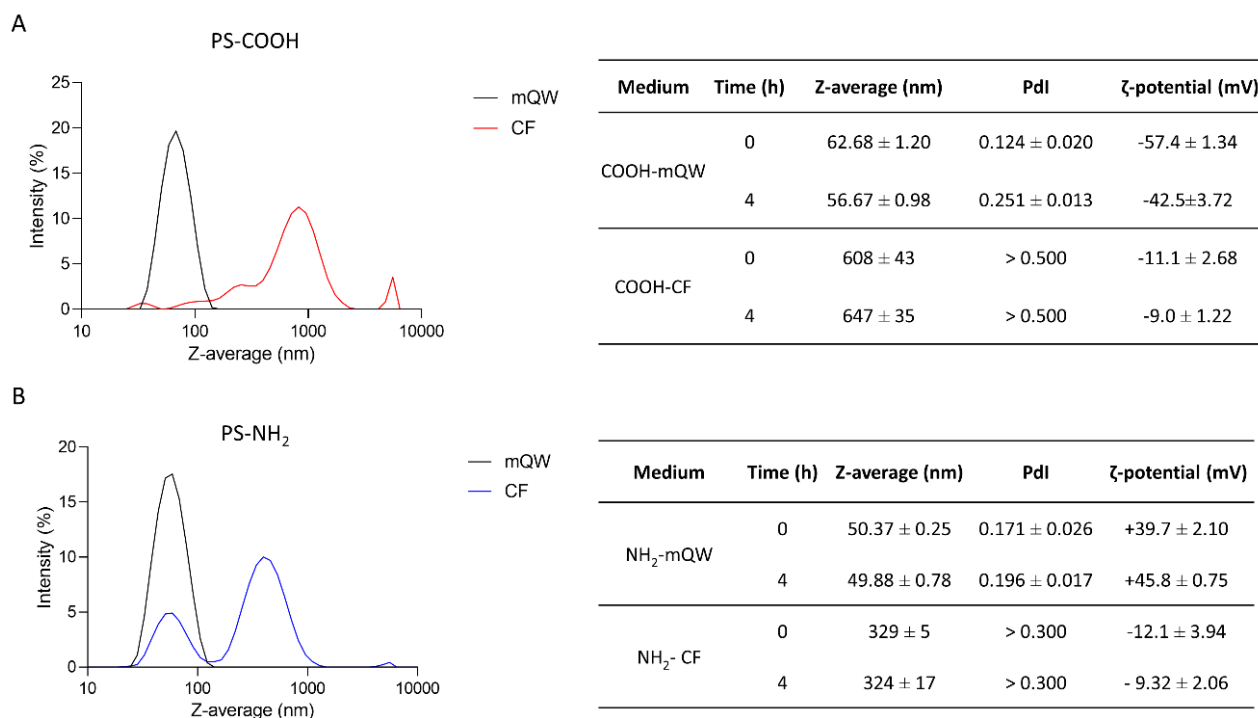
A

PS-COOH

Medium	Time (h)	Z-average (nm)	PdI	ζ-potential (mV)
COOH-mQW	0	62.68 ± 1.20	0.124 ± 0.020	-57.4 ± 1.34
	4	56.67 ± 0.98	0.251 ± 0.013	-42.5 ± 3.72
COOH-CF	0	608 ± 43	> 0.500	-11.1 ± 2.68
	4	647 ± 35	> 0.500	-9.0 ± 1.22

B

PS-NH$_2$

Medium	Time (h)	Z-average (nm)	PdI	ζ-potential (mV)
NH$_2$-mQW	0	50.37 ± 0.25	0.171 ± 0.026	$+39.7 \pm 2.10$
	4	49.88 ± 0.78	0.196 ± 0.017	$+45.8 \pm 0.75$
NH$_2$- CF	0	329 ± 5	> 0.300	-12.1 ± 3.94
	4	324 ± 17	> 0.300	$- 9.32 \pm 2.06$

Figure 4.1 Particles size distribution and Z-average (nm), polydispersity index (PdI) and ζ-potential (mV) of unlabelled PS-COOH (A) and PS-NH$_2$ (B) in mQW and coelomic fluid (CF) at time 0 and 4 h. Data are referred to 25 μg mL^{-1} of PS NPs and reported as mean $\pm$ SD (n = 3).

4.3.2 Immunotoxicity induced by PS NPs on *P. lividus* coelomocytes

Coelomocytes are a heterogeneous group of circulating cells located in sea urchin CF, with a majority of phagocytes (> 80%) and other cell sub-populations present in lower quantities, such as red and white amoebocytes (≈ 13%) and vibratile cells (≈ 7%) (Pinsino and Matranga, 2015). Since each cell sub-population has key functions in sea urchin innate immunity, the immune response towards external challenges can be first assessed through the count of coelomocyte sub-populations (Branco et al., 2013; Migliaccio et al., 2019). Total immune cells count showed no variations in coelomocyte sub-populations, represented by phagocytes, red amoebocytes, white amoebocytes and vibratile cells upon exposure to PS NPs. No significant differences in cell viability upon exposure to PS-COOH at both concentrations tested were observed compared to the control group. Conversely, a significant decrease in cell viability after exposure to PS-NH$_2$ (25 μg mL^{-1}) was found (Figure 4.2) (Figure S3-A).
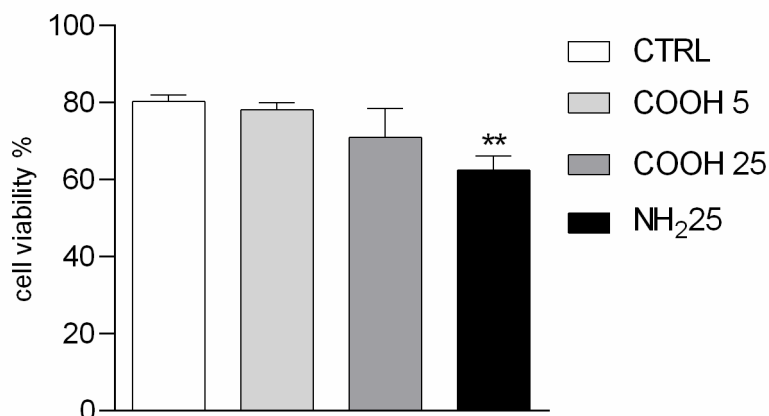
Figure 4.2 Percentage of viable *P. lividus* coelomocytes *vs* total number of cells screened after 4 h of exposure to CF (control), PS-COOH (5 and 25 µg mL^{-1}) and PS-NH$_2$ (25 µg mL^{-1}). Data are reported as mean ± SD (n = 9; Kruskal-Wallis test, Dunn's post-test, p < 0.01). ** indicate significant differences with respect to the control group.

4.3.3 Lysosomal membrane stability decrease at the highest PS-COOH concentration

Lysosomes are cellular organelles involved in different membrane-trafficking pathways, including endocytosis and phagocytosis of foreign particles. The NRRT assay used to assess lysosomal membrane stability is based on the ability of phagocytes to accumulate the NR dye inside their lysosomal compartments. Once lysosomal membranes are destabilized, the dye is then released inside the cytosol (Lowe et al., 1995). A significant increase in the percentage of destabilized lysosomes was observed in coelomocytes exposed to 25 µg mL^{-1} of PS-COOH and PS-NH$_2$ compared to the control group, already after 30 min of incubation with the NR dye (Figure 4.3). Differently, no differences in the percentage of destabilized lysosomes were observed in coelomocytes exposed at the lowest PS-COOH concentration (5 µg mL^{-1}), compared to the control group (in CF only). In general, the effects of PS NPs on the destabilization of the lysosomal membranes appeared to be limited, since no experimental group reached 50% of lysosomal destabilization after 60 min of exposure, which is commonly considered the toxicity end-point of this assay (ICES, 2010; Davies et al. 2012).
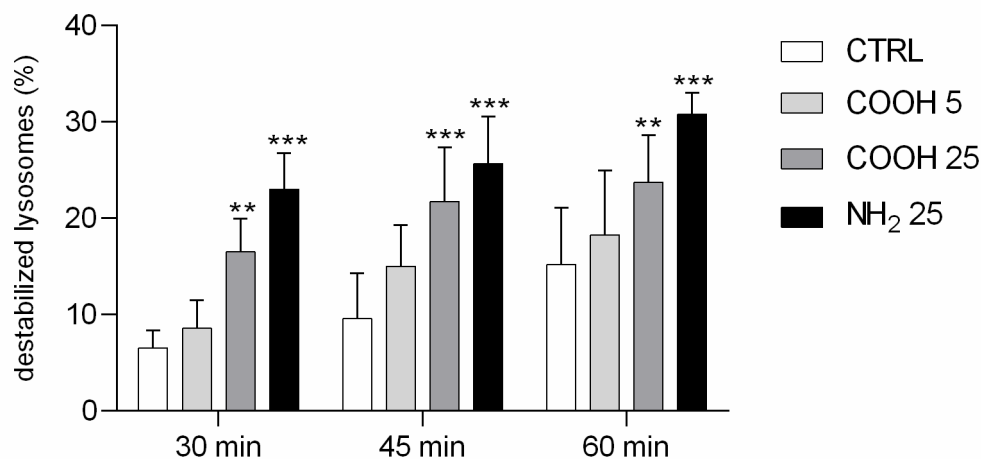
Figure 4.3 Percentage of destabilized lysosomes scored in 100 *P. lividus* coelomocytes after 4 h of exposure to PS-COOH (5 and 25 µg mL^{-1}) and PS-NH$_2$ (25 µg mL^{-1}). Data are reported as mean ± SD (n = 6, One-way, Tukey's post-test, **p<0.01, ***p<0.001). Asterisks indicate significant differences with respect to control and PS-COOH (5 µg mL^{-1}) exposure groups.

4.3.4 Phagocytosis activity is concentration- and surface charge-dependent

Sea urchin phagocytes have a primary role in innate immunity, allowing for clotting and internalization of foreign particles, cytolysis and secretion of humoral factors (reviewed in Smith et al., 2018). A change in the phagocytic activity of these cells, determined through the phagocytosis assay, indicates their ability to cope with a new immune challenge which may affect cell metabolism and viability. Results on PC and PI are shown in Figure 4.4. Phagocytes exposed to 25 µg mL^{-1} of PS-COOH and PS-NH$_2$ showed a significant decrease in PC compared to the control group (Figure S3-C). The lowest concentration of PS-COOH led to a PC and a PI similar to the control group (Figure S4.3-C). A significant decrease in PI was found only for coelomocytes exposed to PS-NH$_2$ (124.2 ± 14.3 %) while no changes were found between those exposed to PS-COOH and the control group. Overall, the results on *P. lividus* cell immune parameters in response to short-term exposure to PS NPs show differences according to PS NP surface charge (PS-COOH vs PS-NH$_2$). Negatively charged PS-COOH did not affect cell viability but caused a destabilization of lysosomal membranes only at the highest concentration (25 µg mL^{-1}). Furthermore, PS-COOH provoked a reduction in PC, but did not affect the quality of the phagocytes, in terms of PI, as found instead for PS-NH$_2$.
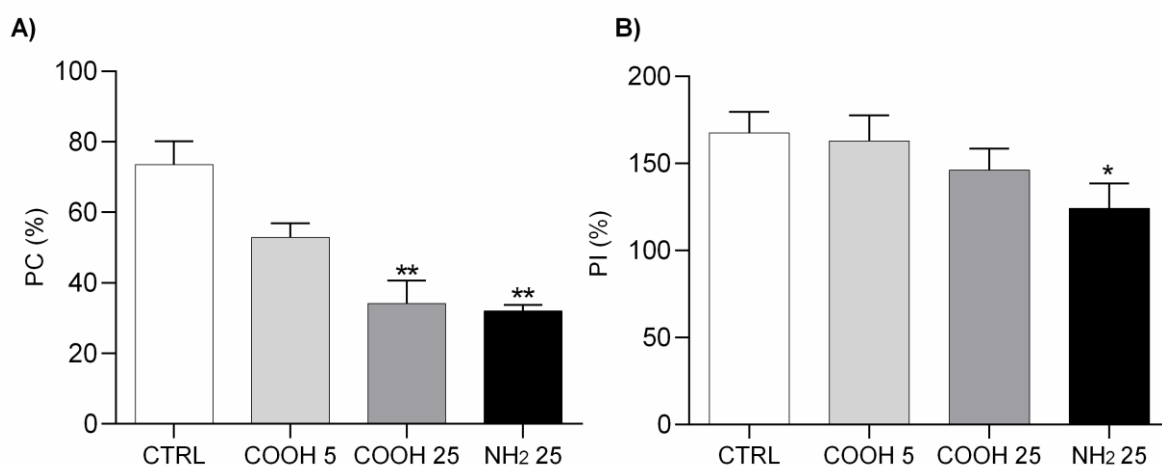
Figure 4.4 Phagocytic capacity (PC, %) (A) and phagocytic index (PI, %) (B) calculated on *P. lividus* phagocytes after 4 h of exposure to PS-COOH (5 and 25 µg mL^{-1}) and PS-NH$_2$ (25 µg mL^{-1}). Data are reported as mean ± SD (n = 9, Kruskal-Wallis test, Dunn's post-test, *p< 0.05, **p< 0.01). Asterisks indicate significant differences with respect to the control group.

4.3.5 Fast uptake and compartmentalization of PS-COOH in phagocytes

The use of yellow-green fluorescently labelled PS-COOH allowed us to evaluate their uptake, translocation and clearance in the phagocytes, the most abundant coelomocyte sub-population of *P. lividus*, having a key role in innate immunity. Optical fluorescence images of coelomocytes exposed to PS-COOH at both concentrations (5 and 25 µg mL^{-1}) show NP uptake already after 15 min and 30 min of exposure (Figure S4.4). Fluorescence signal was still evident after 4 h and more evident on P. lividus phagocytes compared to the other cell populations (Figure S4.5). The fluorescence intensity recorded in lysed phagocytes was significantly higher only in those exposed at the highest PS-COOH concentration (25 µg mL^{-1}) compared to the control group, while no changes were observed for those exposed to 5 µg mL^{-1} up to 4 h of exposure (Figure 4.5) (Figure S4.3-D). The fluorescence intensity of cell lysates exposed to low and high concentrations of PS-COOH was in the ratio 1: 5 in line with the ratio of their nominal concentrations (5 and 25 µg mL^{-1}). Furthermore, the evidence that the intensity measured effectively represented only the internalized PS-COOH is given by the fact that the fluorescence intensity of the PS-COOH suspended in CF only is an order of magnitude higher with respect to the intensity of cell lysates (Figure S4.6).
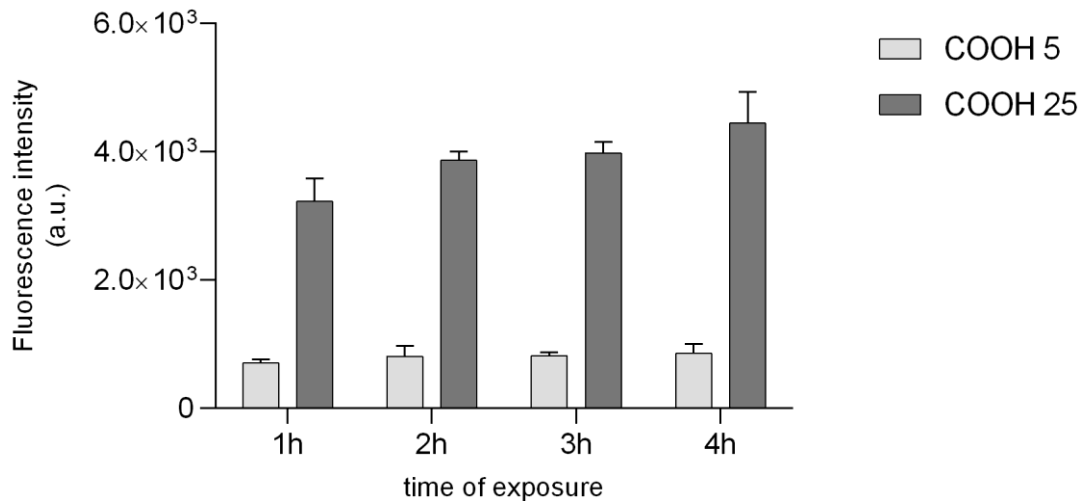
142

Figure 4.5 Fluorescence intensity (arbitrary units, a.u.) of immune cells exposed to fluorescent labelled PS-COOH (5 and 25 μg mL^{-1}) at time 0 and after 1, 2, 3 and 4 h of exposure. Bars represent mean ± SD (n = 3). Fluorescence intensity values are normalized to the auto-fluorescence signal of the control group (*P. lividus* cells exposed to CF only) at each time-point.

Confocal analysis confirmed the internalization of fluorescently labelled PS-COOH agglomerates inside lysosomes of phagocytes at both concentrations tested (5 and 25 μg mL^{-1}) and in a concentration dependent manner (Figure 4.6). PS-COOH were also found close to cell membranes where they could stimulate an inflammatory response. In particular, the images, obtained at the same gain and at the same pinhole, showed that the internalized particles were organized in circular structures recognizable as lysosomes (Figure 4.6). Moreover, confocal microscopy highlighted the presence of multinucleate coelomocytes as a result of cell fusion into a syncytium, a typical process in echinoderm phagocytes (Majeske et al., 2013; Pinsino & Matranga, 2015). Fluorescence measurements of coelomocytes lysates from the recovery experiment showed a significant lower intensity in the fluorescence signal with a reduction of over 50% after 3 h in CF compared to values recorded in cell lysate after 1 h of exposure at both PS-COOH concentrations (5 and 25 μg mL^{-1}) (Figure 4.7) (Figure S4.3-E). A fast uptake (< 15 min) and a time-dependent internalization of the fluorescently labelled PS-COOH NPs in immune cells of sea urchin was shown at 25 μg mL^{-1}. PS-COOH were mostly internalized in lysosomes of coelomocytes but also localized as small agglomerates in the perinuclear area but apparently not inside the nucleus. On the other hand, based on fluorescence microscopy and quantitative fluorimetric analysis, ~50% of PS-COOH seemed to be eliminated from the cells after 1 h of exposure, regardless of tested concentrations (5 and 25 μg mL^{-1}).
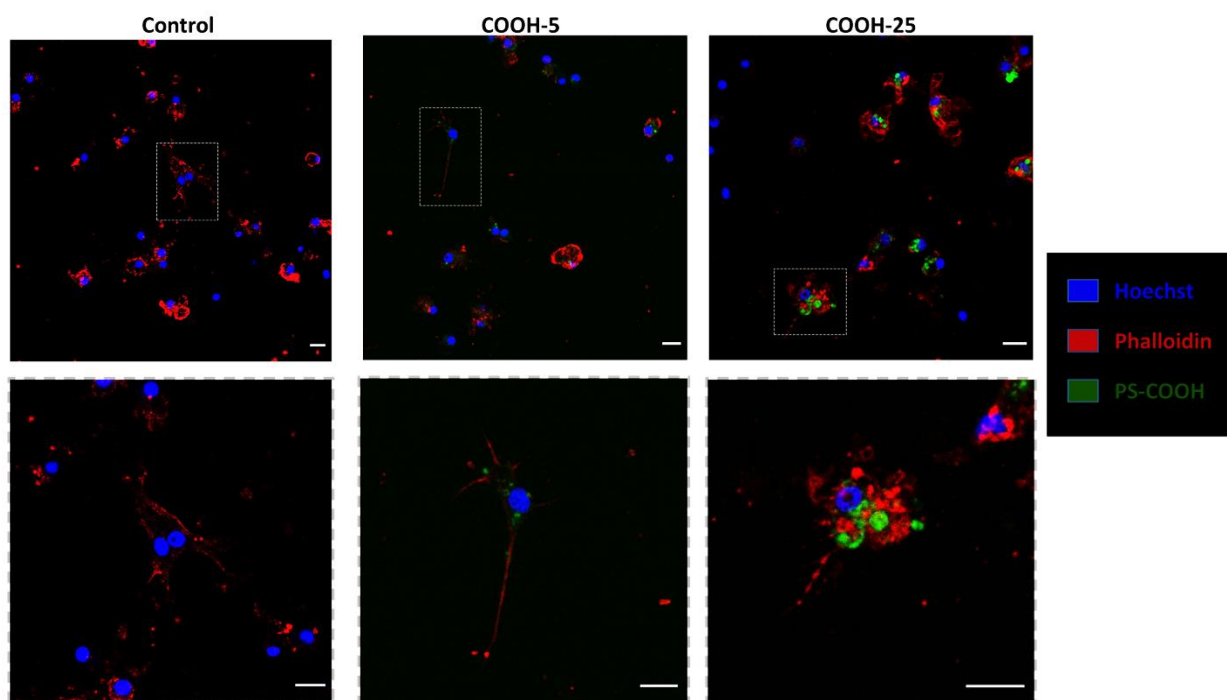
Figure 4.6. Internalization of fluorescent labelled PS-COOH (5 and 25 μg mL^{-1}) in phagocytes of sea urchin *P. lividus* upon 4h of exposure (blue: nuclei, red: actin and green: PS-COOH). Higher magnifications of the areas in the upper images are reported in the images at the bottom. Images were recorded with the same gain using confocal microscope (Leica TCS SP8X). Scale bar: 10 μm.
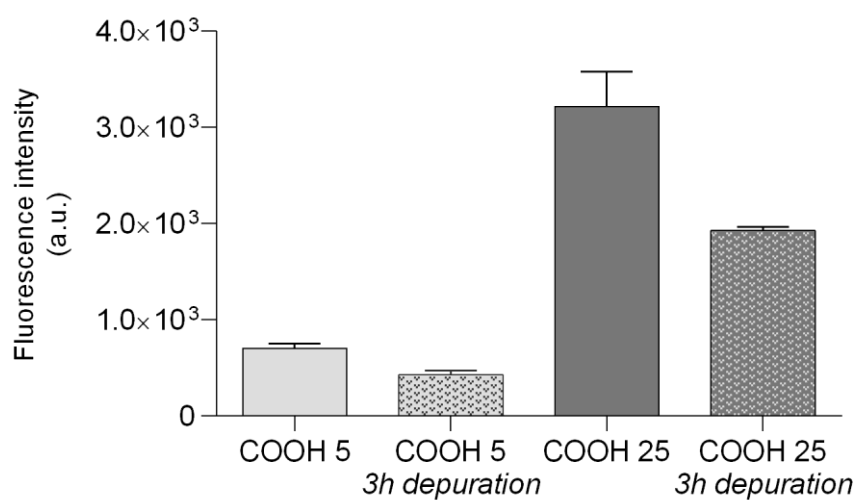
Figure 4.7. PS-COOH elimination from sea urchin coelomocytes. Fluorescence intensity (arbitrary units, a.u.) of lysates of coelomocytes exposed for 1 h to PS-COOH (5 and 25 μg mL^{-1}) and then left for 3 h in CF. Bars represent mean ± SD (n = 3). Fluorescence intensity is normalized to the auto-fluorescence signal of cells exposed to CF only.

4.3.6 Changes in coelomocytes ultrastructural properties

To assess the possibility that PS-COOH could modify coelomocyte ultrastructure, SEM and TEM analyses were performed. SEM images showed a regular and homogeneous surface morphology of the phagocytes of the control group, while a heterogeneous surface was found in PS NP-exposed cells, instead, characterized by the presence of a biological adhesive matrix (flocculate-like structures) presumably resulting from the interaction between CF components and PS-COOH (Figure 4.8 A-B). Although no intracellular localization of PS-COOH agglomerates could be followed, results from TEM analysis also indicated substantial differences among the phagocytes exposed to PS NPs and the control group. While untreated cells showed an elongated conformation and high cytoplasmic-to-nuclear ratio, cells exposed to PS-COOH displayed a narrowed structure, slightly damaged cell membranes and filopodia, low cytoplasmic-to-nuclear ratio as well as the presence of foreign material (indicated by the red arrows) (Figure 4.9). As shown in figure 4.9B, the nucleus of treated coelomocytes appeared abnormal resembling early apoptosis. However, we cannot disregard that chromatin could have exhibited this conformation due the orientation of the ultrathin section. Therefore, SEM and TEM analyses of the phagocyte ultrastructure showed that PS NPs were able to affect cell morphology upon short-term acute exposure.
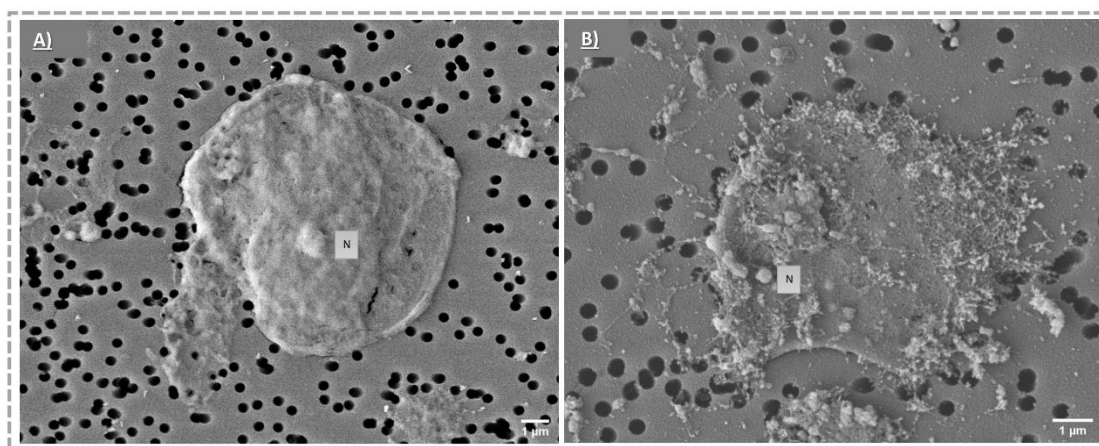
Figure 4.8. SEM analysis of phagocytes. Representative SEM images of control phagocytes (exposed to CF only) (A) and after exposure to PS-COOH at 25 μg mL^{-1} (B). SEM images acquired using a SEM JSM-6700F coupled to LEI detector. Scale bars: 1 μm.
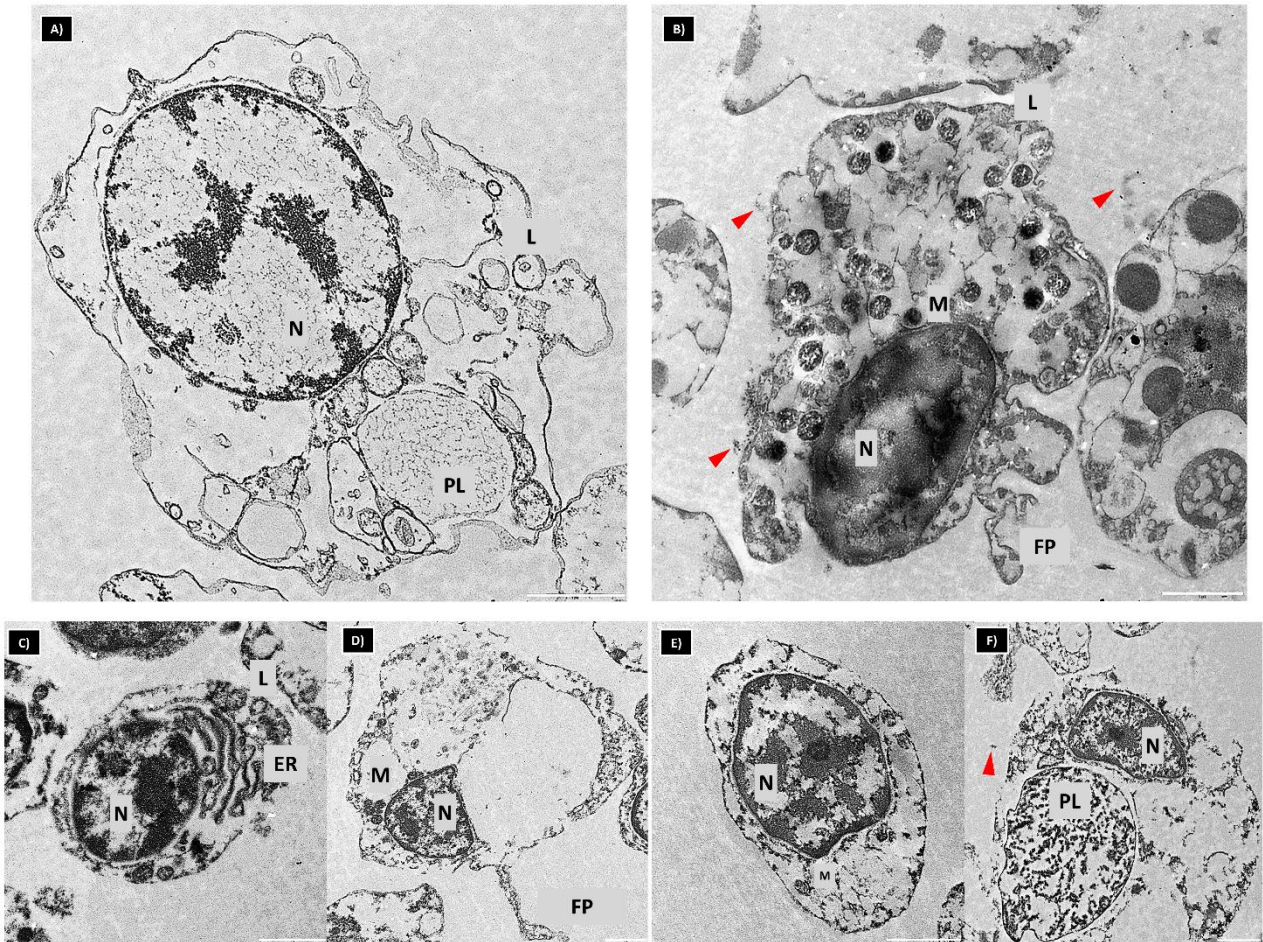
Figure 4.9 TEM analysis of phagocytes. Representative TEM images of control phagocytes (A-C-D) and after exposure to PS-COOH at 25 µg mL^{-1} (B-E-F). Foreign material around cell surface and membrane damage is shown (red arrows). N- nucleus; M- mitochondria; PL- phago-lysosome; L- lysosome; FP- filopodia, ER- endoplasmic reticulum. TEM images were recorded using a LEO 912AB microscope. Scale bars: 1 µm.

4.4 Discussion

4.4.1 The composition of CF drives PS NP behaviour

Upon suspension in alkaline and high ionic strength medium, such as seawater, PS NPs are prone both to hetero-agglomeration (i.e., between non homologous particles) and homo-agglomeration (i.e., among NPs themselves), the latter process driven by high pH (8.0) and ionic composition of the seawater itself (Praetorius et al., 2020). Such behavior is typically more pronounced for anionic PS NPs (i.e., negatively charged PS-COOH) than cationic ones (i.e., positively charged PS-NH$_2$) (Corsi et al., 2020 and references within), although it still occurs with the formation of agglomerates of PS-NH$_2$ with the increase in time of exposure (Eliso et al., 2020; Varó et al., 2019) and decrease in temperature of the media (Bergami et al., 2019). The observed agglomeration of PS NPs in sea urchin CF can be thus ascribed to osmolarity and ion composition of the CF, which is in balance with the

surrounding seawater, since sea urchins are considered osmoconformers, although some sea urchin species can sustain positive gradients for the most relevant ions (Mg^{2+}, Ca^{2+}, and K^+) in case of reduced salinity (Santos et al., 2013; Freire et al., 2011). Moreover, sea urchin CF contains a wide array of biomolecules, produced by the circulating coelomocytes and having key immune functions (Dheilly et al., 2013; Grassi et al., 2019), which are able to adhere on PS NP surface (protein-corona) (Fočak et al., 2019; Marques-Santos et al., 2018; Freire et al., 2011). Our previous findings showed that a highly abundant protein in sea urchin CF, the TPP, tightly bound onto PS NPs surface (hard corona) and provided a new colloidal behaviour to PS NPs regardless of their surface charges. Other proteins found adsorbed onto PS NPs in *P. lividus* CF included flotillins, guanine nucleotide-binding proteins and cytoskeletal proteins (Grassi et al., 2019). The observed changes in the absolute surface charges upon incubation in CF of both NPs and furthermore the full neutralization of positive ones of PS-NH_2 determined by EM analysis provide evidence of surface adhesion of biomolecules present in the CF. This is in agreement with our previous findings in which we reported significant changes in PS NP surface charges once suspended in environmental (i.e., sea water) and biological milieux (internal fluids) (Corsi et al., 2020 and references within). However, although still in the nanoscale range, a variability in PS NP agglomerate sizes in CF suspension between the present study (~300-600 nm) and past investigations (Grassi et al., 2019, Marques-Santos et al., 2018) has been observed and probably related to changes in CF composition in wild caught specimens. While ion composition of sea urchin perivisceral CF can slightly differ from that of external seawater (Santos et al., 2013; Freire et al., 2011), biomolecules, secreted by the circulating coelomocytes and microbes inhabiting the fluid, undergo geographical and seasonal fluctuations also as a consequence of their role in several physiological functions including immune defence (Branco et al., 2014; Matranga et al., 2005). Changes in selected ion composition (Na^+, other cations and Cl^-) have been already documented in sea urchin CF as an adaptive strategy of intertidal species to counteract variations towards external environmental conditions, such as for instance environmental changes in seawater osmolarity (Freire et al., 2011; Fočak et al., 2019). Moreover, a significant increase in the concentration of specific proteins of sea urchin CF (i.e., the toposome, also known as major yolk protein and other molecules) has been reported during the reproductive cycle both in female and male specimens (Ura et al., 2017). Therefore, sea urchin adaptive responses to environmental and physiological changes are reflected by the whole CF composition and thus changes in PS NPs behaviour are likely to occur in wild specimens under natural exposure scenarios, potentially affecting NP-induced biological outcomes. A more in-depth characterization of such realistic exposure scenarios is thus required in order to shed light on PS NPs behaviour and fate once internalized and distributed in biological fluids of exposed species.

4.4.2 PS NPs uptake and clearance

PS-COOH internalization was observed in sea urchin phagocytes, in line with our previous results obtained for cationic PS-NH$_2$ (Marques-Santos et al., 2018). Phagocytes constitute the largest coelomocyte sub-population ($\approx$ 80-90%) and play a significant role in sea urchin innate immune response, being actively involved in phagocytosis and encapsulation of foreign particles and microorganisms, wound repair and vesicular transport, as well as the release of humoral components (Smith et al., 2010; Pinsino & Matranga, 2015). In the Antarctic sea urchin *S. neumayeri*, the up-regulation of genes associated with antimicrobial peptides was reported in coelomocytes exposed in vitro to PS-COOH at 1 and 5 μg mL^{-1} (Bergami et al., 2019), showing that humoral factors can be involved in PS NP recognition and internalization in sea urchin coelomocytes. Being recognized as a first line of defence in all living beings, phagocytosis represents a consistent response towards a large variety of external stimuli including nanoscale particles uptake and clearance (Smith et al., 2018). Confocal images confirmed the localization of fluorescently labelled PS-COOH agglomerates not only inside the lysosomes of phagocytic cells but also close to their cell membranes where they could stimulate an inflammatory response. The analyses of the phagocyte ultrastructure (through SEM and TEM) showed that PS-COOH were able to affect cell morphology, with impairments in cell membrane and filopodia. Moreover, a higher degree of cell compartmentalization (i.e., higher number of vesicles) could be observed compared to the untreated coelomocytes in the control group. PS NPs are known to act as destabilizers of cell membrane and sub-cellular compartments (Rossi et al., 2014), causing membrane disruption and damage with consequences on cell protective functions. NPs can be internalized by the cells through different pathways, transported and accumulated in the lysosomes but only PS-NH$_2$ seemed to be able to strongly interact with biological membranes (Wang et al., 2013a; Wang et al., 2013b). Among these different pathways, phagocytosis is a cellular phenomenon bounded by biophysical constraints and therefore influenced by the concentration as well as the size of the foreign materials (Jamouillè & Waterman, 2020). A fast internalization (within 1 h of exposure) of PS NPs of similar size (50 nm) has been reported in mussel granulocytes, which share a similar active role in phagocytosis as sea urchin phagocytes (Sendra et al., 2020). A higher ratio of granulocytes/basophilic hyalinocytes was found in their haemolymph upon short-term exposure to PS NPs (50 nm), thus indicative of an intensified immune response (Cole et al., 2020). Phagocytic cells clearly represent a target of PS NPs, whose internalization could trigger the innate immune response of marine invertebrate species and raises concern towards chronic exposure scenarios as those most likely occurring in natural environments. Any breakdown in the response of those cells could result in an impaired ability of marine invertebrates to counteract other toxicities (i.e., exposure to physical, chemical and biological stressors) (Smith et al., 2018). In addition, harmful effects could

arise by what PS NPs carry onto their surface, such as for instance contaminants already present in the aquatic environment (e.g., heavy metals, pesticides, hydrocarbons, pharmaceuticals). As a result, PS NPs could act as vectors of other contaminants and enhance their cellular uptake and accumulation in selected organs (i.e., Trojan horse effect) (Trevisan et al., 2020; Zhang & Xu, 2020).

4.4.3 PS NP effects on *P. lividus* immune response

The immune response exerted by sea urchin coelomocytes differed according to PS NP surface charge. Cell viability did not significantly change upon exposure to PS-COOH compared to the control group, while it was significantly reduced in coelomocytes exposed to PS-NH$_2$ (25 µg mL^{-1}), in agreement with our previous findings (Marques-Santos et al., 2018). Lysosomal membrane stability was significantly affected only at the highest PS-COOH concentration (25 µg mL^{-1}), but the damage resulted still lower compared to the one caused by PS-NH$_2$ (25 µg mL^{-1}). Such results are in agreement with our previous findings in which a significant concentration- and time-dependent decrease in lysosomal membrane stability and apoptotic-like nuclear alterations were found in sea urchin phagocytes upon exposure to PS-NH$_2$ (10 and 25 µg mL^{-1}) (Marques-Santos et al., 2018). A disruption in phagocytosis activity in sea urchin coelomocytes following exposure to PS NPs was observed, in agreement with our previous results on Antarctic sea urchin *Sterechinus neumayeri* (Bergami et al., 2019). Here, the decrease in PC of yeast cells was concentration-dependent in response to PS-COOH (5 and 25 µg mL^{-1}) and a similar effect provoked by PS-COOH and PS-NH$_2$ at the highest concentration tested was found. Such results can be associated with the active and quick PS NP internalization by sea urchin phagocytes, which limited their ability to respond to further foreign agents and/or pathogens, such as in this case the yeast. However, the significant decrease in PI in response to PS-NH$_2$ exposure only, compared to the other groups exposed to PS-COOH, suggests that positively charged PS NPs led to a more prominent immunotoxicity, with a reduced activity even among the phagocytes actively internalizing the yeast cells. Alterations in immunological parameters, such as a decrease in PC and an increase in lysozyme activity, have been also reported in mussel haemocytes exposed to PS-NH$_2$ (50 nm) up to 50 µg mL^{-1} (Canesi et al., 2015). Bare PS NPs of different sizes (50 nm, 100 nm, 1 µm) have been found to trigger apoptosis and alter PC in mussel haemocytes, in vitro exposed (3 h) to similar concentrations (10 mg L^{-1}) (Sendra et al., 2019). In addition, PS NPs suspended in mussel haemolymph acquired a Z-potential approximately of -8.6 – -9.6 mV, similar to the one reported for both PS-NPs in this study. To date, the immunotoxicity of negatively charged PS-COOH in marine invertebrates remains largely unexplored. Our first contribution on the Antarctic sea urchin *S. neumayeri* investigated the effects of PS-COOH and PS-NH$_2$ (1 and 5 µg mL^{-1}) in coelomocytes through in vitro short-term exposure (Bergami et al., 2019). PS-COOH exposure caused a stronger modulation of genes involved in

apoptosis and oxidative stress than PS-NH$_2$, suggesting that PS NP surface charge was the key parameter responsible for toxicity, with cells able to counteract the stress caused by PS-COOH rather than by PS-NH$_2$ (Bergami et al., 2019). Interestingly, a similar protein corona composition was shared by PS-COOH and PS-NH$_2$ regardless of their different surface charges (Grassi et al., 2019), nevertheless they were still able to cause a different immune response, with PS-NH$_2$ being more toxic than PS-COOH. In particular, in our study, both PS NPs affected the PC, however only PS-NH$_2$ led to a significant impact on the quality of the phagocytes in terms of PI and on the destabilization of lysosomal membranes. According to Duan & Li (2013), positively charged NPs internalized by the cells could escape from lysosomes after a physical breakdown with an increased influx of chloride ions to counteract their positive charges. Conversely, negatively or un-charged NPs tended to co-localize within lysosomes. Once inside the lysosomes, PS-NH$_2$ appeared to re-acquire the original positive surface charge due to protein degradation by lysosomal enzymes and loss of the bio-corona. This results in a strong lysosomal dysfunction due to interactions with positive charges according to the proton sponge hypothesis (Nel et al., 2009; Wang et al., 2013a; Wang et al., 2018). This theory may explain why PS-COOH and PS-NH$_2$ exerted different effects on sea urchin coelomocytes, although they exhibited similar surface charges and protein corona composition in the CF (Grassi et al., 2019). In addition, the smaller average size of PS-NH$_2$ agglomerates in CF compared to the one of PS-COOH (of ~330 nm and ~600 nm, respectively) could play a significant role in particle fate and behaviour towards plasma membrane and those of internal organelles as lysosomes.

4.5 Conclusions

Our findings support the hypothesis that sea urchin immune cells could be a target of PS NPs and that their surface charge acts as the main driver of potential harmful effects. The efficiency of the sea urchin immune system to counteract the PS-COOH exposure compared to PS-NH$_2$ is shown and seems to limit any potential risk related to environmental exposure scenarios at relevant concentrations. Predicted environmental concentrations for PS NPs are in the range of 1 pg L^{-1} - 10 µg L^{-1}, far lower than those tested in the present study (Al-Sid-Cheikh et al., 2018, 2020). However, current projections of global mismanaged plastic waste generation to the next forty years coupled to ongoing weathering processes and fragmentation, suggest far more critical exposure scenarios in certain marine areas and ecosystems probably not far from the one used in the present study (5-25 µg mL^{-1}) (Lebreton and Andrady, 2019). Plastic accumulation is expected to further intensify in the Mediterranean Sea, recently classified as a hotspot for plastic pollution for both micro- and nanoplastics due local discharges, low dilution and water circulation (Cózar et al., 2015; Suaria et al., 2016; Cincinelli et al., 2019). Recent studies identify in marine sediments the potential reservoir of smaller plastics such as nanoplastics, posing marine benthic species at risk of exposure (Llorca et al.,

2020). PS-COOH are more likely to resemble the naturally occurring negatively surface charged nanoplastics, which may end up in marine coastal waters from primary and secondary sources (Hernandez et al., 2017; Tian et al., 2019). As a result of weathering, most plastics break down into nanoscale plastic fragments, as demonstrated for large PS-based products (Lambert & Wagner, 2016) and they acquire negative surface charges (Fotopoulou and Karapanagioti, 2012; Andrady, 2017). Therefore, the exposure levels for benthic organisms, particularly those inhabiting Mediterranean shallow coastal areas, are likely to exceed toxicity-thresholds. Overall, these findings improve our understanding on the interplay between negatively charged PS NPs, as a proxy for naturally occurring nanoplastics, and *P. lividus* immune system. A fast uptake by phagocytes and sequestration into lysosomal compartments has been demonstrated, with associated low acute toxicity in comparison with their positively charged counterparts. Although experimental conditions considered in the present study reflect acute and probably unrealistic exposure scenarios, they may be representative of local worst-case scenarios, such as the ones occurring in Mediterranean shallow waters. As a matter of fact, under conditions of nanoplastic accumulation in marine coastal sediments and upon acting as vectors of other pollutants, PS-COOH could still pose a threat to the Mediterranean benthic communities.

Chapter 4- Supplementary Material

2. Methods

Composition of PS NP stocks

According to the manufacturer, unlabelled PS-NH$_2$ stock (PA02N, lot: 12839) was supplied at 10% solids (w:v) in deionized water with no stabilizers. The unlabelled PS-COOH stock suspension (PC02N, lot: 11652) contained 10.1% solids (w:v), 0.1% sodium dodecyl sulfate (SDS) and 0.05% sodium azide (NaN$_3$) as stabilizers. Fluorescently labelled PS-COOH stock suspension (FC02F, lot: 11587, Dragon green labeling ex/em 480/520), used for uptake and translocation experiments, contained 1% solids (w:v), 0.1% Tween 20 and 2 mM NaN$_3$. At the concentrations used in our study (5 and 25 µg mL^{-1}), unlabelled and fluorescently labelled PS-COOH suspensions contained a very low residue of stabilizers, as reported in Table S4.1.

Table S4.1. Calculated concentration of SDS, Tween 20 and NaN$_3$ as stabilizers in the unlabelled and fluorescently labelled PS-COOH suspensions at 5 and 25 µg mL^{-1}.

	Unlabelled PS-COOH (PC02N, lot: 11652)		Labelled PS-COOH (FC02F, lot: 11587, Dragon green labeling ex/em 480/520)	
	SDS	NaN$_3$	Tween 20	NaN$_3$
5 µg mL^{-1}	0.05 µg mL^{-1}	0.025 µg mL^{-1}	0.5 µg mL^{-1}	0.001 mM
25 µg mL^{-1}	0.25 µg mL^{-1}	0.125 µg mL^{-1}	2.5 µg mL^{-1}	0.005 mM

By comparing the amount of SDS and NaN$_3$ in the concentrations tested of PS-COOH (5 and 25 µg mL^{-1}) with E(L)C$_{50}$ values in marine model organisms (Table S4.2), the effect of the stabilizers can be considered negligible. E(L)C$_{50}$ values are in fact from 1 to 3 orders of magnitude higher than the concentrations of SDS and NaN$_3$ in PS-COOH working suspensions. We already clarified the negligible effects of stabilizers from different batches of PS-COOH at these final concentrations (Bellingeri et al., 2019; Bergami et al., 2020).

Therefore, the toxicological effects documented for either PS-COOH and PS-NH$_2$ are fully ascribable to the nanoscale dimension of the particles and their surface charges and not to the presence/absence

of stabilizers (i.e., considering also SDS- and NaN_3-free PS-COOH used in Bergami et al., 2016, 2017, 2019; Manfra et al., 2017; Della Torre et al., 2014).

We agree to the need to assess the potential adverse effects of stabilizers present in commercially available NP stocks, however, it is important to take into account also the experimental conditions used to assess the toxicity (e.g., time of exposure, culturing media, temperature, pH, dark/light). So far the majority of the studies to evaluate the role of stabilizers as confounding variables in PS NP testing has mainly been conducted on freshwater species (Pikuda et al., 2019; Heinlaan et al., 2020). With this regards, our previous studies on marine organisms (Bergami et al., 2016, 2017; Pinsino et al., 2017; Della Torre et al., 2014) have wrongly been cited by Pikuda et al. (2019) (i.e., in a study on the freshwater crustacean *Daphnia magna*) as an example of PS NP suspensions containing stabilizers, although they were all stabilizers-free.

Table S4.2. SDS and NaN_3 $E(L)C_{50}$ values and exposure time (h) in different marine taxa. $E(L)C_{50}$ values are reported as mean $\pm$ SD or (95% CI).

Reagent	Model organism	$E(L)C_{50}$ ($\mu g/mL$)	Time (h)	Reference
SDS	*Vibrio fischeri*	2.62 ± 0.90	0.25	(Mariani et al., 2006)
	Artemia spp.	23.20 ± 6.50	24	(Libralato et al., 2016)
NaN_3	*Vibrio fischeri*	> 100	0.5	(Heinlaan et al., 2020)
	Artemia spp.	84 (76-92)	24	(Sleet and Brendel, 1985)

A)

• Cell count results
Total cell concentration: 4.90 x 10⁶ cells/mL
Live cell concentration:
Dead cell concentration:
Viability:
Average cell size: 6.2 µm
Total cell number: 2088
Live cell number:
Dead cell number:

• Protocol
Protocol name: sea urchin cell
Dilution factor: 1
Min. cell size: 3 µm
Max. cell size: 50 µm
Size gating: 3 ~ 50 µm
Noise reduction: 4
Live cell sensitivity: 1
Roundness: 45 %
Declustering level: High
Focusing method: Autofocus
Staining option: Without TB
Counting option: Calibrated value(0x00D3)

B)

• Cell count results
Total cell concentration: 3.80 x 10⁶ cells/mL
Live cell concentration:
Dead cell concentration:
Viability:
Average cell size: 4.4 µm
Total cell number: 1618
Live cell number:
Dead cell number:

• Protocol
Protocol name: Yeast
Dilution factor: 1
Min. cell size: 3 µm
Max. cell size: 8 µm
Size gating: 3 ~ 8 µm
Noise reduction: 3
Live cell sensitivity: 1
Roundness: 85 %
Declustering level: Medium
Focusing method: Autofocus
Staining option: Without TB
Counting option: Calibrated value(0x00D3)

Figure S4.1. Luna II Automated cell counter (Logos Biosystems Inc) instrument settings used for cell counting. Settings for (A) heterogeneous coelomocytes populations (phagocytes, vibratile cells, white and red amebocytes) suspended in CF and (B) yeast cells of *Saccharomyces cerevisiae* suspended in 0.22-µm filtered NSW.

According to the manufacturer's instructions, the fluorescently labelled PS-COOH (60 nm) used in our study have the fluorescent Dragon green dye embedded in the polymer structure (Bangs Laboratories Inc. Product Data Sheet 731). Therefore, a quality control protocol was set up to assess the leaching of the dye and run at the same conditions used for short-term cultures of sea urchin coelomocytes (i.e., sterile vials, 18°C, in the dark). After 4 h of suspension in CF, aliquots of fluorescently labelled PS-COOH (25 µg mL^{-1}) were centrifuged in centrifugal filter units (Microcon®- 10 kDa) at 7000 x g for 30 min at 18°C. CF only was used as a reference. The fluorescence intensity of the resulting filtered solution (radius$_{min}$=1.42 nm of a smooth sphere according to Erickson, 2009) was recorded through the Tecan spectrophofluorometer (Infinite M1000 Pro). Before transferring the aliquots of CF only and CF + NPs to the centrifugal filter units, the fluorescence intensity was determined (CF: 234 ± 10 a.u.; CF + NPs: 42746 ± 120 a.u.). After centrifugation and filtration, no significant differences were observed in the fluorescence intensity of the resulting solution between CF and CF + NPs (CF: 227.3 ± 17 a.u.; CF + NPs: 218 ± 2.5 a.u.) (Fig S2). These results confirm that under the experimental conditions used no loss of the fluorophore from the labelled particles was detected.
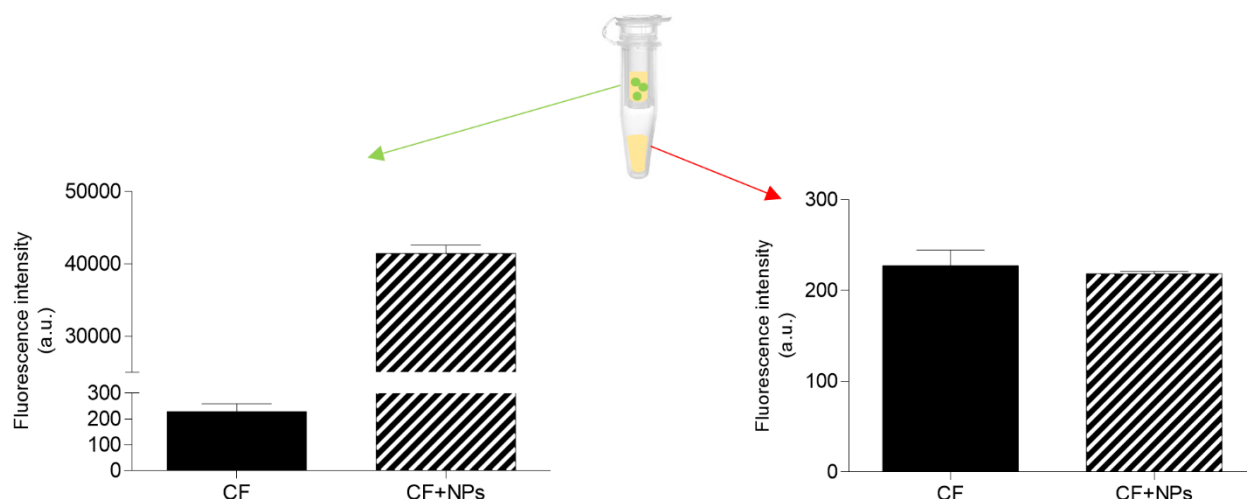
Figure S4.2. PS NP fluorophore leaching test. Fluorescence intensity of the resulting solution before and after centrifugation of CF (only) and PS-COOH suspended in CF at 25 µg mL^{-1} (CF+NPs) in centrifugal sample clarification units of 10 kDa (radius$_{min}$=1.42 nm of a smooth sphere in according to Erickson, 2009).

A) Coelomocytes viability

	Cell viability (%)
CTRL	80.3±1.6
PS-COOH 5	78.1±1.9
PS-COOH 25	70.9±7.5
PS-NH$_2$	62.4±3.7

B) Neutral red retention time

Destabilized lysosomes(%)			
	30 min	45 min	60 min
CTRL	6.5±1.9	9.6±4.7	15.2±5.9
PS-COOH 5	8.6±2.9	15±4.3	18.2±6.7
PS-COOH 25	16.5±3.4	21.7±5.6	23.75±4.9
PS-NH$_2$	23±3.7	25.7±4.9	30.8±2.2

C) Phagocytosis activity

	PC (%)	PI (%)
CTRL	73.6±6.5	167.4±12.1
PS-COOH 5	52.9±4	163±14.5
PS-COOH 25	34.1±6.5	146±12.5
PS-NH$_2$	32±1.8	124.3±14.3

D) PS-COOH uptake

Fluorescence intensity (a.u.)				
	1h	2h	3h	4h
PS-COOH 5	704.3±51.5	806.7±163.9	815±57.7	854.7±145.4
PS-COOH 25	3220±361.45	3861.3±135.6	3975±179	4443±484

E) PS-COOH clearance

Fluorescence intensity (a.u.)		
	1h	3h depuration
PS-COOH 5	704.3±51.5	430±40.4
PS-COOH 25	3220±361.4	1930±37

Figure S4.3. Summary of the results obtained in this study. Results of (A) coelomocytes viability (mean % ± SD); (B) neutral red retention time (mean % ± SD); (C) phagocytic activity (mean % ± SD); (D) PS-COOH uptake (mean a.u. ± SD) and (E) PS-COOH clearance (mean a.u. ± SD).
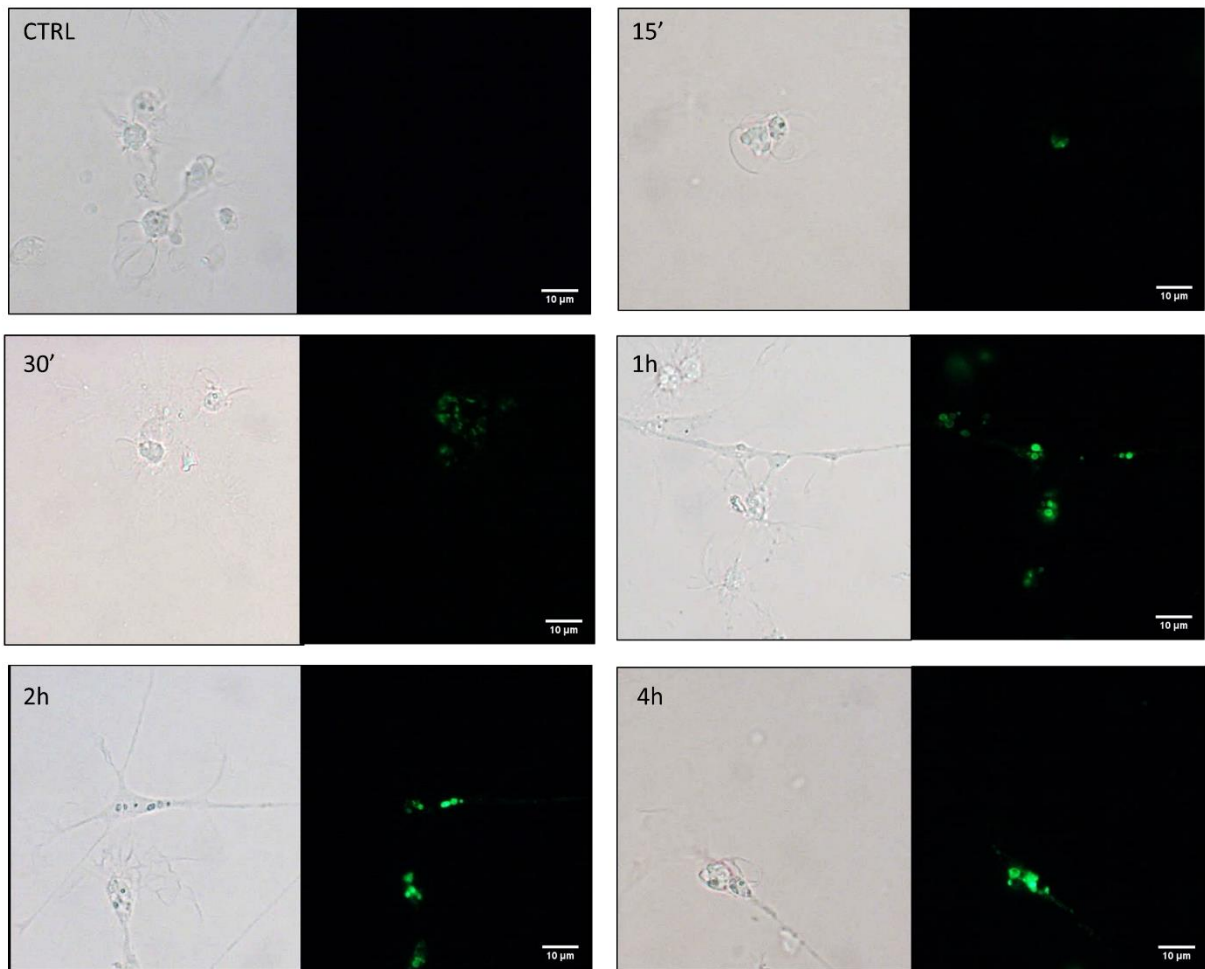
Figure S4.4. **Time-resolved disposition of PS-COOH in sea urchin phagocytes.** Fluorescently labelled PS-COOH (25 µg mL^{-1}) internalization at different times of exposure in phagocytes of sea urchin *Paracentrotus lividus*. Images were recorded at the same gain using an optical microscope (Olympus U-25ND6) equipped with fluorescence GFP-filter (488 λ_{ex}- 510 λ_{em}). Scale bar: 5 µm.
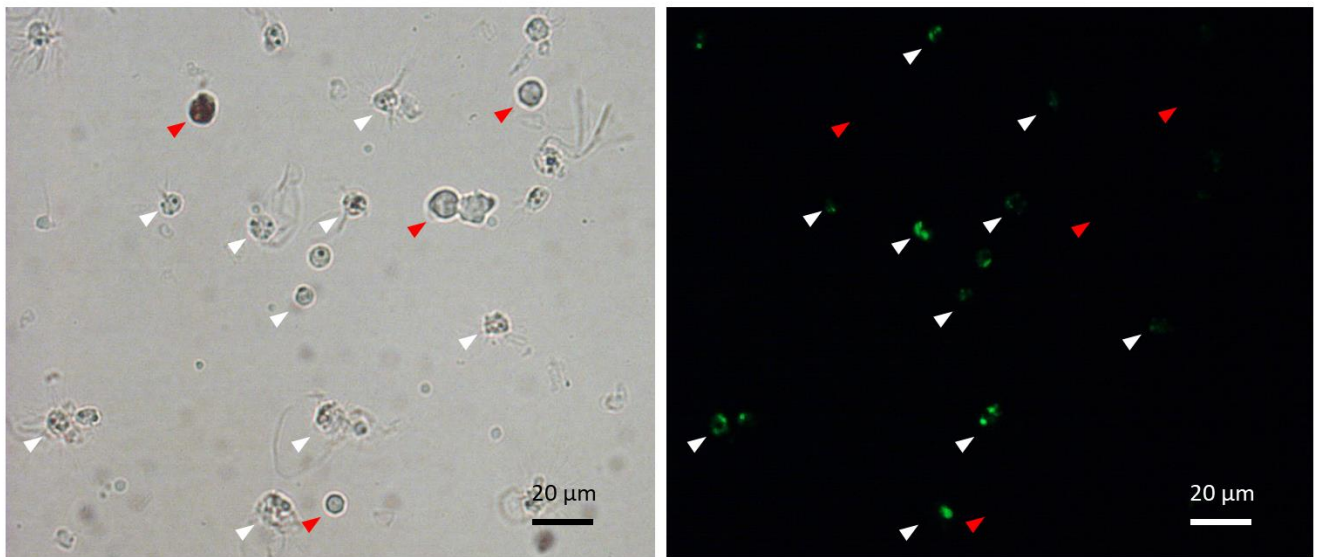
Figure S4.5. **Disposition of PS-COOH in different *P. lividus* coelomocytes sub-populations.** Optical and fluorescence images (on the left and right panel, respectively) of coelomocytes after 4 h of exposure to fluorescently labelled PS-COOH (25 µg mL^{-1}). PS-COOH agglomerates were localized on phagocytes (white arrowheads), while they were absent on other cell sub-populations (red arrow heads), such as vibratile cells and red and white amoebocytes. Scale bar: 20 µm.

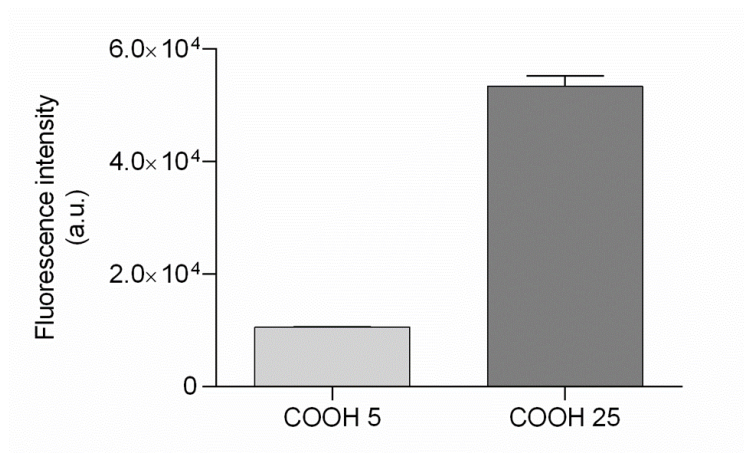**Figure S4.6**. **Labelled PS-COOH suspended in CF.** Fluorescent intensity (arbitrary units, a.u.) of labelled PS-COOH (5 and 25 µg mL^{-1}) suspended in CF and incubated for 4 h in sterile vials in the dark at 18°C. Bars represent mean ± SD (n = 3). Fluorescence intensity values are normalized subtracting the auto-fluorescence of the control group (CF only).
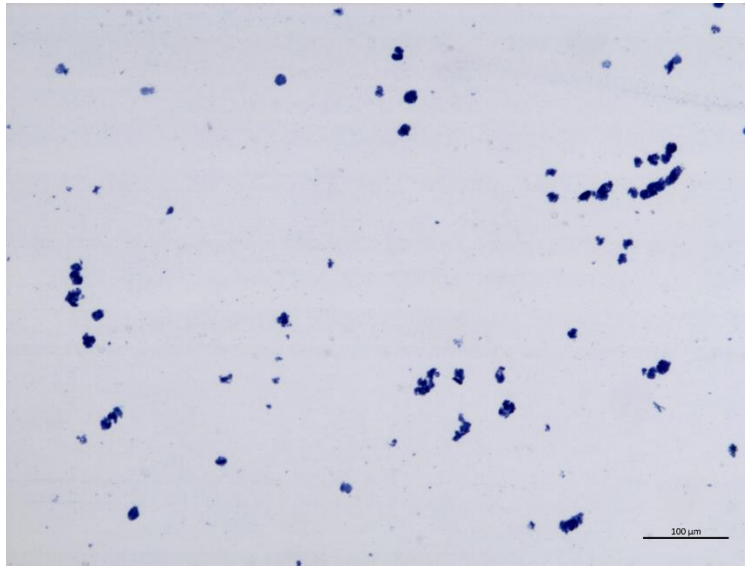
Figure S4.7. Trypan blue exclusion test. Trypan blue (0.4%) does not fully dissolve in *P. lividus* CF (CF: trypan blue 1:1), with the formation of dye clots. Images were recorded using an optical microscope (Zeiss Apotome.2). Scale bar: 100 µm.

References

Abidli, S., Antunes, J. C., Ferreira, J. L., Lahbib, Y., Sobral, P., and Trigui El Menif, N., 2018. Microplastics in sediments from the littoral zone of the north Tunisian coast (Mediterranean Sea). *Estuarine, Coastal and Shelf Science* 205, 1–9. https://doi.org/10.1016/j.ecss.2018.03.006.

Abidli, S., Lahbib, Y., and Trigui El Menif, N., 2019. Microplastics in commercial molluscs from the lagoon of Bizerte (Northern Tunisia). *Marine Pollution Bulletin* 142, 243–252. https://doi.org/10.1016/j.marpolbul.2019.03.048

Alijagic, A., Gaglio, D., Napodano, E., Russo, R., Costa, C., Benada, O., Kofronova, O., Pinsino, A., 2020. Titanium dioxide nanoparticles temporarily influence the sea urchin immunological state suppressing inflammatory-relate gene transcription and boosting antioxidant metabolic activity. *Journal of Hazardous Materials* 384, 121389. https://doi.org/10.1016/j.jhazmat.2019.121389

Alomar, C., Estarellas, F., Deudero, S., 2016. Microplastics in the Mediterranean Sea: Deposition in coastal shallow sediments, spatial variation and preferential grain size. *Marine Environmental Research* 115, 1–10. https://doi.org/10.1016/j.marenvres.2016.01.005

Al-Sid-Cheikh, M., Rowland, S. J., Kaegi, R., Henry, T. B., Cormier, M.-A., Thompson, R. C., 2020. Synthesis of ^{14}C-labelled polystyrene nanoplastics for environmental studies. *Communications Material* 1, 97. https://doi.org/10.1038/s43246-020-00097-9

Al-Sid-Cheikh, M., Rowland, S. J., Stevenson, K., Rouleau, C., Henry, T. B., Thompson, R. C., 2018. Uptake, Whole-Body Distribution, and Depuration of Nanoplastics by the Scallop *Pecten maximus* at Environmentally Realistic Concentrations. *Environmental Science & Technology* 52, 14480–14486. https://doi.org/10.1021/acs.est.8b05266

Andrady, A. L., 2017. The plastic in microplastics: A review. *Marine Pollution Bulletin* 119, 12–22. https://doi.org/10.1016/j.marpolbul.2017.01.082

Angiolillo, M., Lorenzo, B. di, Farcomeni, A., Bo, M., Bavestrello, G., Santangelo, G., Cau, Angelo, Mastascusa, V., Cau, Alessandro, Sacco, F., Canese, S., 2015. Distribution and assessment of marine debris in the deep Tyrrhenian Sea (NW Mediterranean Sea, Italy). *Marine Pollution Bulletin* 92, 149–159. https://doi.org/10.1016/j.marpolbul.2014.12.044

Avio, C. G., Cardelli, L. R., Gorbi, S., Pellegrini, D., Regoli, F., 2017. Microplastics pollution after the removal of the Costa Concordia wreck: First evidences from a biomonitoring case study. *Environmental Pollution* 227, 207–214. https://doi.org/10.1016/j.envpol.2017.04.066

Barnes, D., Verling, E., Crook, A., Davidson, I., O'Mahoney, M., 2002. Local population disappearance follows (20 yr after) cycle collapse in a pivotal ecological species. *Marine Ecology Progress Series* 226, 311–313. https://doi.org/10.3354/meps226311

Bergami, E., Bocci, E., Vannuccini, M. L., Monopoli, M., Salvati, A., Dawson, K. A., Corsi, I., 2016. Nano-sized polystyrene affects feeding, behavior and physiology of brine shrimp *Artemia franciscana* larvae. *Ecotoxicology and Environmental Safety* 123, 18–25. https://doi.org/10.1016/j.ecoenv.2015.09.021

Bergami, E., Krupinski Emerenciano, A., González-Aravena, M., Cárdenas, C. A., Hernández, P., Silva, J. R. M. C., et al. 2019. Polystyrene nanoparticles affect the innate immune system of the Antarctic sea urchin *Sterechinus neumayeri*. *Polar Biology* 42, 743–757. https://doi.org/10.1007/s00300-019-02468-6

Bergami, E., Pugnalini, S., Vannuccini, M. L., Manfra, L., Faleri, C., Savorelli, F., Dawson, K.A., Corsi, I., 2017. Long-term toxicity of surface-charged polystyrene nanoplastics to marine planktonic species *Dunaliella tertiolecta* and *Artemia franciscana*. *Aquatic Toxicology* 189, 159–169. https://doi.org/10.1016/j.aquatox.2017.06.008

Borges, J., Porto-Neto, L., Mangiaterra, M., Jensch-Junior, B., and da Silva, J., 2002. Phagocytosis *in vitro* and *in vivo* in the Antarctic sea urchin *Sterechinus neumayeri* at 0°C. *Polar Biology* 25, 891–897. https://doi.org/10.1007/s00300-002-0431-6.

Boudouresque, C. F., and Verlaque, M. 2020. "*Paracentrotus lividus*," in *Developments in Aquaculture and Fisheries Science* (Elsevier), 447–485. https://10.1016/B978-0-12-819570-3.00026-3

Branco, P. C., Borges, J. C. S., Santos, M. F., Jensch Junior, B. E., and da Silva, J. R. M. C., 2013. The impact of rising sea temperature on innate immune parameters in the tropical subtidal sea urchin *Lytechinus variegatus* and the intertidal sea urchin *Echinometra lucunter*. *Marine Environmental Research* 92, 95–101. https://10.1016/j.marenvres.2013.09.005

Branco, P., Figueiredo, D. and da Silva, J. R. M. C, 2014. New insights into innate immune system of sea urchin: coelomocytes as biosensors for environmental stress. *OA Biology* 18 2(1), 2.

Canesi, L., Ciacci, C., Bergami, E., Monopoli, M. P., Dawson, K. A., Papa, S., Canonico, B., Corsi, I., 2015. Evidence for immunomodulation and apoptotic processes induced by cationic polystyrene nanoparticles in the hemocytes of the marine bivalve *Mytilus*. *Marine Environmental Research* 111, 34–40. https://doi.org/10.1016/j.marenvres.2015.06.008

Canesi, L., Ciacci, C., Fabbri, R., Balbi, T., Salis, A., Damonte, G., Cortese, K., Caratto, V., Monopoli, M.P., Dawson, K., Bergami, E., Corsi, I., 2016. Interactions of cationic polystyrene nanoparticles with marine bivalve hemocytes in a physiological environment: Role of soluble hemolymph proteins. *Environmental Research* 150, 73–81. https://doi.org/10.1016/j.envres.2016.05.045

Canesi, L., and Corsi, I. 2016. Effects of nanomaterials on marine invertebrates. *Science of The Total Environment* 565, 933–940. https://doi.org/10.1016/j.scitotenv.2016.01.085

Castellano, I., Migliaccio, O., Ferraro, G., Maffioli, E., Marasco, D., Merlino, A., Zingone, A., Tedeschi, G., Palumbo, A., 2018. Biotic and environmental stress induces nitration and changes in structure and function of the sea urchin major yolk protein toposome. *Scientific Report* 8, 4610. https://doi.org/10.1038/s41598-018-22861-1

Catarino, A. I., Frutos, A., and Henry, T. B. 2019. Use of fluorescent-labelled nanoplastics (NPs) to demonstrate NP absorption is inconclusive without adequate controls. *Science of The Total Environment* 670, 915–920. https://doi.org/10.1016/j.scitotenv.2019.03.194

Cincinelli, A., Martellini, T., Guerranti, C., Scopetani, C., Chelazzi, D., and Giarrizzo, T., 2019. A potpourri of microplastics in the sea surface and water column of the Mediterranean Sea. *TrAC Trends in Analytical Chemistry* 110, 321–326. https://doi.org/10.1016/j.trac.2018.10.026

Cole, M., Liddle, C., Consolandi, G., Drago, C., Hird, C., Lindeque, P. K., Galloway, T.S., 2020. Microplastics, microfibres and nanoplastics cause variable sub-lethal responses in mussels (*Mytilus* spp.). *Marine Pollution Bulletin* 160, 111552. https://doi.org/10.1016/j.marpolbul.2020.111552

Compa, M., Alomar, C., Wilcox, C., van Sebille, E., Lebreton, L., Hardesty, B. D., Deudero, S., 2019. Risk assessment of plastic pollution on marine diversity in the Mediterranean Sea. *Science of The Total Environment* 678, 188–196. https://doi.org/10.1016/j.scitotenv.2019.04.355

Consoli, P., Falautano, M., Sinopoli, M., Perzia, P., Canese, S., Esposito, V., Battaglia, P., Romeo, T., Andaloro, F., Galgani, F., Castriota, L., 2018. Composition and abundance of benthic marine litter in a coastal area of the central Mediterranean Sea. *Marine Pollution Bulletin* 136, 243–247. https://doi.org/10.1016/j.marpolbul.2018.09.033

Corsi, I., Bergami, E., and Grassi, G., 2020. Behaviour and bio-interactions of anthropogenic particles in marine environment for a more realistic ecological risk assessment. *Frontiers in Environmental Science* 8, 60. https://doi.org/10.3389/fenvs.2020.00060

Courtene-Jones, W., Quinn, B., Gary, S. F., Mogg, A. O. M., and Narayanaswamy, B. E., 2017. Microplastic pollution identified in deep-sea water and ingested by benthic invertebrates in the Rockall Trough, North Atlantic Ocean. *Environmental Pollution* 231, 271–280. https://doi.org/10.1016/j.envpol.2017.08.026

Cózar, A., Sanz-Martín, M., Martí, E., González-Gordillo, J. I., Ubeda, B., Gálvez, J. Á., Irigoien, X., Duarte, C.M., 2015. Plastic Accumulation in the Mediterranean Sea. *PLoS ONE* 10, e0121762. https://doi.org/10.1371/journal.pone.0121762

Davies, I.M., Gubbins, M., Hylland, K., Maes, T., Martínez-Gómez, C., Giltrap, M., Burgeot, T., Wosniok, W., Lang, T., Vethaak, A.D., 2012. Technical annex: assessment criteria for biological effects measurements, 209-212. In Davies, I.M., and Vethaak, A.D (Eds). 2012. Integrated monitoring of chemicals and their effects. *ICES Cooperative Research Report*, 315.

Della Torre, C., Bergami, E., Salvati, A., Faleri, C., Cirino, P., Dawson, K. A., Corsi, I., 2014. Accumulation and Embryotoxicity of Polystyrene Nanoparticles at Early Stage of Development of Sea Urchin Embryos *Paracentrotus lividus*. *Environmental Science & Technology* 48, 12302–12311. https://doi.org/10.1021/es502569w

Dheilly, N. M., Raftos, D. A., Haynes, P. A., Smith, L. C., and Nair, S. V., 2013. Shotgun proteomics of coelomic fluid from the purple sea urchin, Strongylocentrotus purpuratus. *Developmental & Comparative Immunology* 40, 35–50. https://doir.org/10.1016/j.dci.2013.01.007

Duan, X., and Li, Y., 2013. Physicochemical Characteristics of Nanoparticles Affect Circulation, Biodistribution, Cellular Internalization, and Trafficking. *Small* 9, 1521–1532. https://10.1002/smll.201201390

Eliso, M. C., Bergami, E., Manfra, L., Spagnuolo, A., and Corsi, I., 2020. Toxicity of nanoplastics during the embryogenesis of the ascidian *Ciona robusta* (Phylum *Chordata*). *Nanotoxicology*, 1–17. https://doi.org/10.1080/17435390.2020.1838650

Falugi, C., Aluigi, M. G., Chiantore, M. C., Privitera, D., Ramoino, P., Gatti, M. A., Fabrizi, A., Pinsino, A., Matranga, V., 2012. Toxicity of metal oxide nanoparticles in immune cells of the sea urchin. *Marine Environmental Research* 76, 114–121. https://doi.org/10.1016/j.marenvres.2011.10.003

Feng, L.J., Li, J.W., Xu, E. G., Sun, X.D., Zhu, F.P., Ding, Z., Thian, H., Dong, S.S., Xia, P.F., Yuan, X.Z., 2019. Short-term exposure to positively charged polystyrene nanoparticles causes oxidative stress and membrane destruction in cyanobacteria. *Environmental Science: Nano* 6, 3072–3079. https://doi.org/10.1039/C9EN00807A

Feng, Z., Wang, R., Zhang, T., Wang, J., Huang, W., Li, J., Xu, J., Gao, G., 2020. Microplastics in specific tissues of wild sea urchins along the coastal areas of northern China. *Science of The Total Environment* 728, 138660. https://doi.org/10.1016/j.scitotenv.2020.138660

Fočak, M., Džafić, S., and Suljević, D., 2019. Electrolytes and Heavy Metals in Coelomic Fluid of Sea Urchin, *Arbacia lixula* from Adriatic Sea: Biochemical Approach to Ecotoxicological Study. International Journal of Maritime Science & Technology 66, 51–56. https://doi.org/10.17818/NM/2019/2.1

Fotopoulou, K. N., and Karapanagioti, H. K., 2012. Surface properties of beached plastic pellets. *Marine Environmental Research* 81, 70–77. https://doi.org/10.1016/j.marenvres.2012.08.010

Freire, C. A., Santos, I. A., and Vidolin, D., 2011. Osmolality and ions of the perivisceral coelomic fluid of the intertidal sea urchin *Echinometra lucunter* (Echinodermata: *Echinoidea*) upon salinity and ionic challenges. *Zoologia* 28, 479–487. https://doi.org/10.1590/S1984-46702011000400009

Gigault, J., Pedrono, B., Maxit, B., and Ter Halle, A., 2016. Marine plastic litter: the unanalyzed nano-fraction. *Environmental Science: Nano* 3, 346–350. https://doi.org/10.1039/C6EN00008H

Graham, E. R., and Thompson, J. T., 2009. Deposit- and suspension-feeding sea cucumbers (*Echinodermata*) ingest plastic fragments. *Journal of Experimental Marine Biology and Ecology* 368, 22–29. https://doi.org/10.1016/j.jembe.2008.09.007

Grassi, G., Landi, C., Torre, C. D., Bergami, E., Bini, L., and Corsi, I., 2019. Proteomic profile of the hard corona of charged polystyrene nanoparticles exposed to sea urchin *Paracentrotus lividus* coelomic fluid highlights potential drivers of toxicity. *Environmental Science: Nano* 6, 2937–2947. https://doi.org/10.1039/C9EN00824A

Hartmann, N. B., Hüffer, T., Thompson, R. C., Hassellöv, M., Verschoor, A., Daugaard, A. E., Rist, S., Karlsson, T.M., Brennholt, N., Cole, M., Herrling, M., Hess, M., 2019. Are We Speaking the Same Language? Recommendations for a Definition and Categorization Framework for Plastic Debris. *Environmental Science & Technology* 53, 1039–1047. https://doi.org/10.1021/acs.est.8b05297

Hernandez, E., Nowack, B., Mitrano, D. M., 2017. Polyester Textiles as a Source of Microplastics from Households: A Mechanistic Study to Understand Microfiber Release During Washing. *Environmental Science & Technology* 51, 7036–7046. https://10.1021/acs.est.7b01750

Hewitt, R. E., Chappell, H. F., Powell, J. J., 2020. Small and dangerous? Potential toxicity mechanisms of common exposure particles and nanoparticles. *Current Opinion in Toxicology* 19, 93–98. https://10.1016/j.cotox.2020.01.006

ICES, 2010. Report of the ICES\OSPAR Workshop on Lysosomal Stability Data Quality and Interpretation (WKLYS), 13–17 September 2010, Alessandria, Italy. ICES CM2010/ACOM: 61.

Jaumouillé, V., and Waterman, C. M., 2020. Physical Constraints and Forces Involved in Phagocytosis. *Frontiers in Immunology* 11, 1097. https://10.3389/fimmu.2020.01097

Kane, I. A., Clare, M. A., Miramontes, E., Wogelius, R., Rothwell, J. J., Garreau, P., Pohl, F., 2020. Seafloor microplastic hotspots controlled by deep-sea circulation. *Science* 368, 1140–1145. https://10.1126/science.aba5899

Lambert, C., Authier, M., Dorémus, G., Laran, S., Panigada, S., Spitz, J., Van Canneyt, O., Ridoux, V., 2020. Setting the scene for Mediterranean litterscape management: The first basin-scale quantification and mapping of floating marine debris. *Environmental Pollution* 263, 114430. https://10.1016/j.envpol.2020.114430.

Lambert, S., and Wagner, M., 2016. Characterisation of nanoplastics during the degradation of polystyrene. *Chemosphere* 145, 265–268. https://10.1016/j.chemosphere.2015.11.078

Lead, J. R., Batley, G. E., Alvarez, P. J. J., Croteau, M.-N., Handy, R. D., McLaughlin, M. J., Judy, J.D., Schirmer, K., 2018. Nanomaterials in the environment: Behavior, fate, bioavailability, and effects-An updated review: Nanomaterials in the environment. *Environmental Toxicology & Chemistry* 37, 2029–2063. https://10.1002/etc.4147

Lebreton, L., and Andrady, A., 2019. Future scenarios of global plastic waste generation and disposal. *Palgrave Communication* 5, 6. https://10.1057/s41599-018-0212-7

Llorca, M., Vega-Herrera, A., Schirinzi, G., Savva, K., Abad, E., and Farré, M., 2020. Screening of suspected micro(nano)plastics in the Ebro Delta (Mediterranean Sea). *Journal of Hazardous Materials* 404, 124022. https://10.1016/j.jhazmat.2020.124022

Lowe, D., Fossato, V., and Depledge, M., 1995. Contaminant-induced lysosomal membrane damage in blood cells of mussels *Mytilus galloprovincialis* from the Venice Lagoon:an in vitro study. *Marine Ecology Progress Series* 129, 189–196. https://10.3354/meps129189

Lowry, G. V., Gregory, K. B., Apte, S. C., and Lead, J. R., 2012. Transformations of Nanomaterials in the Environment. *Environmental Science and Technology* 46, 6893–6899. https://doi.org/10.1021/es300839e

Macias, D., Cózar, A., Garcia-Gorriz, E., González-Fernández, D., and Stips, A., 2019. Surface water circulation develops seasonally changing patterns of floating litter accumulation in the Mediterranean Sea. A modelling approach. *Marine Pollution Bulletin* 149, 110619. https://doi.org/10.1016/j.marpolbul.2019.110619.

Macic, V., Mandic, M., Pestoric, B., Gacic, Z., Paunovic, M., 2017. First assessment of marine litter in shallow south-east Adriatic Sea. *Fresenius Environmental Bulletin* 26, 4834-4880.

Majeske, A. J., Bayne, C. J., and Smith, L. C., 2013. Aggregation of Sea Urchin Phagocytes Is Augmented *In Vitro* by Lipopolysaccharide. *PLoS ONE* 8, 61419. https://doi.org/10.1371/journal.pone.0061419

Manfra, L., Rotini, A., Bergami, E., Grassi, G., Faleri, C., Corsi, I., 2017. Comparative ecotoxicity of polystyrene nanoparticles in natural seawater and reconstituted seawater using the rotifer *Brachionus plicatilis*. *Ecotoxicology and Environmental Safety* 145, 557–563. https://doi.org/10.1016/j.ecoenv.2017.07.068

Marques-Santos, L. F., Grassi, G., Bergami, E., Faleri, C., Balbi, T., Salis, A., Damonte, G., Canesi, L, Corsi, I., 2018. Cationic polystyrene nanoparticle and the sea urchin immune system: biocorona formation, cell toxicity, and multixenobiotic resistance phenotype. *Nanotoxicology* 12, 847–867. https://doi.org/10.1080/17435390.2018.1482378

Matranga, V., Bonaventura, R., Di Bella, G., 2002. Hsp70 as a stress marker of sea urchin coelomocytes in short term cultures. *Cellular and Molecular Biology* 48(4) 345-349. PMID: 12064441.

Matranga, V., Pinsino, A., Celi, M., Natoli, A., Bonaventura, R., Schröder, H. C., Müller, W.E.G., 2005. Monitoring Chemical and Physical Stress Using Sea Urchin Immune Cells. *Echinodermata* Progress in Molecular and Subcellular Biology., ed. V. Matranga 85–110. https://doi.org/10.1007/3-540-27683-1_5

Mattsson, K., Jocic, S., Doverbratt, I., and Hansson, L.-A., 2018. Nanoplastics in the Aquatic Environment. *Microplastic Contamination in Aquatic Environments* (Elsevier), 379–399. https://doi.org/10.1016/B978-0-12-813747-5.00013-8

Migliaccio, O., Pinsino, A., Maffioli, E., Smith, A. M., Agnisola, C., Matranga, V., Nonnis, S., Tedeschi, G., Byrne, M., Gambi, M.C., Palumbo, A., 2019. Living in future ocean acidification, physiological adaptive responses of the immune system of sea urchins resident at a CO_2 vent system. *Science of The Total Environment* 672, 938–950. https://doi.org/10.1016/j.scitotenv.2019.04.005

Milito, A., Murano, C., Castellano, I., Romano, G., and Palumbo, A., 2020. Antioxidant and immune response of the sea urchin *Paracentrotus lividus* to different re-suspension patterns of highly polluted marine sediments. *Marine Environmental Research* 160, 104978. https://doi.org/10.1016/j.marenvres.2020.104978

Murano, C., Agnisola, C., Caramiello, D., Castellano, I., Casotti, R., Corsi, I., Palumbo, A., 2020. How sea urchins face microplastics: Uptake, tissue distribution and immune system response. *Environmental Pollution* 264, 114685. https://doi.org/10.1016/j.envpol.2020.114685

Nel, A. E., Mädler, L., Velegol, D., Xia, T., Hoek, E. M. V., Somasundaran, P., Klaessig, F., Castanova, V., Thompson, M., 2009. Understanding biophysicochemical interactions at the nano–bio interface. *Nature Materials* 8, 543–557. https://doi.org/10.1038/nmat2442

Pawley, J.B., 2006. Fundamental Limits in Confocal Microscopy. Handbook of Biological Confocal Microscopy, Third Edition, Springer Science+ Business Media, LLC, New York.

Pikuda, O., Xu, E. G., Berk, D., and Tufenkji, N., 2019. Toxicity Assessments of Micro- and Nanoplastics Can Be Confounded by Preservatives in Commercial Formulations. *Environmental Science & Technoogy Letters* 6, 21–25. https://doi.org/10.1021/acs.estlett.8b00614

Pinsino, A., Bergami, E., Della Torre, C., Vannuccini, M. L., Addis, P., Secci, M., Dawson, K.A., Matranga, V., Corsi, I., 2017. Amino-modified polystyrene nanoparticles affect signalling pathways of the sea urchin (*Paracentrotus lividus*) embryos. *Nanotoxicology* 11, 201–209. https://doi.org/10.1080/17435390.2017.1279360

Pinsino, A., and Matranga, V., 2015. Sea urchin immune cells as sentinels of environmental stress. *Developmental & Comparative Immunology* 49, 198–205. https://doi.org/10.1016/j.dci.2014.11.013

Pinsino, A., Russo, R., Bonaventura, R., Brunelli, A., Marcomini, A., and Matranga, V., 2015. Titanium dioxide nanoparticles stimulate sea urchin immune cell phagocytic activity involving TLR/p38 MAPK-mediated signalling pathway. *Scientific Report* 5, 14492. https://doi.org/10.1038/srep14492

Plee, T. A., and Pomory, C. M., 2020. Microplastics in sandy environments in the Florida Keys and the panhandle of Florida, and the ingestion by sea cucumbers (Echinodermata: *Holothuroidea*) and sand dollars (Echinodermata: *Echinoidea*). *Marine Pollution Bulletin* 158, 111437. https://doi.org/10.1016/j.marpolbul.2020.111437

Porter, A., Smith, K. E., and Lewis, C., 2019. The sea urchin *Paracentrotus lividus* as a bioeroder of plastic. *Science of The Total Environment* 693, 133621. https://10.1016/j.scitotenv.2019.133621

Praetorius, A., Badetti, E., Brunelli, A., Clavier, A., Gallego-Urrea, J. A., Gondikas, A., Hassellöv, M., Hofmann, T., Mackevica, A., Marcomini, A., Peijnenburg, W., Quik, J.T.K., Seijo, M., Stoll, S., Tepe, N., Walcha, H., von der Kammera, F., 2020. Strategies for determining heteroaggregation attachment efficiencies of engineered nanoparticles in aquatic environments. *Environmental Science : Nano* 7, 351–367. https://10.1039/C9EN01016E

Rossi, G., Barnoud, J., and Monticelli, L., 2014. Polystyrene Nanoparticles Perturb Lipid Membranes. *Journal Physical Chemistry Letters* 5, 241–246. https://10.1021/jz402234c

Santos, I. A., Castellano, G. C., and Freire, C. A., 2013. Direct relationship between osmotic and ionic conforming behavior and tissue water regulatory capacity in echinoids. *Comparative Biochemistry and Physiology Part A: Molecular & Integrative Physiology* 164, 466–476. https://10.1016/j.cbpa.2012.12.010

Schirinzi, G. F., Llorca, M., Seró, R., Moyano, E., Barceló, D., Abad, E., Farrè, M., 2019. Trace analysis of polystyrene microplastics in natural waters. *Chemosphere* 236, 124321. https://doi.org/10.1016/j.chemosphere.2019.07.052

Schür, C., Rist, S., Baun, A., Mayer, P., Hartmann, N. B., and Wagner, M., 2019. When Fluorescence Is not a Particle: The Tissue Translocation of Microplastics in *Daphnia magna* Seems an Artifact. *Environmental Toxicology & Chemistry* 38, 1495–1503. https://10.1002/etc.4436

Sendra, M., Carrasco-Braganza, M. I., Yeste, P. M., Vila, M., and Blasco, J., 2020. Immunotoxicity of polystyrene nanoplastics in different hemocyte subpopulations of *Mytilus galloprovincialis*. *Scientific Report* 10, 8637. https://10.1038/s41598-020-65596-8

Sendra, M., Saco, A., Yeste, M. P., Romero, A., Novoa, B., and Figueras, A., 2019. Nanoplastics: From tissue accumulation to cell translocation into *Mytilus galloprovincialis* hemocytes. resilience of immune cells exposed to nanoplastics and nanoplastics plus *Vibrio splendidus* combination. *Journal of Hazardous Materials* 388, 121788. https://10.1016/j.jhazmat.2019.121788

Simon-Sánchez, L., Grelaud, M., Garcia-Orellana, J., and Ziveri, P., 2019. River Deltas as hotspots of microplastic accumulation: The case study of the Ebro River (NW Mediterranean). *Science of The Total Environment* 687, 1186–1196. https://10.1016/j.scitotenv.2019.06.168

Smith, L. C., 2010. Diversification of innate immune genes: lessons from the purple sea urchin. *Disease Models & Mechanisms* 3, 274–279. https://10.1242/dmm.004697

Smith, L. C., Arizza, V., Barela Hudgell, M. A., Barone, G., Bodnar, A. G., Buckley, K. M., et al. 2018. Echinodermata: The Complex Immune System in Echinoderms in *Advances in Comparative Immunology*, ed. E. L. Cooper (Cham: Springer International Publishing), 409–501. https://10.1007/978-3-319-76768-0_13

Smith, L. C., Hawley, T. S., Henson, J. H., Majeske, A. J., Oren, M., and Rosental, B., 2019. Chapter 15 - Methods for collection, handling, and analysis of sea urchin coelomocytes, in *Methods in Cell Biology* Echinoderms, Part A., eds. K. R. Foltz and A. Hamdoun (Academic Press), 357–389. https://10.1016/bs.mcb.2018.11.009

Strober, W., 2015. Trypan Blue Exclusion Test of Cell Viability. *Current Protocols in Immunology* 111. https://10.1002/0471142735.ima03bs111

Suaria, G., Avio, C.G., Mineo, A., Lattin, G.L., Magaldi, M.G., Belmonte, G., Moore, C.J., Regoli, F., Aliani, S., 2016. The Mediterranean Plastic Soup: synthetic polymers in Mediterranean surface waters. *Scientific Report* 6, 37551. https://doi.org/10.1038/srep37551

Tallec, K., Huvet, A., di Poi, C., González-Fernández, C., Lambert, C., Petton, B., le Goïc, N., Berchel, M., Soudant, P., Paul-Pont, I., 2018. Nanoplastics impaired oyster free living stages, gametes and embryos. *Environmental Pollution* 242, 1226–1235. https://10.1016/j.envpol.2018.08.020

Taylor, M. L., Gwinnett, C., Robinson, L. F., and Woodall, L. C., 2016. Plastic microfibre ingestion by deep-sea organisms. *Scientific Report* 6, 33997. https://doi.org/10.1038/srep33997

Tian, L., Chen, Q., Jiang, W., Wang, L., Xie, H., Kalogerakis, N., Ma, Y., 2019. A carbon-14 radiotracer-based study on the phototransformation of polystyrene nanoplastics in water versus in air. *Environmental Science: Nano* 6, 2907–2917. https://doi.org/10.1039/C9EN00662A

Trevisan, R., Uzochukwu, D., and Di Giulio, R., 2020. PAH Sorption to Nanoplastics and the Trojan Horse Effect as Drivers of Mitochondrial Toxicity and PAH Localization in Zebrafish. *Frontiers in Environmental Science* 8. https://doi.org/10.3389/fenvs.2020.00078

Ura, K., Wang, H., Hori, T., Aizawa, S., Tsue, S., Satoh, M., Takeii, N., Hoshino, K., Higuchi, I., Sanuki, S., Yuhi, T., Nishimiya, O., Takagi, Y., 2017. The reproductive cycle and transcription-level changes in the major yolk protein of wild northern sea urchin. *Aquaculture Science*. 65 （3）231−237. https://doi.org/10.11233/aquaculturesci.65.231

Varó, I., Perini, A., Torreblanca, A., Garcia, Y., Bergami, E., Vannuccini, M. L., Corsi, I., 2019. Time-dependent effects of polystyrene nanoparticles in brine shrimp *Artemia franciscana* at physiological, biochemical and molecular levels. *Science of The Total Environment* 675, 570–580. https://doi.org/10.1016/j.scitotenv.2019.04.157

Vered, G., Kaplan, A., Avisar, D., and Shenkar, N. 2019. Using solitary ascidians to assess microplastic and phthalate plasticizers pollution among marine biota: A case study of the Eastern Mediterranean and Red Sea. *Marine Pollution Bulletin* 138, 618–625. https://doi.org/10.1016/j.marpolbul.2018.12.013

Wang, F., Bexiga, M. G., Anguissola, S., Boya, P., Simpson, J. C., Salvati, A., Dawson, K.A., 2013a. Time resolved study of cell death mechanisms induced by amine-modified polystyrene nanoparticles. *Nanoscale* 5, 10868. https://doi.org/10.1039/C3NR03249C

Wang, F., Salvati, A., and Boya, P., 2018. Lysosome-dependent cell death and deregulated autophagy induced by amine-modified polystyrene nanoparticles. *Open Biology* 8, 170271. https://10.1098/rsob.170271

Wang, F., Yu, L., Monopoli, M. P., Sandin, P., Mahon, E., Salvati, A., Dawson, K.A., 2013b. The biomolecular corona is retained during nanoparticle uptake and protects the cells from the damage induced by cationic nanoparticles until degraded in the lysosomes. *Nanomedicine: Nanotechnology, Biology and Medicine* 9, 1159–1168. https://10.1016/j.nano.2013.04.010

Zhang, M., and Xu, L. 2020. Transport of micro- and nanoplastics in the environment: Trojan-Horse effect for organic contaminants. *Critical Reviews in Environmental Science and Technology*, 1–37. https://10.1080/10643389.2020.1845531

Conclusions and future perspectives

The present thesis work was one of the first deep investigations of interactions occurring between MPs / nanoplastics and the sea urchin *P. lividus*. According to the general aim of this PhD project, key elements related to the mechanisms of uptake, biodisposition and clearance, toxicity as well as to bio-nano interactions were provided.

In detail, overviewing all the data obtained in each chapter, the following conclusions can be drawn:

- The sea urchin *P. lividus* has proved to be an excellent model organism for the *in vivo* and *in vitro* ecotoxicological investigations of MPs and nanoplastics.

- The sea urchin has shown extraordinary ability to internalize MPs by also implementing selective size-dependent uptake. In this regard, the water vascular system has been shown to play a fundamental role in the uptake of small particles (10μm).

- Sea urchins have also shown the ability to eliminate MPs after their internalization.

- The distinctive immune system of the sea urchin has been confirmed as a valid tool both for either in vitro and *in vivo* studies

- Negatively charged PS NPs, as a proxy for naturally occurring nanoplastics, are quickly captured by phagocytes and sequestred into lysosomal compartments, with associated low acute toxicity in comparison with their positively charged counterparts.

- The interaction between coelomic fluid components and PS-COOH induced changes in coelomocytes's ultrastructural properties.

- PS MPs (45μm and 10 μm) are found to affect the immune response by increasing the levels of reactive species, the number of total cells as well as influencing the ratio between red and white amoebocytes.

- The naturally occurring colonization of PS microbeads in NSW can play a key role in their impact on sea urchin by increasing their internalization and altering the immune response through a decrease of coelomocytes number and an increase of red/white amoebocytes ratio, as well as an increase of intracellular ROS levels and a decrease of intracellular RNS.

- In wild specimens sampled along the coasts of the Gulf of Naples, both polyester and cellulose fibers were found with an average of 2.6 items/individual.

- Since the sea urchin is widely distributed along the Mediterranean coasts, it may represent a suitable bioindicator to easily monitor the presence of MPs and in particular MFs in a benthic environment.

Further investigations using "-omics" approaches can be useful in order to obtain a deeper understanding of mode of action of either MFs and MP and nanoplastics either colonized and virgin in the sea urchin organ/tisuues and immune cells. Moreover, these approaches will be helpful to advance our understanding on the role of *protein-/eco- corona* in toxicodynamics/toxicokinetics processes in sea urchins immune cells upon exposure to PS-COOH and PS-NH$_2$.